UCGE Reports
Number 20254

Department of Geomatics Engineering

Improved Techniques for Measuring and Estimating Scaling Factors Used to Aggregate Forest Transpiration

(URL: http://www.geomatics.ucalgary.ca/research/publications/GradTheses.html)

by

María Rebeca Quiñonez-Piñón

March 2007

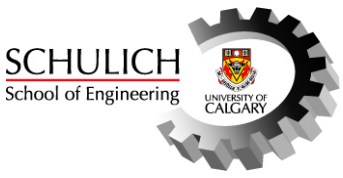

THE UNIVERSITY OF CALGARY

Improved Techniques for Measuring and Estimating Scaling Factors Used to Aggregate Forest Transpiration

by

María Rebeca Quiñonez-Piñón

A DISSERTATION

SUBMITTED TO THE FACULTY OF GRADUATE STUDIES

IN PARTIAL FULFILLMENT OF THE REQUIREMENTS

FOR THE DEGREE OF DOCTOR OF PHILOSOPHY

DEPARTMENT OF GEOMATICS ENGINEERING

CALGARY, ALBERTA

MARCH, 2007

Abstract

This research deals with transpiration scaling issues, and its aim is to improve five boreal species canopy transpiration estimates that are computed by scaling up single tree transpiration to the canopy scale. The improvement of canopy transpiration estimates is made by developing a robust scaling approach. The robustness of the scaling approach rests on fine input scaling parameter data and allometric regression models developed at two different scales, tree and plot (i.e. canopy scale). Moreover, the scaling approach integrates the habitat's vegetation heterogeneity by developing regression models for each species, and by adapting the scaling process to the particular allometric characteristics of each species.

The scaling approach has three spatial scales: microscopic, tree, and plot. The microscopic scale was used to accurately measure tree sapwood depth by means of microscopical wood tissue analysis. Individual sapwood depth variations around the tree trunk were also observed and quantified. There were interspecific allometric differences showing that a tree's sapwood area does not always grow as the tree grows. At the plot scale, pure and mixed vascular vegetation plots of $60{\times}60m$ and $10{\times}10m$ were delimited. Plot's tree quantity and outside bark circumference at the breast height were recorded. LAI was measured using the Tracing Radiation and Architecture of Canopies (TRAC) and the LAI-2000 optical devices.

The results helped to generate the robust regression models. At the tree scale, regression models were fitted between sapwood depth and outside bark diameter at the breast height (DBH_{OB}) to later estimate tree and plot sapwood area. However, not all the models developed were linear relationships. Results for *Pinus banksiana, Pinus contorta*, and *Picea mariana* did not lead to linear relationships, while results for *Pop-*

ulus tremuloides and *Picea glauca* did provide strong linear relationships. These results prove that not all vascular species sapwood depth is directly proportional to their respective DBH_{OB}. Thus, two approaches to aggregate sapwood area to the plot scale were combined. The new combined approach drew strong linear correlations at the plot scale between sapwood area and leaf area. This last outcome conclusively proves the theory claiming a linear correlation between sapwood area and leaf area at different scales, where a lack of conclusive proof existed before.

The heat dissipation technique was used to collect diurnal tree sap flow and estimate transpiration using sapwood area as the scaling parameter. Single tree sap flow was aggregated to the plot scale using the plot's sapwood area estimates. Since vegetation transpiration rates vary among species, mixed forest transpiration is therefore influenced by vegetation heterogeneity. Thus, the internal plot's vegetation heterogeneity was included in the scaling approach. Additionally, tree sap flow radial variations were computed to provide a correction to in situ measurements. The final canopy transpiration estimates were compared with the canopy actual evapotranspiration which was estimated using the Penman-Monteith equation. Canopy transpiration was found to be a large proportion of the canopy's actual evapotranspiration, normally greater than the 50%.

This improved scaling approach includes the error propagation estimation, and showed that the error associated with a plot's leaf area estimate increases with the plot size. The error associated with tree and plot scale sapwood area estimates is practically null. These demonstrate that the error associated with the biometrics can be significantly minimized by using the most robust mensuration methods that currently exist.

Overall, the dissertation outcomes demonstrate that the use of robust methods and the careful formulation of the scaling approach were fundamental in obtaining reliable transpiration estimates. It is recommended that prior characterization of the intraspecific biometrics variations be made in order to develop an adequate scaling approach.

Acknowledgements

This work was financially supported by several organizations. I thank for helping me to accomplish this research The National Council of Science and Technology (CONACyT, Mexico), the Center for Environmental Engineering Research and Education (CEERE, U of C), the Metropolitan University (UAM, Mexico), Alberta Ingenuity, and the Department of Geomatics Engineering. I would like also to thank the Department of Biology and Dr. El-Sheimy for lending me the infrastructure needed to develop part of this research.

I would like to thank especially my supervisor, Dr. Caterina Valeo, for her constant encouragement, patience, valuable feedback, and confidence in all what I have done along this research. I will never find the words to express my gratitude to her. I feel quite lucky for having her as my supervisor. Her help and support will not be forgotten.

I would also like to thank my Supervisory Committee. To Dr. Naser El-Sheimy for his words of support when I started this research. To Dr. Darren Bender for his interesting feedback and suggestions. Thanks to both of them for giving me critical, but always valuable and kind comments during our meetings (thanks for your patience and for listening to my presentations).

I cannot forget to acknowledge the kindness and great help that I always received from the staff of the Kananaskis Field Stations (Barrier Lake facilities). Judy Buchanan-Mappin's help and provision of data was always outstanding and prompt, thanks so much! To Cindy Payne, Mike Mappin, Gary Wainwright, and David Billingham for their constant willing to help. To Ernst, for the great pastries he used to bake.

The field work was a challenging task and without the help of Dr. Valeo, Lynn Raaflaub (thanks for the songs! and the English pronunciation lectures), Angeles Men-

doza (gracias por las fotografías), and David McAllister, it could not be possible to accomplish this work. The four of them were great field mates. Valuable information for this research was collected by David McAllister (LAI measurements). Many thanks to Lynn Raaflaub for allowing me to use part of her $10 \times 10m$ plots data for my own research.

Thanks to Elena Rangelova, Rossen Grebenitcharsky, Alberto Nettel, and Tamara Renkas for their unselfish friendship and interesting discussions about our research. Also, I am deeply thankful to Sharon, and to Janet Gehring, whose insight and clever words helped me to overcome the tough times.

Finally, I would like to thank my family for their great love and support, especially to my siblings, Luis and Carolina, who are the light of my life. To my grandmother, Rebeca, who introduced me into the fascinating world of the books. To my parents, who have always supported me in all that I have done.

Contents

Abstract iii

Acknowledgements v

Contents vii

List of Tables x

List of Figures xiv

List of Symbols xviii

List of Acronyms xxvii

1 Introduction 1
- 1.1 Research objectives . . . 4
- 1.2 Dissertation layout . . . 5

2 Literature Review 8
- 2.1 Ecohydrology of forested areas . . . 8
- 2.2 Transpiration mensuration . . . 10
- 2.3 Velocity of sap flow . . . 11
  - 2.3.1 Radioisotopes and stable isotope tracers . . . 11
  - 2.3.2 Thermal techniques . . . 12
  - 2.3.3 Agreement between techniques . . . 18
- 2.4 Scaling transpiration by means of vegetation characteristics . . . 26
- 2.5 Evapotranspiration derived from remotely sensed data . . . 31
- 2.6 Observed gaps . . . 33

3 The Montane and Boreal forests experimental setup 37
- 3.1 The Montane forest study area . . . 37
  - 3.1.1 Vegetation type . . . 38
  - 3.1.2 Abiotic characteristics . . . 39

3.2 The Boreal forest study area . . . 40
3.2.1 Vegetation type . . . 40
3.2.2 Abiotic characteristics . . . 41
3.3 Equipment setup and data collection . . . 42
3.3.1 Meteorological Station, setup and collected data . . . 42
3.3.2 Thermal Dissipation sensors, field work logistics . . . 43
3.3.3 Soil moisture sensors . . . 45
3.3.4 Data control . . . 45

4 Sapwood area estimates 47
4.1 Introduction . . . 49
4.1.1 Estimation of sapwood depth and sapwood area . . . 49
4.2 Material and methods . . . 55
4.2.1 Injection of dye in situ . . . 55
4.2.2 Microscopical analysis of wood anatomy . . . 55
4.2.3 Visual tracing of the sapwood-heartwood edge by light transmission 57
4.2.4 Tracing boundaries by change in wood coloration . . . 58
4.2.5 Sapwood area calculation . . . 58
4.3 Results and analysis of results . . . 60
4.3.1 Plant material . . . 60
4.3.2 Injection of dye in situ . . . 61
4.3.3 Microscopical analysis of wood anatomy . . . 62
4.3.4 Comparison between methods to measure sapwood depth . . . 98
4.4 Discussion and Conclusions . . . 104
4.4.1 Future work . . . 106

5 Allometric correlations 107
5.1 Modelling SA_{plot}:LA_{plot} relationship . . . 108
5.1.1 Introduction . . . 108
5.1.2 Material and methods . . . 111
5.2 Results and analysis of results . . . 116
5.2.1 Tree scale allometric correlations . . . 116
5.2.2 Aggregation of sapwood area at the plot scale . . . 121
5.2.3 Plot scale allometric correlations . . . 126
5.2.4 Error propagation . . . 138
5.3 Discussion and Conclusions . . . 143

6 Scaling up transpiration 146
6.1 Material and methods . . . 147

6.2 Spatial scaling: Canopy Transpiration 149
6.3 Computing forest evapotranspiration 153
6.3.1 Actual evapotranspiration 153
6.3.2 Potential evapotranspiration 164
6.4 Computing canopy transpiration, modified Penman-Monteith equation 165
6.5 Results and analysis of results 169
6.5.1 Spatial scaling: Canopy transpiration 169
6.5.2 Forest evapotranspiration 174
6.5.3 Canopy transpiration, modified Penman-Monteith equation . . . 177
6.5.4 Agreement between methods 179
6.6 Discussion and Conclusions 183
6.7 Future work 186

7 General discussion and conclusions 187
7.1 Conclusions and novel contribution 190

8 Glossary 192

Appendices 194

A The process of evapotranspiration 194
A.0.1 Evaporation 194
A.0.2 Transpiration 195
A.1 Meteorological factors driving transpiration 198

B Angiosperms and Gymnosperms vascular structure 201

C Regression analyses 203

Bibliography 217

List of Tables

2.1 Summary of research comparing transpiration and evapotranspiration values at the canopy and catchment scales. 21

4.1 Tree species, their wood type, number of trees sampled (n) per each species in the different sites (Prince Albert National Park [PANP], Kananaskis country [KC], and Whitecourt[WC]). Maximum and minimum DBH_{OB} are reported in cm. 61

4.2 Specimen trees diameter and the depth at which the dye was dispersed. . . . 62

4.3 Basic statistics of the sd_{cp} values obtained from the Jack pine sample set (24 trees). Individual's DBH_{OB} ranges from 11.5cm to 23.9cm. 67

4.4 One-way ANOVA Jack pine sd_{cp} as a response of cardinal direction (i.e. repeated measurements, $\alpha = 0.05$). 69

4.5 Variance of Jack pine trees sd_{cp} variances (cm^4) with respect to DBH_{OB}. To keep consistency with the forest survey classification, here the DBH_{OB} classes are reported in inches. 70

4.6 Basic statistics of the sd_{cp} values obtained from the Lodgepole pine sample set. Individual's DBH_{OB} ranges from 16.5cm to 30.9cm. 73

4.7 One-way ANOVA Lodgepole pine sd_{cp} as a response of cardinal direction (i.e. repeated measurements, $\alpha = 0.05$). 75

4.8 One-way ANOVA between Lodgepole pine sd_{cp} and DBH_{OB}. The null hypothesis (H_o) tests the equality between the sd_{cp} and DBH_{OB} means, where sd_{cp} is the response value ($\alpha = 0.05$). 75

4.9 Computed $2\bar{sd}$ variance per SA_{LP} class and the variance of variances of the three classes. 77

4.10 Basic statistics of the sd_{cp} values obtained from the Trembling aspen sample set. Individual's CBH_{OB} ranges from 9.5cm to 38.2cm. 79

4.11 One-way ANOVA between Trembling aspen sd_{cp} and DBH_{OB}. The null hypothesis (H_o) tests the equality between the sd_{cp} and DBH_{OB} means, where sd_{cp} is the response value ($\alpha = 0.05$). 80

4.12 One-way ANOVA Trembling aspen sd_{cp} as a response of cardinal direction (i.e. repeated measurements, $\alpha = 0.05$). 81

4.13 Basic statistics of the sd_{cp} values obtained from the Black spruce sample set. Individual's DBH_{OB} ranges from $9.55cm$ to $37.88cm$. 85
4.14 One-way ANOVA between Black spruce sd_{cp} and DBH_{OB}. The null hypothesis (H_o) tests the equality between the sd_{cp} and DBH_{OB} means, where sd_{cp} is the response value ($\alpha = 0.05$). 86
4.15 One-way ANOVA Black spruce sd_{cp} as a response of cardinal direction (i.e. repeated measurements, $\alpha = 0.05$). 87
4.16 Variance of Black spruce trees sd_{cp} variances (cm^4) with respect DBH_{OB}. To keep consistency with the forest survey classification, here the DBH_{OB} classes are reported in inches. 88
4.17 Basic statistics of the sd_{cp} values obtained from the White spruce sample set. Individual's CBH_{OB} ranges from $11.5cm$ to $50cm$. 92
4.18 One-way ANOVA between White spruce sd_{cp} and DBH_{OB}. The null hypothesis (H_o) tests the equality between the sd_{cp} and DBH_{OB} means, where sd_{cp} is the response value ($\alpha = 0.05$). 93
4.19 One-way ANOVA White spruce sd_{cp} as a response of cardinal direction (i.e. repeated measurements, $\alpha = 0.05$). 94
4.20 Variance of White spruce trees sd_{cp} variances (cm^4)with respect DBH_{OB}. To keep consistency with the forest survey classification, here the DBH_{OB} classes are reported in inches. 95

5.1 Descriptive statistics of the $60 \times 60m$ plots located in the Sibbald areas of Kananaskis Country, Alberta, and Whitecourt [WC], Alberta. ΔSA_{plot} is the error on SA_{plot}. 124
5.2 Descriptive statistics of the $10 \times 10m$ plots located in the Sibbald areas of Kananaskis Country, Alberta. ΔSA_{plot} is the error on SA_{plot}. 125
5.3 Measured LAI_{eff} and LAI estimates for the plots located in Whitecourt, Alberta. Due to logistics, the LAI-2000 was used to obtain LAI estimates for these two sites. The rest of the plots' LAI values were measured with the TRAC optical device. 127
5.4 LAI and estimated LA_{plot} according to plot size for the Coniferous sites. ΔLA_{plot} is the error on LA_{plot} estimates (see § 5.2.4 for details.) 128
5.5 LAI and estimated LA_{plot} according to plot size for the Deciduous sites. ΔLA_{plot} is the error on LA_{plot} estimates (see § 5.2.4 for details). 128
5.6 Estimated sapwood area and their respective leaf area per plot. Results correspond to the Trembling aspen sites. The first two sites are of size $60 \times 60m$ while the last three are of $10 \times 10m$. ρ is the Pearson's correlation coefficient. 130

5.7 The two linear regression models fitted between SA_{plot} and LA_{plot} of Trembling aspen. SE is the model's Standard Error. 131
5.8 Estimated sapwood area and their respective leaf area per plot. Results correspond to the Coniferous sites. The first six sites are of size $10 \times 10m$ while the last four are of $60 \times 60m$. ρ is the Pearson's correlation coefficient ($\alpha = 0.05$). 134
5.9 The two linear regression models fitted between SA_{plot} and LA_{plot} of Coniferous sites. 135
5.10 Coniferous and Deciduous plots' SA_{plot}, LA_{plot}, and LAI 95% C.I. for their COVs by applying Payton's equation. 137

6.1 Steady parameters in the calculation of the aerodynamic resistance to heat and vapour transfer, r_a. All parameters are reported in meters, with exception of ς, which is unitless. 157
6.2 $\bar{F}_{sp}$ and $\bar{F}_{plot}$ at each site. The number of individuals used per plot (Ind. #) to estimate the mass flows and the number of days used to obtain the average values is shown in this table as well. 173
6.3 Penman-Monteith E_{a} and $\bar{E}_{\mathrm{a}}$ estimates during the same days that sap flow was measured at each site. $\bar{E}_{\mathrm{a}}$ is the average of the daily E_{a}. Field campaign 2004. 175
6.4 E_{p} estimates during the same days that sap flow was measured at each site. Field campaign 2004. 177
6.5 Modified Penman-Monteith T_{plant} estimates during the same days that sap flow was measured at the Coniferous site. T_{plant} is the summation of T_{shade} and T_{sun}. $\bar{T}_{plant}$ is the average of the daily T_{plant}. Field campaign 2004. . . 178
6.6 Modified Penman-Monteith T_{plant} estimates during the same days that sap flow was measured at the Deciduos site. Field campaign 2004. T_{plant} is the summation of T_{shade} and T_{sun}. $\bar{T}_{plant}$ is the average of the daily T_{plant}. Field campaign 2004. 178
6.7 Daily average of E_{a} and T_{plot} at the Coniferous (8 days average) and Deciduous (4 days average) sites. SA_{plot} was used as the unit ground area to estimate $\bar{T}_{plot}$. 180
6.8 Daily average of T_{plant} and T_{plot} at the Coniferous (8 days average) and Deciduous (4 days average) sites. SA_{plot} was used as the unit ground area to estimate $\bar{T}_{plot}$. 181
6.9 LA_{plot}, LA_{eff}, and site average canopy transpiration along eight days, Coniferous site. L-p is Lodgepole pine, W-s is White spruce. 182
6.10 LA_{plot}, LA_{eff}, and site average canopy transpiration along four days, Deciduous site. 182

C.1 Regression analysis, ANOVA, and unusual observations for the tree scale fitted linear regression model between $\bar{sd}$ and DBH_{OB} of White spruce. 204
C.2 Regression analysis, ANOVA, and unusual observations for the tree scale fitted linear regression between SA_{plot} and LA_{plot} of Trembling aspen. 207
C.3 Regression analysis, ANOVA, and unusual observations for the first fitted linear regression between SA_{plot} and LA_{plot} of Trembling aspen. 210
C.4 Regression analysis, ANOVA, and unusual observations for the second fitted linear regression between SA_{plot} and LA_{plot} of Trembling aspen. Observations from site "Deciduous-6" was removed to fit this model. 212
C.5 Regression analysis, ANOVA, and unusual observations for the fitted linear regression between SA_{plot} and LA_{plot} of the $10 \times 10m$ Coniferous sites. . . . 213
C.6 Regression analysis, ANOVA, and unusual observations for fitted linear regression between SA_{plot} and LA_{plot} of the Coniferous $60 \times 60m$ plots. 215

List of Figures

3.1 Meteorological station. Notice the trail of the Loop 1 at the back. 43
3.2 Installation of TDP sensors in a set of coniferous trees, site Conifer-4. 45
3.3 Installation of soil moisture sensors in the coniferous site Conifer-4. 46

4.1 Schematic representation of vascular tissues in a tree trunk cross section. . . 52
4.2 Transversal view of a tree trunk disk at the breast height. When a tree transverse cut (I) is flipped 90 deg (II), it gives a cross- sectional view of the wood structure. The tree's figure was modified from Farrar (2003). 59
4.3 Scanning electron micrographs of Jack and Lodgepole pine stems tissues. Notice the clogged resin canals (RC) in the Jack pine heartwood. The sapwood micrographs show the bordered pits (BP) between tracheids (Tr). 64
4.4 Scanning electron micrographs of Black and White spruce stems tissues. The sapwood micrographs for both species show open resin canals (RC) and bordered
pits (BP) between tracheids. Notice that the resin canals are clogged in the heartwood
tissues. The tracheids' walls look thicker as well. 65
4.5 Scanning electron micrographs of Trembling aspen stems tissues. On the right, micrographs are at a scale of $200\mu m$. Micrographs on the right are at higher magnification
($50\mu m$). The sapwood micrographs show the vessels (V) and fibers (F), and arrows show
the lateral pitting between vessels. The heartwood vessels (T) do not conduct sap
anymore since they are sealed by tyloses. 66
4.6 Dot plot of sd_{cp} values (cm) for the Jack pine sample set. Notice the wide spread of the data mostly for the South and East sides. 68
4.7 Jack pine sapwood depth per cardinal point (sd_{cp}) per each tree, versus its DBH_{OB}. Notice that two values are missing: one sd_E and one sd_W due to wood decay. 68
4.8 Jack pine sample set histogram of $2\bar{sd}$ values. 71

4.9 Jack pine sample set histogram of SA_{JP} values. 72
4.10 Bar graph showing values of SA_{JP}, DBH_{OB} and $2\bar{sd}$ register values for each Jack pine individual. Observe how much of the total DBH_{OB} length of each tree is sd_{cp} 72
4.11 Dot plot of sd_{cp} values (cm) for the Lodgepole pine sample set. Notice the wide spread of the data mostly for the North and East sides. 74
4.12 Sapwood depth per cardinal point (sd_{cp}) per each tree, versus its DBH_{OB} for Lodgepole pine. 76
4.13 Lodgepole pine sample set histogram of $2\bar{sd}$ values. 76
4.14 Lodgepole pine sample set histogram of SA_{LP} values. 78
4.15 Bar graph showing values of SA_{LP}, DBH_{OB} and $2\bar{sd}$ register values for each Lodgepole pine individual. 78
4.16 Dot plot of sd_{cp} values (cm) for the Trembling aspen sample set. Notice the wide spread of the data mostly for the South and East sides. 80
4.17 Sapwood depth per cardinal point (sd_{cp}) per each tree, versus its DBH_{OB} for Trembling aspen. 82
4.18 Trembling aspen sample set histogram of $2\bar{sd}$ values. 82
4.19 Trembling aspen sample set histogram of SA_{TA} values. 83
4.20 Bar graph showing values of SA_{TA}, DBH_{OB} and $2\bar{sd}$ values for each Trembling aspen individual. 84
4.21 Dot plot of sd_{cp} values (cm) for the Black spruce sample set. Notice the wide spread of the data mostly for the West and East sides. 86
4.22 Sapwood depth per cardinal point (sd_{cp}) per each Black spruce tree, versus its DBH_{OB}. Notice that two values are missing: one sd_E and two sd_W. Two values were not estimated due to wood decay and one sd_W was an outlier ($CBH_{OB} = 15.28cm$). 88
4.23 Black spruce sample set histogram of $2\bar{sd}$ values. 89
4.24 Black spruce sample set histogram of SA_{BS} values. 90
4.25 Bar graph showing values of SA_{BS}, DBH_{OB} and $2\bar{sd}$ values registered for each Black spruce individual. 91
4.26 Dot plot of sd_{cp} values (cm) for the White spruce sample set. In general, there is a wide spread of sd_{cp} in every cardinal point, being the largest at the East and West sides (Same as it occurs for the other three coniferous species). . . 93
4.27 Sapwood depth per cardinal point (sd_{cp}) per each White spruce tree, versus its DBH_{OB}. There are two missed sd_E values. One sd_E is missed since it was not possible to sample the individual in that side. The second sd_E value was dismissed due to wood decay. 95
4.28 White spruce sample set histogram of $2\bar{sd}$ values. 96

4.29 White spruce sample set histogram of SA_{WS} values. 97
4.30 Bar graph showing values of SA_{WS}, DBH_{OB} and $2\bar{sd}$ values register for each White spruce individual. 97
4.31 Plot of the paired response differences between sd_{cp} values obtained with the microscopical analysis and the translucence methods. White spruce sample set. Notice that five values are missing because they overlap. 99
4.32 Plot of the paired response differences between measured sapwood area with the microscopical analysis and the translucence methods. White spruce sample set. 100
4.33 Plot of the paired response differences between $\bar{sd}$ values obtained with the microscopical analysis and the translucence methods. Jack pine and Lodgepole pine sample set. 101
4.34 Plot of the paired response differences between sapwood area values obtained with the microscopical analysis and the translucence methods. Jack pine and Lodgepole pine sample set. 102
4.35 Measured sapwood depth paired difference between the microscopical analysis and the coloration methods. Trembling aspen wood cores of different DBH_{OB}. 103

5.1 Geographical location of Coniferous plots. The plots are in the Sibbald areas of Kananaskis Country. Contour lines were extracted from the Base Features GIS (AltaLIS, 2006), 1:20,000. Aspect was retrieved from the GEODE archive's Digital Elevation Models (100m grid, [MADGIC (2006)]). 114
5.2 Geographical location of Deciduous plots. The plots are in the Sibbald areas, South-East of Barrier Lake (Kananaskis Country). Contour lines and Hydrographic features were extracted from the Base Features GIS (AltaLIS, 2006), 1:20,000. Aspect was retrieved from the GEODE archive's Digital Elevation Models (100m grid, [MADGIC (2006)]). 115
5.3 Jack pine and Lodgepole pine $\bar{sd}$ in relation to DBH_{OB}. 117
5.4 Black spruce $\bar{sd}$ in relation to DBH_{OB}. 117
5.5 White spruce $\bar{sd}$ in relation to its DBH_{OB}. 119
5.6 Trembling aspen $\bar{sd}$ in relation to its DBH_{OB}. 120
5.7 The $10\times10m$ LAI values taken from East to West and from North to South. 130
5.8 Trembling aspen SA_{plot} in relation to LA_{plot}. 132
5.9 Plots of $60\times60m$. Deciduous Log(SA_{plot}) in relation to their Log(LA_{plot}) and the regression model's fitted line. Dotted lines are the 95% C.I. This Figure is intended to decrease the large difference among LA_{plot} values, and make clearer visualization of the $60\times60m$ regression model. 133

5.10 Conifers' SA_{plot} in relation to their LA_{plot}, and the regression model's fitted line. Plots of $10 \times 10m$. 136
5.11 Conifers' SA_{plot} in relation to their LA_{plot}, and the regression model's fitted line. Plots of $60 \times 60m$. 136
5.12 Plots of $60 \times 60m$. Conifers' $\text{Log}(SA_{plot})$ in relation to their $\text{Log}(LA_{plot})$ and the regression model's fitted line. Dotted lines are the 90% C.I. This figure is intended to decrease the large difference among LA_{plot} values, and make clearer visualization of the $60 \times 60m$ regression model. 137

6.1 Thermal Dissipation Sensors (TDP's) installed in a coniferous tree. 148
6.2 Same coniferous tree with the isolation material (upper part of the picture) ready to cover the sensors. 148
6.3 Typical understory spectral reflectance in KFS study sites during the summer of 2003. 163
6.4 Diurnal sap flow of a Lodgepole pine tree. Tree's $DBH_{OB} = 24\,cm$. Day of the year: 212, in 2004. 170
6.5 Diurnal sap flow of a Lodgepole pine tree. Tree's $DBH_{OB} = 17\,cm$. Day of the year: 216, in 2004. 170
6.6 Diurnal sap flow of a White spruce tree. Tree's $DBH_{OB} = 18\,cm$. Day of the year: 232, in 2004. 171
6.7 Diurnal sap flow of a White spruce tree. Tree's $DBH_{OB} = 32\,cm$. Day of the year: 232, in 2004. 171
6.8 Diurnal sap flow of a Trembling aspen tree. Tree's $DBH_{OB} = 31\,cm$. Day of the year: 228, in 2004. 172
6.9 Diurnal sap flow of a Trembling aspen tree. Tree's $DBH_{OB} = 15\,cm$. Day of the year: 228, in 2004. 172

A.1 The tree main physical phenomena involved in the transpiration process (modified from Dingman, 2002). 197

List of Symbols

English alphabet:

A_{plot}	Total surface area of a plot
B	Emittance of a single leaf
C	Multiple scattering of direct radiation parameter
CBH	Outside bark Circumference at the Breast Height
C_s	Sap heat capacity
D	Outside Bark Diameter at Breast Height (only used in equations)
DBH	Diameter at the Breast Height
DBH_{OB}	Outside Bark Diameter at Breast Height (in text)
DBH_{OB_i}	Outside Bark Diameter at Breast Height of the ith species
E_{a}	Actual forest evapotranspiration
$\bar{E}_{\mathrm{a}}$	Average actual forest evapotranspiration
ET	Evapotranspiration
E_p	Potential Evapotranspiration
F	Sap flow velocity SBH and THB techniques
F_0	Explained variation to unexplained variation ratio, used to determine the P-value, ANOVA
F_s	Single tree's sap mass flow
$\bar{F}_{plot}$	Plot's total sap mass flow
$\bar{F}_{sp}$	Average of the total sap mass flow of a group of individuals of a sp species
$\bar{F}_{sp_{\mathrm{i}}}$	Average sap mass flow of the ith species
G	Soil heat flux
H	Sensible heat transfer
$H_\circ$	Null Hypothesis
J_i	Single individual sap flow or sap flux density, HD technique

$\bar{J}_{sp}$	Average sap velocity or sap flux density of a species *sp*
K	In Chapter 2, Flux index (Granier's technique calibrated constant)
K	In Chapter 5, point estimate of COV
K_R	Empirical factor used to calculate g(R_s)
K_T	Optimum conductance temperature; empirical factor to calculate g(T_a)
K_{VPD}	Empirical factor used to calculate g(VPD)
K_θ	Empirical factor used to calculate g(θ_{sm})
L	Length (units)
LA	Leaf Area
LA_{eff}	Effective Leaf Area
LA_{plot}	Plot's Leaf Area
LA_{sp}	Leaf area of the species *sp*
LAI	Leaf Area Index
LAI_{eff}	Effective Leaf Area Index
LAI_{max}	Maximum LAI along the year
LAI_o	Leaf Area Index of the overstory
LAI_{shade}	LAI for shaded leaves
LAI_{sun}	LAI for sunlit leaves
LAI_u	Leaf Area Index of the understory
$\mathrm{NDVI_u}$	Understory NDVI
P	In Chapter 2, directed power, THB technique
P	In Chapter 6, mean atmospheric pressure
Q_h	Heater power, SHB technique
Q_r	Radial heat conduction, SHB technique
Q_s	Stored heat, SHB technique
Q_v	Vertical heat conduction, SHB technique
R	In Chapter 2, the electric resistance, HD technique
R	In Chapter 6, Specific gas constant ($287 Jkg^{-1}K^{-1}$)
RH	Relative Humidity
R_n	Net solar radiation
$R_{n,\,shade}$	Net solar radiation for shaded leaves
$R_{n,\,sun}$	Net solar radiation for sunlit leaves
R_{nl}	Net outgoing longwave solar radiation
$R_{nl,\,shade}$	Net outgoing longwave solar radiation, shaded leaves
$R_{nl,\,sun}$	Net outgoing longwave solar radiation, sunlit leaves

R_s	Shortwave solar radiation (i.e. global solar irradiation)
$R_{s,\,dif}$	Diffuse shortwave solar radiation
$R_{s,\,dif-under}$	Diffuse shortwave solar radiation under the overstory
$R_{s,\,dir}$	Direct shortwave solar radiation
$R_{s,\,shade}$	Shortwave solar radiation for shaded leaves
$R_{s,\,sun}$	Shortwave solar radiation for sunlit leaves
R^2	Coefficient of determination
R^2_{adj}	Adjusted coefficient of determination
R^2_{pred}	Coefficient of determination for predictions
S	In Chapter 2, Surficial area of heat interchange, HD technique
S	In Chapter 5, Standard deviation, Vangel's equation
SA	Cross-sectional sapwood area
SAI_{actual}	Sapwood area index (LA is the unit ground area)
SA_i	Cross-sectional sapwood area of the ith individual
SA_{BS}	Sapwood area of Black spruce individuals
SAI_{eff}	Sapwood area index (LA_{eff} is the unit ground area)
SA_{JP}	Sapwood area of Jack pine individuals
SA_{LP}	Sapwood area of Lodgepole pine individuals
SA_{plot}	Plot's sapwood area
SA'_{plot}	Plot's sapwood area estimate
SA_{sp}	Sapwood area of a species *sp*
$\overline{SA}_{sp}$	Average sapwood area of the species *sp*
SA_{TA}	Sapwood area of Trembling Aspen individuals
SA_{tree}	Single tree's sapwood area
SA_{WS}	Sapwood area of White spruce individuals
SC	Solar constant ($1367 Wm^{-2}$)
T	Probe temperature, HD technique
T_a	Air temperature
$\bar{T}_a$	Daily average air temperature
T_M	Maximum daily temperature
T_N	Minimum daily temperature
T_{plant}	Actual canopy transpiration, modified Penman-Monteith equation
$\bar{T}_{plant}$	Average actual canopy transpiration, modified Penman-Monteith equation
$\bar{T}_{plot}$	Average actual canopy transpiration
T_{shade}	Actual transpiration of shaded leaves

T_{sun}	Actual transpiration of sunlit leaves
T_v	Virtual temperature
T_∞	Sap temperature in the absence of heat, HD technique
V_h	Heat pulse velocity, HPV technique
VPD	Vapour pressure deficit
VPD_c	Threshold vapour pressure deficit
$\bar{X}$	Sample mean
X_d	Distance from the heater to the sap downstream, HPV technique
X_u	Distance from the heater to the sap upstream, HPV technique

Lowercases:

$a_\circ$	Calibrated polynomial coefficient to estimate e° as a function of T_a (Chebyshev procedure)
a_1	Calibrated polynomial coefficient to estimate e° as a function of T_a (Chebyshev procedure)
a_2	Calibrated polynomial coefficient to estimate e° as a function of T_a (Chebyshev procedure)
a_3	Calibrated polynomial coefficient to estimate e° as a function of T_a (Chebyshev procedure)
a_4	Calibrated polynomial coefficient to estimate e° as a function of T_a (Chebyshev procedure)
a_5	Calibrated polynomial coefficient to estimate e° as a function of T_a (Chebyshev procedure)
a_6	Calibrated polynomial coefficient to estimate e° as a function of T_a (Chebyshev procedure)
c_p	Specific heat of air at constant pressure ($1.010 kJ\, kg^{-1}\, ^\circ\mathrm{C}^{-1}$)
c_w	Specific heat of water
d	Zero-plane displacement
dT	Temperature difference inside the bark, THB technique
e_a	Actual vapour pressure
$\bar{e}_a$	Daily average actual vapour pressure
e°	Saturation vapour pressure

$f(x)$	Sap flow rate index
$\mathrm{g_c}$	Canopy conductance
$\mathrm{g_{c_{max}}}$	Maximum canopy conductance
$\mathrm{g_{env}}$	Minimum value of an environmental parameter reached at a specific time
h	Coefficient of heat transfer, HD technique
h_c	Canopy height
hd	Heartwood depth
$h_\circ$	Coefficient of heat transfer when sap flow is null, HD technique
i	Intensity of electrical current, HD technique
k	von Karman's constant (0.40)
m	Number of individuals of the same species in a single plot
n	Number of trees sampled at each site
n	In Chapter 4, sample size
n	In Chapter 6, number of species in a single plot
$\tilde{r}$	$R_s : SC \cos\theta$ ratio
r_a	Aerodynamic resistance to vapour and heat transfer
r_c	Bulk canopy resistance
$r_{c_{min}}$	Minimum canopy surface resistance
r_s	Stomatal resistance
s^2	Sample variance
sd	Sapwood depth
$sd_{microscopic}$	Sapwood depth measured with the microscopical analysis of wood tissue
$sd_{translucence}$	Sapwood depth measured with the translucence technique
$\bar{sd}$	Average sapwood depth
$\bar{sd}'$	Average sapwood depth estimate
$\bar{sd}_i$	Average sapwood depth of the ith species
$\bar{sd}_i{}'$	Average sapwood depth estimate of the ith species
sd_{cp}	Sapwood depth at each cardinal point
sd_E	An individual's sapwood depth at its East side
sd_N	An individual's sapwood depth at its North side
sd_S	An individual's sapwood depth at its South side
sd_W	An individual's sapwood depth at its West side
$t_\circ$	Time that takes to two thermosensors to gain equal temperature

tq	Trees quantity (i.e. number of trees inside a plot)
tq_A	Number of trees inside a plot of the species A
tq_B	Number of trees inside a plot of the species B
u_z	Wind speed at the height z
$u_\circ$	The wind speed at a reference height $z_\circ$
u_1	Lower bound of the coefficient of variation confidence interval
u_2	In Chapter 5, Upper bound of the coefficient of variation confidence interval
u_2	In Chapter 6, the wind speed at a height of $2m$
v_{max}	A tree maximum sap velocity, or maximum sap flux density
v_{0-3}	Sap velocity or sap flux density in the first $3cm$ of sapwood depth
$v_{0-\bar{sd}}$	Single individual sap flow or sap flux density (same as J_i)
w/v	Ratio of water per volume of certain chemical substance (i.e. safranin-O)
x	In Chapter 5, regressor parameter in linear regression models (independent variable)
x	In Chapter 6, depth at which sap flow is originally measured
x_o	Sapwood depth at which the maximum sap flow rate occurs
$\hat{y}$	Estimate of the true value y, linear regression model
$z_\circ$	Reference height at which wind speed is measured
z_{oh}	Roughness length for the heat transfer
z_{om}	Roughness length for the momentum
z_u	Height at which u_z is recorded

Greek alphabet:

Δ	In Chapter 6, the slope of the saturation vapour pressure curve
$\Delta\, A_{plot}$	Absolute error on A_{plot}
ΔDBH_{OB_i}	Absolute error on DBH_{OB_i}
ΔL	Absolute error on the length of the plot
ΔLA_{plot}	Absolute error on LA_{plot}
ΔLAI	Absolute error on LAI
Δn	Absolute error on n
ΔSA_{plot}	Absolute error on SA_{plot} estimates
$\Delta \overline{SA}_{sp}$	Absolute error on the SA average value of the species sp
ΔT	Temperature differences across a heated section, SHB and HD techniques
ΔT_m	Maximum temperature difference between probes, HD technique
$\Delta\, tq$	Absolute error on tq
$\Delta \bar{sd}'$	Absolute error on $\bar{sd_i}'$
$\Delta \bar{sd}'$	Absolute error on $\bar{sd}'$
χ^2	Chi square test
Ω_E	Overstory clumping index
Ω_u	Understory clumping index
α	In Chapter 2, Coefficient in Granier's final equation (i.e. 0.0206, or 119.01)
α	In Chapter 4 and 5, probability of type I error (significance level of a statistical test)
α	In Chapter 6, surface albedo value
α_l	Woody-to-total area ratio
α_L	Leaf scattering coefficient (0.25)
α_{sa}	Mean leaf-sun angle
β_0	Linear regression model intercept
β_1	Linear regression model slope
β^{-1}	Rate at which sap flow decreases towards the pith's trunk
γ	Psychrometric constant
γ_E	Needle-to-shoot area ratio

ϵ	Vapour ratio molecular weight (0.622)
ϵ_a	Emissivity of the atmosphere
ϵ_g	Emissivity of the ground
ϵ_o	Emissivity of the overstory
ϵ_u	Emissivity of the understory
θ	Solar zenith angle
θ_e	Fraction available of soil moisture for transpiration
θ_{fc}	Soil field capacity
θ_o	Overstory representative transmission zenith angle
θ_u	Understory representative transmission zenith angle
θ_{sm}	Volumetric soil moisture content
θ_{wp}	Soil wilting point
λ	Latent heat of vaporization ($2.45 \times 10^6 JKg^{-1}$)
λ_c	Heat loss coefficient at the measuring point, THB technique
λE	Latent heat of evapotranspiration (Appendix A)
λE_a	Latent heat of actual evapotranspiration
ν	Degrees of freedom (n-1)
π	The ratio of the circumference to the diameter of a circle (≈ 3.1416)
ϖ	Maximum sap flow rate expressed as a fraction (equals 1)
ρ	Pearson's product-moment correlation coefficient
ρ_a	Air density
ϱ	Fraction of temperature available for optimum canopy conductance
σ_{sb}	Stefan-Boltzmann constant ($5.675 \times 10^{-8} Jm^{-2} K^{-4} s^{-1}$)
ς	Empirical factor used to calculate z_{om}

Functions:

Σ	Summation sign
δ	Partial derivative
tan	Tan trigonometric function
$cos\,\bar{\theta}_u$	Transmission of diffuse radiant energy through the understory
$cos\,\bar{\theta}_o$	Transmission of diffuse radiant energy through the overstory
exp	Exponential function

Basic units:

cm	Centimetre
g	Gram
h	Hour
ha	Hectare
J	Joule
K	Kelvin degrees
kg	Kilogram
kPa	Kilo Pascal
MJ	Mega Joule
m	Metre
$mbar$	Millibar
mm	Millimetre
s	Second
W	Watts
°C	Celcius degrees

List of Acronyms

ANOVA	Analysis of Variance
ASCII	American Standard Code for Information Interchange
AVHRR	Advanced Very High Resolution Radiometer
BA	Basal Area
BEPS	Boreal Ecosystem Productivity Simulator
BP	Bordered pits
CBH	Outside Bark Circumference at the Breast Height
C.I.	Confidence Intervals
COV	Coefficient of Variation
C^{++}	High-level programming language
DBH	Diameter at Breast Height
DOY	Day Of the Year
EC	Eddy covariance method
ET	Evapotranspiration
F	Fibers (Wood tissue)
HD	Heat Dissipation (named also Thermal Dissipation)
HEWE	Human Enhanced Water Evapotranspiration
HFD	Heat Field Deformation
HPV	Heat Pulse Velocity
IPCC	Intergovernmental Panel on Climate Change
ILE	Instrument Limit of Error
KC	Kananaskis country
LA	Leaf Area
LAI	Leaf Area Index
Landsat-TM	Landsat-Thematic Mapper
MODIS	Moderate Resolution Imaging Spectroradiometer
NDVI	Normalized Difference Vegetation Index
PANP	Prince Albert National Park
PAR	Photosynthetic Active Radiation
PET	Potential Evapotranspiration
PM	Penman-Monteith equation

$PRESS$	Prediction Error Sum of Squares
RC	Resin canals
RS	Remotely Sensed (data)
SA	Cross-sectional sapwood area
SE	Standard Error
SHB	Stem Heat Balance
TD	Thermal Dissipation
TDP	Thermal Dissipation Probes
THB	Trunk Heat Balance
TRAC	Tracing Radiation and Architecture of Canopies
T	Heartwood vessels
Tr	Tracheids
V	Vessels
VPD	Vapour Pressure Deficit
WB	Water Balance
WC	Whitecourt

1 Introduction

The increment of greenhouse gas emissions due to human activities (e.g. deforestation, fossil fuels combustion) has created an enhanced greenhouse effect. As a consequence, the Earth's climate is changing and it is now crucial that we predict the environmental consequences or advantages of such a change. Most climate change predictions and the effects on biodiversity and natural resources are based on global models. Global model outcomes point to the increment of precipitation and air temperature as climate change indicators (Dias et al., 2002; IPCC, 2001). Still, the IPCC report (2001) stresses that the consequences (or inconsequences) of climate change might vary from region to region; however, the increment of evapotranspiration occurs worldwide (Dias et al., 2002; IPCC, 2001; Gedney and Valdes, 2000). Moreover, in forested regions the evapotranspiration rates could quickly rise due to the trees' physiological need to cool down (i.e. Human Enhanced Water Evapotranspiration [HEWE]). This can be implied since the vegetation of forested ecosystems is the main source of water removal by transpiration, which is normally considered a loss in the water budget for human use (Pimentel et al., 2004). At this point, there are already worldwide water shortages (consequences of overpopulation, human misuse of water and alteration of water balance due to climate change) that have left millions of human beings without even drinkable water (Pimentel et al., 2004).

Even though the global climate change models give plausible prognosis, they still carry uncertainty (IPCC, 2001); therefore, it would not be wise to use global models for predicting evapotranspiration changes at small scales or for environmental management purposes (e.g. water plan management). IPCC (2001) feels that reductions of global model uncertainty should be done by introducing new observational data. Also, in order to improve the global predictions, IPCC (2001) stressed the need to "understand and

characterise more completely dominant processes...in the atmosphere, biota, land...". Thus, natural processes at regional and local scales require in depth study to improve global predictions of climate change.

In the same context, while conducting spatially distributed estimates of evapotranspiration, Jones (1997) stressed that the determination of the appropriate ways to quantify the variation in the factors influencing evapotranspiration, as well as in evapotranspiration itself, "is one of the pressing research issues facing those who need to describe, understand and predict hydrologic and climatic systems especially at regional scales". Thus, it is evident that the quantification of forest evapotranspiration deserves researchers' attention due to first, its importance as a primary component of the water budget of any ecosystem; second, by its dependency to, and at the same time, influence on climate change; and finally by its influence on human water availability. The description and characterization of evapotranspiration at small scales is crucial for the adequate parameterization of global climate change modelling as well. Nonetheless evapotranspiration is a process worth studying because its better understanding, estimation and prediction benefits several fields. Among those fields are ecohydrology, hydrology, ecology, meteorology, agricultural and forest management, and urban planning.

Evapotranspiration accounts for loss of solid or liquid water that is evaporated to the atmosphere, and normally it is partitioned in two components: evaporation and transpiration. Appendix A defines in detail the concepts of evaporation and transpiration. The information in Appendix A will help the reader to become familiar with concepts that are the cornerstone of this research.

Evaporation and transpiration are complex processes to either measure or estimate at any spatial and temporal scale. However, transpiration mensuration is even more complex since spatial and temporal variations in transpiration are large and influenced by biological and meteorological factors. Specifically, the rate at which transpiration takes place is influenced by the spatial and temporal heterogeneity of vegetation type and its physiological functions, in addition to the variations in available energy and

water (Jones, 1997). During a detailed evaluation of studies determining patterns and organization in evapotranspiration, Hipps and Kustas (2000) concluded that the limitations for analysing and modeling evapotranspiration spatial variations are related to: 1) "capabilities of making accurate measurements of critical processes over appropriate scales", 2) "missing theoretical knowledge about processes" and 3) "scaling issues". These three constraints are interrelated and the adequate solution to the first will lead to adequate solutions to the others.

The capability to accurately measure transpiration over appropriate scales is related in first place to the accuracy in mensuration techniques. The use of rough mensuration techniques could carry considerable error estimates while scaling up (i.e. large error propagation). For instance, transpiration mensurations aggregated from trees to a plot scale (a delimited surface area whose vascular vegetation may be composed by individuals of a single vascular species, or more than one) normally differ from transpiration mensurations made at the latter scale. After studying the results of past research (e.g. Wilson et al., 2001; Bovard et al., 2005; Granier et al., 1990; Hogg et al., 1997; Cienciala et al., 1997; Granier et al., 1996; Zhang et al., 1997), differences between scaled and measured transpiration values can be attributed to the technique used to measure single point transpiration, and to the accuracy of the technique used to estimate plot scale transpiration (i.e. canopy transpiration), which normally includes for evapotranspiration and is not just transpiration per se.

At the tree scale, transpiration aggregated from a single point to the whole tree requires the estimation (or mensuration) of the trees' sapwood area to be used as the scaling factor. Sapwood area is complex to measure as well (Vertessy et al., 1997, 1995; Čermák and Nadezhdina, 1998); besides, most of the sapwood mensuration techniques are tree destructive. For these reasons, sapwood area is generally interpolated through linear models obtained from its relationship to other biometrics (e.g. Diameter at the Beast Height (DBH); Poyatos et al., 2005).

To aggregate transpiration from single trees to the canopy scale it is necessary to look for an adequate scaling factor. Past studies established as adequate scaling factor(s) the

plot's basal area (e.g. Whitehead, 1978), sapwood area (e.g. Nadezhdina et al., 2002; Waring et al., 1977; Marchand, 1984), leaf area (e.g. Vertessy et al., 1995, 1997), DBH (e.g. Poyatos et al., 2005; Vertessy et al., 1995), leaf area index (e.g. Poyatos et al., 2005; Vertessy et al., 1995), and solar equivalent leaf area (Čermák, 1989).

Along with the mensuration or estimation of scaling factors and the generation of models for biometric interpolation, there must be an error associated with the mensuration technique. Therefore, not only will the technique used to measure transpiration at a single point contribute to some error while scaling up, but there will also be uncertainty associated with the scaling factors. This does not mean that the techniques are inadequate; however, it is necessary to recognize the existence of uncertainty and look for a solution. Two ways to deal with the uncertainty coming from specific techniques are to estimate and report it, or to improve the technique. This should be a solid step to first improving transpiration estimates at small scales (i.e. tree scale), and second, to either diminishing or at least reporting the error that is propagated during the scaling up process.

1.1 Research objectives

Hence, the main aim of this research is to improve five Boreal species canopy transpiration estimates that are calculated through scaling up single trees transpiration by:

1. Creating robust allometric relationships between the chosen scaling parameters (i.e. sapwood depth, sapwood area, leaf area index, leaf area, and outside bark DBH).
2. Decreasing the uncertainty associated with the scaling parameters mensuration techniques, especially, for sapwood area mensuration.
3. Integrating vegetation heterogeneity during the scaling process.

Once the objectives above are met, the expected final outcome is a new, robust scaling approach that will considerably improve the final canopy transpiration estimates

of Lodgepole pine (*Pinus contorta* Dougl. ex Loud var. *latifolia* Engelm.), Jack pine (*Pinus banksiana* Lambert), White spruce (*Picea glauca* [Moench] Voss), Black spruce (*Picea mariana* [Miller] Britton Sterns, & Poggenburg), and Trembling aspen (*Populus tremuloides* Michx). Furthermore, this research should provide the sapwood area interspecific (between species) and intraspecific (between individuals of the same species) variations with respect to other biometrics such as outside bark DBH (DBH_{OB}) and sapwood depth. Finally, the new scaling approach reliability is validated by comparing the obtained canopy transpiration values with the outcomes of a robust, well known model, the Penman-Monteith equation.

Focus on those vascular species that are common to the Boreal and the Montane forests was of interest, because they not only live in both forests, but they are also part of the large transition zones between these two forests in the Western Canada (Peet, 1988). Thus, it is considered that the characterization of these species in terms of transpiration is a wide contribution to the ecohydrology of both the Boreal and the Montane forests. The chosen vascular species were Trembling aspen, Lodgepole pine, and White spruce. Two more species, Jack pine and Black spruce were of great interest due to their particular ecophysiology. Black spruce is considered the most opportunistic Boreal species with a great capacity to regenerate and to easily populate sites with poor environmental conditions. Jack pine, which is one of the dominant species in the Boreal forest, is not well known in terms of its physiological tolerances (Peet, 1988); thus, the study of its water requirements is a contribution at least to ecohydrology and ecophysiology. Section 3.2.1 describes the main ecological characteristics of Jack pine and Black spruce.

1.2 Dissertation layout

The above objectives are covered in six Chapters as follows:

Chapter 2 begins with a review of the transpiration dependency on vascular vegetation characteristics and questions the influence of each of them at different spatial

scales. This is followed by a detailed revision of actual techniques for measuring tree transpiration as well as observing their pros and cons. This chapter also includes a review of research that has compared scaled transpiration estimates with canopy evapotranspiration measurements. Here, the agreement between techniques and the possible causes for unsuccessful results were examined. Additionally, observations were made whether or not researchers reported the error associated with their estimates.

Chapter 3 is focused on the description of the study areas, their biotic and abiotic characteristics, and the studied vascular species main ecophysiological characteristics. In order to fulfill the dissertation objectives, a three year field data collection was conducted in three different sites: Prince Albert National Park, Saskatchewan; Whitecourt, Alberta; and Sibbald areas (Kananaskis Country), Alberta. Kananaskis country was the site used to aggregate trees' transpiration estimates to the canopy scale. Finally, this Chapter lists the type of collected data, and lists the equipment and the temporal resolutions used for data collection.

You will find that Chapters 4, 5, and 6 have a journal paper structure (i.e. introduction, material and methods, results and analysis of results, discussion and conclusions). Each one of these chapters has a detailed description of the applied methods. For that reason, there is no a single Chapter dedicated to "Material and Methods".

Chapter 4 Focuses on the improved mensuration of trees' sapwood depth, the analysis of each species sapwood depth relationship with two other parameters: DBH_{OB} and sapwood area. The results turned into a detailed description and statistical analysis of the intraspecific sapwood area variations as DBH_{OB} and sapwood depth change.

In **Chapter 5**, previous outcomes lead to the development of allometric correlations between the chosen scaling factors at two different scales: tree and plot. The latter correlations (plot scale) were modelled after developing a combined approach to aggregate scaling parameters from trees to plot. Here, error propagation was estimated (and reported) for each parameter that leads to the final canopy transpiration estimates.

Chapter 6 includes the validation of final canopy transpiration estimates (and therefore of the scaling approach). Firstly, canopy transpiration is computed for some of the

studied plots through in situ sap flow mensurations and a unit ground area. The Heat Dissipation (or Thermal Dissipation) method (Granier, 1985) was used to measure trees' sap flow. Here, just as a mere enquiry, different unit ground areas were used. Secondly, the actual forest evapotranspiration was computed using the well known Penman-Monteith equation. Recently suggested equations were used to incorporate the influence of understory and overstory leaf area on actual forest evapotranspiration.

Finally, **Chapter 7** gives a general discussion, draws overall conclusions, and lists the dissertation's novel contributions.

It is worth mentioning that every chapter begins with an outline giving the reader more detailed information of the chapter's structure and content.

2 Literature Review

Chapter Outline

In this study, it is of primary interest to analyse and mathematically state the spatial and temporal variation in vegetation type, function, and its influence on transpiration rates. Thus, the central point of this chapter focuses on a detailed review of previous works analysing and describing the close correlation between characteristics of vegetation and transpiration. There is also a review of the research work that scales up transpiration from a single tree to the canopy (i.e. stand or plot), catchment and regional scales. This review focuses on the reliability of the different methods used to estimate and scale up transpiration. Finally, there is an analysis of the vegetation characteristics used until now as scaling parameters and each method's variant. This chapter ends with a discussion of the uncertainty and constraints found in these previous works while scaling up transpiration, and a brief discussion of the importance of the present study.

2.1 Ecohydrology of forested areas

Recently, there has been more interest in understanding the links between vegetation and hydrological processes. In fact, it has been recognized that vegetation ecophysiology influences water uptake by plants (Elliot-Frisk, 1988), which is an important modifier of the water yield in forested areas. Consequently, this water uptake influences the available water for other ecological processes and human consumption. Additionally,

species type and age, soil characteristics, and meteorological conditions mingle with vegetation physiology creating different responses in transpiration rates at different spatio-temporal scales.

Moreover, due to differences in vegetation structure, each type of plant differs in its physiological process and therefore in the amount of water required for transpiration (Tyree, 1999). For instance, coniferous trees are less water demanding than deciduous trees because of their more conservative vascular structure and their tolerance to growth in xeric-mesic environments (Elliot-Frisk, 1988). At the same time, each tree's transpiration rates change according to the meteorological conditions, solar energy, and water availability (Veihmeyer and Hendrickson, 1950). This combination of physiological and meteorological factors generates spatio-temporal vegetation heterogeneity. Indeed, it is expected that the total transpiration of a forested area that holds mixed vegetation will be the integration of each tree's transpiration at a certain time and under specific meteorological conditions. Appendix A describes the meteorological parameters governing the evapotranspiration rates. It is suggested that the reader become familiar with these parameters as they will be constantly used in this and future chapters.

Leaf characteristics such as area, shape, orientation, and anatomy influence transpiration from the tree to the global scale (Köstner, 2001; Kramer, 1969). Leaves control transpiration rates through their stomata; and several authors have concluded that the main factor driving stomatal control is the vapour pressure deficit (Meinzer et al., 1993). At the tree scale, the leaves' major influence is normally summarized into the leaf area of the tree. At the canopy scale, the Leaf Area Index (LAI) has played an important role on indirectly estimating leaf area and correlating it to transpiration (see § 2.4). At this scale, other factors might influence the amount of water uptake, such as tree stand density (Cienciala et al., 2000), as well as the spatial location of vegetation into its habitat (Matlack, 1993). Hence, it is based on the spatial and temporal scales at which transpiration will be estimated or later scaled up that will define which vegetation characteristics should be measured and integrated into the equation.

To give an example, effects of forest fragmentation and forest edges are reflected in

the whole hydrological cycle. Vegetation that is found at the forest edges shows different transpiration and growth rates because water availability varies from the forest interior to its edges. Normally, trees found at the edges have access to that water accumulated in the clearings; besides the microclimatic conditions and solar radiation are different at the edges (Matlack, 1993). Thus, estimating water use without taking into account the edge and fragmentation effects on vegetation can bring some underestimations when aggregating to a whole catchment (Cienciala et al., 2002).

At the tree scale most of the actual transpiration mensuration methods require measuring the tree sapwood area to scale up sap flow from a single point to the entire tree. Here, the vegetation characteristic to be measured is already stated; however, it is now the mensuration method which will determine the uncertainty associated with the transpiration estimates. Thus, besides the careful determination of the vegetation characteristics to be used as scaling factor, it is necessary to carefully choose the adequate mensuration method. For that reason, the actual methods to measure transpiration in situ are described and discussed in the following section.

2.2 Transpiration mensuration

Some of the most recent compilations and analysis of the different methods to measure transpiration have been made by Swanson (1994), Kozlowski and Pallardy (1997), and Roberts (1999). The authors classified the methods by the type of techniques used and by the spatio-temporal scale at which transpiration is measured.

This section is a revision of the most common methods used to measure transpiration in terms of sap flow velocity, the pros and cons that several authors have reported for each method and their estimated accuracy, if it was reported.

2.3 Velocity of sap flow

As mentioned in § A.0.2, the velocity at which the sap ascends towards the leaves is determined by the rate of evaporation from the same leaves. Thus, measuring the rate at which sap travels along the tree trunk gives its rate of transpiration. Sap flow velocity is measured either by using radioisotopes and stable isotope tracers or by thermal techniques such as the heat pulse and heat balance methods.

2.3.1 Radioisotopes and stable isotope tracers

Although this technique was introduced fourteen years ago, few works have applied it (Waring and Roberts, 1979). The theoretical principle of the radioisotopes and stable isotopes tracers technique is based on the conservation of mass principle, the amount of mass concentration injected into the tree trunk equals the mass concentration transpired by the tree leaves.

The method consists of injecting a certain amount of a tracer into the tree trunk and measuring the rate at which the tracer concentration is transpired by the tree leaves. The total amount of evaporated tracer is related to sap flow by means of the conservation of mass equation. The method is explained in detail by Calder (1992). Two conditions should be met to accomplish the estimation of transpiration. First, the input of tracer must completely leave the tree to respect the law of mass conservation; and second, before the tracer travels along the tree and separates into the branches, it must completely mix at the trunk level.

The most commonly used tracer is deuterium oxide (D_2O). With this tracer, authors have reported that transpiration rates have showed good agreement between trees of the same species and diameter, with a standard mean error considered "adequate" for most hydrological studies (Calder et al., 1986). Calder (1992) stated that one of the method's constraints is the limitation to collect the transpired tracer from the leaves. Since the whole canopy cannot be sampled, some of the shoots are selected at different levels to collect the transpired tracer in plastic bags (transpired water and

tracer are trapped in the bag, causing condensation). Meinzer et al. (2006) believed that the radial diffusion of tracer causes a loss and the measured velocity of sap flow is an underestimation. Besides, the transpiration rates are measured at no less than a daily basis, which might become a constraint when finer time scales are needed. Still, the transpiration values obtained with this method have been found to be in good agreement with evapotranspiration values obtained, for instance, with the Penman-Monteith equation. The use of radioisotopes and stable isotopes tracers is an alternative method when the use of more demanding methods, in terms of input values, are not suitable, and also when the time-resolution required is daily or seasonally based.

2.3.2 Thermal techniques

As mentioned, there are two main thermal techniques, the heat pulse and the heat balance methods. These techniques are distinguished by the power characteristics used to warm up the sap, and of course, it makes a difference in the theoretical bases to estimate the sap flow velocity. The first attempts with the thermal techniques were in 1932, with Huber's heat pulse instrumentation published work (Swanson, 1994; Čermák et al., 2004). Early attempts at heat balance techniques were in the 1960's, but the first applicable method and instrumentation was in 1973 by Čermák et al.

Heat balance techniques.

The heat balance principle was described by Čermák et al. (1973). The theory is based on the conservation principles, and it states that a certain amount of heat injected into a tree trunk (and assuming that there will be no heat loss) equals the total heat transported upwards by the sap flow stream.

The heat balance techniques have instrumentation variants with invasive and non-invasive sensors and heaters; and the instruments are specific for certain sizes and sections of the plant. The most widely used techniques are Stem Heat Balance (SHB), developed by Sakuratani (1981); Trunk Heat Balance (THB) by Čermák et al. (1973);

Heat Dissipation (HD) by Granier (1985); and Heat Field Deformation (HFD) by Čermák et al. (2004). The heat balance techniques are quantitative and the outcome is the sap flux density over normally short periods of time. Swanson (1994) gives a detailed description of each technique.

Stem Heat Balance.

The SHB is mainly used in herbaceous plant stems, and consists of heating a vertical section of the tree trunk exterior and the sap velocity is measured by determining the changes in sap temperature between the heated and non-heated sections of the trunk. The sap flow velocity F $[gs^{-1}]$ is determined by:

$$F = \frac{Q_h - Q_r - Q_v - Q_s}{C_s \Delta T} \tag{2.1}$$

which is the ratio of the differences between the heat fluxes and the changes in the power heat. The heat fluxes account for the heater power Q_h, the radial heat conduction Q_r, the vertical heat conduction Q_v, and the stored heat Q_s. The changes in power heat are estimated by multiplying the specific heat capacity of the sap (C_s) by the temperature differences across the heated section (ΔT).

The use of the SHB method is restricted to certain trees because they are specific for certain tree diameters and also requires stem invasion (Dugas, 1990). Steinberg (1988) concluded that SHB worked adequately under the conditions consistent with the physical principles by which it is governed.

Trunk Heat Balance.

The THB technique is useful for tree trunks of large diameter ($DBH_{OB} > 0.1m$). Main characteristics of the technique is the internal heating and sensing of sap temperature changes (invasive instrumentation). Its particular characteristic is that it follows the compensation principle; that is, the temperature difference inside the bark (dT) is kept

constant by varying the power source, or vice versa. The heat balance of a specific space in the trunk is given by:

$$P = FdTc_w + dT\lambda_c \tag{2.2}$$

where P is the directed power (Watts, [W]), F is the sap flow rate $[kgs^{-1}]$, dT is the temperature difference inside the bark at the measuring point (K), c_w is the specific heat of water $[Jkg^{-1}K^{-1}]$, and λ_c is the heat loss coefficient from the measuring point $[WK^{-1}]$. λ_c is an adjustable variable, and sometimes is considered negligible and eliminated from the equation (Čermák et al., 2004).

According to Dugas (1990), the THB technique effectively measures changes in F. The technique does not need a previous calibration. Some of the drawbacks of the technique is the type of instrumentation needed (complex) and the power for internal heating.

Heat Field Deformation.

The technique was first presented in 1998 by Nadezhdina in an International Workshop on Measuring sap flow in intact plants. The technique's description given here is based on Čermák et al. (2004). The basics of this technique is that it measures the "deformations" on the field heated around a small heater. The sap flow is a function of a series of constant values that consider the geometry of the measuring point, the stem heat conductivity and specific heat of water besides the ratio between the axial and tangential gradients of temperature around the heater. The method is suggested for modelling radial sap flow in large vascular trees, which requires the correction of the distances between the different thermocouple pairs. A detailed explanation of the methodology is found in Čermák et al. (2004). The technique is still new and Čermák et al. felt that its theoretical analysis needs greater explanation before it can be said that the method is complete.

Heat Dissipation.

Granier (1985) proposed a slightly different thermal balance approach, the heat dissipation (HD) technique. The instrumentation is invasive and consists of two probes of 2mm in diameter, and 20mm in length and a parallel separation of 5cm (original instrument). The upper probe has a thermosensor and a heater while the lower probe has a thermosensor. The heater provides a constant heating power, and the thermosensors are used to measure the temperature difference (ΔT) between the two probes. In theory, the amount of heat provided must equal the amount of heat dissipated by the sap flux (Granier, 1985). Originally, the theory is mathematically represented by:

$$hS(T - T_{\infty}) = R\mathrm{i}^{\,2} \tag{2.3}$$

were h is the coefficient of heat transfer $[Wm^{-2}\ {}^{\circ}C^{-1}]$, S is the surficial area of interchange $[m^2]$, T is the probe temperature $[^{\circ}C]$, T_{∞} is the sap temperature in the absence of heat $[^{\circ}C]$, R is the electric resistance [ohms] and i is the intensity of electrical current [amps].

The coefficient of heat transfer is a function of the velocity of sap flow and the heat transfer coefficient when the sap flow is null $h_{\circ}$.

In theory, when the sap flow is constant, Granier assumed that the sap's velocity is:

$$J_i = \frac{1}{\alpha}\left[\frac{\Delta T_m - \Delta T}{\Delta T}\right] \tag{2.4}$$

where ΔT_m is the maximum temperature difference given when the sap flow is null (i.e. $J_i = 0$), ΔT is the difference in temperature between the two probes at a specific time. The ratio between the temperature differences becomes the calibrated constant K (flux index) in Granier's technique. With a sample size of 53 trees of three different species and diameters, Granier determined that the flux index has an exponential

relationship with the velocity of sap flow:

$$K = 0.0206 J_i{}^{0.8124} \tag{2.5}$$

with a $R^2 = 0.96$, and units of J_i are $10^{-6} m s^{-1}$. J_i is expressed in the same way as sap flux density, that is, flow rate of sap volume per unit of sapwood area (i.e. $10^{-6} m^3_{sap}\, m^2_{SA}\, s^{-1}$). Substituting K into Equation (2.5) by Equation (2.4), and considering the α term independent of the experimentation the sap flow velocity is estimated by:

$$J_i = 0.0119 \left[\frac{\Delta T_m - \Delta T}{\Delta T} \right]^{1.231} \tag{2.6}$$

where J_i is in units of $cm s^{-1}$ (or $cm^3_{sap}\, cm^2_{SA}\, s^{-1}$). Granier validated his results with the Penman equation outcomes, finding a good agreement between both set of results (of course, Penman estimates were greater than the ones obtained with the Granier method). The studied species were Douglas fir (*Pseudotsuga menziesii*), European black pine (*Pinus nigra*), and Oak tree (*Quercus pedunculata*). The velocity of sap flow is converted into total trunk's mass flow (F_s, $[cm^3 s^{-1}]$) by scaling from the point of measurement to the total sapwood cross-sectional area (SA, $[cm^2]$):

$$F_s = SA J_i \tag{2.7}$$

Advantages of the HD technique is the obtention of sap flow values at a very low time resolution (seconds if needed). The HD probes are very sensitive and are able to record slight changes in temperature, which finally correspond to changes in sap flow. If SA is known, transpiration for the entire tree can be estimated.

The estimation of ΔT_m by assuming that the maximum temperature is reached when

J_i is null has been questioned (Green et al., 1989), since a null sap flow could be observed when meteorological conditions change drastically, mainly the vapour pressure deficit. However, the problem occurs when there is not enough data to observe the diurnal response together with meteorological data and decide whether the high temperature value corresponds to a null sap flow or a drastic change in meteorological conditions (i.e. vapour pressure deficit is high or very low).

The use of HD instrumentation is relatively simple; however, to maintain and provide the constant heat, a large amount of power is needed. Moreover, the instrumentation is invasive and may damage the sampled trees if they are not adequately treated after sampling (e.g. seal the holes).

According to Hogg et al. (1997) sap flow readings may be influenced by the tree's response to nightly vapour pressure deficits and the tree's water storage capacity.

Dynamax Inc. commercialized the HD instrumentation and named it Thermal Dissipation Probes (TDP), providing choices for trees of different diameters. TDP are known for their accurate estimations of sap flow in single trees (Schulze et al., 1985; Samson, 2001) without requiring an empirical calibration factor. Two important advantages are that it is possible to measure the transpiration of a single tree in mixed forests, and that the sap flow patterns of different tree species can be described for different diameters. The main constraint in the estimation of transpiration for a single tree is the differentiation and quantification of the sapwood area for including the radial variation of sap flow and for scaling purposes.

Heat Pulse Velocity technique.

The Heat Pulse Velocity (HPV) technique is based on the conservation principle as well. With this technique, the velocity of sap flow is measured by estimating the period of time in which a heat pulse moves away by convection from the heated point in the trunk. This technique is based on maintaining a constant temperature along the stem by varying the heating power (i.e. compensation principle). A detailed explanation of the theory and the equipment characteristics is given by Swanson (1994) and Čermák

et al. (1976).

The instrumentation is invasive and consists of a set of two thermosensors and a heater. The heater is placed between the two thermosensors. The distance between the heater and the upper thermosensor is normally smaller than between the heater and the lower thermosensor.

The heat pulse velocity is estimated by:

$$V_h = \frac{X_d - X_u}{2t_\circ} \tag{2.8}$$

where X_d and X_u are the distances from the heater to the downstream and upstream thermosensors, $t_\circ$ is the time that it takes the two sensors to gain an equal temperature after a heat pulse has been released.

There are some important drawbacks of the HPV technique that should be kept in mind. The HPV does not differentiate between sap flow in the early-wood and the one that occurs in the late-wood (Granier et al., 1994). The conversion of sap heat pulse velocity, which is the measured value, requires a conversion factor to estimate the velocity of sap flow. This conversion factor is species-specific.

2.3.3 Agreement between techniques

Transpiration is complex to measure and there is no single method that can determine the actual transpiration at multiple scales (single tree, canopy, catchment or region). Some methods have been claimed as more accurate and reliable than others. And, as normally happens with environmental variables, the true transpiration value is rarely known, and the only way to observe the reliability of each method is by comparing results between the different methods.

In order to scale up sap flux density to whole stands, it is very common to estimate the sap flux density in a representative stand sample. The sample can be chosen by observing the tree size histogram and selecting at least one tree of each size for sap flow

mensuration. Another approach is to choose trees that are evenly distributed along the stand in order to take into account the dominance of trees' canopy. Moreover, in fragmented areas, the trees that are close to open areas have normally larger transpiration rates. Thus, for transpiration estimates of fragmented areas, transition zones, or areas close to clearings, it is necessary to sample trees at the stand's edges as well.

To estimate the sap flux density of the stand, most authors are prone to estimate a stand average sap flux density. Čermák et al. (1995) argued that only stand's mean sap flux density is comparable to evapotranspiration values, such as the Potential Evapotranspiration (PET).

Some authors have chosen to compare transpiration estimates with evapotranspiration values obtained with well recognized techniques such as the eddy correlation (i.e. eddy covariance, [EC]) method, or the Penman-Monteith equation. The differences between values change from region to region, and they are a function of vegetation type, density, health and heterogeneity. For instance, in dense forested areas, transpiration is considered the largest proportion of total evapotranspiration; the rest is soil or water surface evaporation. Thus, one is expected to observe a slightly larger evapotranspiration value than transpiration. Table 2.1 gives a summary of some of the research comparing transpiration values obtained with different techniques.

Granier (1985) validated his HD technique by comparing the evapotranspiration obtained with the Penman equation. Granier found good agreement between both sets of results, and reported that the largest differences between them were when the environment reached a dew point, or the trees were close to open areas.

Hogg et al. (1997) compared the HD and HPV transpiration values with eddy water vapour fluxes above the canopy of a Trembling aspen (*Populus tremuloides*) stand. Hogg et al. found a significant difference between absolute transpiration estimates. Authors concluded that Trembling aspen physiological characteristics influenced the relationship between tree scale and canopy scale transpiration values.

Granier et al. (1990) compared HD transpiration with the stand's PET obtained with the Penman equation and the total water vapour flux from the eddy correlation.

Studies were conducted in a Maritime pine (*Pinus pinastra*) of low tree density. Stand transpiration results are 55% of PET obtained with the Penman equation and 70% of total water vapour flux (measured by the EC technique). Granier et al. considered that there was a low interspecific transpiration variability due to the low tree density of the stand which allowed each canopy tree to have a full cover of sunlight. Another interesting observation is the influence of microtopography in tree transpiration, being larger in trees located in the higher (in elevation) part of the stand.

Cienciala et al. (1997) estimated the HPV transpiration of coniferous mixed stands with different ages. Transpiration HPV results were lower than those of eddy fluxes. Authors felt that the transpiration values were incomparable; however, there was an acceptable correlation between EC and HPV transpiration. What it is noticeable and obvious is that HPV stand transpiration was lower that the actual fluxes of EC. In cases in which HPV transpiration was higher than EC values, Cienciala et al. felt that there was a footprint influence on the EC fluxes.

Granier et al. (1996) reported that HPV transpiration rates were 75% of PET in a mixed stand of 8 different species in the rain forest. On the contrary, Čermák et al. (1995) obtained THB transpiration values were a minimum fraction of PET (e.g. 0.07% for spruce trees) in mixed stands of Scots pine (*Pinus sylvestris*) and Norway spruce (*Picea abies*). The large discrepancy between values was not discussed.

Bovard et al. (2005) reported that HD stand transpiration estimates were in closer agreement with EC evapotranspiration during small water vapour fluxes. When water vapour fluxes increased, HD transpiration estimates were lower than EC evapotranspiration values.

Granier et al. (2000) compared HD transpiration estimates with EC water vapour fluxes in stands dominated by Beech (*Fagus sylvatica*), finding a high linear correlation between HD and EC outcomes during a drought period ($R^2 = 77.0\%$). Like the rest of the previous research, Granier et al. obtained smaller daily transpiration values from the HD technique than the daily water vapour fluxes coming from the EC measurements. Barbour et al. (2005) reported that HD sap flow was 51% and 22% of the total EC

Table 2.1: Summary of research comparing transpiration and evapotranspiration values at the canopy and catchment scales.

Techniques	**Tree species**	**Scale**	**Agreement**	**Author, year**
EC HD HPV	*Populus tremuloides*	Canopy	$HD \neq EC$ $HPV \neq EC$	Hogg et al. 1997
HD EC PET (Penman)	*Pinus pinaster*	Canopy	$0.70EC$ 0.55PET	Granier et al. 1990
HPV EC	*Pinus sylvestris* *Picea abies*	Canopy	$HPV < EC$	Cienciala et al. 1997
HD PET (Penman)	Mixed rain forest, 8 species	Canopy	0.75PET	Granier et al. 1996
HD EC Water balance (WB)	*Quercus montana* *Quercus alba* *Nyssa sylvatica* *Acer rubrum*	Canopy	$HD \approx EC$ $HD \approx WB$	Wilson et al. 2001

Table 2.1: Summary of research comparing transpiration and evapotranspiration values at the canopy and catchment scales (cont.).

Techniques	**Tree species**	**Scale**	**Agreement**	**Author, year**
HD EC Water balance (WB)	*Quercus montana* *Quercus alba* *Nyssa sylvatica* *Acer rubrum*	Catchment	$HD \neq EC$ $HD \neq WB$	Wilson et al. 2001
HD EC	*Quercus montana* *Quercus alba* *Nyssa sylvatica* *Acer rubrum*	Canopy	$HD \neq EC$	Wilson et al. 2001
HD EC	*Pinus grandidentata* *A. rubrum* *B. papyrifera* *Quercus rubra*	Canopy	$HD \approx EC$ and $HD < EC$	Bovard et al. 2005
HD EC	*Dacrydium cupressinum*	Canopy	$HD = 0.51EC$ and $HD = 0.22EC$	Barbour and Whitehead 2003

during days with no rainfall and with rainfall, respectively.

Other common comparisons are between techniques that only account for transpiration. Granier et al. (1994) compared three techniques, water absorption, HPV, and TDP. The HPV and TDP transpiration estimates showed a good agreement, and the diurnal transpiration trends obtained with both techniques were similar. Contrary to what it is normally expected, the TDP results were slightly higher than the HPV ones. The water absorption method underestimated the sap flow values with respect to the TDP method, however, it was felt by the authors to be a good approximation to transpiration estimates. In the same work, Granier et al. introduced the water absorption technique, which consists of attaching a Mariotte system to the tree trunk and is filled with a safranin solution that is absorbed by the tree through previously drilled holes. The technique was more useful in determining sap flow pathway than velocity. It is well known that once the tree trunk is chiseled to expose the sapwood, the pressure gradients are altered and consequently the sap flow changes as well.

Čermák et al. (2004) made a detailed comparison of THB and HFD techniques based on previous results obtained by different authors. Čermák et al. found that THB's outcomes are considered reliable and thus it is commonly used as a standard to examine the results of other techniques. The main constraint with the THB is its weakness in estimating the sap flow at very low rates in ring-porous trees. Unlike the THB, the HFD technique is considered "extremely sensitive" to the sap flowing at very low rates. Studies comparing HFD transpiration results with other techniques results have demonstrated that the method could be reliable enough once the validation is completed.

Zhang et al. (1997) compared values of *Populus* transpiration estimated by means of two different methods: the sap flow mensuration and the Penman-Monteith (PM) equation. The latter equation was modified to obtain transpiration estimations for a whole tree, by integrating the leaf area parameter. Another important modification to the combination equation was to the net solar radiation R_n term (see Appendix A for a detailed definition of the term), which was needed for a single tree. Mensuration of sap flow was performed using the heat balance method. Sap flow values were scaled up

by means of an average leaf area value and the number of branches present in a specific layer (upper, middle or lower). Transpiration rates obtained with the sap flow method and the PM equation (using the stomatal conductance average value) were very similar for about 66% of the time they conducted the experiment. Authors found that even if there was a good agreement between estimates obtained with both methods, they suggested care in using the modified PM equation, since it considers the environmental conditions to be the same for each leaf in the tree. This assumption of homogeneity is not quite correct because there exists a gradient of climatic parameters across the canopy that normally decreases from the outermost to the innermost part of the canopy (e.g. solar radiation decreases as it passes through the canopy crown).

In forested areas, values of transpiration and evapotranspiration at larger spatio-temporal scales are even more similar. In fact, Wilson et al. (2001) concluded that evaporation was a not significant fraction of the annual evapotranspiration process in a forested catchment. Wilson et al. compared the soil water budget, HD, EC, and catchment water balance techniques on a daily and annual basis. In an annual basis, the EC and the catchment water balance were comparable. In a daily basis, authors found a significant linear correlation between EC and HD transpiration outcomes.

Intraspecific and interspecific variability on sap flow velocity is given by each individual's particular anatomy, species characteristics and environmental conditions. Such variability will be reflected while aggregating transpiration to the canopy scale. Besides, the carefulness and experience applying the technique to measure sap flow influences the final estimates at the tree level and determines the propagated uncertainty while scaling up. The literature has indicated the main sources of error in sap flow techniques (Nadezhdina et al., 2002; Dugas, 1990; Swanson, 1994); and therefore, new projects should take these into account to avoid large sources of error. In some cases, it should be even possible to suggest new methods in which those errors are decreased to their minimum.

The estimation of a tree transpiration rates using the TDP technique carries errors from two main sources. Firstly, the estimation of the tree's water storage capacity; and

secondly, the fact that sap flow radially varies around the tree trunk. As mentioned, the water storage capacity can be estimated by knowing a whole day-night sap flow pattern. Several authors have estimated the water storage capacity of a tree using different approaches (e.g. Hogg et al., 1997; Goldstein et al., 1998; Kumagai et al., 2004; Loustau et al., 1996). These authors have concluded that the water storage capacity is a negligible fraction and does not influence transpiration estimates at larger scales. Although the conclusions might direct us to dismiss the estimation of water storage capacity, it is important to acknowledge that these conclusions are site and species-specific. Thus, for scaling purposes, it is still necessary to assess the influence of the water storage capacity of the species present at the study area (Phillips et al., 1996).

The sap flow variability around a tree's trunk should be accounted for scaling purposes as well. Most approaches have measured sap flow in different points around the tree, and at different depths (Granier et al., 1994; Phillips et al., 1996; Nadezhdina et al., 2002). The constraint by measuring sap flow at different depths is that not one of the thermal techniques are sensitive enough to determine the boundary between the sapwood and heartwood (i.e. sapwood depth), and some radial flow and moisture transfer between sapwood and heartwood can be confounded with transversal sap flow. These radial variations in sap flow are related to the species vascular structure, specifically the radial distribution and length of sapwood depth around the tree circumference (Nadezhdina et al., 2002; Čermák and Nadezhdina, 1998). Thus, the influence of a single tree's sapwood depth variability on estimating sap flow velocity should be acknowledged. The key point for most of the thermal techniques is that the accurate mensuration of sapwood depth or sapwood area is required to take into account the sap flow radial pattern. Obtaining accurate measurements of sapwood depth and therefore sapwood area, will help to better understand the mass flow variations due to tree size (Oren et al., 1999). In Chapter 4 this problem is addressed by using proper sapwood depth measurements around each tree trunk.

Once these two main constraints for accurately measuring sapwood depth are addressed, the scaling process depends on finding the adequate scaling parameter(s) at

larger scales than a tree. The handful of approaches for scaling up transpiration suggests that the estimation of a scaling parameter is complex and time consuming. Hence, most of the studies look for simpler methods to finally obtain rough transpiration estimates at the canopy scale without reporting the uncertainty associated with the scaling process. As it has been described in this chapter, the most common way to observe the accuracy of transpiration estimates is by comparing results with measured or modelled evapotranspiration estimates.

The variability and sources of errors using the HD technique can be accounted for by measuring sap flow in a representative sample of the plot under study. For instance, Kumagai et al. (2005) studied the intraspecific and radial sap flow variations in a stand of Japanese cedar (*Cryptomeria japonica*), concluding that the intraspecific sap flow variation is more significant than the radial sap flow variation for scaling purposes. Still sap flow radial variation has been of some concern arguing that the use of TDP thermocouples does not account for radial variation (James et al., 2002). As mentioned, the radial variation is given by the sapwood depth variation; thus, once the sapwood variation is known, the TDP technique becomes a reliable source of sap flow velocity measurements.

2.4 Scaling transpiration by means of vegetation characteristics

There have been many approaches for estimating transpiration at different scales. The difference between them is the input parameters and the weight given to them. Most of these approaches are based on the influence of vegetation characteristics on transpiration rates. At the tree scale, sapwood area coupled with leaf anatomy can determine the capacity of a tree to hold and transport specific amounts of water. At the canopy scale, transpiration is influenced by leaf area, leaf anatomy, basal area, species composition, stand density and canopy aerodynamic roughness (Schipka et al., 2005).

Scaling transpiration from a single tree to a whole stand has been attempted from

using single quantities of tree diameters to allometric correlations and remotely sensed data. DBH is commonly used as a scaling parameter because of its close relationship with sapwood area. In theory, sapwood area increases as the DBH increases as well. In addition to this theory, some power functions have been developed based on a parallel theory establishing that sap flow increases with DBH (e.g. Marc and Robinson, 2004; Calder, 1992).

Authors have used basal area as scaling factor even if basal area accounts not only for the sapwood area but the non active part of the tree, the heartwood. However, it seems that basal area correlates well with transpiration values at the tree scale. Čermák et al. (1995) concluded that basal area is an easy anatomical characteristic for measuring in situ, and Cienciala et al. (1997) felt that basal area is a suitable scaling factor when there is a large variability in sap flow velocity between trees of different stands. The same method was applied by Jiménez et al. (1996) in a Mediterranean forest of *Laurus azorica* (Laurel trees), finding that the correlation between sap flow and basal area was exponential and just 5% of the sap flow variability was not explained by the basal area. Using the exponential model, Jiménez et al. scaled up single tree sap flow mensurations to the stand scale. One interesting conclusion in Jiménez et al. is that the Laurel forest total transpiration accounted for just 65% of the PET, which addresses the transpiration differences between cold, dry forests (such as the Boreal forest) and humid, tropical forests. The lower transpiration rates in the Mediterranean forest may be related to the stomatal control against large water loss in hot environments.

The sapwood area estimates of a whole stand are used to scale up transpiration from single trees. Hogg et al. (1997) determined a stand's sapwood area as the product of the stand's basal area and the fraction of sapwood area present in the basal area. The fraction of sapwood area was estimated from a set of 16 wood increment cores where the sapwood depth was stained with methyl blue. As mentioned before, Hogg et al. stand transpiration values demonstrated a lack of consistency between the three methods used. One of the reasons, besides the ones mentioned by the authors, may be that the sapwood area estimates were a general approximation to the real value.

Cienciala et al. (2000) used a linear correlation between each tree's sapwood area and its mean daily sap flow value. The fitted linear regressions gave large coefficients of determination (74% and 82%) for the two studied stands of *Acacia mangius*. Authors observed that the rate of increment of the two linear models (represented by the slope) were similar and concluded that sapwood area was a robust scaling parameter independent of the stands' tree density. In the same manner, authors studied the effectiveness of basal area to scale up, and they found discrepancies between the fitted models for both stands.

Other attempts for scaling up transpiration used either average transpiration or average sapwood area (Oren et al., 1998, 1999). Granier et al. (1990) used sapwood area as a scaling factor and calculated a Maritime pine (*Pinus pinaster*) stand's transpiration as the product of the fraction of mean sap flow velocity at a specific tree class and the stand's sapwood area. Authors did not specify how the tree classes were arranged. When Granier et al. compared transpiration results with PET from Penman equation and total vapour flux from eddy correlation, they found a reasonable agreement, which implied that their scaling factor and use of mean sap flow velocity values were adequate.

Poyatos et al. (2005) estimated canopy transpiration in a forested area by multiplying individual sap fluxes by the total sapwood area of each stand. Poyatos et al. adjusted a logarithmic equation that relates canopy transpiration to PET estimated with the Penman-Monteith equation. In that way, Poyatos et al. took into account the influence of stomatal control and therefore the influence of vapour pressure deficit into the transpiration process. The logarithmic equation was considered as an acceptable approach to scale up transpiration to the canopy scale. Based on this logarithmic equation, Poyatos et al. calibrated a model that estimates canopy transpiration based on soil moisture content and tree water uptake.

There have been a few attempts for scaling up HD transpiration values from single trees to a whole catchment on an annual basis. Unfortunately, the results were not promising. For instance, Wilson et al. (2001) found that scaled HD measurements from single trees to a whole catchment are not representative of the expected transpiration

(based on results obtained with other techniques). Authors concluded that there must be some other factors influencing the process of aggregation to a whole catchment that were not included. Thus, further work is needed to improve estimates of transpiration at large scales.

Oren et al. (1999) used the sap flux weighted value multiplied by the fraction of stand sapwood area per unit ground area. With sap flux weighted values, Oren et al. included the sap flux variation around the tree trunk.

It goes without saying that radial patterns of transpiration vary around the tree because of the natural variation in sapwood thickness. In order to determine the thickness of sapwood, some authors opted for determining the radial patterns of sap flow and together with the stand's sapwood area estimates, determined the fraction of active sapwood for scaling purposes (Wullschleger and Norby, 2001; James et al., 2002; Barbour et al., 2005). Oren et al. (1999) observed similar diurnal patterns of sap flow around a tree trunk but the sap flow values differed in magnitude. Oren et al. attributed it to the radial variation of sapwood around the tree trunk (i.e. sapwood depth variation).

An important sap flow scaling issue, which will be later elaborated, is the use of sapwood area as the scaling factor at the tree scale. When scaling sap flow measurements from a single point to the whole tree, it is necessary (in most of the Thermal techniques) to know the tree's sapwood area. Sapwood area becomes an accurate scaling factor when it is properly estimated. However, accurate mensurations of sapwood area are time consuming and there is still a polemic about which is the most adequate method to measure sapwood area. Several authors have recognized this issue as a source of error while scaling up transpiration (Poyatos et al., 2005; James et al., 2002; Čermák and Nadezhdina, 1998). Hence, it is necessary to address this problem before attempting to scale up from a single tree to the canopy scale.

Čermák (1989) evaluated several vegetation characteristics at the stand scale in order to obtain the most adequate parameter to scale up transpiration. Based on the comparison of the standard errors of transpiration estimates obtained with the different scaling parameters, Čermák decided that the "solar equivalent leaf area" parameter was the

most adequate parameter to scale up transpiration values.

Another interesting attempt to scale up transpiration was by means of "leaf mass" estimates, which is the product of the trees leaf area and the leaf mass per area values (Čermák, 1998). Leaf mass was considered an adequate scaling factor due to its close correlation with the amount of sunlight trapped by a tree canopy in both deciduous and coniferous trees.

Barbour et al. (2005) integrated wood density as an important factor for scaling up sap velocity values to a whole stand. The work is based on the theory of the Poiseuille's law as modified by Roderick and Berry (2001), which considers the influence of wood density and other structural wood characteristics to the sap flow velocity. This approach was introduced when Barbour et al. found that none of the common scaling parameters were suitable for rainforest vascular vegetation.

Leaf area and plant density are other parameters used as scaling factors. Ham et al. (1990) followed a very particular approach to scale up sap flow velocities of a cotton crop (*Gossypium hirsutum*). Ham et al. scaled SHB sap flow velocities to larger areas by means of normalizing SHB sap flow velocities using plant density or leaf area values. The normalization with plant density overestimated plot transpiration values due to the large vegetation size variance inside the plot. The normalization with leaf area values was made at the tree scale. The use of a single tree's leaf area to normalize its sap flow velocity was considered an adequate predictor of transpiration at the canopy scale.

There has been some controversy about transpiration patterns at the regional scale. Authors working in similar regions have opposite conclusions with respect to the variability of regional transpiration rates. Schipka et al. (2005) reviewed this fact for the Western and Central European forests, finding that while some authors (Roberts, 2000) concluded that forest transpiration is homogenous between individuals of different species and meteorological conditions, others concluded that there are large differences in different species' transpiration rates (e.g. Köstner, 2001; Granier et al., 2003). Schipka et al. proposed that those differences are related to the methods used to estimate canopy transpiration. Methods include different parameters and of course, the

combination of those parameters determines the accuracy of the estimate at different spatio-temporal scales. For that reason, it is important to understand the method used to measure/estimate well transpiration and to report the error propagation for making our results available for comparison.

2.5 Evapotranspiration derived from remotely sensed data

At larger scales than the canopy scale, remotely sensed (RS) information is often used to indirectly estimate ET. Estimates are commonly approached by means of retrieving meteorological or vegetation parameters that regulate ET. Finally, these parameters are integrated into ET equations, hydrological models, or into algorithms to estimate ET. This section briefly describes the actual methods used to estimate ET at larger scales than the canopy scale. Even if it is not of the scope of the present research to use remotely sensed data to scale up transpiration, it is important to mention the efforts made to obtain transpiration estimates at larger scales, and the role that estimates at small scales play in these efforts.

Most common meteorological parameters retrieved from RS data are Temperature, R_n, and Vapour Pressure Deficit (VPD) (Granger, 1997, 2000). Radiometric temperatures and R_n are used to estimate components of the energy balance method (Hasager and Jensen, 2001) or they are correlated to aerodynamic temperatures (Bussières and Granger, 2000). Retrieved vegetation parameters are commonly LAI, through correlations with NDVI or other vegetation indices (Price, 1990; Kondoh and Higuchi, 2001; Szilagy, 2002).

At large scales, changes in surface temperature are related to moisture fluxes and thereupon to ET. In other words, surface temperature is extracted from RS for relating a surface cool down to a loss of energy which implies a direct surface water evaporation. For instance, Granger (1997) developed an algorithm that combines land surface temperatures and R_n, which are extracted from RS data, and ground meteoro-

logical parameters such as air temperature, ground heat transfer, and wind speed. In 2000, Bussières and Granger applied this algorithm (named feedback algorithm) to the Mackenzie basin, and assessed their final daily average ET map with a high level of uncertainty since there was limited knowledge on how to apply the algorithm to certain regions of the basin, specifically water bodies and mountains.

Most of the ET estimations using RS surface temperature values are based on AVHRR data (Yunhao et al., 2003; Kite et al., 2001; Bussières and Granger, 2000; Kakane, 1998) and MODIS (Naglera et al., 2005; Nishida et al., 2003). Some attempts for improving ET estimates include the integration of NDVI for weighting the contribution of vegetation to changes in surface temperature which have been assumed to be related to changes in transpiration rates (Price, 1990) due to its direct correlation to photosynthesis (Yunhao et al., 2003). Also, some authors have retrieved LAI from Landsat-TM and correlated to energy fluxes estimated with MODIS or AVHRR in order to obtain a more detailed information of the spatial distribution of vegetation (Hasager et al., 2003; Caselles et al., 1998) for improving the estimates of evapotranspiration from vegetated areas.

The energy balance method for estimating evaporation has been modified to estimate evapotranspiration by including LAI or NDVI, and surface vegetation temperatures. LAI or NDVI accounts for the fraction of vegetated areas and to estimate the contribution of transpiration to the total evapotranspiration. The energy balance method is the most applied in RS because most of its parameters can be retrieved from RS data (Kite et al., 2001; Liu et al., 2003; Kant and Badarinath, 1998). Other RS approaches are the application of combination equations, such as Penman-Monteith and/or Priestley-Taylor (Nishida et al., 2003; Szilagy, 2002; Biftu and Gan, 2001).

Field tower EC evapotranspiration estimates have been correlated to vegetation indices and surface temperatures derived from RS data, in order to generate model equations to interpolate ET estimates to other areas. These methods gave acceptable results in a riparian zone (Naglera et al., 2005).

Remotely sensed based evapotranspiration estimates have a few sources of error that

cover spatial ranges from field data to sensor specifications and correction/calibration of the raw *RS* data. One of the most important constraints is that still surface temperature extracted from RS carries errors associated with matching the radiometric temperatures to the atmospheric or aerodynamic ones (Kustas et al., 2001; Price, 1990). On the other hand, the use of point based field data to characterize larger areas (i.e. pixel) carries error because it roughly generalizes a real value. This is of concern when dealing with parameters such as soil moisture, vegetation density, air temperatures, and so forth. Another constraint is the spatial resolution of the final evapotranspiration estimates. Since the sensors which provide the finest radiometric resolution lack a fine spatial resolution, evapotranspiration outcomes are for pixels of about 1 kilometre.

Still, as in any other *RS* application, field data and description of processes governing transpiration at small scales is of importance for reliable modelling of hydrological processes and for obtaining more accurate estimates of each component of water balance in vegetated areas (Prueger et al., 2001). Liu et al. (2003) stated that there is still work to do to improve satellite imagery based *ET* estimates. Liu et al. addressed attention to the importance of improving the determination of using imagery of higher spatial resolution and the generation of more elaborate understanding and modelling of the processes involved in *ET*.

In the present dissertation, one of the main objectives is to characterize transpiration rates due to vegetation spatial heterogeneity at the canopy (i.e. plot) scale, in order to contribute to a better understanding of such variability's impact on scaling transpiration estimates using *RS* derived parameters, specifically *LAI*.

2.6 Observed gaps

After reviewing previous research attempts to scale up single tree transpiration to the canopy scale, one can conclude that it is necessary to address four main issues: 1) the chosen scaling parameters and the lack of conclusive evidence of the correlation of these parameters at large scales; 2) the accuracy in mensuration methods and the

applicability to specific types of vascular species; 3) the influence of tree physiological characteristics on estimating tree transpiration; and 4) the validate of the final canopy transpiration estimates. These four issues are elaborated in the following paragraphs.

Scaling process accuracy depends on finding the adequate scaling parameters. An adequate scaling parameter estimated at certain scale, should have a strong relationship with another scaling parameter at a larger scale. All the previous research demonstrates that the common scaling parameters (i.e. sapwood area, basal area, DBH_{OB}) are not always adequate for every vegetated forest. Thus, the canopy transpiration scaling parameters for each forested area need to be tested and finally defined.

From all the known scaling parameters, sapwood area, as mentioned before is an accurate biometric if it is properly estimated. On the other hand, interspecific anatomical differences restrict the applicability of every mensuration method to every species. Therefore, it is necessary to have more research determining the accuracy of the actual mensuration methods in order to decide which one is the most adequate for a particular species, and for the particular research purposes. Or at least, to report the error associated with the mensuration method used.

At the same time, there is not enough research proving the scaling parameters' relationships at large scales. Most of the canopy aggregation is based in the assumed linear allometric relationship between the most common scaling parameters (e.g. sapwood area and leaf area). Thus, more research should focus on proving these allometric relationships at large scales.

Tree physiological characteristics are claimed to be one of the reasons for observing large variations between the canopy transpiration aggregated estimates and other methods that measure evapotranspiration at large scales (e.g. EC method). If so, it is necessary to describe each tree species transpiration patterns before attempting any scale in any region. Here, it is also questionable the way in which canopy transpiration values should be validated. There is no better way to prove the reliability of the canopy transpiration estimates, but by comparing with modelled or estimated canopy evapotranspiration values. Another problem is that only mean canopy transpiration

values or sap flow are comparable with most of the methods used to observe reliability. Therefore, it is necessary to look for more adequate validation methods. Here, it is suggested that on top of a conventional comparison of results, one should also consider developing transpiration scaling approaches that address the reduction of error propagation. This could be another way to establish the validity of the scaling approach and its final outcomes. Thus it is necessary to generate scaling approaches that integrate the estimation of uncertainty.

Inter and intraspecific variability in sap flow is given by each individual's particular anatomy, species characteristics and environmental conditions. Such variability should be taken into account to scale up. The two main issues that arise from sap flow variability are the radial patterns of sap flow and the water storage capacity. Radial patterns of sap flow influence the measured sap flow velocity and should be estimated in order to avoid under or overestimations of transpiration due to this physiological condition. There are several ways in which water storage capacity can be taken into account while estimating tree sap flow. Still, there is no a formal method that can accurately determine it, and each species has a different pattern in water storage capacity. Thus it is particularly necessary to define each species water storage capacity diurnal trends.

As mentioned before, given the sources of error in sap flow techniques, it should be possible to suggest new methods in which those errors are minimized. Doing this requires a thorough understanding of the method used to measure/estimate transpiration and will allow for error propagation reporting that will facilitate comparing the results obtained in this study to other results.

At larger scales (i.e. catchment, regional scale), improved estimation or mensuration of the transpiration process at the tree and stand scales is necessary. This will be a valuable tool to global model parameterization. For global model parameterization purposes, the reduction of error propagation and reporting the error associated with the final transpiration estimates is essential. Thus, transpiration scaling approaches that significantly reduce error propagation effects are necessary. It is suggested that new scaling approaches should mainly focus on two aims; first, on obtaining reliable,

representative single tree transpiration values; and second, on measuring as accurately as possible, scaling parameters values.

In RS, the issues associated with the estimation of transpiration at large scales are:

1. To decrease the error associated with matching atmospheric or aerodynamic temperatures with radiometric temperatures.
2. Point based sampling to characterize large areas is a serious source of error when scaling up or comparing with pixel values. Thus, better methods of field data collection should be addressed in order to have representative values comparable to large scale information.
3. Field data and description of processes governing transpiration at small scales is of importance for reliable modelling of hydrological processes and for obtaining more accurate transpiration estimates.

3 The Montane and Boreal forests experimental setup

Chapter Outline

The experimental sites were established in Montane and Boreal forest areas. The Montane forest experimental sites are located in the Sibbald areas in Kananaskis Country, Alberta. The Boreal forest experimental sites are near Whitecourt, Alberta. This Chapter describes these two areas in terms of abiotic and biotic characteristics with close attention to the studied vascular vegetation in this research. Thereafter, the equipment set up and data collection are described, with close description of the meteorological and soil moisture data collection. The experimental sites, location, and main characteristics are highlighted in § 5.1.2. Therefore, the main focus of this Chapter is on describing the study areas and the equipment set up.

3.1 The Montane forest study area

The Barrier Lake Kananaskis Field Station is located in the Kananaskis Valley, which is considered a Montane Forest. The experimental sites were classified into two vegetation communities, coniferous and deciduous. The coniferous sites as well as the meteorological station were established within the Sibbald areas, in the base of the Baldy mountain, to the North-West of the Kananaskis Field Station facilities. The deciduous sites were established at the South-East of the Barrier Lake, within the Bow Valley Wildland

Provincial Park. Maps of the study area are shown in Figures 5.1 and 5.2.

3.1.1 Vegetation type

The study area inside of Kananaskis Valley is a Montane closed forest formation (Peet, 1988) within the Rocky Mountains (Rowe, 1972; Strong and Leggat, 1992). Inside the study area, the dominant vascular species are Lodgepole pine (*Pinus contorta* Dougl. ex Loud. var. *latifolia* Engelm.), White spruce (*Picea glauca* [Moench] Voss), Trembling aspen (*Populus tremuloides* Michx.), and Balsam poplar (*Populus balsamifera* L.). The first two species are softwood, while the last two are hardwood. Forest ecologists consider the vegetation composition of the Montane forest to be driven by the elevation, topography, soil composition, soil moisture, and climate (Peet, 1988).

Trembling aspen is a deciduous tree of broad, oval leaves, and cylindrical trunk whose roots are widely spread very close to the soil surface. Trembling aspen is considered a species of high tolerance that grows within pure and mixed communities in a wide variety of soil types and climatic conditions. Still, Trembling aspen prefers the Valley bottoms with low acidity (i.e. basic pH), and mesic soil with high nutrient concentrations. Yearly average temperatures of 16 °C have been recorded in Trembling aspen sites (Burns and Honkala, 1990b). Trembling aspen is as shade-intolerant as Lodgepole pine. Inside the study area, Trembling aspen frequently mixes with White spruce and Lodgepole pine. In the study area, the largest density of Trembling aspen surrounds the Barrier Lake, especially in the Lake's South-West.

Lodgepole pine is considered the Montane and Boreal species that most easily spreads after fire. This coniferous species grows in a wide variety of soils but dominates in coarse, granitic, moist soils (Peet, 1988; Burns and Honkala, 1990a). Its root system is normally shallow and narrow spread, which makes it prone to falling if exposed to strong winds. Extreme climatic conditions do not constrain Lodgepole pine growth. For instance, large stands of this species settle in areas that reach temperatures between -57 °C and 38 °C. Consequently, the species is widespread within the Rocky Mountains along elevations between $400m$ and $3600m$ (Burns and Honkala, 1990a). In the study

area, Lodgepole pine occupies the Baldy Mountain North-facing base in mixed stands with White spruce and a few Trembling aspen individuals.

Like Lodgepole pine, White spruce spreads in a wide variety of soil types and climatic conditions; however, they differ in their tolerance to shade (Farrar, 2003). White spruce preferably grows in basic-loam, xeric-mesic substrates. Within the Rocky Mountains, this species occupies sites with elevations from $1220m$ to $1520m$ above sea level, which exposes it to extreme temperatures (e.g. -29 °C and 24 °C in winter and summer times respectively, Burns and Honkala, 1990a). White spruce's root system is very flexible and widely spreads close to the ground surface. In the study area, White spruce dominates the stands where it mixes with Lodgepole pine.

An important factor in this study is the capacity of these species to conduct and use water. The water use capacity and water conduction efficiency is determined by each species' vascular structure, which also changes between Gymnosperm and Angiosperm species. Appendix B describes the main characteristics of angiosperms and gymnosperms vascular structure. This information will introduce the reader with some of the principles behind the mensuration methods explained in Chapter 4.

3.1.2 Abiotic characteristics

The Montane forest is classified as an ecoregion within the Cordilleran ecoprovince, whose particular mix of physiography and air masses creates particular climatic conditions (Strong and Leggat, 1992). In general, the Montane forest has an average annual precipitation of about $515mm$. The summer mean annual temperatures range from 5.1 °C to 18.9 °C, while the winter mean annual temperatures are from -11.3 °C to -0.2 °C. The temperatures can easily drop to freezing at anytime of the year. Within Alberta, the Montane forest maintains the warmest temperatures during the winter than any other forested ecosystem.

According to Strong and Leggat (1992), the reference soil is eutric-brunisol, which generates moderately-well drained substrates. Gray-luvisols are also common in the Montane forest. Topographically, the study area is characterized by ridged foothills and

a marked rolling topography (Strong, 1992). The complex topography together with climate and soil type create a wide variety of habitats suitable for different vegetation communities. Lodgepole pine is considered as the reference species in the Montane forest, followed by Trembling aspen and White spruce. Strong and Leggat (1992) include Douglas-fir (*Pseudotsuga menziesii* var. *menziesii* Mirb. Franco) as a Montane species for practical purposes; however, this species is better identified as a Subalpine one (Judy Buchanan-Mappin, personal communication, 2006).

3.2 The Boreal forest study area

According to the Ecological Land Classification (Strong and Leggat, 1992), the Whitecourt forested area is within the Mid Boreal Mixedwood ecoregion. Two experimental sites were set up in the Whitecourt forested area, one of Jack pine individuals and one of Black spruce. The Jack pine site was established just at the edge of the Hilltop Industrial Area. The Black spruce site was located towards the West Whitecourt area, in a site parallel to the Highway 43 (Grand Prairie).

3.2.1 Vegetation type

Whitecourt is considered as a closed forest formation (Elliot-Frisk, 1988) in the Southern Alberta uplands (Strong, 1992). In the Whitecourt forested area, there are Trembling aspen and Balsam poplar individuals, as well as Jack pine, Lodgepole pine and Black spruce. It was possible to distinguish large amount of pure stands; however, there were also mixed sites of coniferous and deciduous trees. Both experimental sites of Jack pine and Black spruce were inside pure stands.

Jack pine is a Boreal species widely distributed in North-Eastern of Canada. In the West of Canada, there are Jack pine patches in central Alberta and North-Eastern British Columbia. Individuals of this species grow in low nutrient soils, such as coarse sands, shallow soils, including permanently frozen soils (Elliot-Frisk, 1988; Farrar, 2003). Its climate tolerance changes from the Maritimes to the interiors. In general, the

species survives to annual maximum temperatures between 29°C and 38°C and annual minimum temperatures between -29°C and -4°C (Burns and Honkala, 1990a). Jack pine's root system spreads widely in the horizontal and vertical ground, and it is shade-intolerant that mixes with other shade intolerant species (e.g. Trembling aspen, Lodgepole pine) (Farrar, 2003).

As mentioned, Black spruce is considered an opportunistic species that easily grows in poorly drained sites, preferably in xeric-hygric, organic soils with low nutrient concentration. Black spruce individuals have a very shallow root system (Farrar, 2003) that allows them to easily grow in high water table sites. Black spruce, as with most of the Boreal species, tolerate extreme atmospheric temperatures. Low extreme temperatures range between -62 °C and -34 °C, and the high extreme ranges between 27 °C and 41°C (Burns and Honkala, 1990a). Probably, the main characteristic of Black spruce is its ability to grow in bogs and swamps, but still it is known that the densest stands are found in well-drained sites with sandy soils (Burns and Honkala, 1990a).

3.2.2 Abiotic characteristics

The combination of low insolation and circulation patterns (i.e. Arctic air masses and Westerlies) define the climatic conditions of the Boreal forest ecoprovince. Furthermore, there are slight climatic variations from one ecoregion to another due to the changes in local topography (Strong and Leggat, 1992). In fact, the Mid Boreal Mixedwood ecoregion is characterized by its moister atmospheric conditions than the rest of the Boreal ecoregions (Strong and Leggat, 1992). In this ecoregion, the average annual precipitation is about $240mm$ during the summer and $64mm$ in winter time (Strong and Leggat, 1992). The summer mean annual temperatures range from 7.3 °C to 19.6 °C, while the winter mean annual temperatures range from -18.6 °C to -7.7 °C. Thus, the average precipitation is larger in the Montane area than in this ecoregion; however, the Mid Boreal Mixedwood forest is slightly warmer than the Montane forest. The Mid Boreal Mixedwood forest lacks a complex topography. The topography in this ecoregion is mainly composed of a rolling terrain that creates low height hills as well as

some uplands (Rowe, 1972).

Although the two forests differ in climatic conditions, both of them share the same soil types, eutric-brunisol and gray-luvisol. Gray-luvisol is the reference soil in this area, though (Strong and Leggat, 1992; Rowe, 1972). The substrate ranges from well-drained to very poorly drained. The soil type in the very-poorly drained sites is mainly gleysol with high concentration of organic matter, which are the preferred sites of Black spruce (Rowe, 1972). Opposite to this, the well-drained areas with eutric-brunisols are populated by Jack pine individuals (Strong and Leggat, 1992; Rowe, 1972).

3.3 Equipment setup and data collection

3.3.1 Meteorological Station, setup and collected data

In the Montane Forest, the meteorological station was set up in a $25m$ radius clearing located inside the Loop 1 of the Barrier Lake Forestry Trails, in the South corner of the Coniferous plot 5 (Conifer-5, see Figure 5.1). In the Mid Mixedwood Boreal Forest, the station was established in the West side of the Whitecourt town, about $200m$ away from the experimental sites.

The installed sensors measured temperature, relative humidity, dew point, rainfall, atmospheric pressure, wind speed, gust speed, wind direction, solar radiation, and Photosynthetically Active Radiation. The sensors were placed at height of about $3.0m$ above the ground level. The sensors are made to work with the HOBO weather station logger (H21-002). All the variables values were collected every minute and downloaded every week to a laptop using the HOBO Weather station software (Boxcar Pro ver. 4.0; Figure 3.1). The data was initially stored in the format of Excel files and lately processed as ASCII files to match by time (hour and minutes) the data variables with the sap flow mensurations (C^{++} program).

Figure 3.1: Meteorological station. Notice the trail of the Loop 1 at the back.

3.3.2 Thermal Dissipation sensors, field work logistics

Dugas (1990) analyzed the different methods to estimate transpiration and concluded that sap flow measurement methods have the advantages of being an integrated value for the whole plant and being appropriate for measurements in small plots. There are two common thermal techniques: the Thermal Dissipation Probe method (TDP) (Delta-T Devices Ltd., 2003) or Granier's Continuous Heating Method (Granier, 1985) and the Steam Heat Balance (SHB) (Steinberg, 1988; Steinberg et al., 1989). The use of the SHB method is restricted to certain trees because they are specific for certain tree diameters and also requires stem invasion (Dugas, 1990). Steinberg (1988) concluded that SHB worked adequately under the conditions consistent with the physical principles by which it is governed.

On the other hand, TDP techniques are known for their accurate estimations of sap flow in single trees (Schulze et al., 1985; Samson, 2001) without requiring an empirical calibration factor. Two important advantages are that it is possible to measure transpiration of single trees in mixed forests and that the sap flow patterns of different tree species can be described at different diameters. The main constraint in the estimation

of transpiration for a single tree is the differentiation and quantification of the sapwood area for scaling purposes. Thus, TDP-30 sensors (Dynamax, Inc.) were used in trees' sap flow mensuration. The sensors' and system description are given in Chapter 6.

Sap flow was measured in sets of four trees during periods of 48 hours. For each species, trees were chosen by their size in order to cover the whole size range found in the study area. Once the period of 48 hours was met, another set of four trees was chosen and TDP equipment installed in them for obtaining a new data set. At the end of the summer 2003 there were sap flow data of 34 individuals, of which eight were White spruce, five Jack pine, nine Lodgepole pine and twelve Trembling aspen. Black spruce individuals were not included in sap flow measurements due to weather and site constraints.

Sap flow mensurations were collected every five minutes and stored in a Data Dolphin data logger with 4 differential, 24 bit inputs (Data Dolphin logger DD-124). The data logger was fed by a 12V battery. Extra gel batteries were used to keep the 12V battery fully charged; the gel batteries are Power-Sonic, model PS-2330 NB (12 Volt, 35 Amperes hour). The power for heating the thermocouples was controlled by installing an adjustable dual voltage regulator-controlled power (AVRDC, Dynamax Inc.). The collected sap flow data was downloaded to a laptop every 24 hours using the Data Dolphin data logger software. The files were in ASCII format and the information was processed in Excel (Microsoft Office Excel 2003), Minitab (ver. 13.32) or S-Plus (ver. 7.0, student version) according to the purpose. The accuracy of the sensor for measuring changes in sap temperature is 0.025 °C(AVRDC, Dynamax Inc.)[1]. Figure 3.2 illustrates the set up in a group of coniferous trees.

[1]Lab tests were conducted in order to verify the sensors accuracy reported by the manufacturers. Distilled water was heated and then left at room temperature. Changes in water temperature were measured every five minutes with a high accuracy thermometer and the thermocouples. There was no difference between the two sets of observed temperatures

Figure 3.2: Installation of TDP sensors in a set of coniferous trees, site Conifer-4.

3.3.3 Soil moisture sensors

For each tree set, one tree was chosen for measuring the soil moisture in the perimeter surrounding the tree. The distance at which the sensors were installed was about $1m$, and the soil moisture data was collected every four minutes. Six soil moisture sensors were set up $1m$ away from the tree; four sensors were installed in the direction of the main four cardinal points, one more in the South-West and the sixth one in the North-East (Figure 3.3). Every time the TDP equipment was changed to a new tree set, the soil moisture data was downloaded before uninstalling the sensors. The data was downloaded into a laptop using the DL6 software.

3.3.4 Data control

The meteorological data was controlled by comparing the variables values with those registered at the Meteorological station of the Kananaskis Field Station. It was considered that the distance between the two stations should not create a large difference in measured values. Besides, the two stations were located in open areas, facing the

Figure 3.3: Installation of soil moisture sensors in the coniferous site Conifer-4.

North-East. For instance, the sets of solar radiation values were compared against those registered with the solar radiation sensor of the Kananaskis Field Station. A good agreement was found between the two data sets. The same was done with other variables values available at the Field Station, such as temperature and wind speed/direction.

The sap flow values were controlled by observing the order or magnitude and their agreement between some meteorological variables and the sap flow trends. It was expected that sap flow rates would be greater in sunny, calm days than in rainy, cold, cloudy days. There are periods of the day when sap flow decreases to avoid desiccation, and some other periods in which it is known that all trees reach their maximum sap flow rates.

The soil moisture data was controlled by comparing the amount of water lost by the soil and the amount of water sucked up by the tree. Also, the rainfall periods were observed and soil moisture data checked; thus, after a rainfall it was expected to observe an increase in soil moisture.

4 Sapwood area estimates

Chapter Outline

Sapwood cross-sectional area (or sapwood area) is calculated as the annulus formed by two circles of different sizes. The smaller circle's diameter equals the heartwood's diameter and the larger circle's diameter equals the Diameter at Breast Height (DBH). The complex part of estimating sapwood area is the mensuration of sapwood depth for each species.

Due the complexity of obtaining accurate sapwood depth mensurations, researchers have developed different methods claiming to differentiate sapwood from heartwood and thus estimate sapwood and heartwood depths. Those methods are normally based on physiological and morphological characteristics that make a distinction between both sapwood and heartwood. Sapwood-heartwood distinction has been obtained by: staining specific wood tissues (e.g. Shelburne et al., 1993; Baynes and Dunn, 1997), injecting the tree with methyl-blue dye (e.g. Goldstein et al., 1998; Samson, 2001), visually tracing the sapwood-heartwood edge through their differences in colour and water content (e.g. Marchand, 1984; Gilmore et al., 1996; Delzon et al., 2004; Eckmüllner and Sterba, 2000), by measuring the concentrations of organic, chemical and bacteriological wood components (Jeremic et al., 2004), perfusing a chemical dye through branch or trunk segments (e.g. Zimmermann and Jeje, 1981; Sperry et al., 1991) and by microscopical analysis of wood anatomy (e.g. Aloni et al., 1997; Jeremic et al., 2004). The accuracy of the results that are obtained with any of these methods are dependent on tree species type, differences between individuals of the same species, and the environmental

conditions.

There is also a wide variety of indirect methods for estimating sapwood area. At the tree scale, sapwood area has been statistically correlated to DBH_{OB}, LAI and BA (Basal Area), and there is a considerable amount of linear and non-linear equations explaining such correlations for different tree species and forest environments.

The main objectives of this chapter are:

1. To obtain tree sapwood area estimates for the five boreal tree species of interest: Trembling aspen, Lodgepole pine, Jack pine, Black spruce and White spruce; and
2. To describe and statistically evaluate the intraspecific sapwood area variations as a function of DBH_{OB} and sapwood depth.

In this work, direct estimates of sapwood depth were used to estimate sapwood area for a single tree, and later used to calculate sap flux density (J_i) (Chapter 6), while the allometric correlations were applied to estimate transpiration rates at the plot scale.

Three different direct methods for measuring sapwood depth were tested and statistically analysed: the injection of dye in situ, the microscopical analysis of wood anatomy to differentiate sapwood from heartwood, and the visual differentiation and tracing of the sapwood-heartwood edge by light transmission and wood change coloration. The first method was the first option and used in situ during the field campaign of 2003; however the results were not successful, and during the same field campaign, increment cores (also known as wood cores) were collected to perform the microscopical analysis of wood anatomy. The third method was performed to investigate its reliability since it is widely used, and it has been applied with little concern. Comparison between the last two methods revealed the over and underestimation that may occur using the third method, and possible causes are discussed. Results of sapwood depth obtained from differences in the anatomy of wood microscopic tissues are later used to estimate transpiration at the tree level and for scaling up to the plot level by allometric correlations.

4.1 Introduction

4.1.1 Estimation of sapwood depth and sapwood area

The method used to estimate sapwood area may considerably influence sap flow values scaled to the whole tree (Čermák and Nadezhdina, 1998; James et al., 2002). The main factor that carries error into the sapwood area estimates is the measurement of sapwood depth. Studies that required the estimation of sapwood area normally used one method, and just a couple of studies have compared the results obtained with different methods (Čermák and Nadezhdina, 1998; James et al., 2002).

In this study, estimation of sapwood depth was addressed by applying three different methods in order to compare results and estimate the error associated with each method. The main objective of this exercise is to avoid large errors in sapwood depth mensuration. The sapwood depth values with the least error should be used for scaling sap flow to the whole tree and to obtain the allometric correlations. To the author's knowledge, there is no previous study that compares the three methods used here.

Injection of dye in situ.

This method involves injecting the tree with methyl-blue dye, which is an organic solution that easily travels through the sapwood conducting tissues while staining them. The stained wood is measured as the total sapwood depth. Goldstein et al. (1998) used the method in tropical species, while Samson (2001) used it with mixed deciduous forest species (following Goldstein et al.'s method). Neither work reported accuracy assessments, and only Goldstein et al. commented on the need for coring the trees in different places in order to locate traces of the dye.

Anatomical and physiological characteristics of trees influence the success of the ascent of a chemical solution injection. Tyree and Zimmermann (2002) analysed the drawbacks dye injection due to the trees' physiology. These authors stressed that previous knowledge of probable dye ascent patterns of the species of interest is necessary

because every species has a particular tangential spread "that varies from 1° to 3° " and this diffuses the solution more around the trunk than into its inner structure. Tyree and Zimmermann (2002) proposed that the number of injection holes around the trunk should be enough for spreading the dye towards the crown without damaging the tree. Another important point is the pattern of water conduction governed by the type of vessels or tracheids present in the tree. These authors also felt that diffuse-porous species (e.g. Trembling aspen) are not complicated since most of their sapwood is mainly composed of conducting vessels and a single target may allow the dye to move towards the crown. However, ring-porous species are much more problematic, since in these species, the earliest sapwood is the active conducting tissue. Tyree and Zimmermann also determined that is not easy to successfully use the dye injection method in these species unless special techniques are used to inject the earliest sapwood with the dye.

Probably the most important point mentioned by Tyree and Zimmermann (2002) is the fact that the sap is under a negative pressure. The authors explained that once the tree is cored, there is a drastic change in pressure due to the intrusion of air into the cored hole. The torus-margo pit membranes are normally broken, which alters the original sapwood path. Therefore, there will not be an acropetal movement of the injected dye once the vessels or tracheids are damaged. Still knowing all those drawbacks, the injection of the dye method was attempted and results are presented here.

On the other hand, using air pressure for injecting the dye (i.e. perfusion of the chemical dye) through a branch or trunk segments could improve the method; however, this method was firstly developed with the main objective of measuring vessels/tracheids lengths (Skene and Balodis, 1968). Still, Sperry and Tyree (1990) and Sperry et al. (1991) used the dye perfusion to differentiate between functional and non-functional sapwood while studying embolism. Spicer and Gartner (2001) firstly used the alizarine-red dye to mark the heartwood-sapwood boundary. Authors perfused the same samples with 0.5% w/v safranin-O solution where they determined that in 27% of their samples, the innermost sapwood was wrongly marked as actively conductive by the alizarine-red dye; however, they do not reported any further assessment of the methods used.

Microscopical analysis of wood anatomy.

Differentiation of sapwood by anatomic analysis requires one to identify the capillary structures (vessels/tracheids), density of these conducting elements, and some other characteristics such as the presence of ray parenchyma and starch grains. In this study, it is expected to observe a distinguishable gradient in the number of active vessels/tracheids, decreasing inwards to the pith. Another anatomical characteristic that might be useful (if possible to apply) is the decrement of alive ray parenchyma cells, as explained by Yang (1993). His results on the survival rate of ray parenchyma in Jack pine, Black spruce, Trembling aspen and Balsam fir (*Abies balsamea*) explained that the amount of death ray parenchyma cells increases from the outer sapwood towards the inner sapwood. Thus, there is the possibility of defining the sapwood-heartwood boundary by their anatomic differences at the microscopic level.

In order to microscopically differentiate sapwood from heartwood tissues, it is necessary to know and distinguish the anatomic characteristics of the different vascular tissues at a microscopic level. The vascular tissues that are expected to be microscopically differentiable in a trunk cross-section are the phloem, cambium and sapwood, going from the outermost part (cork) to the innermost part (pith), where the heartwood should be differentiated as well (Figure 4.1).

Results of a recent work have stated that wood anatomy, extractives, and bacteria concentrations are the main differences between heartwood and sapwood. Jeremic et al. (2004) studied the physical, anatomical, chemical and bacteriological characteristics of sapwood, heartwood and wetwood in Balsam fir (*Abies balsamea*). The physical study showed that wetwood and sapwood have similar water content, and even wetwood can reach higher water content than sapwood. Therefore, there is the possibility of reading wet heartwood as sapwood. The results of the anatomical study demonstrated obvious differences in the cellular structure of heartwood-wetwood and sapwood. Those differences were explained by the presence of bordered, clean pits in sapwood, while pits in heartwood and wetwood looked generally incrusted and aspirated. Sapwood showed the highest number and concentration of bacteria and methanol dissolved extractives

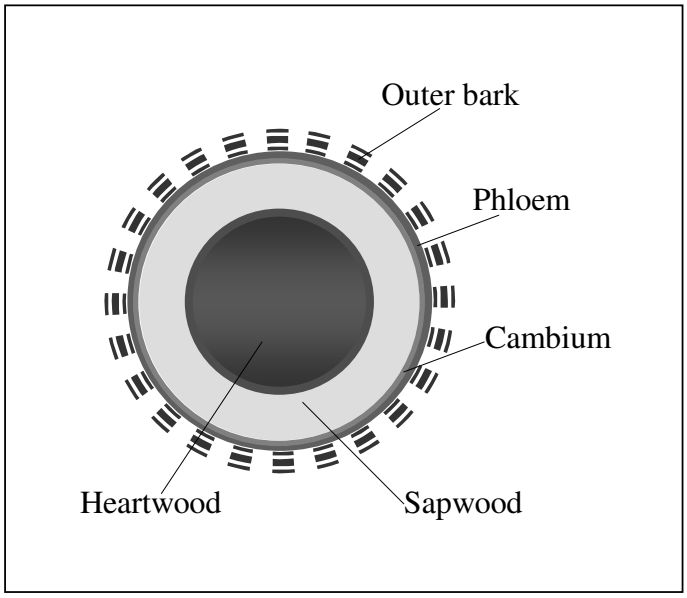

Figure 4.1: Schematic representation of vascular tissues in a tree trunk cross section.

as well. Authors concluded that the only confident way of differentiating heartwood and wetwood from sapwood is by means of wood anatomy.

Visual tracing of the sapwood-heartwood edge by light transmission or change in wood coloration.

A trunk's cross-section normally presents two different coloured zones: a light one located at the outermost part of the trunk, and a zone with a darker coloration, located at the innermost part of the tree (Jeffrey, 1922; Kozlowski and Pallardy, 1997). The lighter in colour zone is generally translucent due to a high water concentration and considered to be the active sapwood. The darker zone is opaque due to a high accumulation of extractives (e.g. tannins, gums, oils, resins), and it is considered the heartwood (ibidem).

For a majority of woody species, their sapwood has a lighter coloration than the heartwood. However, this principle does not apply to species such as Black spruce and White spruce that have very slight sapwood-heartwood colour differences; in Black spruce the

sapwood is not translucent enough to distinguish it against the light (personal observation). Also, not all individuals of the same species show this remarkable difference in sapwood-heartwood coloration. Gartner (2002) noticed that the boundary marked by difference in coloration in individuals of Douglas-fir (*Pseudotsuga menziesii*) in general matched the sapwood-heartwood edges highlighted with alizarine-red dye, but there were exceptions.

López et al. (2005) studied and described the wood anatomy of *Prosopis pallida* (algaroba) by means of scanned images of cross-sections at the base of the stem. Authors noticed a slightly darker coloration of the late (older) sapwood in a few section samples of *Prosopis pallida*, and being aware of this situation, they measured the sapwood depth taking into account those darker rings as part of the sapwood.

Some researchers had visually traced the sapwood-heartwood edges in boreal species (coniferous and deciduous), and reported that those boundaries were evident due to the semitransparency of the sapwood, but difficult to bound by difference in coloration (Kaufmann and Troendle, 1981).

The sapwood-heartwood bounding by means of difference in coloration and light transmission in the sapwood is commonly applied due to its apparent ease. Besides, this method's sapwood area estimates generally gives high correlations with other morphological characteristics of the trees (Dean and Long, 1986; Sievänen et al., 1997; Marchand, 1984). Very little concern has been shown for the accuracy of the method used in a study, and no one has conducted a study specifically on this issue.

More concern has been shown with respect to sapwood area estimates required for scaling up transpiration from a single point in the tree to the entire tree and to the plot. Čermák and Nadezhdina (1998) performed a comparison between results obtained with two different sapwood area estimation methods: xylem water content and radial patterns of sap flow rate. For Arizona cypress (*Cupressus arizonica*), a coniferous species, the results from the two methods were almost similar. However, significant differences were found with the rest of the species analysed (4 coniferous and 4 deciduous) because sapwood-heartwood water content largely varied; while some species had higher

water content in their sapwood than in their heartwood other species had a much lower water content (e.g. $20\%_{vol}$ in sapwood and $80\%_{vol}$ in heartwood [Poplars, *Populus interamericana*]). Even some species had similar water content between their heartwood's outermost part (transitional zone between sapwood and heartwood) and their sapwood. Hence, the boundaries between sapwood and heartwood were not defined by water content. Moreover, radial patterns of sap flow demonstrated that for most of the species, sap flow occurs in approximately 60% of the outermost part of the tree radius, after the cambium. The authors concluded that for scaling purposes (of transpiration) either method of estimating sapwood depth by water content or by colour differentiation would involve considerable errors.

The same observation with respect to a tree's water content radial variations was made by Yazawa et al. (1965). Based on his results of transitional sapwood-heartwood zone water content, the authors classified the transitional zones into three categories: the moisture content of the transitional area can be equal to either the sapwood or the heartwood zones, it can be lower than either zone, or it can be an average of both zones.

Pathological conditions of the wood (e.g. wood invasion for pathogens, tree injury, age-growth) can create false sapwood-heartwood zones. For example, wound-induced discoloration, which is a mechanism of defence against the dispersion of pathogens in the whole tree, consists of the generation of a protective, discoloured sapwood that surrounds the invaded zone. Change in wood coloration generates what is known as *false heartwood*, which actually has been described as an extension of sapwood with a coloration similar to heartwood (Kozlowski and Pallardy, 1997; Ward and Pong, 1980). Another example is the presence of wetwood in standing trees. Wetwood is actual heartwood that has suffered an internal infusion of water, and therefore, it has a high moisture content. The causes of this malfunction are still unknown; however, the wetwood has a translucent look and it is always located at the outermost part of the heartwood, close to the sapwood, which confuses it with sapwood (Ward and Pong, 1980; Jeremic et al., 2004).

High concentrations of water content is what makes the wood look semitransparent,

and observing the results obtained in the previous work, there may not be complete reliability in the translucence of the wood for bounding the heartwood-sapwood. Transitional zones are not marked by coloration either, and sometimes the sapwood stops functioning before the darker coloration takes place and vice versa. Thus, there might be an over or underestimation of sapwood depth by bounding sapwood-heartwood edges using changes in coloration and translucence of sapwood. This research reports results on tracing the heartwood-sapwood edges by means of differences in coloration and translucence of the sapwood. Also, these values are compared with those obtained using the microscope to identify the sapwood depth based on wood anatomy (see § 4.3.4).

4.2 Material and methods

4.2.1 Injection of dye in situ

Attempts at measuring the sapwood depth by injecting methyl-blue in the tree trunk were made in Prince Albert National Park. The injection of the dye was through a hole made by an increment borer (Haglof borer, $200mm$ of length, and $5.15mm$ of diameter). As Goldstein et al. (1998) did, the hole and injection was made at the breast height, i.e. $1.3m$. After 2 hours, a wood core was extracted at $2cm$ above each dye injection point. The total conducting area of sap was determined from the depth of the wood coloured by the dye as it is moved up in the transpiration stream (Goldstein et al., 1998; Samson, 2001). According to Goldstein et al. (1998), a larger distance to extract the core may be used; however, the shorter distance minimizes damage to the tree. The selected dye, methyl-blue, is soluble in water and does not cause alterations in the composition of the sap (Samson, 2001).

4.2.2 Microscopical analysis of wood anatomy

Section 4.3.1 describes in detail the collection of plant material, which mainly consisted of collecting the wood cores that would be used to estimate sapwood depth. Once the wood cores were extracted, the procedure was as follows:

Every core was submerged in distilled water after leaving it at room temperature for at least 8 hours. When the core was completely soaked, it was placed in a Petri dish full of distilled water, and free-hand cut into very thin cross-sections. The reason for soaking the cores and cutting them under water was to avoid air embolism (Aloni R., e-mail communication, 2003).

To cut the cores for identifying the sapwood region and quantifying its depth was conducted as follows:

i The core total length was measured in order to eventually calculate the percentage of xylem, sapwood, cambium and phloem in the sample.

ii The core rings were counted and their length measured as well.

iii The first cut was always made in the innermost part of the core. It was a longitudinal cut of about 2mm or more. The length of the cut was determined according to the width of the rings to keep them complete and to maintain the elements of every ring as a whole. These cuts are referred to as *small cores* in the rest of the present work.

iv The small core was cut to obtain at least 4 thin cross-sectional slices and 4 longitudinal thin slices.

v The half of both the cross-sectional and the longitudinal slices were stained with safranin dye and the other half were stained with methyl-blue.

vi The dyes were left for 10 minutes to obtain well-stained sections (i.e. uniform coloration). After that, the sections were washed with a few drops of distilled water to eliminate the excess of dye.

vii Sections were used to prepare temporal microscopic preparations.

viii The sections were placed in microscope slides and observed in a light microscope (Olympus Optical Co., LTD, model CH30RF100). The process was repeated, cutting sample sections towards the innermost part of the core, until the sapwood region appeared. Then, the rest of the core length was measured.

ix At this stage, 1mm slices were cut tangentially at the outermost part of the core, to identify the cambium and phloem regions.

x The small sample was treated as explained in steps iv to vi.

xi The last two steps were repeated until the sapwood region appeared in this side of the core.

xii The total depth of the sapwood is the resultant core length.

4.2.3 Visual tracing of the sapwood-heartwood edge by light transmission

Bounding the sapwood-heartwood edge by difference in light transmission consisted of exposing the wood cores samples to a source of artificial light (bulb of white light, 14W). The cores were soaked in distilled water, as explained in § 4.2.2, in order to easily observe the translucence zone and differentiate it from the opaque zone. The depth of the translucent zone was then measured and is reported here as the sapwood depth. For comparison of methods, selected samples of Jack and Lodgepole pine and White spruce were analysed by both the translucence and microscopical differentiation of wood anatomy methods.

After the boundary was set by translucence, each core was longitudinally cut from the marked boundary towards the sapwood (about two rings). Same procedure was performed from the marked boundary towards the heartwood (about two rings). Thin cross-sectional slices were prepared for both sections (as explained in § 4.2.2). If the wood anatomy did not concur with translucence method results (i.e. sapwood depth did not end where wood translucence ended), more sections were cut and microscopically analysed to delimit the sapwood depth based on wood anatomy.

4.2.4 Tracing boundaries by change in wood coloration

Samples were soaked in distilled water, as explained in § 4.2.2. This made the difference in coloration between sapwood and heartwood more evident. The wood core section with lighter coloration was identified and measured as the sapwood depth.

In order to compare both microscopical differentiation of wood anatomy and coloration methods, sapwood depth of Trembling aspen core samples was estimated by means of both methods. Once the boundary was set by coloration, each core was longitudinally cut from the marked boundary towards the sapwood (about two rings). The same procedure was performed from the marked boundary towards the heartwood (about two rings). Thin cross-sectional slices were prepared for both sections (as explained in § 4.2.2). If the wood anatomy did not concur with coloration results (i.e. sapwood depth did not end at the coloured boundary), more sections were cut and microscopically analysed to delimit the sapwood depth based on wood anatomy.

4.2.5 Sapwood area calculation

Sapwood cross-sectional area can be defined as the region bounded by two concentric circles: the outermost part of the tree that is formed by the bark and vascular cambium (forming the external circle), while the innermost circle is the one formed by the tree's heartwood. Under natural conditions these circles are of nonuniform shape, which make them thicker or thinner around tree trunk's basal area. However, it is considered that for many cases tree trunks come close to a circle (Husch et al., 1972). Thus, for each species the total sapwood area was estimated assuming that the trees under study are of consistent cylindrical shape (Figure 4.2).

Consequently, the sapwood cross-sectional area, SA, is quantified as an annulus by:

$$SA = \frac{\pi}{4}(D^2 - hd^2) \tag{4.1}$$

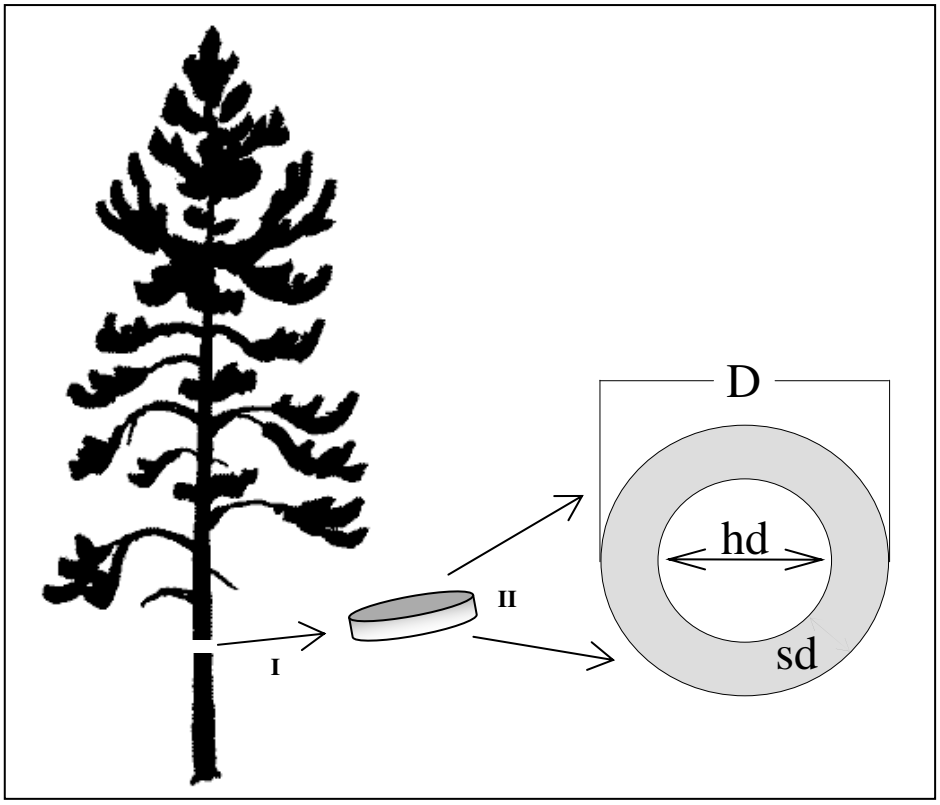

Figure 4.2: Transversal view of a tree trunk disk at the breast height. When a tree transverse cut (I) is flipped 90 deg (II), it gives a cross- sectional view of the wood structure. The tree's figure was modified from Farrar (2003).

where D is the DBH of outside bark (DBH_{OB}), calculated from field measurements of the Circumference of outside bark at Breast Height (CBH):

$$D = \frac{CBH}{\pi} \tag{4.2}$$

hd is the tree's heartwood diameter that is estimated based on the average tree's sapwood depth and DBH_{OB}:

$$hd = D - 2\bar{sd} \tag{4.3}$$

where $\bar{sd}$ is estimated as an average sapwood depth:

$$\bar{sd} = \frac{sd_N + sd_S + sd_E + sd_W}{4} \tag{4.4}$$

sd_N, sd_S, sd_E and sd_W are the individual's sapwood depth $[L]$ at each cardinal point (North [N], South [S], East [E], West [W]).

A simplified form of estimating SA is obtained by substituting Equation (4.3) into Equation (4.1):

$$SA = (\bar{sd}D - \bar{sd}^2)\pi \tag{4.5}$$

4.3 Results and analysis of results

4.3.1 Plant material

Table 4.1 lists the five species considered in this study, their respective wood types, the field sites, the number of trees sampled in each site (**n**), and the maximum and minimum DBH_{OB} of the trees sampled. The first set of wood cores was collected in Prince Albert National Park, Saskatchewan, during the summer of 2003.

During the summer of 2004, a second set of wood cores was collected in Kananaskis country, AB, and Whitecourt, AB (Table 4.1). The first set collected was used to develop allometric correlations. The second set of sapwood area results was integrated with the first set to increase the number of samples used in the correlations, but also, the second set corresponds to those trees used to measure sap flow.

Every tree was cored out at the breast height in its North, South, East and West sides. The diameter of the cores was 5.15mm and the length varied as a function of the total diameter of the tree. The circumference at the breast height (CBH) was

Table 4.1: Tree species, their wood type, number of trees sampled (n) per each species in the different sites (Prince Albert National Park [PANP], Kananaskis country [KC], and Whitecourt[WC]). Maximum and minimum DBH_{OB} are reported in *cm*.

Species type	**Wood type**	**n**	**Site**	**DBH_{OB}**	
				Maximum	Minimum
Trembling aspen	diffuse-porous	23	PANP	46	10
		12	KC	31	12
Black spruce	coniferous	25	PANP	38	15
		6	WC	13	10
White spruce	coniferous	18	KC	50	11
Lodgepole pine	coniferous	9	KC	31	17
Jack pine	coniferous	21	PANP	24	11
		6	WC	24	13

measured to calculate each tree's DBH_{OB} (Equation [4.2]).

Cores were immediately wrapped in aluminium foil and kept in polyethylene bags under a cold environment. While the analyses were being conducted, samples were kept in refrigeration and occasionally misted with distilled water to avoid cracks and dehydration.

Since the tracheids of every conifer and vessels of Trembling aspen can support extreme changes in weather (Sperry et al., 1994; Woodward, 1995), the specimens can be preserved under refrigeration without damaging their active xylem structure. To avoid the invasion of the remaining holes in the trees by insects and then the possibility of infestations by fungus, the holes were completely sealed using a special wax (Tree wax [combination of natural resins] Trimona, Germany.).

4.3.2 Injection of dye in situ

After two hours of injecting the dye, there was no clear indication of a radial dye dispersion. The time and dye were incremented: six hours, injecting the dye every

hour until the hole was completely soaked. The dye was injected in 23 specimens of Trembling aspen, 21 of Jack pine and 25 of Black spruce. Traces of dye were observed in 4 specimens of Black spruce, two in Trembling aspen and one in Jack pine (Table 4.2).

Table 4.2: Specimen trees diameter and the depth at which the dye was dispersed.

Tree species	**DBH_{OB}** (cm)	**Dye depth** (cm)
Black spruce	22.00	2.10
	17.00	1.64
	22.00	1.70
	22.00	1.25
Trembling aspen	38.00	5.40
	24.00	2.40
Jack pine	11.00	0.35

4.3.3 Microscopical analysis of wood anatomy

The mensuration of sapwood depth in the four cardinal points was performed for individuals of the 5 species of interest. A total of 480 wood cores were observed through the microscope. For most of the wood cores (396), it was possible to measure sapwood depth with an accuracy of 0.01mm by using the microscope ocular micrometer. Factors that affected the observation of wood microscopic anatomy are related to wood decay, high concentrations of bacteria, malformations, and some other factors that are species specific (these factors will be addressed later). Thus, for 17.5% of collected samples, it was not possible to differentiate and measure their sapwood.

To illustrate each species' microscopic anatomy (described in § 4.1.1), images of sapwood and heartwood were captured on Scanning Electron Micrographs by using the Environmental Scanning Electronic Microscope Philips [FEI]-ESEM, Model: XL30 (Figures 4.3, 4.4, 4.5). Micrographs of conifer trees show some singular sapwood character-

istics, such as the presence of bordered pits and open resin canals. Bordered pits are microscopical cavities formed between the tracheids that allow the transversal sap flow. The bordered pits have a membrane (torus-margo pit membrane) which is centred between the tracheids' walls (Jeffrey, 1922; Hacke et al., 2004). The open resin canals are rounded, empty holes randomly distributed in the sapwood; and they are larger than the tracheids. The heartwood lacks bordered pits and pit membranes adhere to one side of the pit. The pits are filled with fibres and the tracheids' walls become thicker. the heartwood tissues lose their living contents such as protoplasm, starch grains and nuclei as well.

In deciduous trees, like Trembling aspen, the vessels are widely spread in the sapwood (diffuse-porous) and fibers between them sustain the entire sapwood structure. When the sapwood loses its sap-conducting capability, those vessels are sealed either with tyloses or gums, and the sapwood becomes heartwood (see micrographs in Figure 4.5). The presence of tyloses is more common in angiosperm trees such as those pertaining to the genus *Populus* (Kozlowski and Pallardy, 1997). Tyloses are the key feature for distinguishing between sapwood and heartwood. Trembling aspen has tyloses in its sapwood as well; however the increment of tyloses in its heartwood is considerably high.

Other features used for sapwood recognition were the presence of bacteria and starch grains (not visible in the micrographs), as well as pitting between tracheids and the ray tracheids. Once each individual's sapwood depth at each cardinal point was measured (sd_{cp}), its $\bar{sd}$, and SA were estimated. The following paragraphs report the results per species.

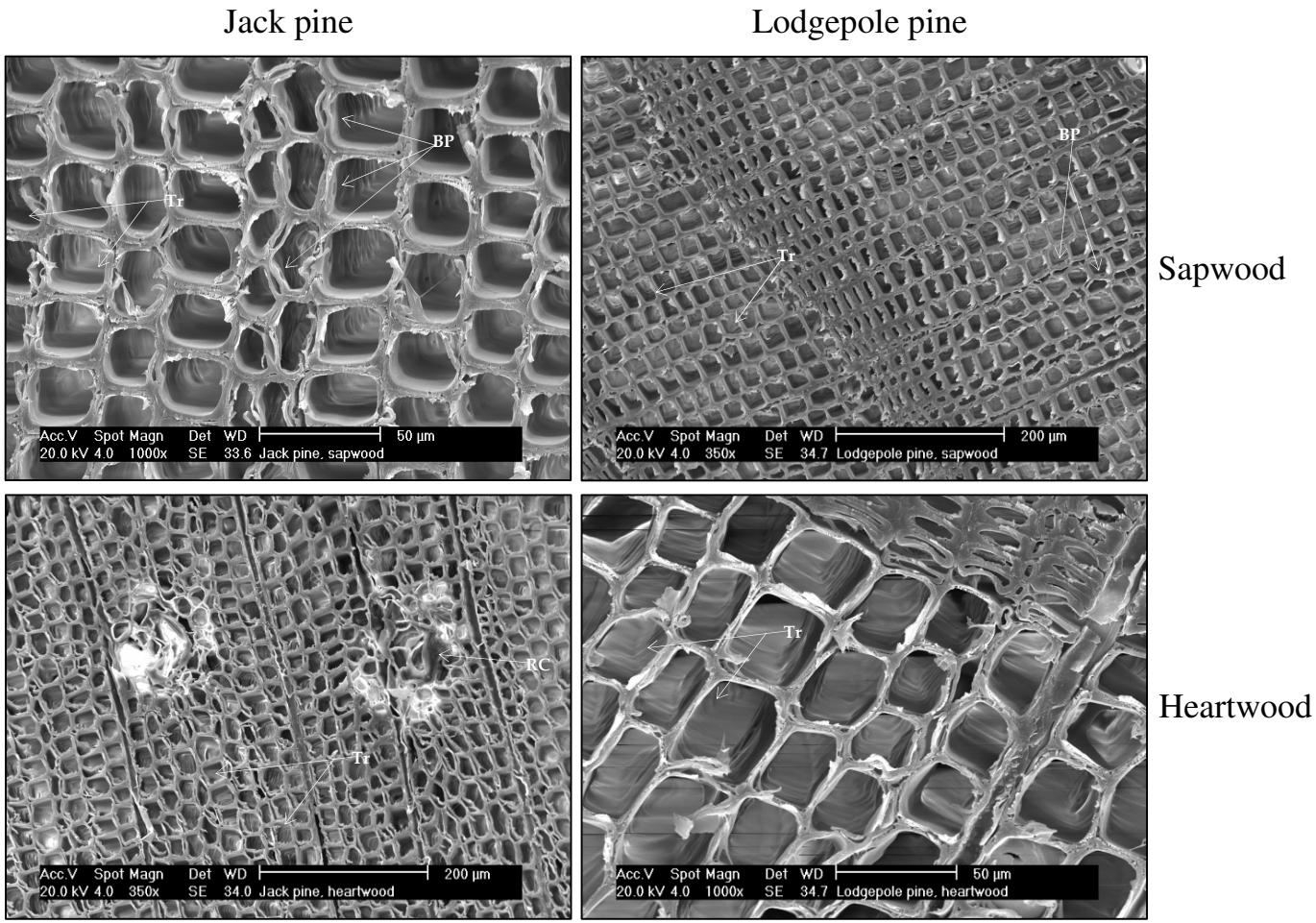

Figure 4.3: Scanning electron micrographs of Jack and Lodgepole pine stems tissues. Notice the clogged resin canals (RC) in the Jack pine heartwood. The sapwood micrographs show the bordered pits (BP) between tracheids (Tr).

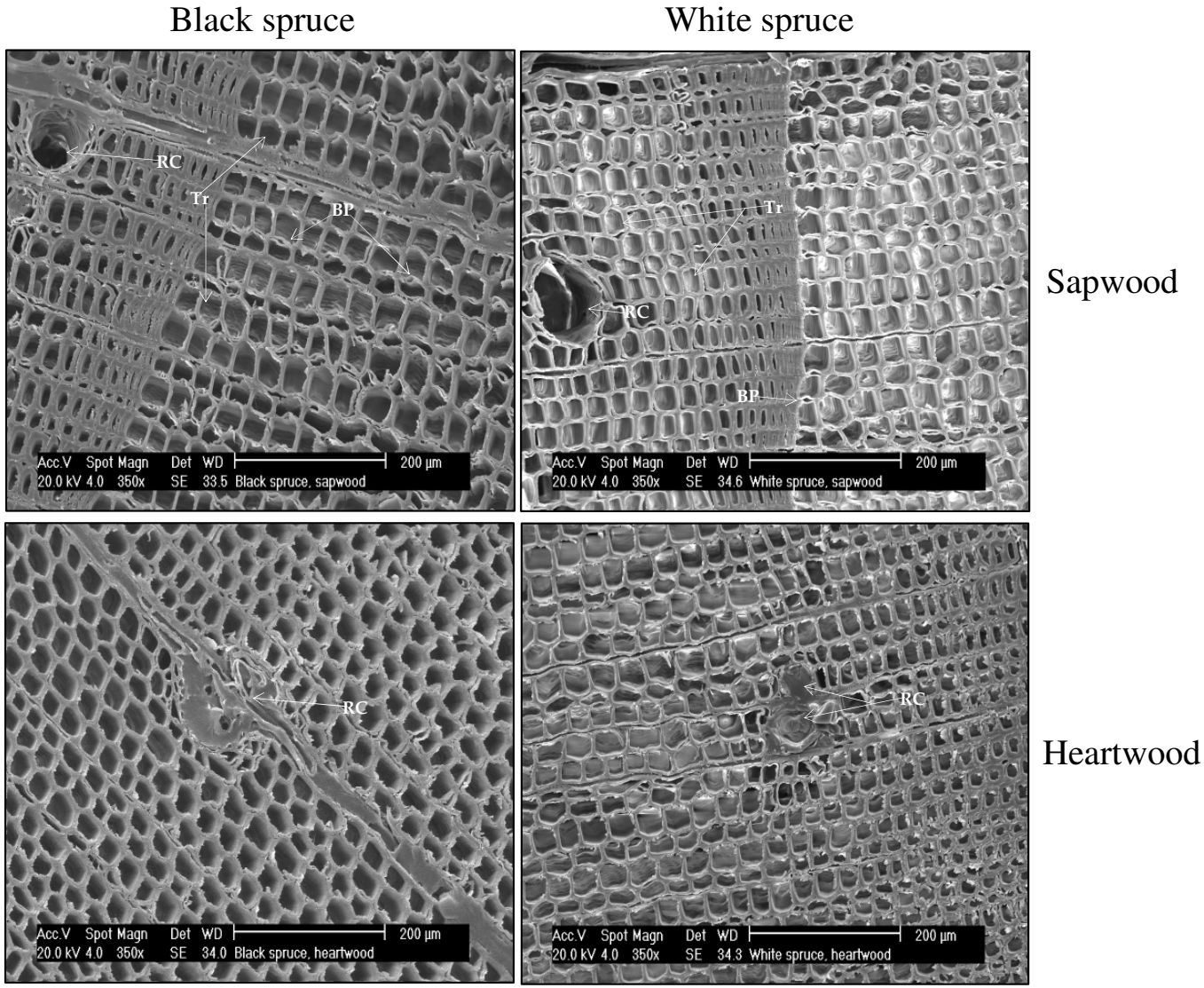

Figure 4.4: Scanning electron micrographs of Black and White spruce stems tissues. The sapwood micrographs for both species show open resin canals (RC) and bordered pits (BP) between tracheids. Notice that the resin canals are clogged in the heartwood tissues. The tracheids' walls look thicker as well.

Figure 4.5: Scanning electron micrographs of Trembling aspen stems tissues. On the right, micrographs are at a scale of $200\mu m$. Micrographs on the right are at higher magnification ($50\mu m$). The sapwood micrographs show the vessels (V) and fibers (F), and arrows show the lateral pitting between vessels. The heartwood vessels (T) do not conduct sap anymore since they are sealed by tyloses.

Jack pine. The tissues of 24 Jack pine trees (96 cores) were successfully analysed under the microscope. The remaining three individuals (12 cores) were analysed but sapwood depth was not measured, since the presence of tylosis (a mechanism to seal injured or dead parts [Tyree and Zimmermann (2002)]) in intermediate zones of the whole sapwood depth made it impossible to differentiate heartwood from sapwood. Therefore, the new Jack pine sample set remains a 24 individuals, whose DBH_{OB} range from 11.5cm to 23.9cm. Statistics of sapwood depths for the Jack pine sample set are given in Table 4.3.

Table 4.3: Basic statistics of the sd_{cp} values obtained from the Jack pine sample set (24 trees). Individual's DBH_{OB} ranges from 11.5cm to 23.9cm.

	Sapwood depth				
Cardinal point	**Maximum** (cm)	**Minimum** (cm)	**Mean** (cm)	**Mode** (cm)	**Variance** (cm^2)
North	5.20	1.34	3.37	3.30	0.89
South	5.06	1.25	3.05	2.10	0.91
East	5.90	1.90	4.00	4.00	1.01
West	5.20	2.00	3.54	3.00	0.62

Jack pine maximum sd_{cp} ranges from 5.06cm to 5.9cm. These maximum values are related to trees whose $DBH_{OB} \leq 17.83$ (i.e. the DBH_{OB} sample mean). The minimum sd_{cp} values pertain to trees whose $DBH_{OB} \leq 17.83cm$ with the exception of one tree whose $DBH_{OB} = 21.65cm$ (minimum $sd_W = 2.00cm$). For the Jack pine sample set, it could be told that the smallest sd_{cp} values pertain to trees whose DBH_{OB} is smaller than the sample mean; but also, the larger sd_{cp} were recorded for smaller trees. This suggests that trees' sapwood depth compensates the large sapwood growth in some sides with thinner sapwood depth in other sides of the trees, creating the well known heterogeneity of sapwood depth around the tree trunk. This is better observed with the following plots and statistical analyses. Here, what it is suggested is that the larger sapwood depths do not necessarily pertain to the larger trees, and the smaller sapwood depths do not necessarily pertain to the smaller trees.

Figure 4.6 is the Jack pine sample set dotplot showing the sapwood depth variability at each cardinal point. This figure shows that the largest variance is for sd_E values, with lower variations for sd_W and sd_N; also the South side registered low sd_S for most of the samples.

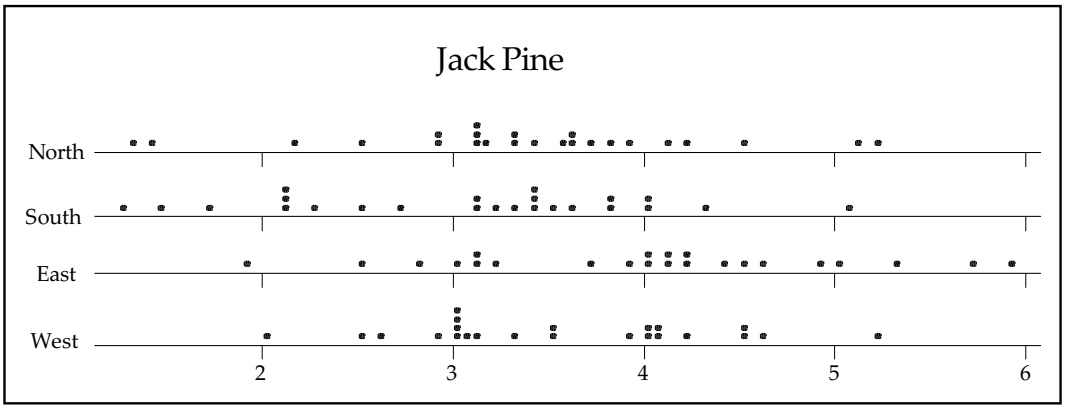

Figure 4.6: Dot plot of sd_{cp} values (cm) for the Jack pine sample set. Notice the wide spread of the data mostly for the South and East sides.

Each individuals's sd_{cp} values plotted against its DBH_{OB} is shown in Figure 4.7. The variance in each individual's sd_{cp} does not show a pattern with respect to its DBH_{OB}; that is, changes in sd_{cp} are not dependent on the increment of DBH_{OB}. On the contrary, each individual shows a pattern of variation in sd_{cp} around the tree. For instance, most of the individuals have a maximum, minimum, and intermediate sd_{cp} values, which in general gives large variance between sd_{cp} values (Figure 4.7). Once again, these results support the knowledge that sapwood depth varies along the tree trunk.

The next question is do the trees commonly grow thicker sapwood in certain directions versus others? It was observed that sixty six percent of the sample set has the largest sapwood depth at the North and East sides, while 68% has the shortest sapwood depth at the South and West sides; however, there were individuals having the largest sapwood depth at the South-West sides (34%) and the shortest at the North and East sides as well (32%). The results seem to indicate that there is a preference to grow larger sapwood

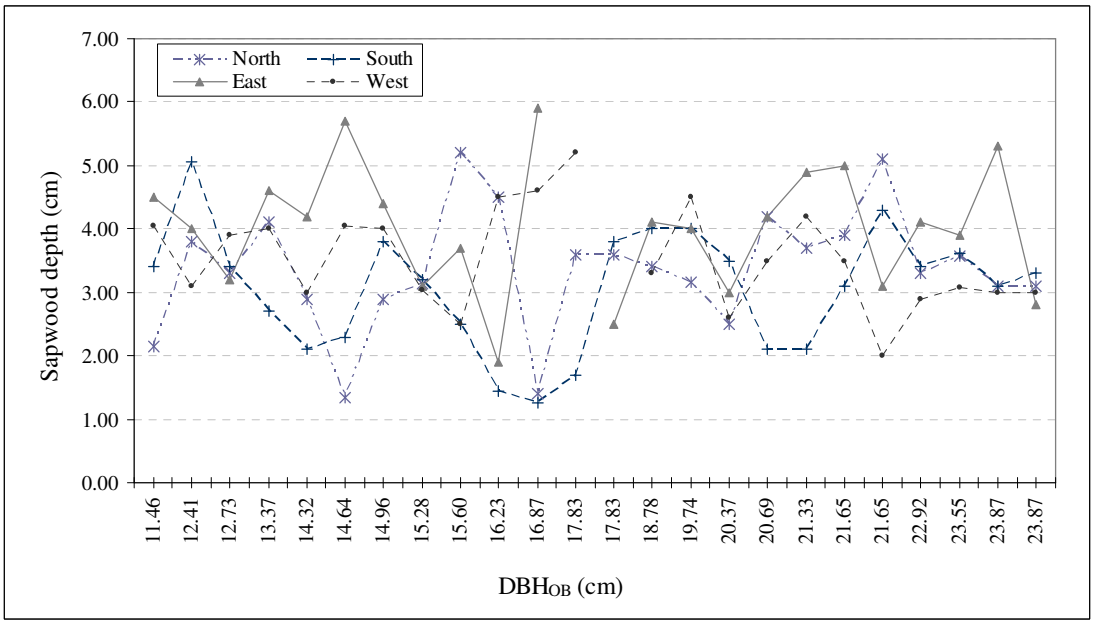

Figure 4.7: Jack pine sapwood depth per cardinal point (sd_{cp}) per each tree, versus its DBH_{OB}. Notice that two values are missing: one sd_E and one sd_W due to wood decay.

depth in a particular direction. In order to support these results, a one-way ANOVA with repeated measures was computed (Table 4.4). The statistical analysis suggests that indeed, cardinal direction has a significant effect on Jack pine sd_{cp} values ($\alpha = 0.05$). What can be concluded is that in this Jack pine sample set there is preference to grow in a specific cardinal direction. A pairwise comparison indicates that there is a significant statistical difference between the sd_S and sd_E (with Bonferroni P-value= 0.031). Also, a slight significant difference between the sd_E and sd_W (with Bonferroni P-value= 0.031) was also observed.

In order to observe how each individuals sd_{cp}'s variability behaves with respect to the tree size (i.e. if variance increases for certain DBH_{OB} classes), the 24 tree samples were grouped in diameter classes and the variance of sd_{cp} variances was calculated for each DBH_{OB} class. The highest sd_{cp} variance was for trees of the 6-inch class, while the lowest variance of sd_{cp} was recorded for trees larger than 8 inches (Table 4.5).

About 58% of the $2\bar{sd}$ values fall between $7.0cm$ and $8.0cm$ with a variance between

Table 4.4: One-way ANOVA Jack pine sd_{cp} as a response of cardinal direction (i.e. repeated measurements, $\alpha = 0.05$).

Source of variation	Degrees of Freedom	Sum of squares	Mean square	F_0	P-value
Cardinal direction	3	11.667	3.889	3.990	0.011
Residual Error	63	61.402	0.975		
Total	66	73.069			

Table 4.5: Variance of Jack pine trees sd_{cp} variances (cm^4) with respect to DBH_{OB}. To keep consistency with the forest survey classification, here the DBH_{OB} classes are reported in inches.

Diameter class (inches)	**Variance of variances** (depth)
4-5	1.47
6-7	3.62
8-9	0.43

$2\bar{sd}$ values of $0.1cm^2$. These $2\bar{sd}$ values pertain to trees with a DBH_{OB} ranging between $11.5cm$ to $23.9cm$ ($s^2 = 17.1cm^2$). The remaining 42% have $2\bar{sd}$ values between $5.8cm$ and $6.9cm$ (also a $s^2 = 0.1cm^2$, with DBH_{OB} values that range from $12.7cm$ to $20.4cm$, with a variance between DBH_{OB} values of $14.0cm^2$ (Figure 4.8). For those two individuals whose sd_E and sd_W are missing due to wood decay, the $\bar{sd}$ is the average of the remaining three sides.

With respect to the sapwood area (SA_{JP}), 25% of the sampled trees fall into the class of $120cm^2$, which corresponds to trees with a DBH_{OB} of $12.7cm$ to $15.2cm$; 16% have an SA_{JP} between $140 - 160cm^2$, corresponding to trees between $16.8cm$ and $20.4cm$. Also, trees with a DBH_{OB} between $21.3cm$ and $23.9cm$ fall into the SA_{JP} class of $200 - 220cm^2$ (Figure 4.9). However, in particular cases a large SA_{JP} is registered for relatively small trees that have a large sapwood depth. For instance, a tree with an SA_{JP} of $194.15cm^2$ registered a $2\bar{sd}$ of $7.83cm$ and a DBH_{OB} of $19.7cm$. As it can

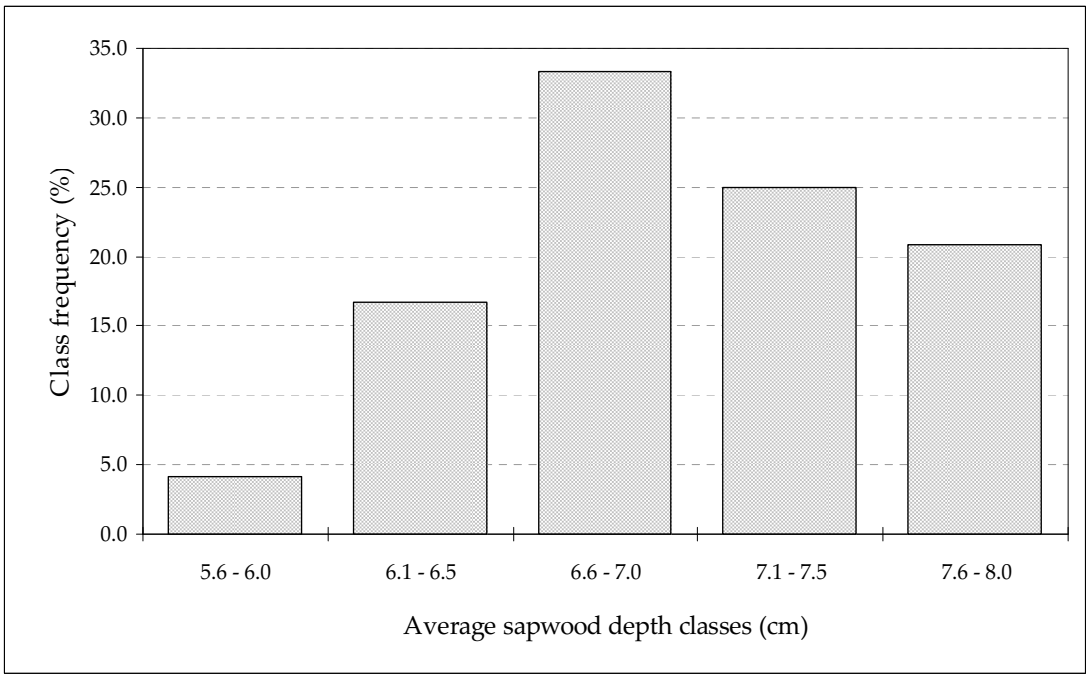

Figure 4.8: Jack pine sample set histogram of $2\bar{sd}$ values.

be appreciated in Figure 4.10[1], the increments in SA_{JP} do not correspond to sapwood depth increments, but to tree size. It means that trees with a large DBH_{OB} could have smaller or similar sapwood depths than trees with a small DBH_{OB}; however, the larger trees will still be observed to have a larger sapwood area due to their larger DBH_{OB}. It is also appreciated in this plot that $2\bar{sd}$ does not increases as the trees' DBH_{OB} increases, which raises the assumption that in mature Jack pine, the sapwood depth may be quasi constant as the individual grows (at least when its DBH_{OB} grows from $11.5cm$ to $23.9cm$). This constancy in sapwood depth was also found by Granier et al. (1996), curiously, for eight different rain forest species.

[1]This plot is an unconventional way of presenting this type of data. A scatterplot over a bar graph is normally preferred. However, the author feels that this graph explicitly shows which values pertain to each tree. Be aware of the x-axis scale, which is not continuous. Furthermore, scatterplots of the data proved that the scale does not trick the eye with respect to the lack of continuity. This same comment applies for the rest of the species.

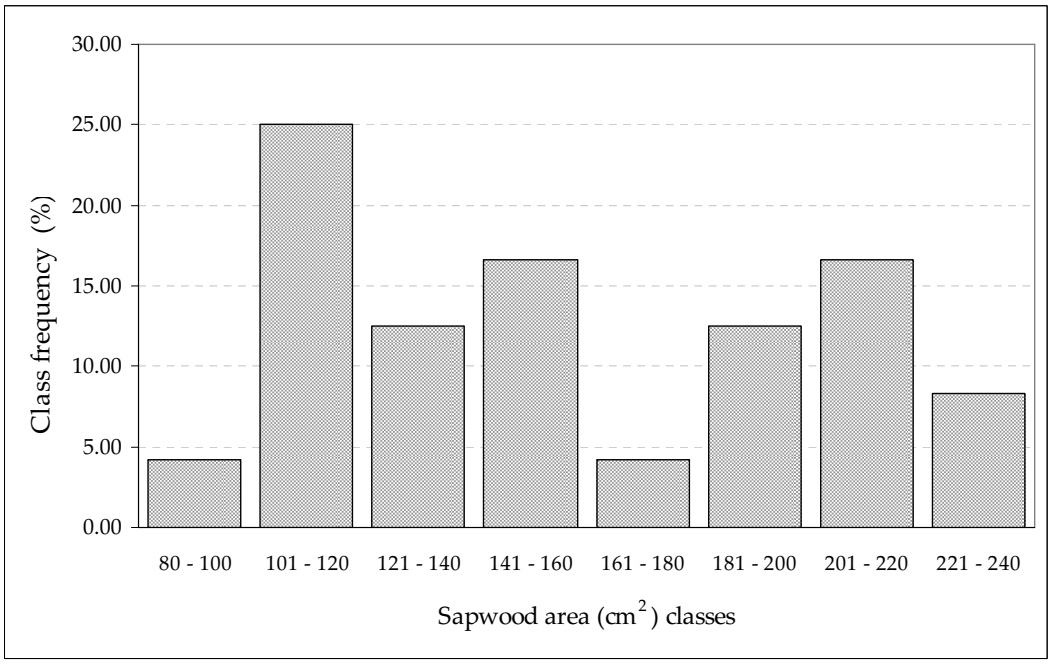

Figure 4.9: Jack pine sample set histogram of SA_{JP} values.

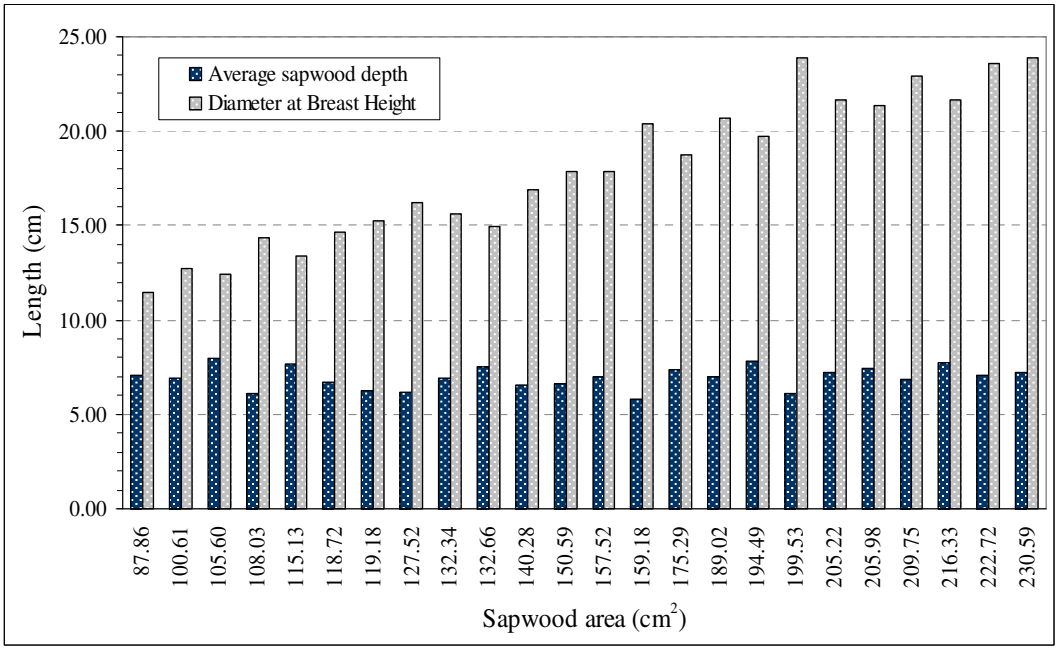

Figure 4.10: Bar graph showing values of SA_{JP}, DBH_{OB} and $2\bar{sd}$ register values for each Jack pine individual. Observe how much of the total DBH_{OB} length of each tree is sd_{cp}.

Lodgepole pine. Jack pine and Lodgepole pine pertain to the same taxonomic group and they have a similar vascular structure (personal observation); therefore, it is felt that sapwood depth and sapwood area estimates for both Jack pine and Lodgepole pine can be obtained by integrating their sample sets. The Paired t-test was applied to analyse if the mean values of the two sample sets are the same. From the results, the confidence interval for the mean difference between the two sets of $\bar{sd}$ suggests a similarity between them (the interval includes zero: $-0.77, 0.061$); furthermore, the resultant P-value of the Paired t-test ($\simeq 0.1$) suggests that the two sample sets are from the same population type ($\alpha = 0.05$). Thus, the Lodgepole pine sapwood depth estimations of 9 individuals (35 cores) were integrated into the set of Jack pine for setting allometric correlations. The following analysis is just on Lodgepole pine individuals; statistics of sapwood depths for the Lodgepole pine sample set are given in Table 4.6.

Table 4.6: Basic statistics of the sd_{cp} values obtained from the Lodgepole pine sample set. Individual's DBH_{OB} ranges from $16.5cm$ to $30.9cm$.

	Sapwood depth				
Cardinal point	**Maximum** (cm)	**Minimum** (cm)	**Mean** (cm)	**Mode** (cm)	**Variance** (cm^2)
North	5.10	2.00	3.40	2.20	1.17
South	4.80	3.70	3.75	4.30	0.11
East	5.80	0.90	2.93	2.00	2.63
West	4.80	2.40	3.70	4.10	0.44

At the four cardinal points, maximum values range from $4.80cm$ to $5.80cm$. These maximum values pertain to trees whose $DBH_{OB} > 23.80cm$ (i.e. the DBH_{OB} sample mean). The sd_{cp} minimum values that range from $0.9cm$ to $3.70cm$ were recorded for trees whose $DBH_{OB} > 23.80cm$. For this particular sample set, it could be told that the smallest sd_{cp} values pertain to trees whose DBH_{OB} is larger than the sample mean; but also, the larger sd_{cp} were recorded for larger trees. Also, these results denote the heterogeneous sapwood growth pattern around the tree trunk. For instance, the smallest sd_{cp} ($0.9cm$) was found in the East side of one of the largest trees ($DBH_{OB} \simeq 27.40$).

As a consequence, such a small sd_E value makes the sd_{cp} considerable larger at the other cardinal points (e.g. this tree sd_N is $5.10cm$). The smallest variance was observed for the sd_S and sd_W set of values, while larger variances in sd_{cp} were registered for the East and North sides (Figure 4.11). These variations in sapwood depth around every tree trunk were definitely expected.

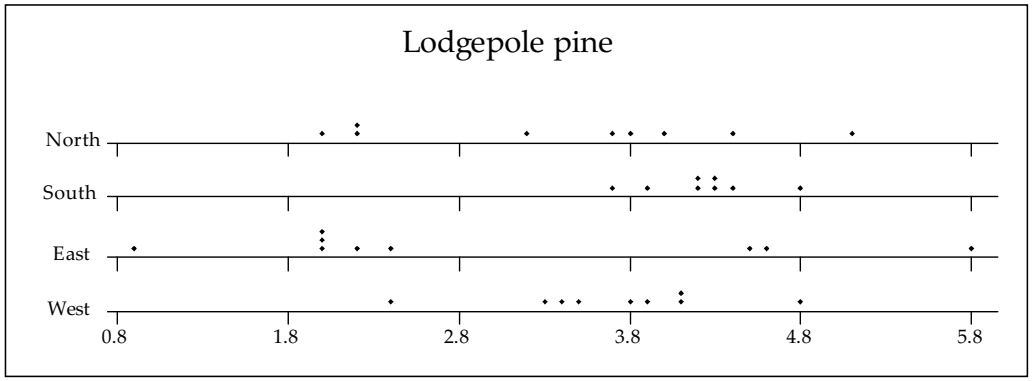

Figure 4.11: Dot plot of sd_{cp} values (cm) for the Lodgepole pine sample set. Notice the wide spread of the data mostly for the North and East sides.

Also, these sapwood depth variations around the tree trunk cause one to observe a maximum, minimum, and intermediate sd_{cp} values in every tree. Each individual's sd_{cp} values were plotted against its DBH_{OB} is shown in Figure 4.12. From the Lodgepole pine sample set, 33.3% has the largest sapwood depths at the East side, 33.3% at the North side, and 33.3% at the South side. Just 11% of the sample has the shortest sapwood depth in the West side, 67% at the East side, and 22% at the North side. A one-way ANOVA with repeated measurements shows that cardinal direction does not have a significant effect on Lodgepole pine sd_{cp} values (Table 4.7). This may imply that Lodgepole pine does not have a preference to growth thicker or thinner sapwood in any direction.

Figure 4.12 also shows that each individual's sd_{cp} does not show a pattern with respect to its DBH_{OB} (i.e. sd_{cp} does not increases as DBH_{OB} increases), and these results are similar to the results observed for the Jack pine sample set. These conclusions

Table 4.7: One-way ANOVA Lodgepole pine sd_{cp} as a response of cardinal direction (i.e. repeated measurements, $\alpha = 0.05$).

Source of variation	Degrees of Freedom	Sum of squares	Mean square	F_0	P-value
Cardinal direction	3	3.83	1.28	0.73	0.546
Residual Error	24	42.17	1.76		
Total	35	54.41			

are supported by the one-way ANOVA testing the hypothesis of the means of DBH_{OB} and sd_{cp} being equal (Table 4.8). With the one- way ANOVA results, it is observed that there is not significant difference between the mean values of sd_{cp} and DBH_{OB} (assuming that sd_{cp} is independent of the cardinal direction). Thus, it can be said that in Lodgepole pine, incremental growth in DBH_{OB} does not directly drive sd_{cp} growth.

Table 4.8: One-way ANOVA between Lodgepole pine sd_{cp} and DBH_{OB}. The null hypothesis (H_o) tests the equality between the sd_{cp} and DBH_{OB} means, where sd_{cp} is the response value ($\alpha = 0.05$).

Source of variation	Degrees of Freedom	Sum of squares	Mean square	F_0	P-value
DBH_{OB}	6	8.26	1.38	0.87	0.532
Residual Error	29	46.15	1.59		
Total	35	54.41			

About 67% of the $2\bar{sd}$ values fall between $7.2cm$ and $7.9cm$ with a variance between $2\bar{sd}$ values of $0.03cm^2$. These $2\bar{sd}$ values pertain to trees with a DBH_{OB} ranging between $16.5cm$ to $30.9cm$ ($s^2 = 35.3cm^2$). The 33% left have $2\bar{sd}$ values between $6.0cm$ and $6.3cm$ ($s^2 = 0.004cm^2$), with DBH_{OB} that range from $20.0cm$ to $26.1cm$, and a variance between DBH_{OB} values of $12.2cm^2$ (Figure 4.13). Since $2\bar{sd}$ values had a range within one centimetre, the $2\bar{sd}$ variability for this set of individuals is relatively small ($s^2 = 0.4cm^2$).

With respect to the sapwood area (SA_{LP}), about 56% of the sampled trees fall into

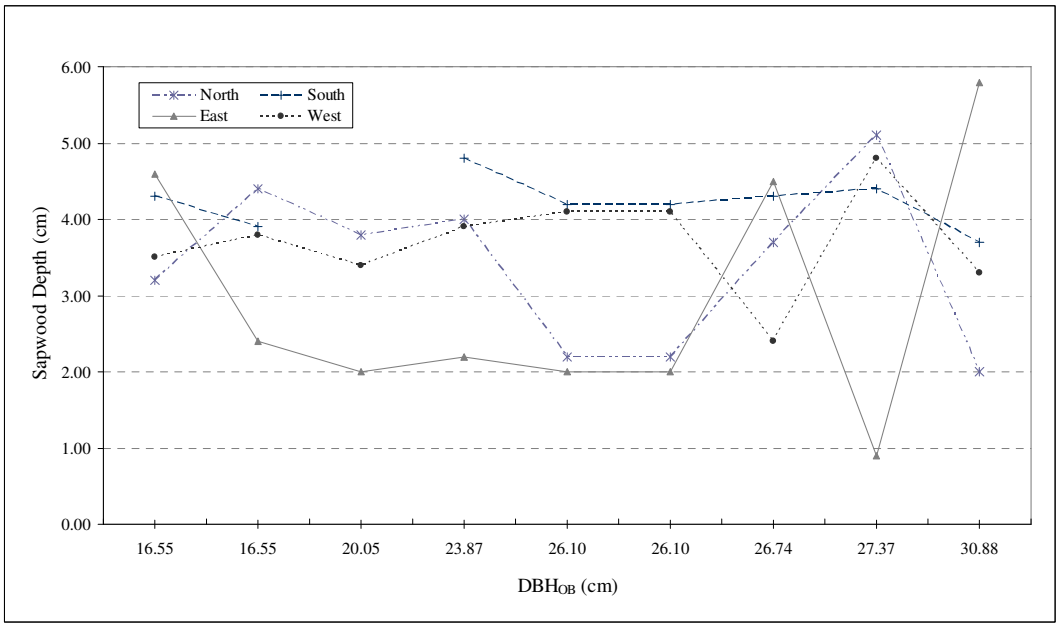

Figure 4.12: Sapwood depth per cardinal point (sd_{cp}) per each tree, versus its DBH_{OB} for Lodgepole pine.

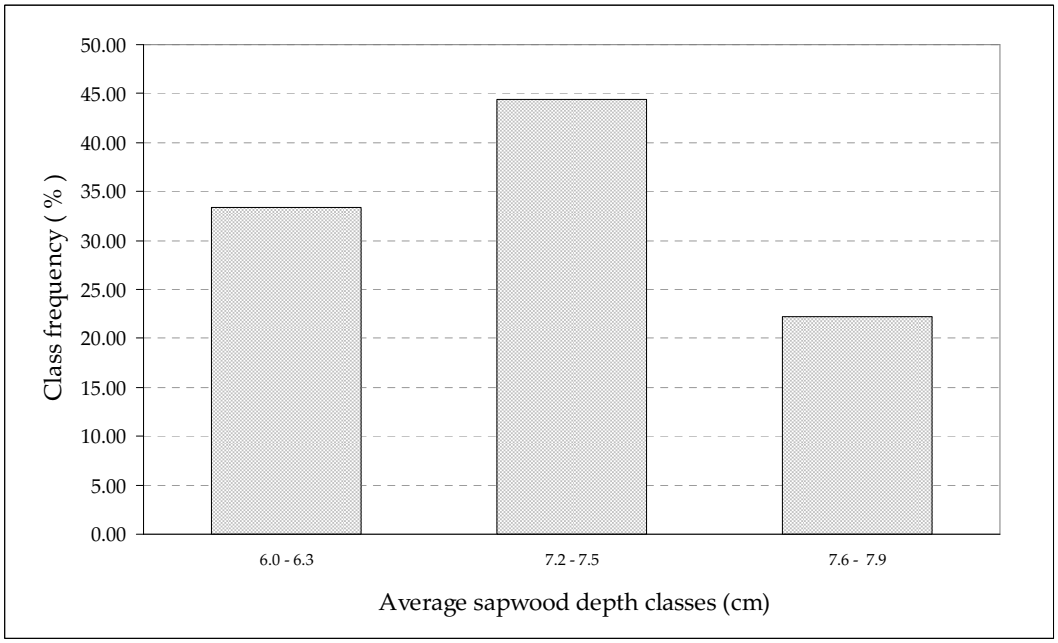

Figure 4.13: Lodgepole pine sample set histogram of $2\bar{sd}$ values.

the class of $150 - 250cm^2$, which corresponds to trees with a DBH_{OB} of $16.5cm$ to $23.9cm$; 33% have an SA_{LP} between $250 - 350cm^2$, corresponding to trees between $26.7cm$ and $30.9cm$ in DBH_{OB}. Also, one tree with a DBH_{OB} of $16.5cm$ falls into the SA_{LP} class of $150cm^2$ (Figure 4.14).

Figure 4.15 shows the corresponding values of $2\bar{sd}$ and DBH_{OB} for each tree's estimated SA_{LP}. Trees between $160cm^2$ and $225cm^2$ in SA_{LP} (DBH_{OB} of $20 - 26cm$) have $2\bar{sd}$ ranging from $6.13cm$ to $6.25cm$ ($s^2 = 0.004cm^2$). As Lodgepole pine individuals reach a DBH_{OB} of $26 - 30cm$ and SA_{LP} of $225 - 235cm^2$, the $2\bar{sd}$ is between $7.25 - 7.45cm$ for this group of trees. As observed with Jack pine individuals, the increments in SA_{JP} do not correspond to sapwood depth increments, but to the tree size. Two individuals whose DBH_{OB} is $16.5cm$, have an SA_{LP} of $145cm^2$ and $155cm^2$, while the $2\bar{sd}$ are $7.25cm$ and $7.8cm$. As mentioned, the $2\bar{sd}$ variance for this set of individuals is relatively small ($s^2 = 0.4cm^2$); now, it is observed that the largest $2\bar{sd}$ difference between bigger and smaller trees is $1.7cm$ and that the lowest is 0.0. Thus, it might be concluded that the differences between $2\bar{sd}$ is due to some random error; that sapwood depth does not vary as the tree grows; and SA_{LP} becomes larger due to the individual's bigger basal area. These are the same conclusions made for Jack pine. In order to support these conclusions, the variance of $2\bar{sd}$ variances per SA_{LP} class was computed. The computed variance of variances is $0.04cm^8$, which is a negligible value; hence, it is concluded that the difference in $2\bar{sd}$ is negligible as well. Table 4.9 displays the obtained results that support previous conclusions.

Table 4.9: Computed $2\bar{sd}$ variance per SA_{LP} class and the variance of variances of the three classes.

SA_{LP} **class** (m^2)	**Variance per class** (m^4)	**Variance of variances**
145-155	0.15	
160-225	0.39	
225-235	0.007	
		$0.04m^8$

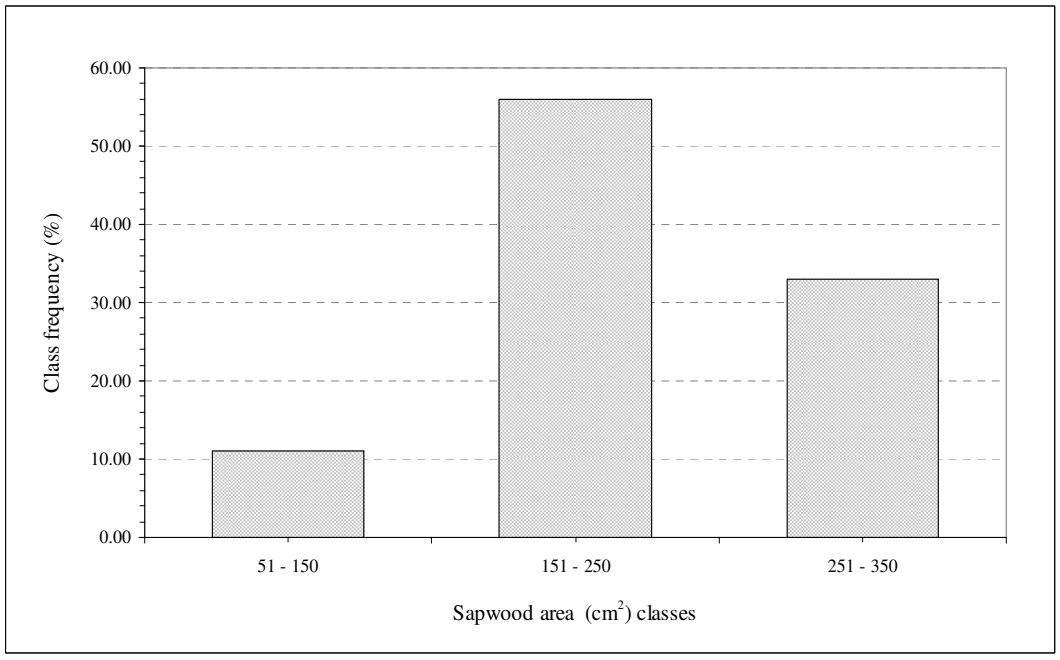

Figure 4.14: Lodgepole pine sample set histogram of SA_{LP} values.

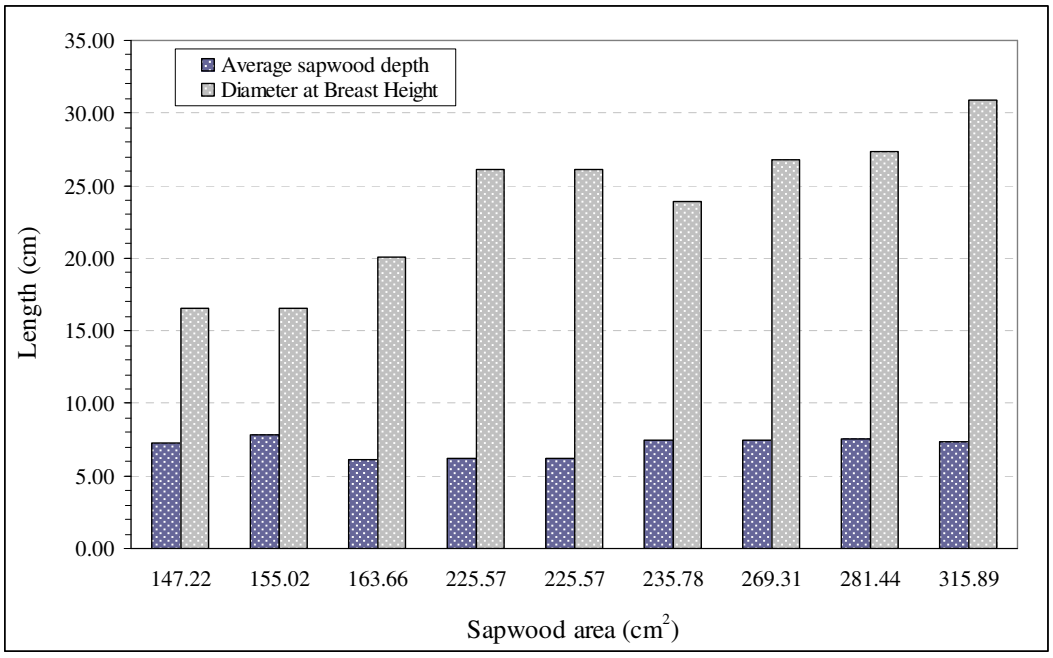

Figure 4.15: Bar graph showing values of SA_{LP}, DBH_{OB} and $2\bar{sd}$ register values for each Lodgepole pine individual.

Trembling aspen. Mensuration of sapwood depth was done in 26 Trembling aspen individuals (104 cores). Due to the anatomical structure of this species, it was the most complex one to microscopically differentiate sapwood-heartwood boundaries. During the analysis of the Trembling aspen sample set, 9 sampled trees (36 samples) were lost due to the complexity involved in differentiating the wood structure. The remaining 26 samples not only were analysed through this method, but also through the difference in colour (see § 4.3.4 for results). DBH_{OB} ranges from $9.5cm$ to $38.2cm$. Statistics per cardinal point for the Trembling aspen sample set are given in Table 4.10.

Table 4.10: Basic statistics of the sd_{cp} values obtained from the Trembling aspen sample set. Individual's CBH_{OB} ranges from $9.5cm$ to $38.2cm$.

Cardinal point	**Sapwood depth**				
	Maximum (cm)	**Minimum** (cm)	**Mean** (cm)	**Mode** (cm)	**Variance** (cm^2)
North	7.90	0.50	4.27	4.40	4.81
South	9.90	1.20	4.70	7.00	6.06
East	13.90	0.00	4.26	4.40	9.85
West	7.80	0.00	3.98	1.10	6.56

Maximum sd_{cp} ranges from $7.80cm$ to $13.90cm$ ($s^2 = 8.14cm^2$), and minimum sd_{cp} from $0.5cm$ to $1.20cm$ ($s^2 = 0.32cm^2$). Maximum sd_{cp} values correspond to trees whose $DBH_{OB} > 22.9cm$ (i.e. the average DBH_{OB}), while minimum sd_{cp} were measured in trees whose $9.55cm \geq DBH_{OB} \leq 27.60cm$. In this case, Trembling aspen maximum sd_{cp} values were related to the trees larger than the average DBH_{OB}, while minimum sd_{cp} were found either in trees larger or smaller than the average DBH_{OB}.

The Trembling aspen sd_{cp} values are shown in Figure 4.16. The variances of sd_{cp} are the largest of the five studied species (see also Table 4.10), being for sd_E the largest variance of the whole data set, followed by the West and South sides. The lowest sd_{cp} variance is registered in the North side. The large sd_{cp} values in Trembling aspen concur with the knowledge that angiosperms vascular tissues are less efficient to transport water (Tyree and Zimmermann, 2002); thus, more sapwood area is required to fulfill the tree's water demands.

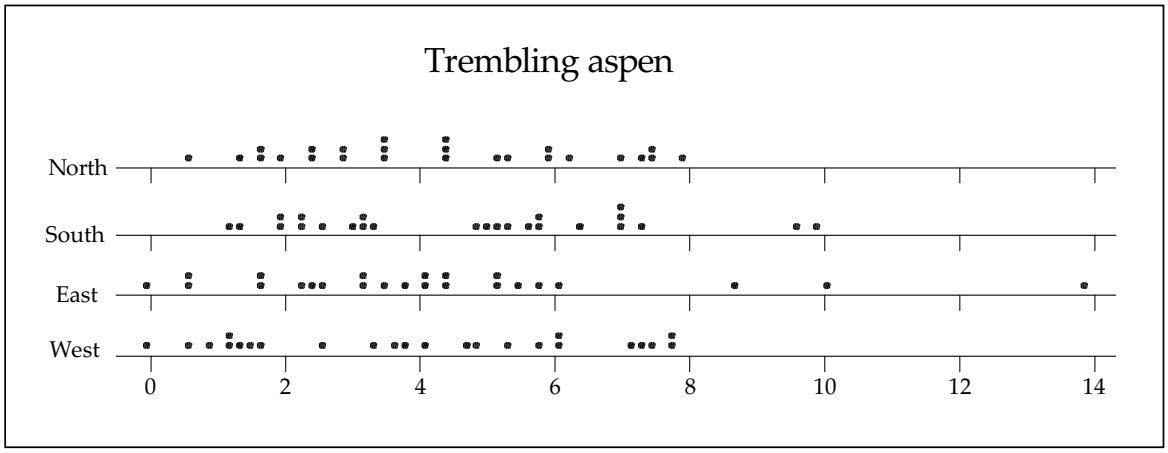

Figure 4.16: Dot plot of sd_{cp} values (cm) for the Trembling aspen sample set. Notice the wide spread of the data mostly for the South and East sides.

Each individual's sd_{cp} values were plotted against its DBH_{OB} and is shown in Figure 4.17. Every individual's sd_{cp} value shows a pattern with respect to its DBH_{OB}; that is, sd_{cp} tend to increase as DBH_{OB} increases. The ANOVA for observing the relationship between sd_{cp} and DBH_{OB} (Table 4.11) shows that changes in sd_{cp} respond to changes in DBH_{OB} (assuming that sd_{cp} is independent of the cardinal direction) as well.

Table 4.11: One-way ANOVA between Trembling aspen sd_{cp} and DBH_{OB}. The null hypothesis (H_o) tests the equality between the sd_{cp} and DBH_{OB} means, where sd_{cp} is the response value ($\alpha = 0.05$).

Source of variation	Degrees of Freedom	Sum of squares	Mean square	F_0	P-value
DBH_{OB}	20	412.78	20.64	7.97	<0.001
Residual Error	75	194.24	2.59		
Total	95	607.02			

What remains similar to the coniferous trees is that each individual shows a pattern of variation in sd_{cp} around the tree (i.e. individuals have a maximum, minimum and intermediate sd_{cp} value). The largest variance between sd_{cp} for a single tree occurs for

the bigger trees (DBH_{OB} from $27.7cm$ to $38.2cm$). Fifty eight percent of the sample set has the largest sapwood depth at the North and East sides, while 50% has the shortest sapwood depth at the South and West sides; also, there are individuals having the largest sapwood depth at the South-West sides (42%) and the shortest at the North and East sides as well (38.5%). About 11.5% of the sample set register the same minimum sd_{cp} at their North-East, North-West and East-West sides (Figure 4.17). A one-way ANOVA with repeated measurements ($\alpha = 0.05$) suggests that there is no significant cardinal direction effect on sd_{cp} (Table 4.12). Thus, it seems that there is not preference to growth thicker or thinner sd_{cp} in a specific direction.

Table 4.12: One-way ANOVA Trembling aspen sd_{cp} as a response of cardinal direction (i.e. repeated measurements, $\alpha = 0.05$).

Source of variation	Degrees of Freedom	Sum of squares	Mean square	F_0	P-value
Cardinal direction	3	9.85	3.28	0.733	0.536
Residual Error	75	332.78	4.48		
Total	78	342.73			

As it is shown in Figure 4.18, the range of $2\bar{sd}$ values for Trembling aspen have a larger range than any of the coniferous species reported here. The $2\bar{sd}$ ranges from minimum values of $1.95cm$ to a maximum of $18.1cm$. About 50% of the $2\bar{sd}$ values fall between $8.1cm$ and $12.0cm$ with a variance between $2\bar{sd}$ values of $1.5cm^2$. These $2\bar{sd}$ values pertain to trees with a DBH_{OB} ranging between $11.4cm$ to $30.1cm$ ($s^2 = 39.33cm^2$). About 15.4% of the $2\bar{sd}$ fall into the $4cm$ class ($s^2 = 0.3cm^2$) with DBH_{OB} values ranging between 13.4 and $21cm$ ($s^2 = 12.8cm^2$). The 11.5% of the Trembling aspen sample set falls into the $6cm$ class, with DBH_{OB} values of $17.8cm$ and $20.05cm$ ($s^2 = 1.6cm^2$). This $6cm$ class has the lowest $2\bar{sd}$ variance ($s^2 = 0.09cm^2$). The 19.2% falls into the $14cm$ and $2\bar{sd} > 14.1cm$ classes, with $2\bar{sd}$ variances of $0.9cm^2$ and $3.8cm^2$ respectively. DBH_{OB} of these last two classes range between $22.9cm - 23.2cm$ ($s^2 = 0.05cm^2$) and $28.6 - 38.20cm$ ($s^2 = 26.2cm^2$) respectively. Notice as well that the

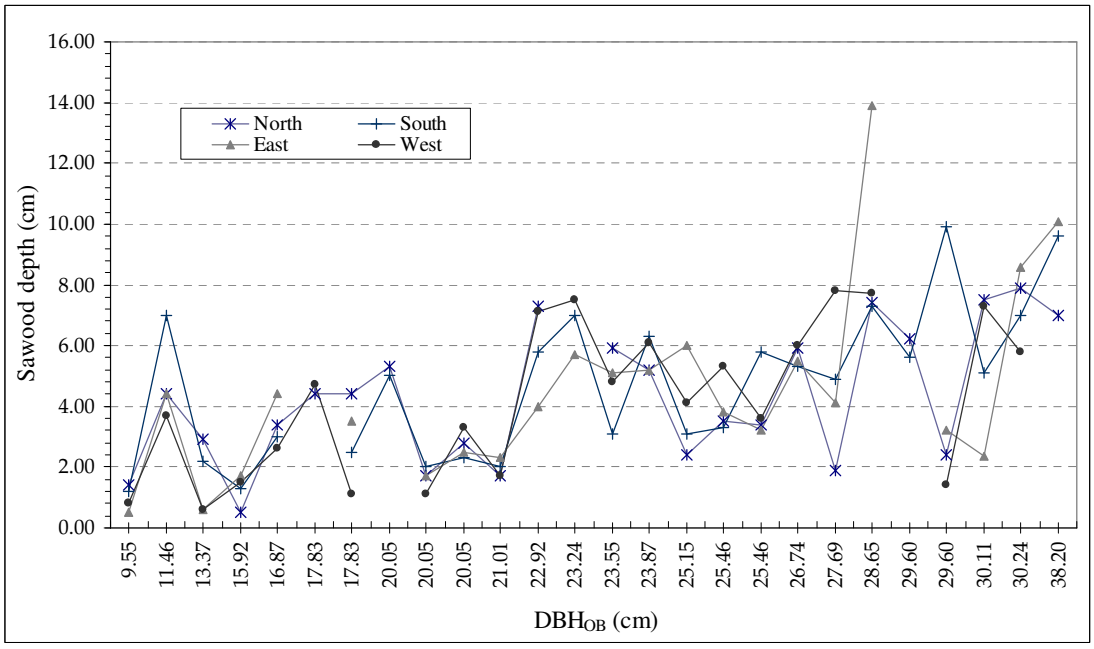

Figure 4.17: Sapwood depth per cardinal point (sd_{cp}) per each tree, versus its DBH_{OB} for Trembling aspen.

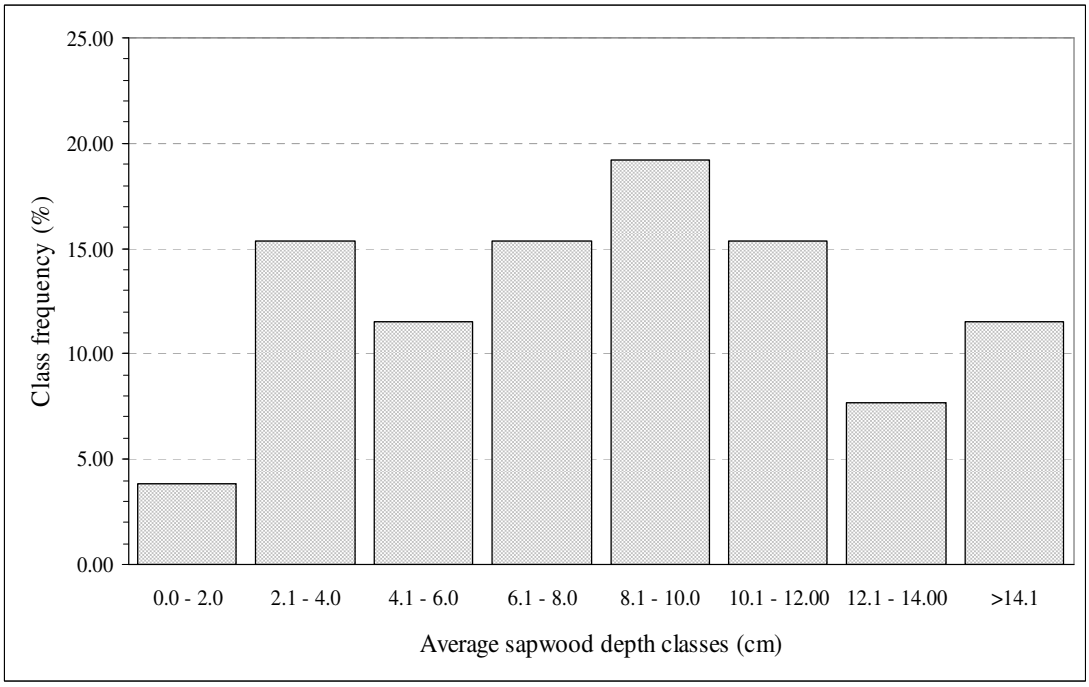

Figure 4.18: Trembling aspen sample set histogram of $2\bar{sd}$ values.

$2\bar{sd}$ histogram shows a distribution close to Normal. The remaining 3.9% falls into the $2cm$ class that includes trees with a DBH_{OB} ranging between $9.5cm - 21.01cm$.

With respect to the sapwood area (SA_{TA}), 42% of the sampled trees fall into the class of $200cm^2$, whose DBH_{OB} is between $9.55cm$ and $21.0cm$. About 38.5% have an SA_{TA} between $201 - 400cm^2$ with DBH_{OB} values in the range of $22.9 - 29.6cm$. The SA_{TA} class of $600cm^2$ gathers 15.5% of the whole sample set, whose DBH_{OB} is between $28.7cm$ and $30.2cm$. The last class includes the sample set's largest tree that reached an SA_{TA} of $819.2cm^2$ (Figure 4.19).

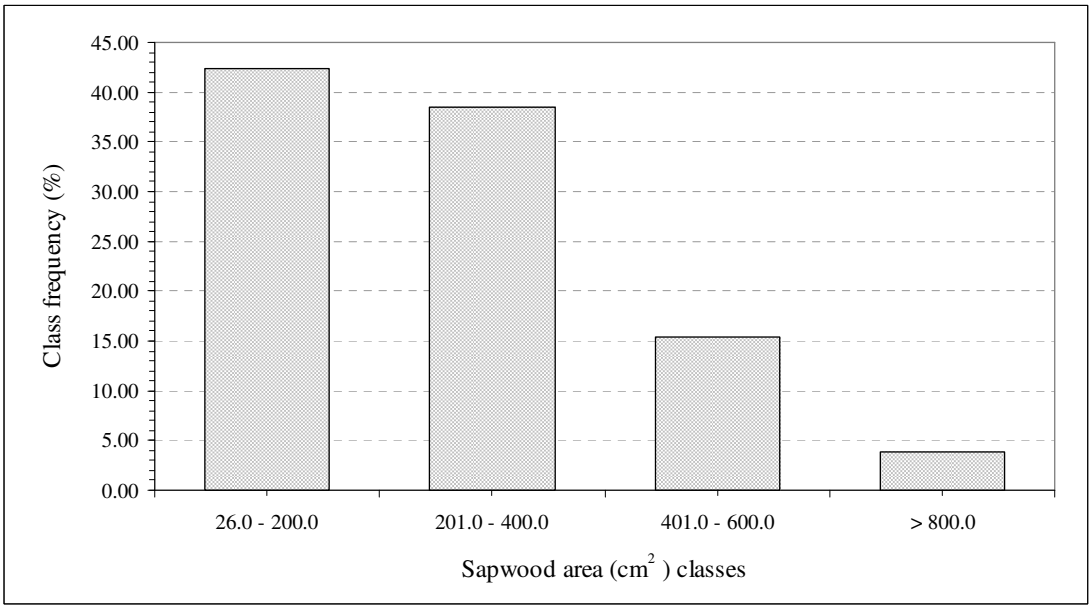

Figure 4.19: Trembling aspen sample set histogram of SA_{TA} values.

Figure 4.20 shows the corresponding values of $2\bar{sd}$ and DBH_{OB} for each tree's estimated SA_{TA}. In the whole sample set, there is a large variability in both $2\bar{sd}$ and DBH_{OB} as SA_{TA} increases. The clearest trend is for the last six individuals, where $2\bar{sd}$ increases together with size (DBH_{OB}) and SA_{TA}. From this figure, it can be appreciated that sapwood area depends on both individual's DBH_{OB} and $2\bar{sd}$. Small individuals can reach large SA_{TA} if $2\bar{sd}$ is large (e.g. individual whose SA_{TA} is $558.02cm^2$), and vice versa, larger trees have a small SA_{TA} if $2\bar{sd}$ is small (e.g. individual whose SA_{TA} is $148.35cm^2$).

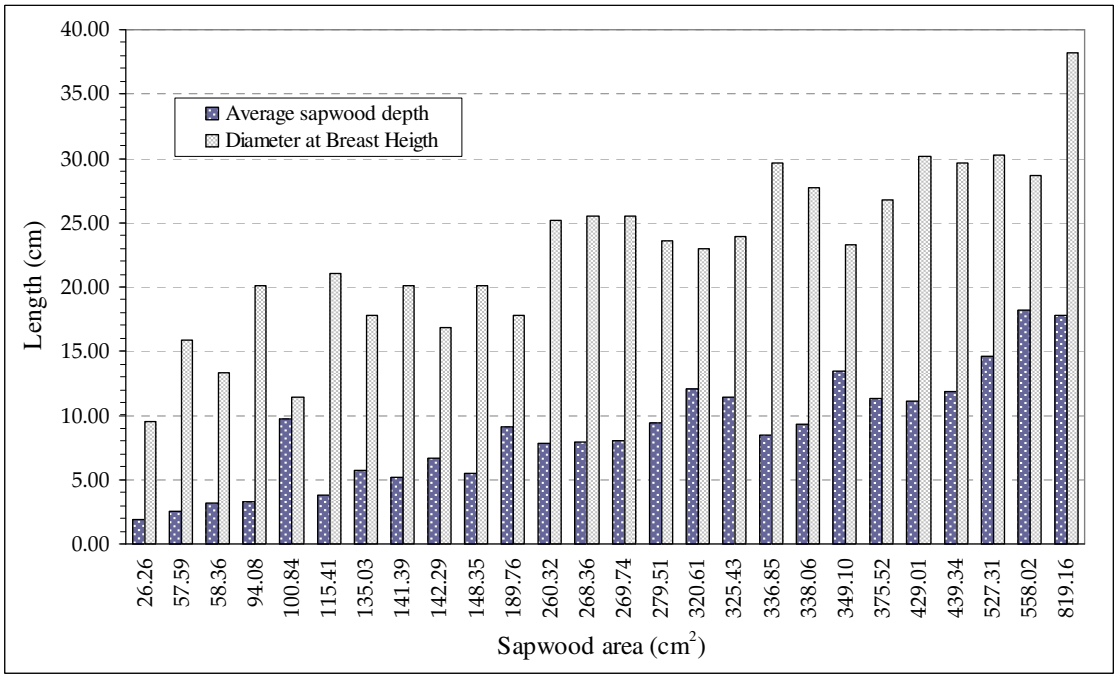

Figure 4.20: Bar graph showing values of SA_{TA}, DBH_{OB} and $2\bar{sd}$ values for each Trembling aspen individual.

Black spruce. Twenty two Black spruce trees (88 cores) out of 33 were suitable for analysis with the microscope. This coniferous species presented several problems due to wood decay and malformations that made the differentiation of sapwood-heartwood boundaries difficult. As a consequence, 11 trees were dismissed from the sample set, and 6 of them were the ones collected in Whitecourt. Finally, the new Black spruce sample set remains with 22 individuals, with DBH_{OB} ranging from $9.5cm$ to $37.9cm$. In this sample set, an outlier was found on the West side of an individual with a DBH_{OB} of $15.28cm$ ($sd_{cp} = 7.30cm$). Statistics of sapwood depths for the Black spruce sample set are given in Table 4.13.

Table 4.13: Basic statistics of the sd_{cp} values obtained from the Black spruce sample set. Individual's DBH_{OB} ranges from $9.55cm$ to $37.88cm$.

Cardinal point	**Sapwood depth**				
	Maximum (cm)	**Minimum** (cm)	**Mean** (cm)	**Mode** (cm)	**Variance** (cm^2)
North	5.00	1.60	3.20	2.72	0.92
South	5.10	0.90	3.12	0.90	1.98
East	6.00	0.60	3.64	3.30	2.49
West	5.80	0.90	3.36	0.90	1.82

Maximum sd_{cp} values range between $5.00cm$ and $6.00cm$ that pertain to trees whose $9.55cm < DBH_{OB} \leq 24.51cm$. Minimum sd_{cp} values range between $0.60cm$ and $1.60cm$ that pertain to trees whose $9.55cm \leq DBH_{OB} \leq 27.06cm$. Thus, it seems that sd_{cp} indistinctly grows around the tree trunk; or at least, with this sample set there is no evidence to correlate thicker/thinner sd_{cp} to larger/smaller trees.

The last column of Table 4.13 shows each cardinal point's sapwood depth variance; this is also appreciated in Figure 4.21. The smallest variance is registered for the sd_N values, followed by the sd_W values. On the other hand, sd_S values register a slightly larger variance than sd_W values; however, the largest variance is registered for the sd_E values. Note that these sd_{cp} values have similar patterns to the Lodgepole pine and Jack pine individuals.

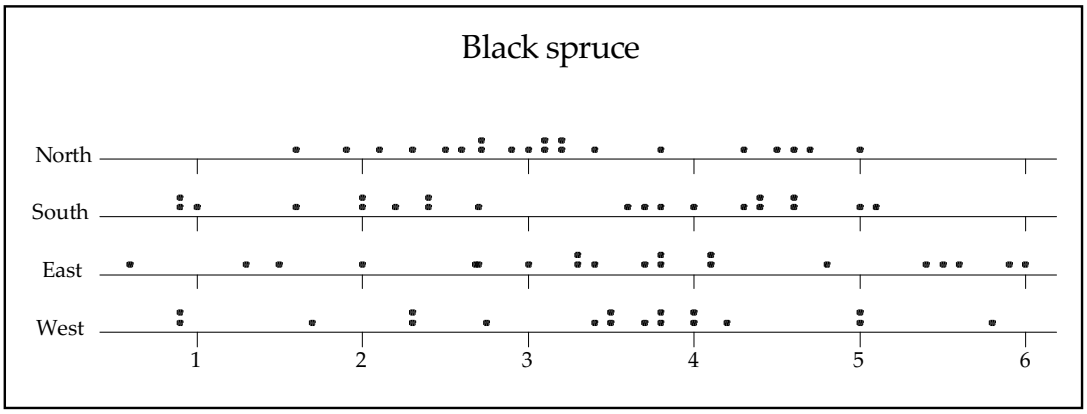

Figure 4.21: Dot plot of sd_{cp} values (cm) for the Black spruce sample set. Notice the wide spread of the data mostly for the West and East sides.

Each individuals's sd_{cp} value is plotted against its DBH_{OB} and is shown in Figure 4.22. The variance in each individual's sd_{cp} values does not show a clear pattern with respect to its DBH_{OB}. However, ANOVA results concluded that there is still a significant difference between the mean values of sd_{cp} and DBH_{OB} (Table 4.14). In this particular case, the regression analysis will conclusively demonstrate the correlation between the Black spruce average sd_{cp} and DBH_{OB} (Chapter 5).

Table 4.14: One-way ANOVA between Black spruce sd_{cp} and DBH_{OB}. The null hypothesis (H_o) tests the equality between the sd_{cp} and DBH_{OB} means, where sd_{cp} is the response value ($\alpha = 0.05$).

Source of variation	Degrees of Freedom	Sum of squares	Mean square	F_0	P-value
DBH_{OB}	18	75.69	4.20	4.01	<0.001
Residual Error	61	63.90	1.05		
Total	79	139.59			

Despite previous results, each Black spruce individual shows a pattern of variation in sd_{cp} around a tree (as it was for the Jack pine and Lodgepole pine sd_{cp} values). Sixty seven percent of the Black spruce sample set has the largest sapwood depth at the North

and East sides (38% from the East side and 29% from the North side), while 52% has the shortest sapwood depth at the South and West sides (38% from the South and 14% from the West). Furthermore, there are individuals having the largest sapwood depth at the South-West sides (33% [4% from the South and 29% from the West]) and the shortest at the North and East sides as well (48% [24% from the East and 24% from the North]). Thus, results show now that North-East side dominates in the largest sapwood depth values, and the South-West side develops the smallest sd_{cp}. A one-way ANOVA with repeated measurements shows that indeed there is not a significant effect from cardinal direction on sd_{cp} values (Table 4.15).

Table 4.15: One-way ANOVA Black spruce sd_{cp} as a response of cardinal direction (i.e. repeated measurements, $\alpha = 0.05$).

Source of variation	Degrees of Freedom	Sum of squares	Mean square	F_0	P-value
Cardinal direction	3	3.87	1.29	0.906	0.444
Residual Error	60	85.51	1.43		
Total	63	89.38			

The variance of sd_{cp} variances was calculated for the 21 Black spruce individuals by grouping them into DBH_{OB} classes. Each diameter class encompasses two 2-inch classes (i.e. instead of 2-inch classes [as normally is used in forestry], they are 4-inch classes) to have almost the same quantity of trees per class. The highest sd_{cp} variance was for trees of 4-inch class, while the lowest variance of sd_{cp} was recorded for trees larger than 12 inches (Table 4.16). These results point to the fact that the larger the tree, the lower each individual's sd_{cp} variance (i.e. each individual's variance between sd_N, sd_S, sd_E and sd_W).

Each Black spruce individual's $2\bar{sd}$ was estimated by applying Equation (4.4). Figure 4.23 shows a negative skewed distribution on the Black spruce $2\bar{sd}$ values. Two large accumulations of $2\bar{sd}$ values occur in the $7.5cm$ and $10.0cm$ classes. The former class accumulates 38% with a variance between $2\bar{sd}$ values of $0.5cm^2$. Moreover, the $7.5cm$

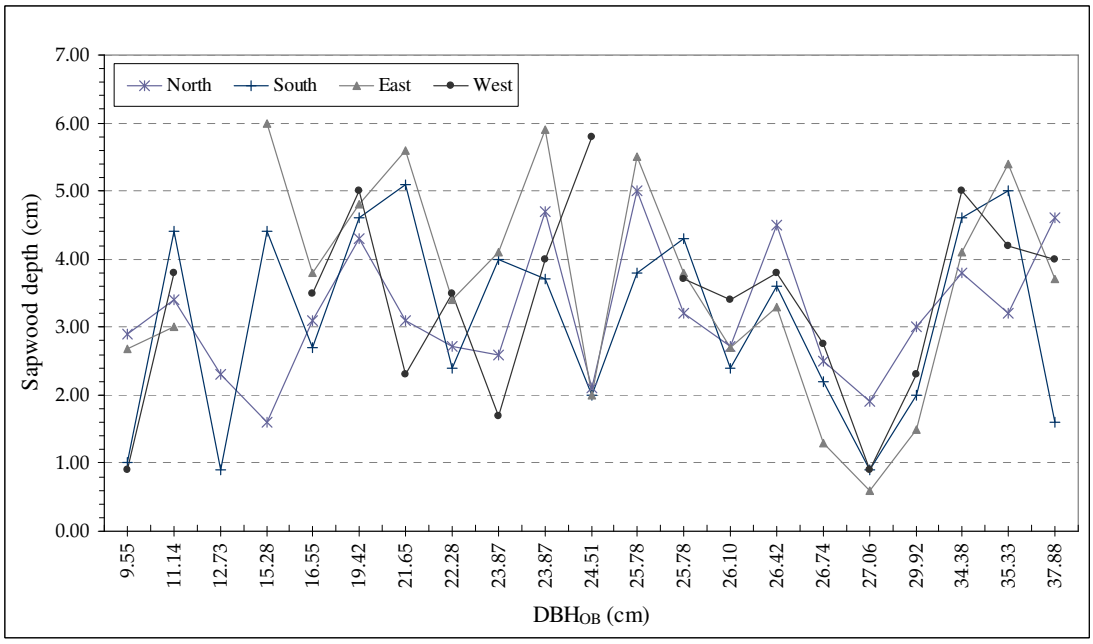

Figure 4.22: Sapwood depth per cardinal point (sd_{cp}) per each Black spruce tree, versus its DBH_{OB}. Notice that two values are missing: one sd_E and two sd_W. Two values were not estimated due to wood decay and one sd_W was an outlier ($CBH_{OB} = 15.28cm$).

Table 4.16: Variance of Black spruce trees sd_{cp} variances (cm^4) with respect DBH_{OB}. To keep consistency with the forest survey classification, here the DBH_{OB} classes are reported in inches.

Diameter class	**Variance of variances**
(inches)	(depth)
4-7	3.82
8-11	1.27
12-15	0.42

$2\bar{sd}$ class is integrated by trees with a DBH_{OB} ranging between $11.1cm$ to $37.9cm$ ($s^2 = 60.34cm^2$). Similarly, the latter class of $2\bar{sd}$ values is about 38% with an $s^2 = 0.5cm^2$; and DBH_{OB}'s ranging between $15.3cm$ and $35.3cm$ ($s^2 = 47.8cm^2$). Nineteen percent of the Black spruce individuals are in the $5cm$ $2\bar{sd}$ class, with DBH_{OB} values

that varied from $9.5cm$ to $29.9cm$ ($s^2 = 101.9cm^2$). The remaining 5% pertains to the $2.5cm$ $2\bar{s}d$ class and includes one individual of $25cm$ in DBH_{OB}. From these results, it is observed that there is a large variance of DBH_{OB} values in each $2\bar{s}d$ class. In fact, individuals with a DBH_{OB} of $\approx 24cm$ can be found in the $7.5cm$ or the $10.0cm$ $2\bar{s}d$ classes. Even individuals with a DBH_{OB} of $\approx 26cm$ can be found in the $5cm$, the $7.5cm$ or the $9.5cm$ classes. Thus, $2\bar{s}d$ seems to be independent of the individual's DBH_{OB}.

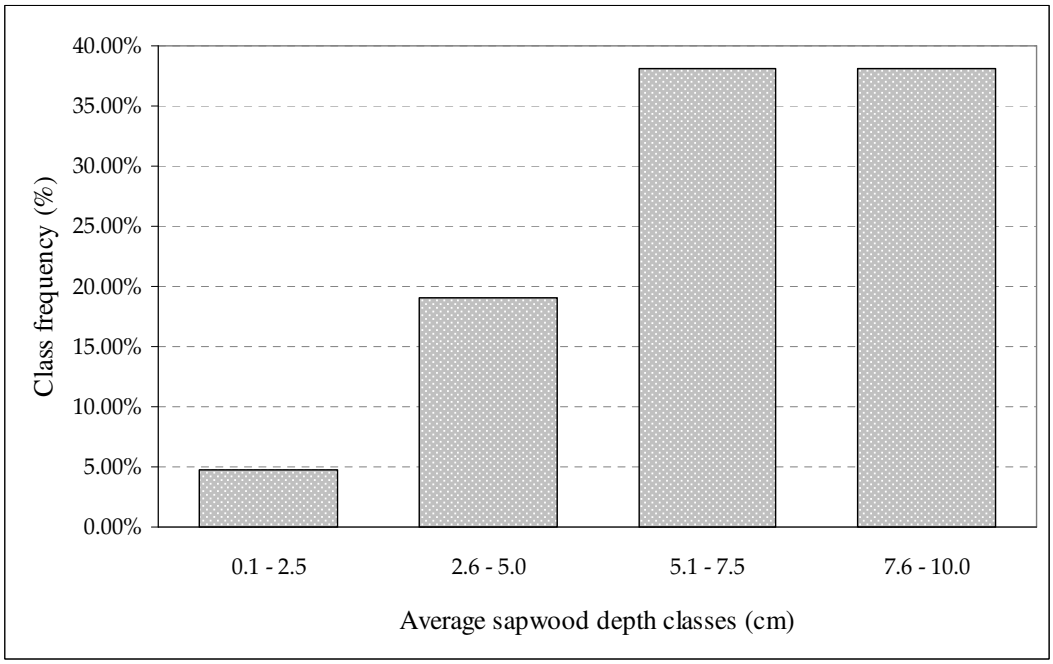

Figure 4.23: Black spruce sample set histogram of $2\bar{s}d$ values.

The Black spruce sapwood area (SA_{BS}) histogram shows a positive skewed distribution (Figure 4.24). The most common SA_{BS} values fall into the class of $250cm^2$ and holds 38% of the sampled trees, whose DBH_{OB} range from $19.4cm$ to $29.9cm$. Next common SA_{BS} values are in the $150cm^2$ class (29% of the total sample set) corresponding to trees between $9.5cm$ and $27.1cm$ in DBH_{OB}. The last two SA_{BS} classes hold the remaining 33% of the sample set, and also the largest trees (DBH_{OB} between $23.9cm$ and $37.9cm$).

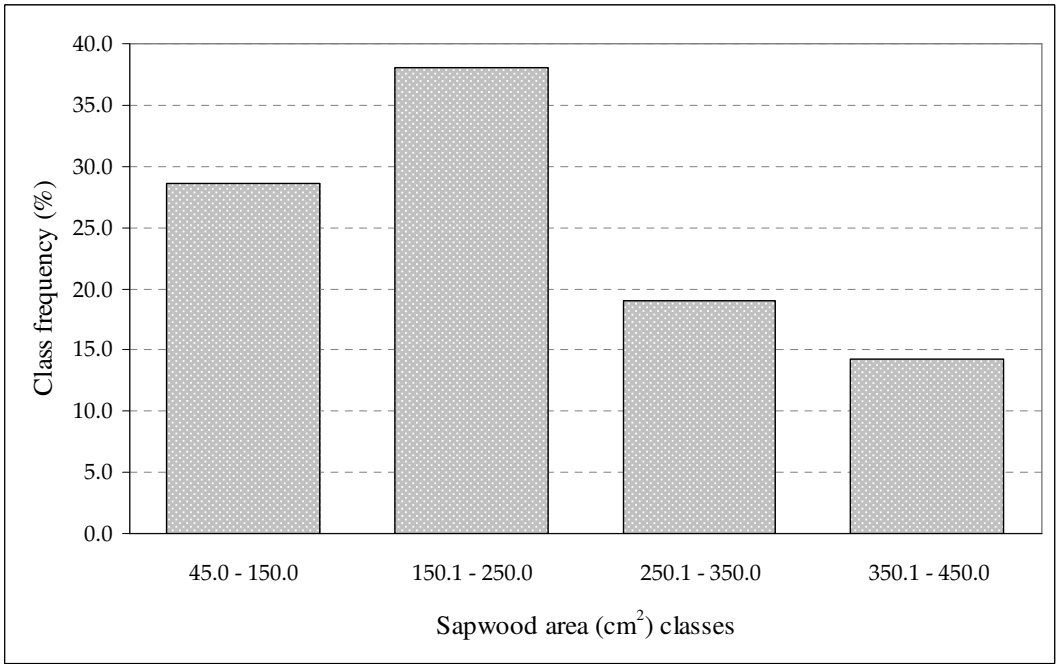

Figure 4.24: Black spruce sample set histogram of SA_{BS} values.

Figure 4.25 shows the corresponding $2\bar{sd}$ and SA_{BS} values for each Black spruce individual according to its DBH_{OB}. As it did occur with the other coniferous species, there are particular cases in which a large SA_{BS} is registered for relatively small trees that have large sapwood depth. Indeed, individuals with very small $2\bar{sd}$ but large DBH_{OB}, register large SA_{BS} values. Specifically, a tree as large as $27.1cm$ in DBH_{OB} having a small $2\bar{sd}$ ($2.15cm$) will of course have its SA_{BS} equal to $87.7cm^2$. Also, look at the tree with an SA_{BS} of $375.59cm^2$, whose DBH_{OB} is one of the largest, but its $2\bar{sd}$ is even smaller than a tree with one of the smallest DBH_{OB}. Thus, the increments in SA_{BS} do not correspond to sapwood depth increments, but the tree size.

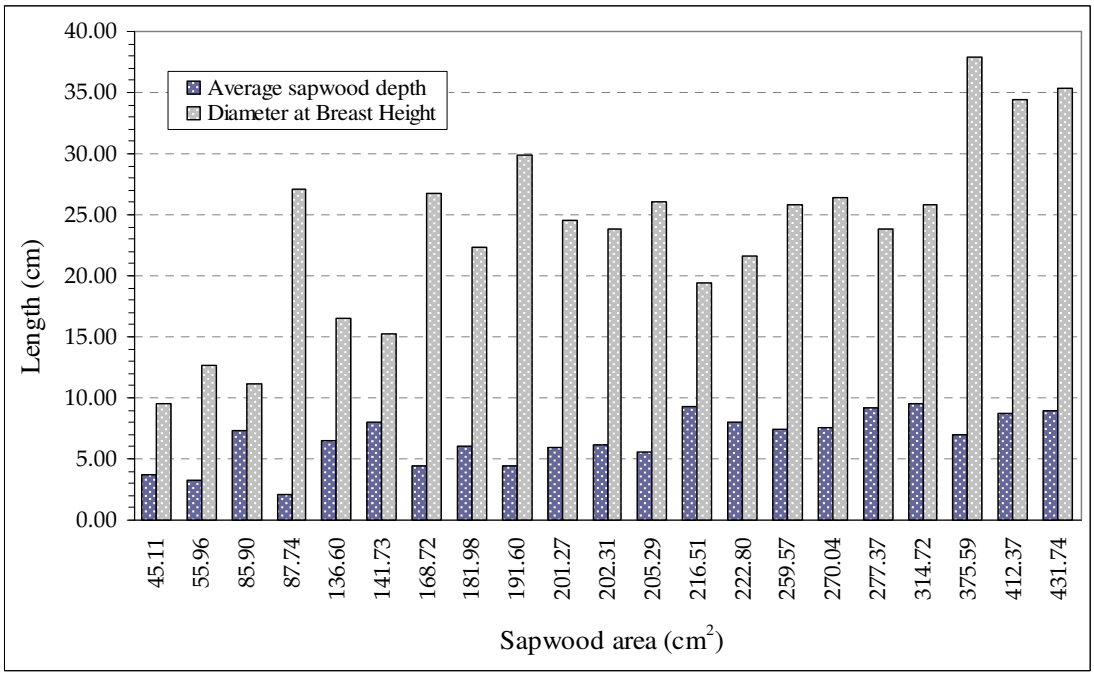

Figure 4.25: Bar graph showing values of SA_{BS}, DBH_{OB} and $2\bar{sd}$ values registered for each Black spruce individual.

White spruce. It was possible to analyse under the microscope the whole White spruce sample set (68 wood cores). Thus, the sample set size did not change and remains with 18 individuals, whose CBH_{OB} range from $11.5cm$ to $50cm$. Statistics of measured sapwood depths in the four cardinal points are given in Table 4.17.

Table 4.17: Basic statistics of the sd_{cp} values obtained from the White spruce sample set. Individual's CBH_{OB} ranges from $11.5cm$ to $50cm$.

Cardinal point	Sapwood depth				
	Maximum (cm)	**Minimum** (cm)	**Mean** (cm)	**Mode** (cm)	**Variance** (cm^2)
North	5.20	1.50	3.22	4.40	1.17
South	5.60	1.72	3.37	2.30	1.50
East	4.90	0.69	2.87	3.10	1.64
West	5.90	0.35	3.19	4.20	2.33

Maximum sd_{cp} values range between $4.90cm$ and $5.90cm$ that were measured in trees whose $DBH_{OB} > 28.18cm$ (i.e. the average DBH_{OB}). Minimum sd_{cp} values range between $0.35cm$ and $1.72cm$ that pertain to trees whose $DBH_{OB} \leq 28.18cm$. Here, there is not a window for considering any correlation between the thickness of sapwood depth and the tree size, because three of the minimum values pertain to a tree whose $DBH_{OB} = 11.46cm$. With respect to the maximum sd_{cp} values, all of them pertain to different trees, and as mentioned before, they are larger than the mean DBH_{OB} of the White spruce sample set.

In Figure 4.26 and the last column of Table 4.17, it is shown that the largest variance is for sd_W values, with lower variations for sd_E and sd_S. The smallest variance was observed for the sd_N values; nevertheless, it is still a large variance ($1.17cm^2$) taking into account the registered lengths in sapwood depth.

As a result, there is a change of sd_{cp} values as the individual's DBH_{OB} changes. This change is observed in Figure 4.27, where each individuals's sd_{cp} values is plotted against its DBH_{OB}. Similar to Trembling aspen, each individual's sd_{cp} generally tend to increase as their DBH_{OB} increases. The ANOVA testing the similarity between mean

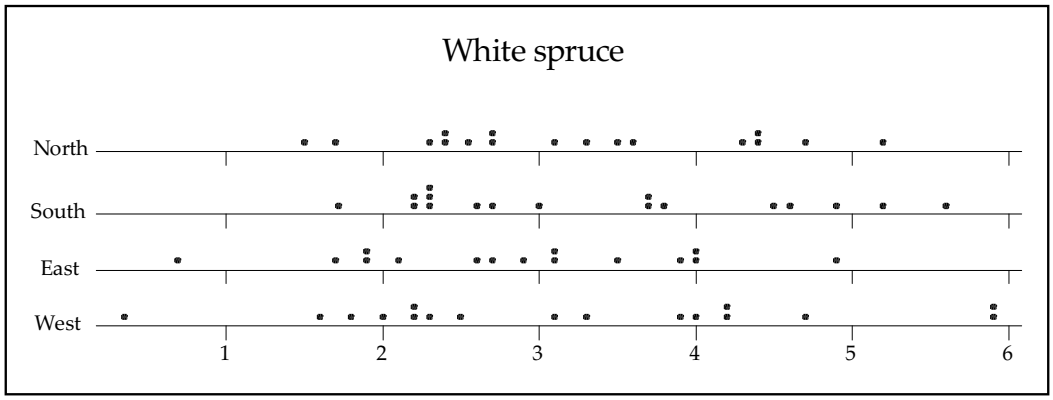

Figure 4.26: Dot plot of sd_{cp} values (cm) for the White spruce sample set. In general, there is a wide spread of sd_{cp} in every cardinal point, being the largest at the East and West sides (Same as it occurs for the other three coniferous species).

values of sd_{cp} and DBH_{OB} drew similar conclusions: there is a significant difference between mean values (Table 4.18). Therefore, it can be concluded that changes in sd_{cp} are driven by changes in DBH_{OB} (assuming that the cardinal direction has no significant effect on sd_{cp}). Still, more information will be derived after the regression analysis between these two variables.

Table 4.18: One-way ANOVA between White spruce sd_{cp} and DBH_{OB}. The null hypothesis (H_o) tests the equality between the sd_{cp} and DBH_{OB} means, where sd_{cp} is the response value ($\alpha = 0.05$).

Source of variation	Degrees of Freedom	Sum of squares	Mean square	F_0	P-value
DBH_{OB}	16	68.968	4.311	7.01	<0.001
Residual Error	49	30.137	0.615		
Total	65	99.105			

As it occurs with the rest of the species studied here, each White spruce individual registers a maximum, minimum and intermediate sd_{cp} value. On the other hand, each individual's sd_{cp} variance remains fairly small, and it tends to increase in the bigger trees

($DBH_{OB} \geq 31.8cm$). Fifty nine percent of the sample set has the largest sapwood depth at the South and West sides, while 53% of the sample set has the smallest sapwood depth at the North and East sides. Furthermore, the smallest sd_{cp} values were also observed at the South and West sides (47%), and 41% of the sample set registers the largest sd_{cp} values at the North and East sides. The maximum and minimum sd_{cp} values seem to be quasi evenly distributed around the tree trunk. A one-way ANOVA with repeated measurements shows that indeed there is no significant effect from cardinal direction on sd_{cp}. Thus, it seems that there is no preference in White spruce to grow thicker or thinner in a specific direction (Table 4.19). Be aware that the last conclusion is totally independent of the fact that each White spruce individual still has a maximum, minimum and intermediate sd_{cp} around the tree trunk.

Table 4.19: One-way ANOVA White spruce sd_{cp} as a response of cardinal direction (i.e. repeated measurements, $\alpha = 0.05$).

Source of variation	Degrees of Freedom	Sum of squares	Mean square	F_0	P-value
Cardinal direction	3	6.31	2.10	2.41	0.078
Residual Error	51	44.51	0.87		
Total	54	50.82			

The variance of sd_{cp} variances is shown in Table 4.20. The highest sd_{cp} variance was for trees of the 8-inch class, while the lowest variance was recorded for trees in the 6-inch class. Unlike the other species, White spruce has a larger variance in sd_{cp} values for larger individuals. For middle size individuals (6-inch class), the variance in between sd_{cp} values was minimal.

With respect to the calculated $2\bar{sd}$, the sample set values have a distribution close to Normal (Figure 4.28). The largest accumulation of $2\bar{sd}$ values is for the two middle classes (i.e. $5.5cm$ and $8.0cm$). Specifically, 41% of the $2\bar{sd}$ values fall between $5.6cm$ and $8.0cm$ with a variance between $2\bar{sd}$ values of $0.45cm^2$. Into this $8cm$ $2\bar{sd}$ class, DBH_{OB} values varied from $25.5cm$ to $35.6cm$ ($s^2 = 14.6cm^2$). The $5.5cm$ $2\bar{sd}$ class

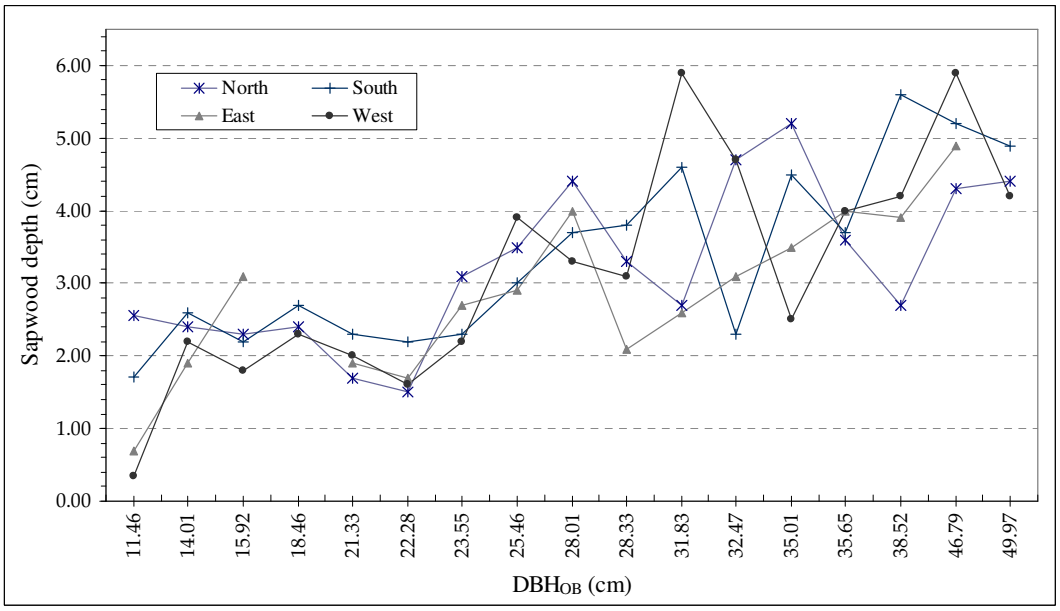

Figure 4.27: Sapwood depth per cardinal point (sd_{cp}) per each White spruce tree, versus its DBH_{OB}. There are two missed sd_E values. One sd_E is missed since it was not possible to sample the individual in that side. The second sd_E value was dismissed due to wood decay.

Table 4.20: Variance of White spruce trees sd_{cp} variances (cm^4)with respect DBH_{OB}. To keep consistency with the forest survey classification, here the DBH_{OB} classes are reported in inches.

Diameter class (inches)	**Variance of variances** (depth)
4-5	0.20
6-7	0.03
8-9	0.78

holds 35% of the total sample set and its variance between $\bar{sd}$ values equals $0.40cm^2$; DBH_{OB} values in this class range from $14.0cm$ to $23.5cm$. Eighteen percent of the sample set integrates the $10.5cm$ class, whose individuals' DBH_{OB} range from $38.5cm$ to $50.0cm$. The remaining 6% is a tree with a $2\bar{sd}$ of $2.66cm$ and DBH_{OB} of $11.5cm$, which is the smallest tree of the sample set. For two individuals, their sd_E value was

dismissed due to wood decay; thus, their $2\bar{sd}$ was estimated as an average of the sd_N, sd_S and sd_W values.

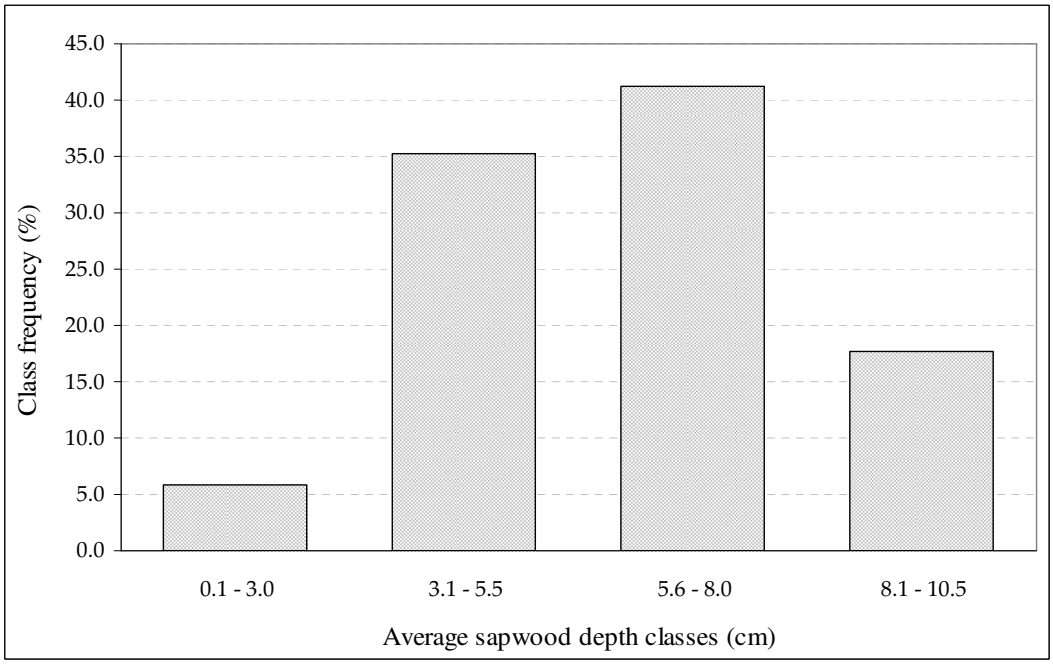

Figure 4.28: White spruce sample set histogram of $2\bar{sd}$ values.

The White spruce sapwood area (SA_{WS}) histogram is in Figure 4.29. The histogram shows two large accumulations of SA_{WS} values, the first and largest one pertains to the $101 - 200cm^2$ class (with 29% of the SA_{WS} values), and the next one pertains to the $301 - 400cm^2$ class (with 23.5% of the SA_{WS} values). The SA_{WS} class of $101 - 200cm^2$ includes trees with a DBH_{OB} of $15.9cm$ to $23.5cm$, while the $301-400cm^2$ class includes trees with a DBH_{OB} between $38.8cm$ and $35.7cm$.

Following these two classes, there are four more SA_{WS} classes that hold the rest of the sample set. First, 18% of the sample set falls into the $201 - 300cm^2$ class, including those trees whose DBH_{OB} values range between $25.5cm$ and $28.3cm$. Second, 12% of the White spruce trees fall into the $42 - 100cm^2$ SA_{WS} class, corresponding to the smallest trees of the sample set (DBH_{OB} ranges between $11.5cm$ and $14cm$). Next class includes trees whose SA_{WS} falls between $601cm^2$ and $700cm^2$ and whose DBH_{OB} are the largest of the sample set ($46.8cm$ and $50cm$). Finally, one tree ($\approx$ 6% of the

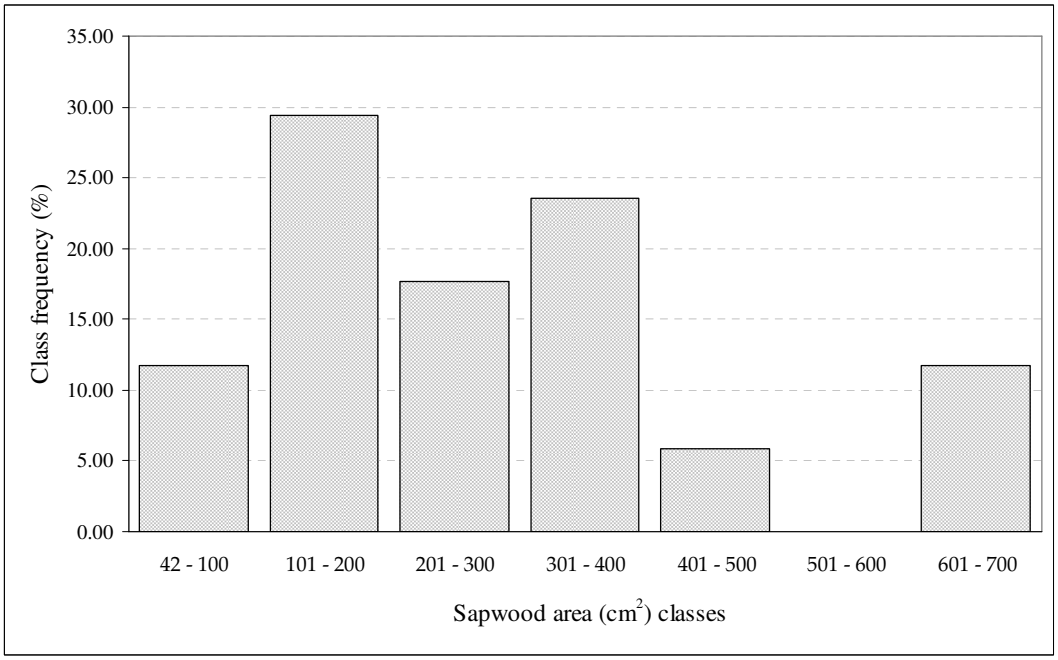

Figure 4.29: White spruce sample set histogram of SA_{WS} values.

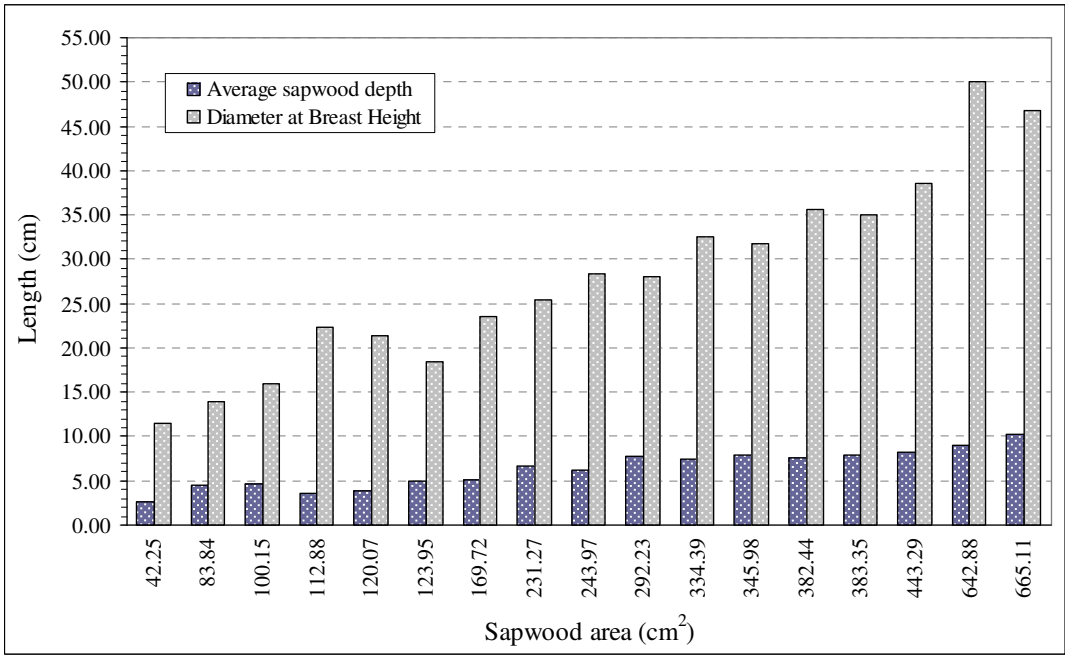

Figure 4.30: Bar graph showing values of SA_{WS}, DBH_{OB} and $2\bar{sd}$ values register for each White spruce individual.

sample set) with a DBH_{OB} of $38.5cm$ fall into the $400 - 500cm^2$ SA_{WS} class.

In the particular case of the White spruce, each SA_{WS} class corresponds to only one range of DBH_{OB} values. That is, the DBH_{OB} ranges do not overlap with one another, and as the DBH_{OB} increases, the SA_{WS} increases as well. This relationship is also observed in Figure 4.30 where $2\bar{sd}$ values are also included. In general, the graph shows that increments in SA_{WS} correspond to increments in DBH_{OB}, while $2\bar{sd}$ values remain fairly constant along the DBH_{OB} range. Thus, unlike the other three coniferous species, increments in SA_{WS} are driven by tree size, and there are changes in $2\bar{sd}$ as the tree grows.

4.3.4 Comparison between methods to measure sapwood depth

Microscopical analysis and translucence methods. The sample sets of White spruce, Jack pine, and Lodgepole pine were used for measuring sapwood depth by the translucence and microscopical analysis.

For the White spruce sample set, a Paired-T test proved that the two set of results are significantly different (P=0.00, N=36) with $\alpha = 0.05$. Similarly, in the Jack pine and Lodgepole pine sample set, the obtained sapwood depth values with the two different methods are significantly different (P=0.00, N=50) with $\alpha = 0.05$. It is concluded that the two methods for measuring sapwood depth will give different estimates for individuals of White spruce, Jack pine and Lodgepole pine individuals.

In White spruce, the difference between the sapwood depth measured by the translucence method and microscopical analysis ($sd_{translucence}$ - $sd_{microscopic}$ [i.e. the paired response differences]) ranged between $-1.10cm$ and $1.60cm$. Figure 4.31 is the plot of the paired response differences that clearly shows a constant overestimation of the sapwood depth by the translucence method. More importantly is how the method used to estimate sapwood depth affects the estimation of total sapwood area. The estimated White spruce sapwood areas by means of the $\bar{sd}$ values obtained with the two methods showed a significant difference that ranged between $-18.02cm^2$ and $71.92cm^2$ (Figure 4.32). In 77% of the cases, White spruce's sapwood area was overestimated by the

translucence method. The maximum overestimation was of 34% of the total sapwood area estimated with the microscopical method. On average, the overestimations were approximately 15% of the total sapwood area estimated with the microscopical method.

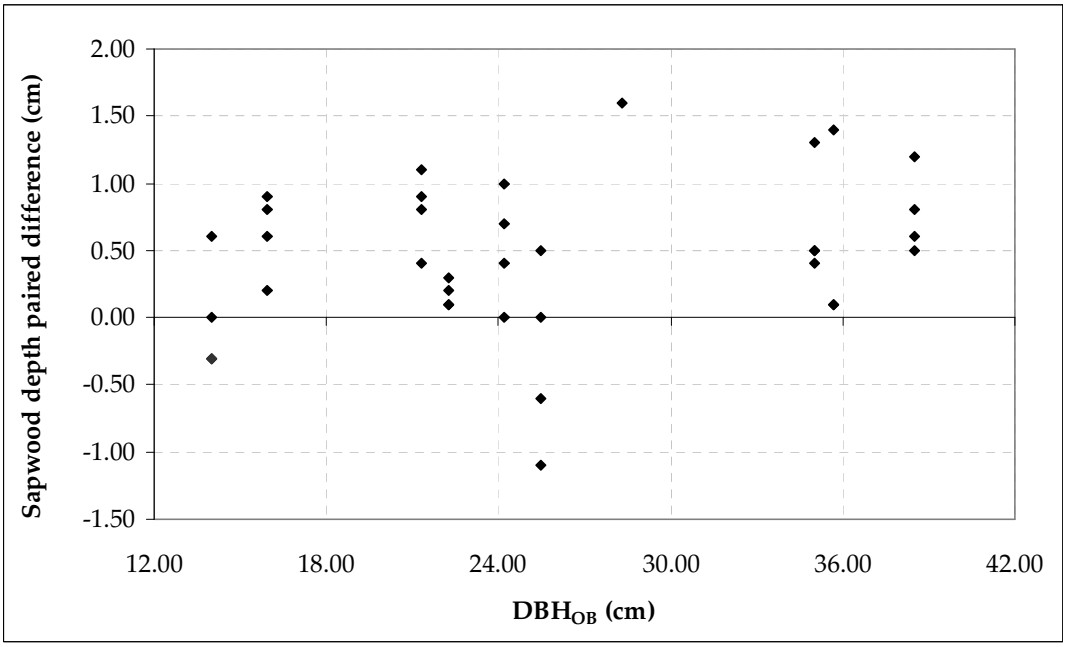

Figure 4.31: Plot of the paired response differences between sd_{cp} values obtained with the microscopical analysis and the translucence methods. White spruce sample set. Notice that five values are missing because they overlap.

In the Jack pine and Lodgepole pine sample set, the difference between the sapwood depth measured by microscopical analysis and the translucence method ranged between $-4.90cm$ and $1.90cm$. The plot of the response differences (Figure 4.33) shows that it was more common to have an underestimation of the sapwood depth by the translucence method. The estimated Jack pine and Lodgepole pine sapwood areas by means of the $\bar{sd}$ values obtained with the two methods showed residuals that ranged between $-102.06cm^2$ and $37.86cm^2$ ($s = 36.52cm^2$). There is a constant underestimation (86% of the cases) of the sapwood area by the translucence method (Figure 4.34) with an average of 35% of the total sapwood area estimated with the microscopical method. The largest underestimation was of 61% of the total sapwood area calculated with the microscopic method.

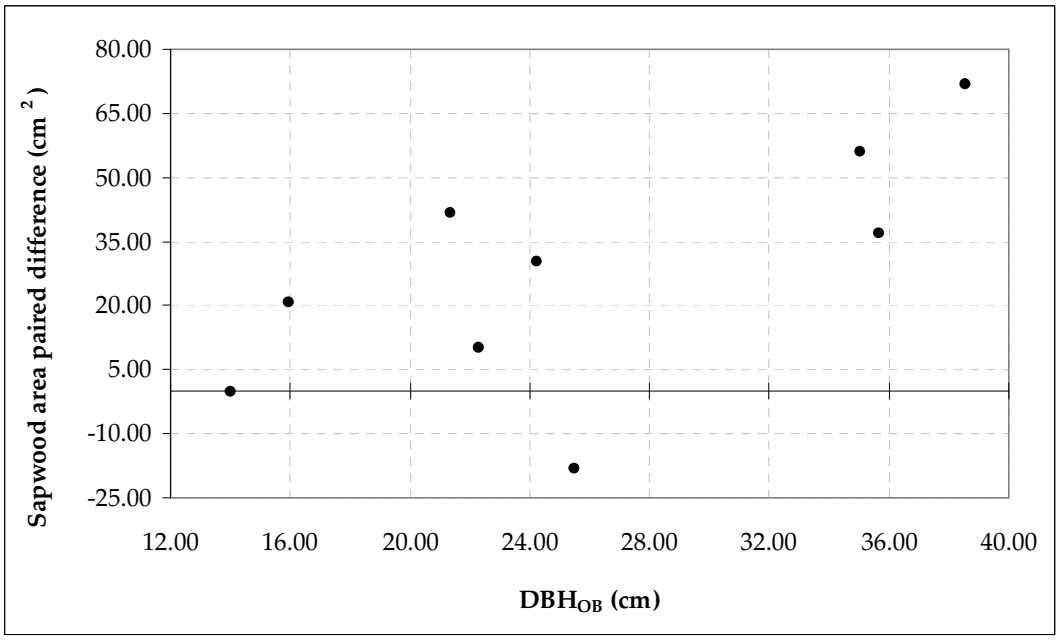

Figure 4.32: Plot of the paired response differences between measured sapwood area with the microscopical analysis and the translucence methods. White spruce sample set.

In terms of the uncertainty associated with the translucence method, it is difficult to estimate it because it is a function of the gross and systematic errors. Both types of error are difficult to measure because they are related to the person who determines the translucent sapwood depth. The only guidance for the translucence method is that the sapwood transmits light while the heartwood does not. This criterion does not have a solid basis (as explained in § 4.1.1) since the wood water content varies and confounds both sapwood and heartwood. On the contrary, the uncertainty associated with the wood tissues microscopical analysis method can be estimated, and taken into account for further estimations or predictions.

Microscopical analysis and Coloration methods. The coloration method was tested with the Trembling aspen sample set. For a total of seventeen wood cores, sapwood depth values were obtained with both the microscopical analysis and the coloration methods. The number of tested wood cores was limited by how problematic it was to

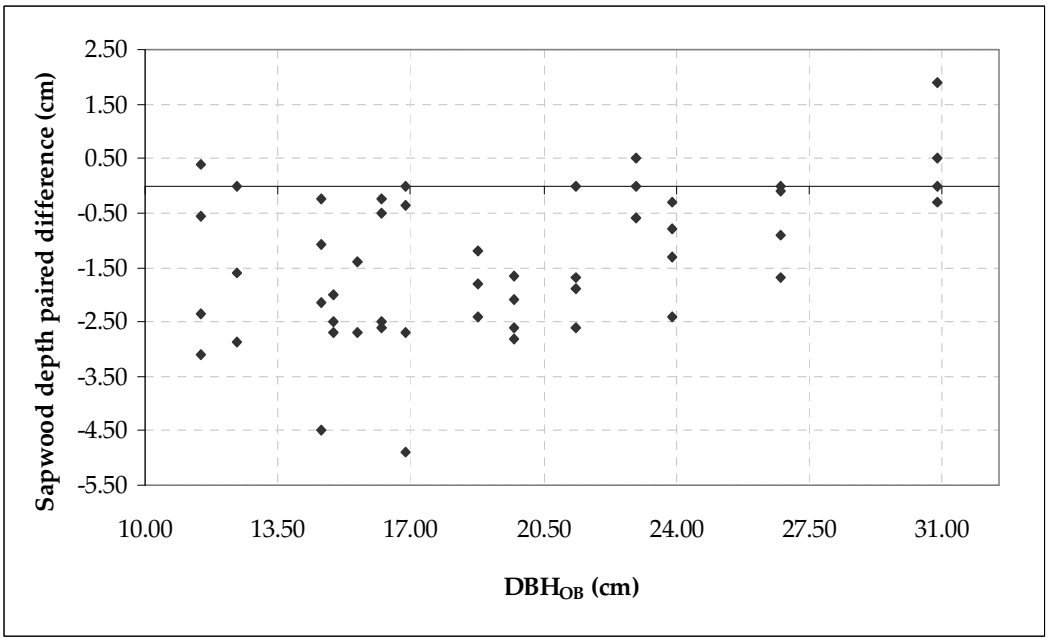

Figure 4.33: Plot of the paired response differences between $\bar{sd}$ values obtained with the microscopical analysis and the translucence methods. Jack pine and Lodgepole pine sample set.

distinguish the difference in coloration between the sapwood and heartwood. Still, the sample size is adequate for performing a Paired t-test ($\alpha/2 = 0.1$ and $\beta = 0.8$). Thus, the obtained sapwood depth values with the two different methods are significantly different (P=0.012, $\alpha/2 = 0.1$). It can be concluded that the two methods for measuring sapwood depth will give different estimates when it comes to Trembling aspen individuals. For sapwood depth values, the paired difference between the microscopical analysis and the coloration methods ranged from $0.00cm$ to $-1.8cm$ (Figure 4.35). In 65% of the cases, Trembling aspen's sapwood depth was underestimated by the coloration method; in the remaining 35% of the cases the measured sapwood depth was exactly the same for both methods (i.e. the paired difference was null). In terms of sapwood area, the largest underestimation was approximately 18% of the total area calculated with the microscopical analysis method. On average, the underestimations were 10% of the total area calculated with the microscopical analysis method.

In summary, the translucence and coloration methods are already considered unreli-

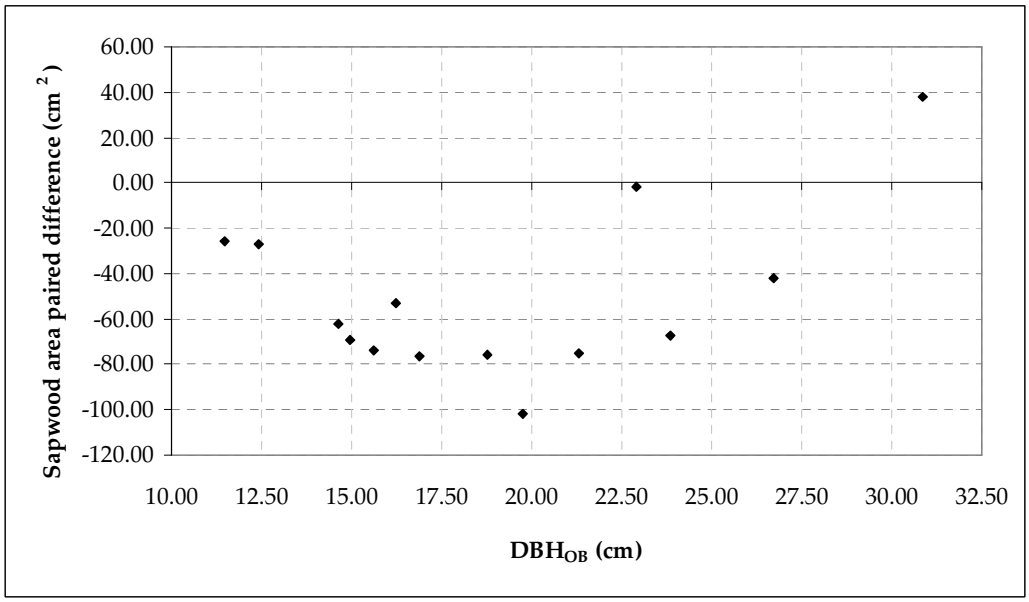

Figure 4.34: Plot of the paired response differences between sapwood area values obtained with the microscopical analysis and the translucence methods. Jack pine and Lodgepole pine sample set.

able (Čermák and Nadezhdina, 1998). Here, the obtained results quantify the reliability of the methods, which is closely related the physiological criteria for distinguishing sapwood from heartwood. Thus, the two methods over and underestimated sapwood depth. The overestimation was notorious in White spruce individuals, while underestimations commonly occurred in Trembling aspen and Jack/Lodgepole pine individuals. The reported percentages quantify the over and underestimations and they could be used as a way of estimating the translucence and coloration methods' uncertainty.

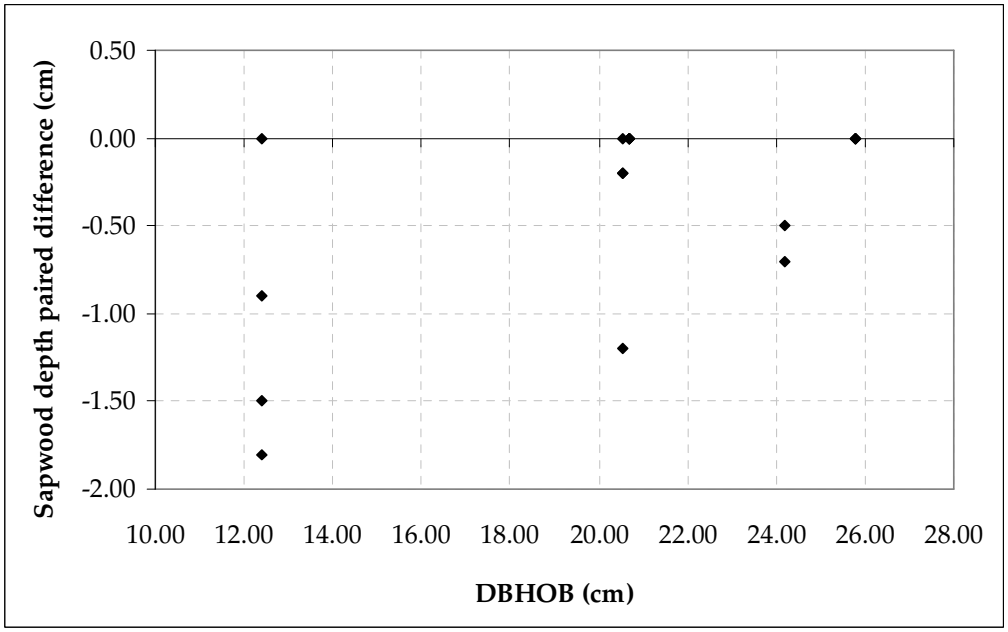

Figure 4.35: Measured sapwood depth paired difference between the microscopical analysis and the coloration methods. Trembling aspen wood cores of different DBH_{OB}.

4.4 Discussion and Conclusions

To evaluate the preciseness of sapwood depth as scaling factor, it was necessary to analyze within-tree variation, and the sapwood depth variability with respect to the species and tree size. And at the same time, it was important to recognize the influence of the bio-physical factors in tree growth. Thus, the following discussion is based on the obtained results and previous knowledge of the bio-physical conditions under which the five studied species grow.

Each studied species' sd_{cp} results concur with previous works stating that the depth in sapwood is not homogenous around the tree annulus along the tree trunk (Kozlowski and Pallardy, 1997; Philipson et al., 1971b,a). Thus, sapwood depth heterogeneity at the four cardinal points suggests that it is necessary to measure sapwood depth at least in the four cardinal points for obtaining a reliable sapwood depth estimate.

Also, the five studied species tend to have a small sd_S values which, is attributed to the fact that in the Northern Hemisphere, the South sides are exposed to much more solar radiation than North-facing slopes (Auslander et al., 2003); thus, the South sides tend to have xeric conditions that are a constraint for the trees with respect to water availability and variability in microclimate. Hence, it is believed that trees tend to have less sd_S as a mechanism of defence (i.e. to avoid loosing large amounts of water).

In comparison with the other three coniferous species, the Black spruce sd_{cp} and $\bar{sd}$ values have the lowest variance which could be attributed to tree growth requirements. This species is prone to grow under high soil moisture conditions. Thus, Black spruce individuals are normally found in flat areas, where there are high water concentrations and the sunlight will be more evenly distributed at the four cardinal points along the day than on terrains with slope. As a consequence, sapwood in Black spruce has similar chances to grow at any side of the tree.

In Jack pine and Lodgepole pine individuals there is low variance in sd_W and sd_N that may be attributed to a well balanced supply of water (mesic conditions) in the North-facing sides (remember that most of the samples were collected in sites with a

North-East aspect). Moreover, in Lodgepole pine and Jack pine individuals there is a small variance of $2\bar{sd}$ as the individuals grow. It may imply that for these two species in particular, the tree sapwood depth does not largely vary as the individuals grow. Unlike these two species, White spruce and Trembling aspen species $2\bar{sd}$ increases at larger DBH_{OB}. Thus, in the case of White spruce and Trembling aspen it is concluded that indeed, sapwood depth is directly proportional to DBH_{OB}. Consequently, SA_{WS} and SA_{TA} estimates show proportional increments with respect to DBH_{OB} and $2\bar{sd}$. In contrast, increments on SA_{JP}, SA_{LP}, and SA_{BS} estimates are mainly related to increments in DBH_{OB} and not to $2\bar{sd}$. As mentioned, some of the largest trees in DBH_{OB} registered small $2\bar{sd}$ values, but still they have large SA_{sp} due to the influence of their CBH_{OB}.

All crown classes of sampled trees were relatively high. It has been suggested that crown class my be another factor influencing sapwood depth. For instance, one White spruce tree of $44cm$ in DBH_{OB} showed a $2\bar{sd}$ similar to that of a small tree of $22cm$ in DBH_{OB} due to its very low crown class. Thus, it may be suggested to integrate crown class as another factor influencing sapwood depth; however, crown class is not rigorously defined. Thus, if the crown class classification is a subjective method, it could be a hindrance in obtaining objective outcomes.

In conclusion, sapwood depth and sapwood area seem to behave differently in each studied species and are not always proportional to the tree size as it is normally assumed. It appears that the structural design and growth of sapwood depth and sapwood area is species-specific and one should be cautious in assuming similar tree growth patterns in non-studied tree species. Thus, in order to effectively use either sapwood depth or sapwood area as scaling factors, it is recommended that one observe each species sapwood depth variations before making any inference. Also, it is important to specify the environmental conditions and species growth requirements as factors that might influence the allometric correlations of sapwood depth. These results help to better understand of how sapwood varies along a tree trunk and between different tree sizes, which will allow one to obtain more reliable predictions of sapwood depth and sapwood area.

4.4.1 Future work

Similar studies are needed in order to reinforce previous results and to observe the variations of sapwood depth and sapwood area in different site conditions, such as slope, aspect, and climate. Also, studies rigorously classifying trees by crown class will give an insight of sapwood depth variations in relation to the trees spatial location, and its influence on plot transpiration rates.

5 Allometric correlations

Chapter outline

The calculation of a tree transpiration rate by means of sap flow density uses the sapwood area as the scaling factor (Granier, 1985). Measuring sap flow density and sapwood area at each studied tree becomes a complex and destructive method when estimating a whole tree stand's transpiration. As a consequence, it would be convenient to adopt an alternative method for aggregating transpiration rates at the stand (i.e. plot) scale.

For this research it is crucial to obtain a scaling parameter to aggregate tree transpiration rates to the plot scale. For that, it is necessary to develop an allometric relationship between two measurable vegetation factors per plot. Based on Shinozaki's pipe model theory that a proportion of sapwood cross-sectional area transports water and nutrients to a specific amount of leaf area (Smith and Hinckley, 1995), it is expected that this relationship holds true at the plot scale. Furthermore, it is supposed that sapwood area and leaf area are the adequate scaling parameters due to their close relationship with transpiration.

Thus, the expected aims of this research dissertation chapter are:

1. Develop $\bar{sd} : DBH_{OB}$ allometric correlations for the five species of interest.
2. Develop an approach to aggregate a single tree's sapwood area to the plot's scale (i.e. plot's sapwood area).
3. Develop plot sapwood area : leaf area correlations taking into account the plot's vegetation heterogeneity.

To the author's knowledge, there is no published work developing a plot's sapwood area - leaf area relationship ($SA_{plot} : LA_{plot}$). The published work in this matter deals with single tree relationships (e.g. Gilmore et al. (1996); Kaufmann and Troendle (1981); McDowell et al. (2002); Meadows and Hodges (2002)). These works have reported different sapwood area : leaf area correlations for the same species, attributing the discrepancy to site-specific characteristics, stand density, and tree competition.

The concept used to estimate a plot's sapwood area and leaf area defines a vegetated plot as a surface area that holds a big, single tree, whose vascular and leafy parts will be the summation of all the tree's vascular and leafy parts inside the plot. For instance, the big tree's sapwood area could become an integration of each species sapwood area present in the plot.

This chapter then presents the results of single tree sapwood area models, the aggregation of sapwood area to the plot scale, and plot sapwood area models. At the tree scale, sapwood area was estimated by previously defining the $\bar{sd} : DBH_{OB}$ relationship. At the plot scale, Leaf Area is the parameter used as the predictor of Sapwood Area. The obtained linear regression models were tested and statistically analysed.

5.1 Modelling $SA_{plot}:LA_{plot}$ relationship

5.1.1 Introduction

Sapwood area supports several physiological functions, such as photosynthesis, gas exchange, cooling, nutrient transport, and naturally transpiration. Also, sapwood area has been theoretically related to leaf area (Shinozaki's pipe model theory, Smith and Hinckley, 1995). The pipe model theory has been sufficiently proven by several researchers' work. Most of these works have modeled the leaf area : sapwood relationship area ($LA_{sp}:SA_{sp}$) to estimate a single tree's leaf area having sapwood area as the predictor. These works have reported linear models for about 20 conifers, such as Scotch pine ([*Pinus sylvestris*], Whitehead, 1978), Ponderosa pine ([*Pinus ponderosa*], War-

ing, 1982), Loblolly pine ([*Pinus taeda*], Blanche et al., 1985), Douglas fir ([*Pseudotsuga menziesii*], Borghetti et al., 1986; Waring, 1982; McDowell et al., 2002), Lodgepole pine ([*Pinus contorta*, Dean et al., 1988; Hungerford, 1987; Keane and Weetman, 1987; Kaufmann and Troendle, 1981), Engelmann spruce and Subalpine fir ([*Picea engelmanni* and *Abies lasiocarpa*], Kaufmann and Troendle, 1981), Pinyon pine and One-seeded Juniper ([*Pinus edulis* and *Juniperus monosperma*, Schuler and Smith, 1988), Balsam fir ([*Abies balsamea*], Coyea and Margolis, 1992; Marchand, 1984), and so forth.

Deciduous species haven't been as studied as coniferous species; however, still there is some published work by Vertessy et al. (1995) for Mountain ash (*Eucalyptus regnans*), Kaufmann and Troendle (1981) for Trembling aspen (*Populus tremuloides*), Meadows and Hodges (2002) for Cherry bark oak (*Quercus falcata*) and Green ash (*Fraxinus pensylvanica*). In this last work, Meadows and Hodges (2002) improved their model for predicting leaf area by not only having sapwood area as a predictor, but by adding total height and live crown ratio to the equation.

Researchers that have studied the same species under different site conditions, have reported different $LA_{sp}:SA_{sp}$ linear (even sometimes non-linear) equations. The discrepancy between results have helped to understand that the $LA_{sp}:SA_{sp}$ relationship is driven by the site's conditions such as stand density (Binkley and Reid, 1984; Shelburne et al., 1993; White et al., 1998), climatic factors (Mencuccini and Grace, 1994), and physical characteristics (Hillis, 1987). Naturally, it is expected that the $LA_{sp}:SA_{sp}$ relationship is species-specific (Hillis, 1987), but it does not always happen. For instance, Dean and Long (1986) determined that the Lodgepole pine's allometric relationship $LA_{sp}:SA_{sp}$ is linear, while Kaufmann and Troendle (1981) determined that a non-linear regression better explains the relationship. Thus, while in theory the correlation $LA_{sp}:SA_{sp}$ is explained as linear, it could change due to site conditions.

In the present study, it is suggested that besides the site conditions, the methods used to measure sapwood area and leaf area significantly influence the $LA_{sp}:SA_{sp}$ relationship. It is well known that not all the methods to measure sapwood area will give the same results (Čermák and Nadezhdina, 1998), and direct or indirect leaf area

mensuration gives different outcomes as well (Jonckheere et al., 2004).

In more recent work, the average sapwood thickness (i.e. average sapwood depth, $\bar{sd}$) has been used instead of sapwood area to indirectly estimate some other forest stand characteristics such as canopy cover densities and foliage biomass by combining remotely sensed data and field data (Lefsky et al., 1999; Means et al., 1999). The method consists of estimating foliage biomass as a function of DBH by previously modelling $\bar{sd}:DBH$ relationships to predict DBH for a whole tree stand (Means et al., 1999). The authors used previous equations to estimate foliage biomass and sapwood area. In a similar way, Lefsky et al. (1999) used an already published $\bar{sd}:DBH$ relationship to estimate foliage biomass as an indicator of DBH. The $\bar{sd}:DBH$ relationship used by both authors was obtained from Lassen and Okkonen (1969).

To the author's knowledge, Lassen and Okkonen (1969) could be one of the few published works reporting results for single tree $\bar{sd}:DHB$ relationships (Lassen and Okkonen's paper cited 3 more published works on this issue). Lassen and Okkonen reported that in Douglas-fir (*Pseudotsuga menziesii*) and some other conifers, sapwood depth increases as the tree's diameter (inside bark) increases. Most of the species showed that trees had an exponential sapwood depth growth until they reached a diameter of $25.4 - 38.1cm$; thereafter, sapwood depth nearly reached a plateau. Thus, trees' sapwood depth tend to increase "only slightly" in older/bigger trees. That was the general tendency, with the exception of Lodgepole pine that showed a large variability in sapwood depth, and actually some trees that were smaller in diameter showed a larger sapwood depth than those with a larger diameter. Authors also concluded that Douglas-fir trees with the same diameter had different sapwood depths according to their location (coast area or interior land), and elevation.

Even though there is sufficient work supporting the strong relationship between a single tree's sapwood area and leaf area, these models cannot be used to scale up to larger scales. In a forested region, it is expected that leaf area increases as the ground area increases, it is not possible to use single tree models to interpolate either leaf area or sapwood area values for a group of trees. Thus, it is necessary to develop specific

models for the $SA_{plot}:LA_{plot}$ relationship.

5.1.2 Material and methods

Statistical Analysis. All the statistical analyses were mainly performed with Minitab, version 13.32 (Minitab Inc., State College, PA USA). For each species, there was an exhaustive study of the statistical results to determine the most adequate model. These statistical results include the Pearson's correlation coefficient, detection of outliers, the regression analysis, the ANOVA, list of unusual observations, and the lack-of-fit test. Finally, each linear model's residuals were examined in order to check the model adequacy. Model adequacy checking includes a Normal plot of residuals and the plot of residual versus fitted values.

Besides the correlation analysis, the pairwise comparison of the Coefficient of Variation (COV) confidence intervals (C.I.) is used as an indication of the relationship between the scaling parameters at the plot scale (i.e. between Sapwood Area [SA_{plot}] and Leaf Area Index, and between SA_{plot} and Leaf Area [LA_{plot}]). The pairwise comparison consists of comparing the parameters' C.I. to see if they overlap or not. This is another way to test if there is correlation between the variables; since they are different parameters and the units differ, it is not suitable to use mean values or standard deviations to test the similarity between the two sample populations (Payton et al., 2000; Vangel, 1996; Verrill, 2003).

Thus, for $100\,(1-\alpha)\%$ and $\nu = n-1$ degrees of freedom, the modified McKay Confidence Interval for a COV (Vangel, 1996) is:

$$\left[\left(\frac{u_1+2}{n}-1\right)K^2+\frac{u_1}{\nu}\right]^{-0.5} K \leq COV \leq K\left[\left(\frac{u_2+2}{n}-1\right)K^2+\frac{u_2}{\nu}\right]^{-0.5} \quad (5.1)$$

where K is the point estimate of COV ($K = S/\bar{X}$), $u_1 = \chi^2_{\nu,1-\alpha/2}$, and $u_2 = \chi^2_{\nu,\alpha/2}$. Therefore, K is a function of the sample standard deviation (S), and the sample mean ($\bar{X}$).

Another modified approach to MacKay C.I. is suggested by Payton (1997):

$$\chi^2_{\nu,1-\alpha/2}\left[\frac{1+K^2}{nK^2}\right]^{-0.5} \leq COV \leq \chi^2_{\nu,\alpha/2}\left[\frac{1+K^2}{nK^2}\right]^{-0.5} \tag{5.2}$$

The main difference between both Equations is that the latter one can be used for any COV value, while Equation (5.1) is restricted to $0 < COV \leq 0.33$ (Vangel, 1996; Verrill, 2003). C.I. are reported together with the pairwise comparison results.

Development of allometric correlations. To study the $SA_{plot} : LA_{plot}$ relationship, a vegetated plot has been conceptualized as a surface ground area with a single big tree whose sapwood area is the summation of all the trees' sapwood area inside the plot. Likewise, the big tree's leaf area will be the summation of all trees' leaf area inside the plot. Despite the simplicity of the concept, it takes into account vegetation heterogeneity.

Based on this concept, allometric correlations and linear models were developed here in order to measure sapwood area at the tree and at the plot scale. At the tree scale, the models are firstly based on each species $\bar{sd}$ and DBH_{OB} data. The obtained correlations were used to estimate each tree's sapwood area inside the delimited plots and to aggregate sapwood area at the plot scale.

The plot's sapwood area estimates were derived by two different approaches. The first approach was by the previously defined $\bar{sd}:DBH_{OB}$ correlations per species. The second approach was by using sapwood area average values, and it was taken as an alternative when the $\bar{sd}:DBH_{OB}$ correlation was null. The leaf area per plot, LA_{plot}, was derived from LAI mensurations and the surface ground area of interest. It was understood that modelling $SA_{plot} : LA_{plot}$ carries uncertainties while aggregating to large areas. Thus, uncertainties were estimated through propagation error equations and reported here in this chapter.

Sampling design. Plots of different sizes are used to compare the responses of SA_{plot}: LA_{plot}. Four plots are of $60 \times 60m$, and nine of $10 \times 10m$. These plots are located in the Sibbald Areas of Kananaskis Country, Alberta. The species composition of these plots was either dominated by deciduous trees (mainly Trembling aspen), or coniferous trees (Lodgepole pine and White spruce). Figures 5.1 and 5.2 show the location and delimitation of the plots. Two more plots were delimited at Whitecourt, one dominated by Jack pine individuals and one dominated by Black spruce individuals. The Jack pine plot was $20 \times 20m$, and the Black spruce plot was $15 \times 15m$. The plots were labelled as **Coniferous** for those whose species composition was dominated by a conifer tree, and **Deciduous** for those whose species composition was dominated by a deciduous tree. The site characteristics are considered to be uniform between plots with similar species composition, with the exception of the Black spruce plot. The Black spruce plot is located in a lowland area with hydric, organic soil (very poor drainage conditions). The smallest plots ($10 \times 10m$) were distinguished from the largest ones ($\geq 300m^2$) by adding a prime symbol in front of their assigned number.

Field data collected at each plot include number of trees per plot, each tree's DBH_{OB}, and Leaf Area Index. Mensurations of LAI were taken in the $60 \times 60m$ plots using the Tracing Radiation and Architecture Canopies (TRAC, 3rd Wave Engineering Co.; Nepean, Canada) device. The Canopy Analyzer LAI-2000 (LI-COR Incorporated; Lincoln Nebraska, US) was used at the two plots located in Whitecourt.

Saplings. It goes without saying that saplings practically lack heartwood, being mostly composed of sapwood (Kramer and Kozlowski, 1979; Hillis, 1987; Čermák and Nadezhdina, 1998). Thus, saplings correlations between DBH_{OB} and $\bar{sd}$, or between DBH_{OB} and SA_{sp} will be different and it is assumed therefore that such correlations have to be treated separately from the rest of the trees. Saplings are considered to be those trees whose DBH_{OB} range is $\approx 2.41cm - 10.2cm$ (or a $CBH \approx 7.6cm - 32.0cm$), and $38.1cm - 76.2cm$ tall. Saplings are not included in any of the allometric correlations. Thus, all trees found inside of the plots with a $DBH_{OB} \leq 10cm$ were dismissed. The studied sites do not hold significant quantities of saplings (see § 5.2 for details).

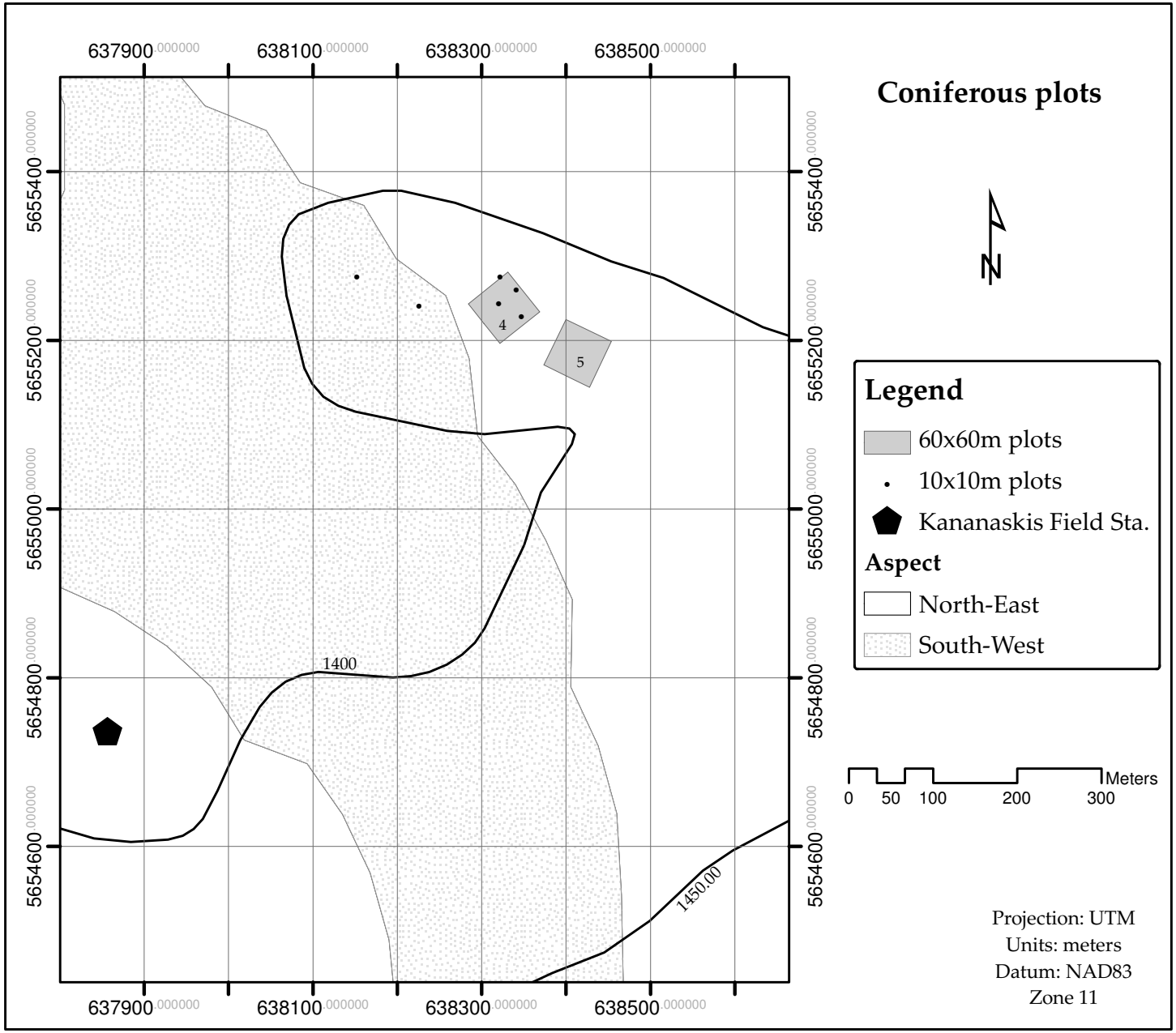

Figure 5.1: Geographical location of Coniferous plots. The plots are in the Sibbald areas of Kananaskis Country. Contour lines were extracted from the Base Features GIS (AltaLIS, 2006), 1:20,000. Aspect was retrieved from the GEODE archive's Digital Elevation Models (100m grid, [MADGIC (2006)]).

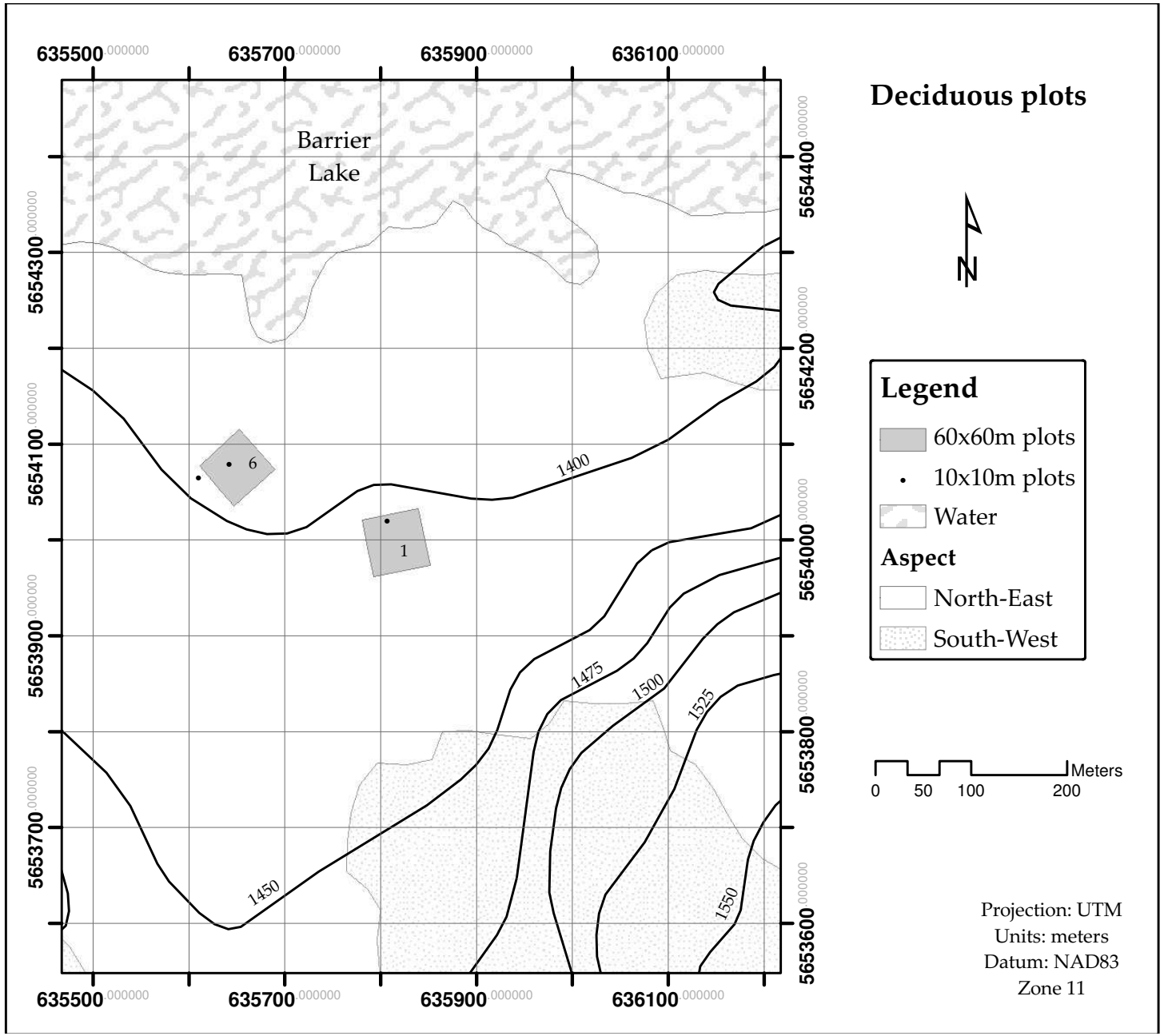

Figure 5.2: Geographical location of Deciduous plots. The plots are in the Sibbald areas, South-East of Barrier Lake (Kananaskis Country). Contour lines and Hydrographic features were extracted from the Base Features GIS (AltaLIS, 2006), 1:20,000. Aspect was retrieved from the GEODE archive's Digital Elevation Models (100m grid, [MADGIC (2006)]).

5.2 Results and analysis of results

The obtained results are divided in three main parts. The first part describes and analyses each species $\bar{sd} : DBH_{OB}$ allometric correlations. The second part is the description of the theory behind the estimation of sapwood area per species (SA_{sp}) and plot's Leaf Area (LA_{plot}). The theory also describes the aggregation of sapwood area to the plot scale (SA_{plot}) by combining two scaling approaches. The third and last part describes and analyses the $SA_{plot} : LA_{plot}$ relationship. Finally, the developed equations for estimating error propagation are described.

5.2.1 Tree scale allometric correlations

Jack pine, Lodgepole pine. The sample sets of Jack pine and Lodgepole pine are integrated in a single group to obtain sapwood depth and sapwood area estimates. Looking at the crossplot of $\bar{sd}$ and DBH_{OB}, it is evident that individuals of similar DBH_{OB} could have an $\bar{sd}$ that approximately ranges between $2.90cm$ and $3.99cm$ and there is no specific pattern that may suggest a linear model or any other type of model (Figure 5.3). The Pearson's correlation (ρ) between $\bar{sd}$ and DBH_{OB} is 0.005, and the tested hypothesis of the correlation coefficient being zero ($H_o : \rho = 0$) gives a P-value of 0.979 ($\alpha = 0.05$); therefore, it is concluded that there is no linear correlation between the variables of interest.

Black spruce. For Black spruce, a similar behaviour was observed as in the previous two species. The correlation between $\bar{sd}$ and DBH_{OB} was practically null ($\rho = 0.202$), with a P-value of 0.379 ($\alpha = 0.05$). Also, there is no evidence for fitting any other type of model to this data set. Figure 5.4 shows the crossplot between $\bar{sd}$ and DBH_{OB}, and it is clearly apparent that there is no relationship at all between these two variables. Moreover, for trees with similar DBH_{OB}, their $\bar{sd}$ may vary between $\approx 1.08cm$ and $\approx 4.77cm$.

In these two particular cases (i.e. Jack pine and Lodgepole pine, and Black spruce),

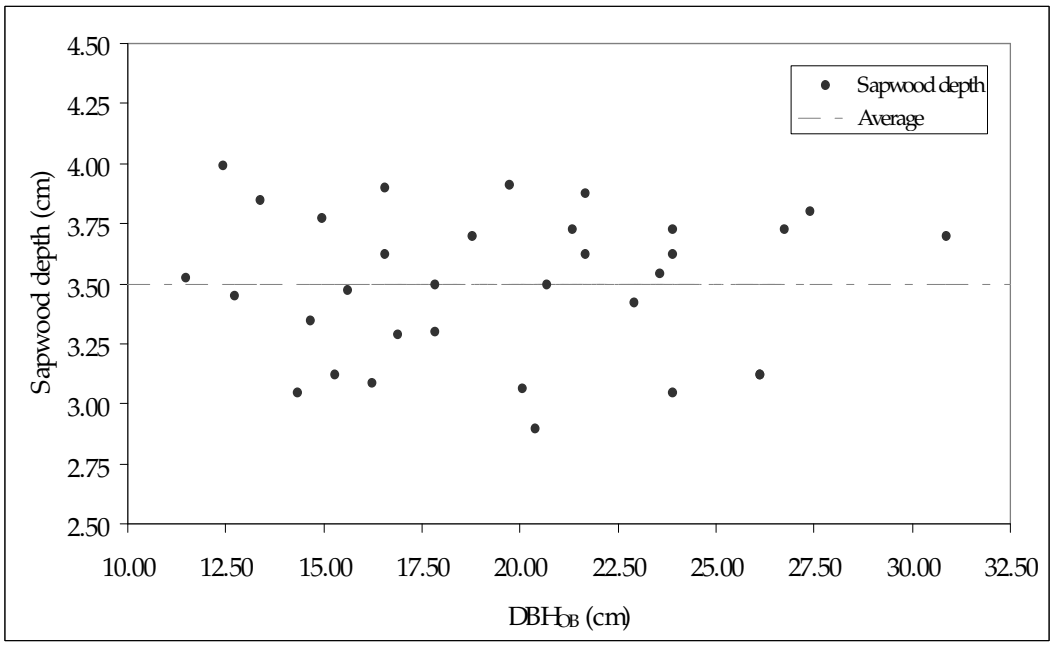

Figure 5.3: Jack pine and Lodgepole pine $\bar{sd}$ in relation to DBH_{OB}.

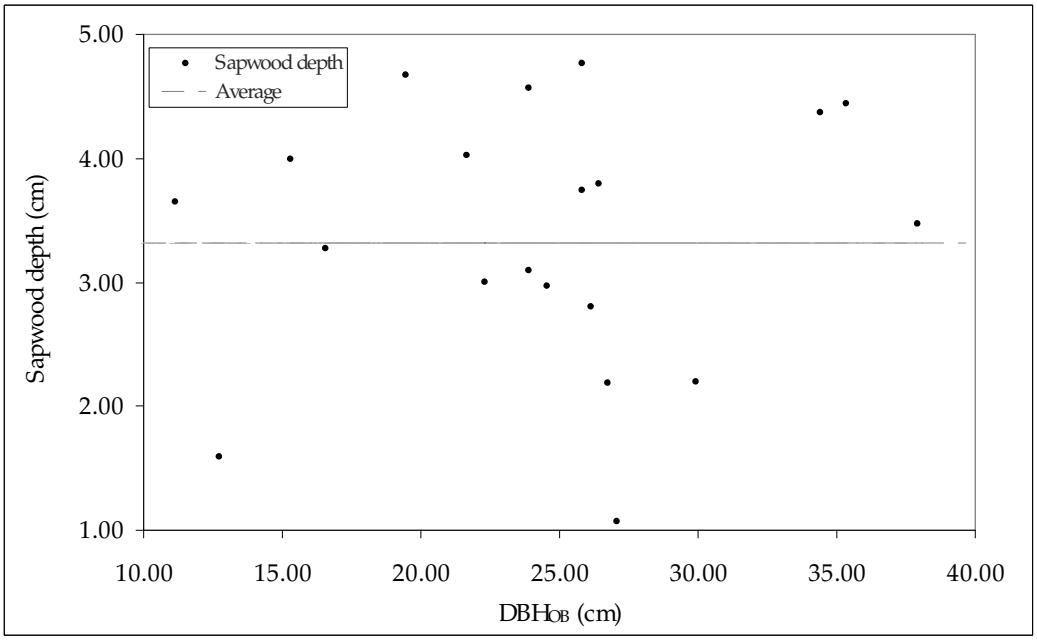

Figure 5.4: Black spruce $\bar{sd}$ in relation to DBH_{OB}.

Pearson's correlation shows that $\bar{sd}$ does not depend on tree's DBH_{OB}. This result is in agreement with the previous Jack Pine, Lodgepole pine and Black spruce results showing that big trees tend to have large sapwood area because of the tree size and not because of their sapwood depth (Chapter 4).

White spruce. There is a significant, positive linear correlation between White spruce's $\bar{sd}$ and DBH_{OB} ($\rho = 0.916$). The P-value of the tested hypothesis of the correlation coefficient being zero ($H_o : \rho = 0$) gives enough evidence to conclude that the correlation is linear (P-value < 0.0001, $\alpha = 0.05$). The fitted linear regression model is of the form:

$$\bar{sd_i}' = 0.0887\, DBH_{OB_i} + 0.6828 \tag{5.3}$$

with a Standard Error (SE) of $0.1131cm$. For the fitted regression model, the regression analysis, the ANOVA, and list of unusual observations are given in Table C.1 (Appendix C). The regression analysis shows the significance of DBH_{OB} as a predictor of $\bar{sd}$ (P-value < 0.0001, $\alpha = 0.05$), and the ANOVA results point at its significant contribution to the model as well (P-value < 0.0001, $\alpha = 0.05$). The coefficient of determination (R^2) implies that 83.9% of the variation in $\bar{sd}$ is well explained by DBH_{OB}. The coefficient of determination for predictions (R^2_{pred}), which describes the regression model predictive capability (Montgomery, 2001), is in reasonable agreement with the adjusted coefficient of determination (R^2_{adj}). The regression plot with its 95% C.I. is shown in Figure 5.5, and it shows that DBH_{OB} mostly explains the variation in $\bar{sd}$ and the C.I. naturally widens at the plot's extrema. Finally, the plot of residuals shows no pattern and the normal probability plot of residuals tend to be linear in the center. Hence, these two plots are a good evidence of a linear correlation between White spruce's DBH_{OB} and $\bar{sd}$ values.

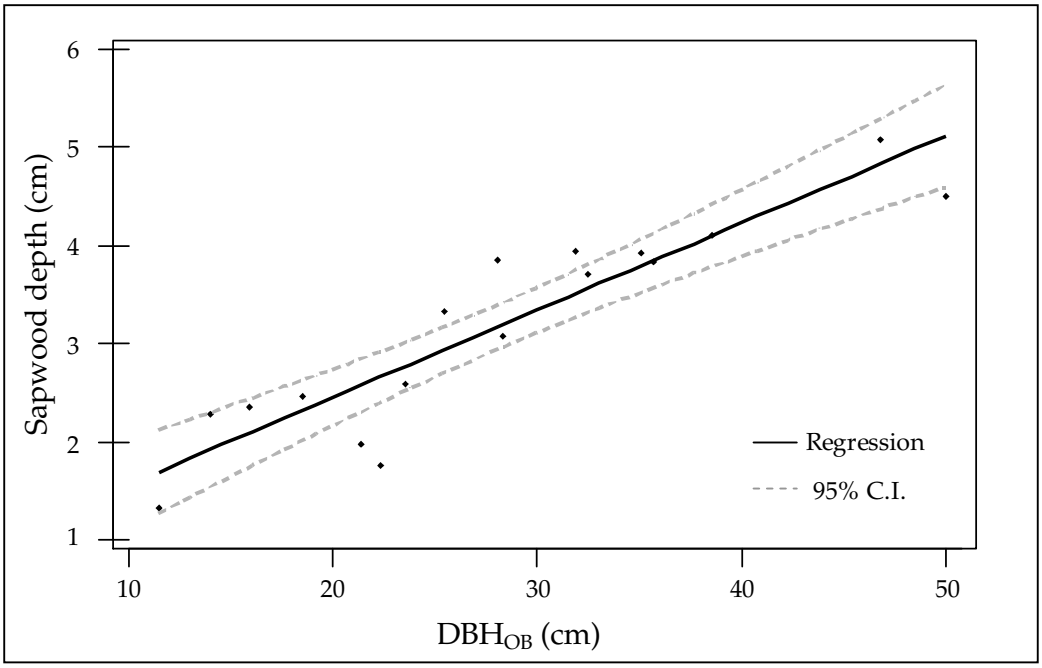

Figure 5.5: White spruce $\bar{sd}$ in relation to its DBH_{OB}.

Trembling aspen. For Trembling aspen, there is a significant, positive linear correlation between DBH_{OB} and $\bar{sd}$ ($\rho = 0.735$). The P-value of the tested hypothesis of the correlation coefficient being zero ($H_o : \rho = 0$) gives enough evidence to conclude that the correlation is linear (P-value < 0.0001, with an $\alpha = 0.05$). Thus, linear regression was the approach to obtaining Trembling aspen $\bar{sd}$ estimates ($\bar{sd}'$). The linear regression model is as follows:

$$\bar{sd_i}' = 0.2441\, DBH_{OB_i} - 1.166 \tag{5.4}$$

with an SE of $0.3092cm$. The regression analysis, the ANOVA for significance of the regression model, and the list of unusual observations are given in Table C.2. The regression analysis shows that, in Trembling aspen individuals, the DBH_{OB} is a significant predictor of $\bar{sd}$ (P-value < 0.0001, $\alpha = 0.05$). The R^2 implies that 54% of the

variation in $\bar{sd}$ is well explained by DBH_{OB}. In comparison with the White spruce case, Trembling aspen trees' DBH_{OB} explain less of their variability in $\bar{sd}$. Still, the coefficient of determination for predictions, R^2_{pred}, is in reasonable agreement with the R^2_{adj}. The ANOVA also indicates the significant contribution of DBH_{OB} to the regression model ($\alpha = 0.05$). Figure 5.6 shows the Trembling aspen regression plot and its 95% Confidence Intervals (95% C.I.) for the mean response. The regression plot shows that there is still a fair amount of variation in $\bar{sd}$ that is not explained by DBH_{OB} per se. Nonetheless, there is no evidence of lack of fit (P-value>0.1), meaning that the regression function is linear. In the list of unusual observations, two observations are marked as having a large influence and large standardized residual; however, they are not outliers ($\bar{sd}$ and DBH_{OB} values were verified) and they remain in the data set. The plotted residuals versus estimated values show no pattern, which helps to establish that the model is adequate and that the assumptions of linear, positive correlation between Trembling aspen's DBH_{OB} and $\bar{sd}$ are satisfied.

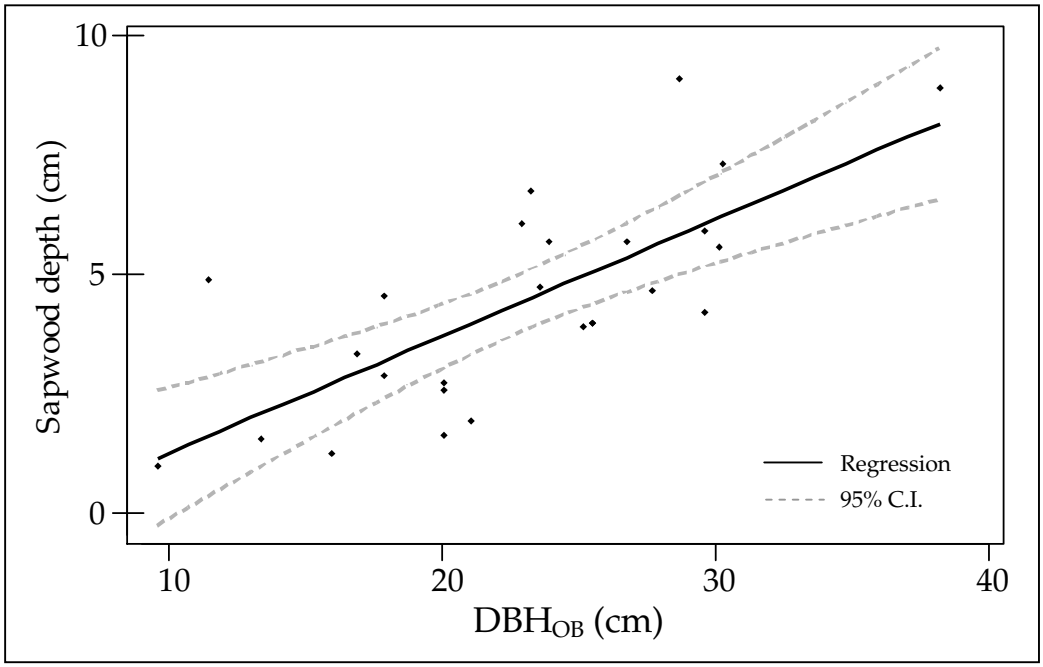

Figure 5.6: Trembling aspen $\bar{sd}$ in relation to its DBH_{OB}.

5.2.2 Aggregation of sapwood area at the plot scale

Since it was feasible to fit a model for just two of the five studied species, the aggregation of Sapwood Area at the plot scale is performed by fusing two approaches. Thus, to estimate the Sapwood Area at every plot (SA_{plot}), if White spruce and/or Trembling aspen trees are present, their respective linear model is applied (first approach); while under the presence of Jack pine and Lodgepole pine, and/or Black spruce, their respective average sapwood area ($\overline{SA}_{sp}$) is applied (second approach).

In more detail, if the linear models of White spruce or Trembling aspen are used to aggregate; the estimated SA per tree will be obtained by applying Equation (4.5). Therefore, the estimated SA_{plot} will be the summation of each tree's SA:

$$\begin{aligned} SA_{plot} &= \sum_{i=1}^{tq} SA_i \\ &= \sum_{i=1}^{tq} (DBH_{OB_i}\, \bar{sd_i}' - [\bar{sd_i}']^2)\, \pi \end{aligned} \tag{5.5}$$

where tq is the total number of trees inside the plot (i.e. tree quantity), DBH_{OB_i} is the ith individual's DBH_{OB}, and $\bar{sd_i}'$ is ith individual's estimated sapwood depth that, in the case of White spruce is estimated by Equation (5.3), or in the case of Trembling aspen, is estimated by Equation (5.4).

Based on previous results (Chapter 4) it is assumed that SA_{JP}, SA_{LP}, and SA_{BS} remain relatively constant as the tree grows. Therefore, the estimated SA_{plot} in the presence of these species is:

$$SA_{plot} = \overline{SA}_{sp}\, tq \tag{5.6}$$

where $\overline{SA}_{sp}$ is the species average sapwood area calculated by:

$$\overline{SA}_{sp} = \frac{\sum_{i=1}^{n} (DBH_{OB_i}\, \bar{sd}_i - [\bar{sd}_i]^2)\, \pi}{n} \tag{5.7}$$

Notice that $\overline{SA}_{sp}$ is calculated from the sample sets obtained to measure $\bar{sd}$ by microscopical differentiation of sapwood-heartwood boundaries, and to develop the correlations between $\bar{sd}$ and DBH_{OB}. Thus, n is the size of the sample set, DBH_{OB_i} is the sample set's ith individual's DBH_{OB}, and $\bar{sd}_i$ is ith individual's average sapwood depth (Equation [4.4]).

For mixed vegetation areas, the two approaches should be combined in order to estimate the total SA_{plot}. To illustrate, suppose a plot holding individuals of the species A and B, with a number of trees tq_A and tq_B of the species A and B respectively; therefore, the total number of trees is $tq = tq_A + tq_B$. Also, each individual's DBH_{OB} has been measured. It is already known that species A fits a linear model, while species B has an average sapwood area ($\overline{SA}_B$). To estimate the total SA_{plot}, both Equations (5.5) and (5.6) are used as follows:

$$SA_{plot} = \sum_{i=1}^{tq_A} SA_A + \overline{SA}_B\, tq_B$$

$$SA_{plot} = \left[\sum_{i=1}^{tq_A} (DBH_{OB_i}\, \bar{sd}_i{}' - [\bar{sd}_i{}']^{\,2})\, \pi \right] + \overline{SA}_B\, tq_B$$

and depending on which species is A, the Equation (5.3) or (5.4) is applied to calculate $\bar{sd}_i{}'$.

Furthermore, estimations of SA_{WS} can be reduced by substituting Equation (5.3) into (5.5) and leaving it all in terms of DBH_{OB}:

$$SA_{WS} = (0.0808\, [DBH_{OB}]^2 + 0.5617\, DBH_{OB} - 0.4662)\, \pi \tag{5.8}$$

For SA_{TA}, Equation (5.4) is substituted into Equation (5.5) to obtain:

$$SA_{TA} = (0.1845\,[DBH_{OB}]^2 - 0.5958\,DBH_{OB} - 1.3596)\,\pi \tag{5.9}$$

The calculation of SA_{plot} estimates by means of using two approaches (Equations [5.5] and [5.6]) is considered to be reliable for a group of trees whose CBH_{OB} falls between the maximum and minimum CBH_{OB} of sampled trees (Tables 4.3, 4.6, 4.10, and 4.13).

The SA_{plot} calculated for each $60 \times 60m$ and $10 \times 10m$ plot, including tree species, tree quantity, plot's DBH_{OB} statistics and the error associated with SA_{plot} are given in Tables 5.1 and 5.2 (refer to § 5.2.4 for details on the error estimation).

The Conifer sites are those whose tree composition is of White spruce, Lodgepole pine, Jack pine, and Black spruce. The Deciduous sites are mainly composed of Trembling aspen. If Deciduous individuals were present in the Coniferous plots, their number should count for less than 10% of the total tree quantity or be mainly saplings. Such is the case of the site Conifer-5, whose Trembling aspen tree quantity is 114; however, 92 individuals were saplings. Thus, the count of deciduous trees inside the plot was considered to be minimum. Most of the Deciduous sites were 100% pure, and if any other tree was present, its count was less than 5% of the total plot's tree quantity (e.g. Deciduous-6). Most of the Coniferous sites ($10 \times 10m$ and $60 \times 60m$) are composed of White spruce and Lodgepole pine trees. The two pure Coniferous sites are Conifer-11 and Conifer-12 (see Table 5.1).

Notice that the contribution of Lodgepole pine individuals to the total SA_{plot} is larger than the White spruce contribution, even if the number of White spruce trees is larger than Lodgepole pine's. Naturally, this may be related to the approach used to estimate Lodgepole pine's sapwood area. In general terms, all $60 \times 60m$ Coniferous sites' SA_{plot} increments corresponds to increments in their tree quantity. However, for all $10 \times 10m$ Coniferous sites' there is no correspondence between SA_{plot} and the increment in tree quantity. All the Deciduous sites show a larger SA_{plot} as tree quantity increases.

Table 5.1: Descriptive statistics of the 60×60m plots located in the Sibbald areas of Kananaskis Country, Alberta, and Whitecourt [WC], Alberta. ΔSA_{plot} is the error on SA_{plot}.

Plot	**Tree species**	**Tree quantity**	**DBH_{OB}**			**SA_{sp}** (m^2)	**SA_{plot}** (m^2)	**ΔSA_{plot}** (m^2)
			Maximum	Minimum	Average			
Conifer-4[1]	White spruce	434	43.30	2.20	13.14	2.92		
	Lodgepole pine	276	33.42	5.73	20.15	4.87	7.79	±0.03
Conifer-5[1]	White spruce	164	48.38	2.86	18.31	2.29		
	Lodgepole pine	48	26.10	1.59	14.09	0.85		
	Trembling aspen	114	19.42	2.86	7.23	0.14	3.28	±0.03
Conifer-11[2]	Jack pine	129	25.15	6.37	16.57	2.28	2.28	±0.03
Conifer-12[2]	Black spruce	60	23.55	5.09	15.69	1.28	1.28	±0.01
Deciduous-1[1]	Trembling aspen	83	25.46	9.55	18.57	1.42	1.42	±0.01
Deciduous-6[1]	Trembling aspen	498	31.19	8.91	19.10	9.03		
	White spruce	14	48.38	7.00	23.40	0.31	9.34	±0.08

[1]Sibbald areas

[2]Whitecourt, AB

Table 5.2: Descriptive statistics of the $10 \times 10m$ plots located in the Sibbald areas of Kananaskis Country, Alberta. ΔSA_{plot} is the error on SA_{plot}.

Plot	**Tree species**	**Tree quantity**	**DBH_{OB}**			**SA_{sp}** (m^2)	**SA_{plot}** (m^2)	**ΔSA_{plot}** (m^2)
			Maximum	Minimum	Average			
Conifer-1'	White spruce	29	24.51	5.09[1]	6.53	0.16		
	Lodgepole pine	12	26.74	14.01	19.89	0.21	0.37	±0.001
Conifer-2'	White spruce	15	27.06	7.64[1]	14.88	0.21		
	Lodgepole pine	9	27.37	16.23	20.23	0.16	0.37	±0.001
Conifer-3'	White spruce	19	25.78	4.46[1]	12.48	0.19		
	Lodgepole pine	13	29.60	10.82	19.98	0.23	0.42	±0.0007
Conifer-4'	White spruce	9	21.33	3.50[1]	12.59	0.04		
	Lodgepole pine	14	27.06	11.78	20.35	0.25	0.29	±0.0003
Conifer-5'	White spruce	4	28.33	12.41	18.94	0.05		
	Lodgepole pine	13	32.79	15.92	22.33	0.23	0.28	±0.0002
Conifer-10'	White spruce	5	33.74	5.09[1]	16.87	0.19		
	Lodgepole pine	14	34.70	12.73	21.99	0.11		
	Trembling aspen	1	21.01			0.03	0.33	±0.0005
Deciduous-7'	Trembling aspen	31	32.79	9.87[1]	17.15	0.70	0.70	±0.004
Deciduous-8'	Trembling aspen	28	28.01	14.01	20.29	0.87	0.87	±0.005
Deciduous-9'	Trembling aspen	22	23.24	14.64	19.92	0.65	0.65	±0.004

[1]Remember that even if sapling trees were present, they were not included for SA_{plot} estimations.

5.2.3 Plot scale allometric correlations

LAI measurements and Leaf Area estimations.

Mensurations of LAI were taken in the $60 \times 60m$ plots using the Tracing Radiation and Architecture Canopies (TRAC, 3rd Wave Engineering Co.; Nepean, Canada). The Canopy Analyser LAI-2000 (LI-COR Incorporated; Lincoln Nebraska, US) was used at the two plots located in Whitecourt; thus, the obtained values at these two plots are effective LAI (LAI_{eff}). Consequently, it was necessary to convert the LAI_{eff} to LAI by using the proposed Chen's equation (Chen and Cihlar, 1996):

$$LAI = (1 - \alpha_l) LAI_{eff}\, \gamma_E / \Omega_E \tag{5.10}$$

where α_l is the woody-to-total area ratio (i.e. tree's woody fraction), γ_E is the needle-to-shoot area ratio (i.e. fraction of needles per shoot), Ω_E is the clumping index. In order to derive the α_l and γ_E values from the typical values reported by Leblanc et al. (2002), the age and productivity of the stand needs to be known. Thus, age and productivity characteristics were defined by comparing the LAI_{eff} with typical LAI_{eff} reported by Chen et al. (1997). The LAI_{eff} of the Jack pine plot is similar to an intermediate/medium productivity stand ($LAI_{eff} = 2.20$), thus α_l is assumed as 0.05 and γ_E as 1.35. The Black spruce plot LAI_{eff} value is similar to a mature medium/high productivity stand ($LAI_{eff} = 2.78$), thus α_l is assumed as 0.14 and γ_E as 1.35. Finally, Ω_E was derived from typical values reported by Chen et al. (1997); thus, the Black spruce and the Jack pine Ω_E values are respectively set as 0.65 and 0.75. The LAI estimates of the Jack pine and Black spruce plots are shown in Table 5.3.

Leaf Area per plot (LA_{plot}) is estimated by following the definition of LAI (Chen and Black, 1992): "The total one-sided (or one half of the total all-sided) green leaf area per unit ground surface area". In this particular case, the unit ground area is the plot

Table 5.3: Measured LAI_{eff} and LAI estimates for the plots located in Whitecourt, Alberta. Due to logistics, the LAI-2000 was used to obtain LAI estimates for these two sites. The rest of the plots' LAI values were measured with the TRAC optical device.

Site	$\boldsymbol{LAI_{eff}}$	$\boldsymbol{\alpha}$	$\boldsymbol{\gamma_E}$	$\boldsymbol{\Omega}$	$\boldsymbol{LAI}$
Conifer-11	2.20	0.05	1.35	0.75	3.76
Conifer-12	2.78	0.14	1.35	0.65	4.96

surface area expressed in m^2, thus:

$$LAI = \frac{LA_{plot}}{A_{plot}} \tag{5.11}$$

Thus, the total LA_{plot} is defined as the plot's LAI multiplied by the plot's total surface area (A_{plot}):

$$LA_{plot} = (LAI)A_{plot} \tag{5.12}$$

Values of LAI, plots' size, LA_{plot}, and the error on LA_{plot} estimations are given in Tables 5.4 (Coniferous sites) and 5.5 (Deciduous sites). Each plot's LAI concurs with previous reported values by Chen et al. (1997), Chen and Cihlar (1996) and Robinson et al. (2002) (Tables 5.4 and 5.5). The error on a plot's LAI is ± 0.10 for Deciduous and ± 0.13 for Coniferous. As it is shown in Table 5.4, the Coniferous $10 \times 10m$ plots' area is adjusted and reported as $150m^2$ in order to take into account what is known as the "TRAC footprint". TRAC footprint is created by trees whose shadows are large enough to fall into the delimited plot influencing the TRAC measurements. Thus, the LAI obtained belongs to a larger area than the delimited one. This effect is not evident in the $10 \times 10m$ Deciduous plots as it is demonstrated in §5.2.3. According to Leblanc et al. (2002), the TRAC footprint is influenced by the tree height and the solar zenith angle (θ). It is assumed that in Kananaskis Country the coniferous trees' average height is about $15m$; the Solar noon zenith angle is about $45.21°$ at the date when LAI measurements where taken ($DOY = 238$). Therefore, the extent of the

footprint ($tree\ height \times tan\theta$) is $15.00m$. This extent occurs in just one side of the plot, giving a LAI for a plot's area of $10 \times 15m$.

Table 5.4: LAI and estimated LA_{plot} according to plot size for the Coniferous sites. ΔLA_{plot} is the error on LA_{plot} estimates (see § 5.2.4 for details.)

Site	***LAI***	**Plot size** (m^2)	$\mathbf{LA_{plot}}$ (m^2)	$\mathbf{\Delta LA_{plot}}$ (m^2)
Conifer-1'	6.90	150.00	1,035.00	±19.90
Conifer-2'	6.04	150.00	906.00	±19.04
Conifer-3'	6.57	150.00	985.00	±19.57
Conifer-4'	5.34	150.00	801.00	±18.34
Conifer-5'	4.51	150.00	676.50	±17.51
Conifer-10'	6.12	150.00	918.00	±19.12
Conifer-4	5.71	3,600.00	20,556.00	$\pm 1,338.20$
Conifer-5	2.54	3,600.00	9,144.00	±855.10
Conifer-11	3.76	400.00	1,502.52	±259.32
Conifer-12	4.96	300.00	1,486.97	±242.82

Table 5.5: LAI and estimated LA_{plot} according to plot size for the Deciduous sites. ΔLA_{plot} is the error on LA_{plot} estimates (see § 5.2.4 for details).

Site	***LAI***	**Plot size** (m^2)	$\mathbf{LA_{plot}}$ (m^2)	$\mathbf{\Delta LA_{plot}}$ (m^2)
Deciduous-1	2.64	415.00	1,093.53	±405.85
Deciduous-6	3.14	3,600.00	11,304.00	$\pm 1,411.27$
Deciduous-7'	2.30	100.00	230.00	±12.30
Deciduous-8'	3.57	100.00	357.00	±13.57
Deciduous-9'	3.22	100.00	322.00	±13.22

Deciduous SA_{plot}-LA_{plot} correlation.

In the case of the Trembling aspen sites, a close similarity was found between the two sets of plots in terms of LAI. In order to support this observation, a Bartlett's test and F-test (for equality of variances) was applied to the LAI values obtained in the plots of $10\times10m$ and $60\times60m$. Based on the two statistical test results, it is concluded that the LAI variances of the two sample sets are equal (C.I. = 95%) and that the two sets can be merged to generate a single regression model for aggregating SA_{TA} at the plot scale. It is considered that the explanation for such similarity between Trembling aspen's leaf area at different scales is related to canopy type. Unlike coniferous trees, Trembling aspen canopy is horizontally wide, creating small gaps between the canopy of neighbouring trees.

This effect of Trembling aspen canopies is due to their wide-circular leaves and their alternate (not clumped) distribution. At the same time, the leaves are practically at the top of the tree, creating a rounded crown with a large diameter. Moreover, in the studied sites, the Trembling aspen tree height is similar. The combination of these characteristics gives wider tree shadows that practically cover the entire plot's floor at noon. Thus, inside the plot there is little room for observing the footprint of external trees in any direction; meaning that the TRAC device mostly measures the LAI inside the plot with a negligible footprint. This is proven by plotting the LAI measured in the East-West and North-South transects (Figure 5.7). In both East-West and North-South directions, LAI is practically the same value (a Paired T-test proved that the difference in the population means is equal to zero, with an $\alpha = 0.05$). Hence, it is concluded that it is possible to merge both data sets to obtain a linear regression model.

The estimated SA_{plot} and LA_{plot} for the Trembling aspen sites, their Pearson's correlation coefficient (ρ), and the P-value of the tested hypothesis of the correlation coefficient being zero ($H_o : \rho = 0$) are shown in Table 5.6. For all Trembling aspen sites, there is a strong linear correlation between SA_{plot} and LA_{plot} ($\rho \approx 1.0$), and the P-value gives sufficient evidence to conclude that indeed, the correlation is not zero ($\alpha = 0.05$).

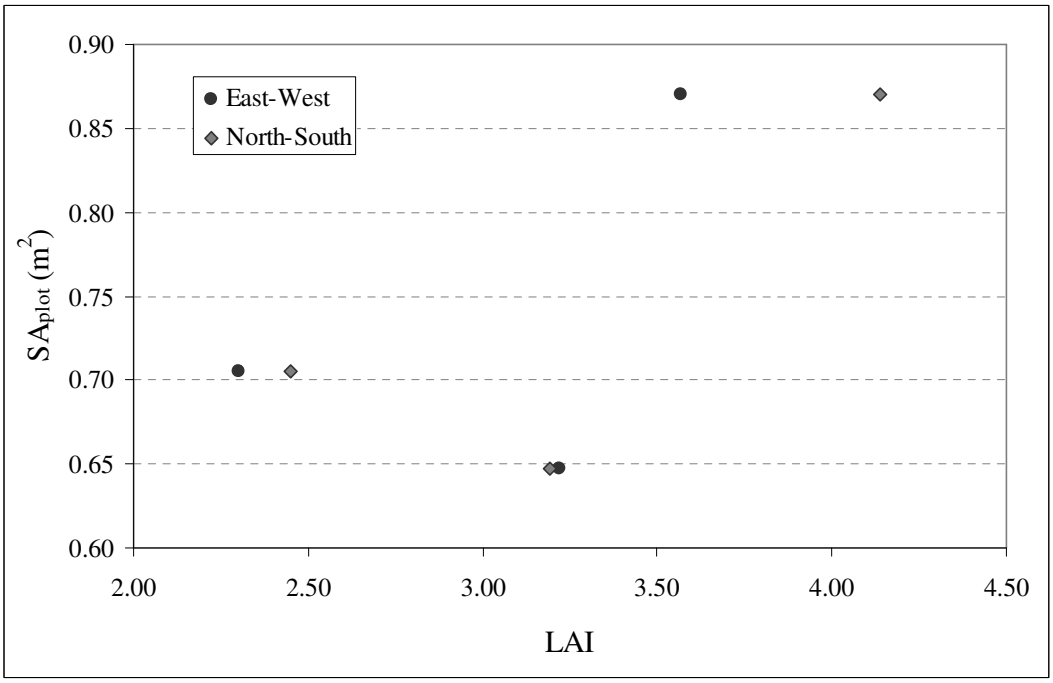

Figure 5.7: The $10 \times 10m$ LAI values taken from East to West and from North to South.

Table 5.6: Estimated sapwood area and their respective leaf area per plot. Results correspond to the Trembling aspen sites. The first two sites are of size $60 \times 60m$ while the last three are of $10 \times 10m$. ρ is the Pearson's correlation coefficient.

Site	$\mathbf{SA_{plot}}$ (m^2)	$\mathbf{LA_{plot}}$ (m^2)	ρ	**P-value**
Deciduous-1	1.42	1,093.53		
Deciduous-6	9.35	11,304.00		
Deciduous-7'	0.70	230.00		
Deciduous-8'	0.87	357.00		
Deciduous-9'	0.65	322.00	0.9998	<0.0001

Table 5.7 shows the two regression models fitted to the Trembling aspen data set at the plot scale. Both models were assessed based on the results of the regression analysis, the ANOVA for significance of regression, and the Standardized Residuals (StdRes).

Table 5.7: The two linear regression models fitted between SA_{plot} and LA_{plot} of Trembling aspen. SE is the model's Standard Error.

Model ($\hat{y} = \beta_0 + \beta_1 x$)	$\mathbf{R^2}$	$\mathbf{R^2_{adj}}$	$\mathbf{R^2_{pred}}$	**SE** (m^2)
$SA'_{plot} = 0.518 + 0.0007816\, LA_{plot}$	100%	99.9%	98.61%	0.04933
$SA'_{plot} = 0.478 + 0.0008619\, LA_{plot}$	95.0%	92.4%	87.83%	0.06856

Results of the regression analysis support the decision of fitting a linear model to the data (Table C.3), showing that LA_{plot} resulted in a significant predictor of SA_{plot} with a P-value < 0.0001 ($\alpha = 0.05$). Table C.3 also includes the results of the ANOVA for significance of the regression model. Once more, the ANOVA results determined that LA_{plot} contributes significantly to the model ($\alpha = 0.05$). The large value of the coefficient of determination ($R^2 = 100\%$) implies that the whole variation in SA_{plot} is perfectly explained by the obtained regression model. The R^2_{adj} does not greatly differ from the R^2 (0.01% of difference), and the R^2_{pred} is in reasonable agreement with the R^2_{adj}.

All previous results support the regression model for estimating Trembling aspen SA_{plot} by having LA_{plot} as a predictor. However, the list of unusual observations (third Table on C.3) draws attention to the large influence that the LA_{plot} of the Deciduous-6 site gives to the model. Even if the observation is not considered an outlier (StdRes < 2.00), it was removed from the sample set, and the regression model was fitted with the other four observations (latter model in Table 5.7). The second model's Regression analysis, ANOVA, and list of unusual observations are given in Table C.4.

In the second model, all the coefficients of determination values are lower than the ones of the first model. The R^2 shows a decrement of 5% with respect to the R^2 of the first model, and the R^2_{pred} is in reasonable agreement with the R^2_{adj}. Comparing

the two regression models, their slopes differ by about 9%, and the intercepts differ by about 7% (Table 5.7). Thus, the slope and intercept in both models do not drastically change. This demonstrates that the LA_{plot} observation in the Deciduous-6 site is not determining regression model fit, but supports the strong relationship between SA_{plot} and LA_{plot}. Thus, it is possible to use the first model for future predictions. The first linear model with its 95% C.I. is plotted in Figure 5.8. Figure 5.9 is the $60\times60m$ model with SA_{plot} and LA_{plot} in a logarithm base 10. The latter Figure is only to improve the graphical representation of the regression model, and no further analysis or discussion is based on this graph.

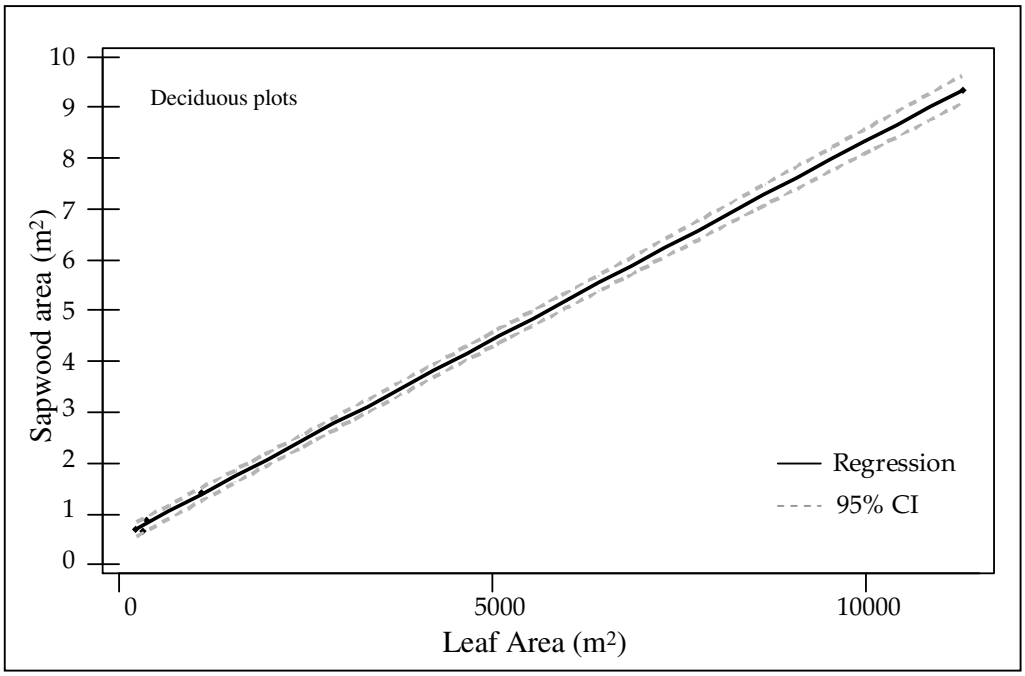

Figure 5.8: Trembling aspen SA_{plot} in relation to LA_{plot}.

Coniferous SA_{plot}-LA_{plot} correlation.

The coniferous SA_{plot} and LA_{plot} estimates for the $10\times10m$ and $60\times60m$ plots are given in Table 5.8. For all coniferous sites, there is a strong linear correlation between SA_{plot} and LA_{plot}, and the P-value supports that the correlation is not zero. However, if a

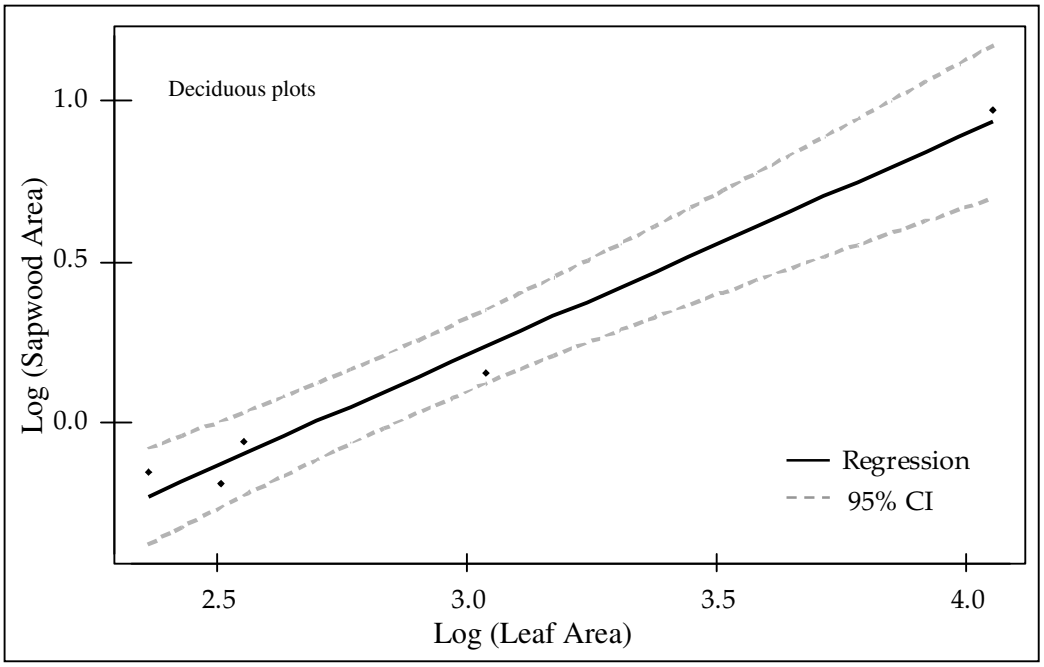

Figure 5.9: Plots of $60 \times 60m$. Deciduous Log(SA_{plot}) in relation to their Log(LA_{plot}) and the regression model's fitted line. Dotted lines are the 95% C.I. This Figure is intended to decrease the large difference among LA_{plot} values, and make clearer visualization of the $60 \times 60m$ regression model.

regression model is derived by using both sample sets ($10 \times 10m$ and $60 \times 60m$ plots), the Lack-of-fit test is significant at a P-value of 0.019. The Lack-of-fit test suggests a possible curvature in the model and that some other type of model should be fitted. It is assumed that the mismatch between the two data sets is due to the overestimation of LAI due to the influence of the footprint at the $10 \times 10m$ scale. As a consequence, the sapwood area for the $10 \times 10m$ plots are underestimated between 20% and 29.6%. Hence, in the case of the coniferous sites, the obtained values for the $10 \times 10m$ plots are not suitable for combination with the $60 \times 60m$ plots because of the footprint caused by the canopy type (which is not randomly distributed [clumped] and have large open areas that allow trees outside of the plot to reflect their shadows inside of it).

The two fitted regression models, the coefficients of determination and the models' SE are given in Table 5.9. First model corresponds to the $10 \times 10m$ plots, and the latter

Table 5.8: Estimated sapwood area and their respective leaf area per plot. Results correspond to the Coniferous sites. The first six sites are of size $10\times10m$ while the last four are of $60\times60m$. ρ is the Pearson's correlation coefficient ($\alpha = 0.05$).

Site	$\mathbf{SA_{plot}}$ (m^2)	$\mathbf{LA_{plot}}$ (m^2)	ρ	**P-value**
Conifer-1'	0.37	1035.00		
Conifer-2'	0.37	906.00		
Conifer-3'	0.42	985.50		
Conifer-4'	0.29	801.00		
Conifer-5'	0.28	676.50		
Conifer-10'	0.33	918.00		
			0.847[1]	0.033
Conifer-4	7.79	20,556.00		
Conifer-5	3.28	9,144.00		
Conifer-11	2.28	1,502.52		
Conifer-12	1.28	1,486.97		
			0.978[2]	0.022
			0.972[3]	<0.001

[1] ρ between $10\times10m$ plots. [2] ρ between $60\times60m$ plots.
[3] ρ includes all plots.

model is the fit for the $60\times60m$ plots. Both models have similar slopes, that differ by just about 11%. However, due to the underestimation of SA_{plot}, the $10\times10m$ data set shows a linear model that sits below from the $60\times60m$ model (Figures 5.10 and 5.11). Figure 5.12 is the $60\times60m$ model with SA_{plot} and LA_{plot} in a logarithm to base 10.

Tables C.5 and C.6 show the regression analysis, ANOVA and list of unusual observations for the $10\times10m$ and $60\times60m$ regression models respectively. In both models, the regression analysis and ANOVA results suggest that LA_{plot} is a significant predictor of SA_{plot} ($\alpha = 0.05$). However, the model's R^2_{pred} for the $10\times10m$ plots denotes inadequacy for future predictions (check plot of residuals and Normal plot). Moreover, the R^2_{pred} significantly differs from the R^2_{adj} (≈ 26.33). Contrary to the first model, the

Table 5.9: The two linear regression models fitted between SA_{plot} and LA_{plot} of Coniferous sites.

Plot size	**Model** $(\hat{y}=\beta_0+\beta_1 x)$	$\mathbf{R^2}$	$\mathbf{R^2_{adj}}$	$\mathbf{R^2_{pred}}$	**SE** (m^2)
$10\times10m$	$SA'_{plot} = 0.0341 + 0.000349\,LA_{plot}$	71.8%	64.7%	38.37%	0.0159
$60\times60m$	$SA'_{plot} = 1.1102 + 0.000312\,LA_{plot}$	95.5%	93.2%	68.60%	0.5281

$60\times60m$ one shows a better agreement between its coefficients of determination. Still the difference between R^2_{adj} and the R^2_{pred} is large, but the model adequacy check gives enough evidence to support the decision of fitting a linear model to the $60\times60m$ data set.

COV confidence intervals. The pairwise comparison of C.I. for COV is an extra analysis to support the applicability and reliability of the Equations given in Table 5.9, because the sample size for both data sets is not as large as desired when fitting a linear regression model. Therefore, this analysis reinforces the suggested relationship between the scaling factors, no matter the sample size. Since most of the COVs are larger than 0.33, Payton's equation (Equation [5.2]) was used to estimated the C.I. Table 5.10 displays the obtained COVs and C.I. of SA_{plot}, LAI, and LA_{plot}.

For the coniferous data set, the LA_{plot}, SA_{plot}, and LAI C.I. are not significantly different; therefore, there is an indication of correlation between these scaling factors. For the deciduous data set, the LA_{plot} and SA_{plot} C.I. are not significantly different, while the LAI C.I. is significantly different to LA_{plot} and SA_{plot} C.I. Therefore, there is an indication of correlation between LA_{plot} and SA_{plot} and of no correlation between SA_{plot} and LAI in the deciduous data set. These results are in reasonable agreement with the results obtained with the Pearson's correlation hypothesis test and the regression analysis.

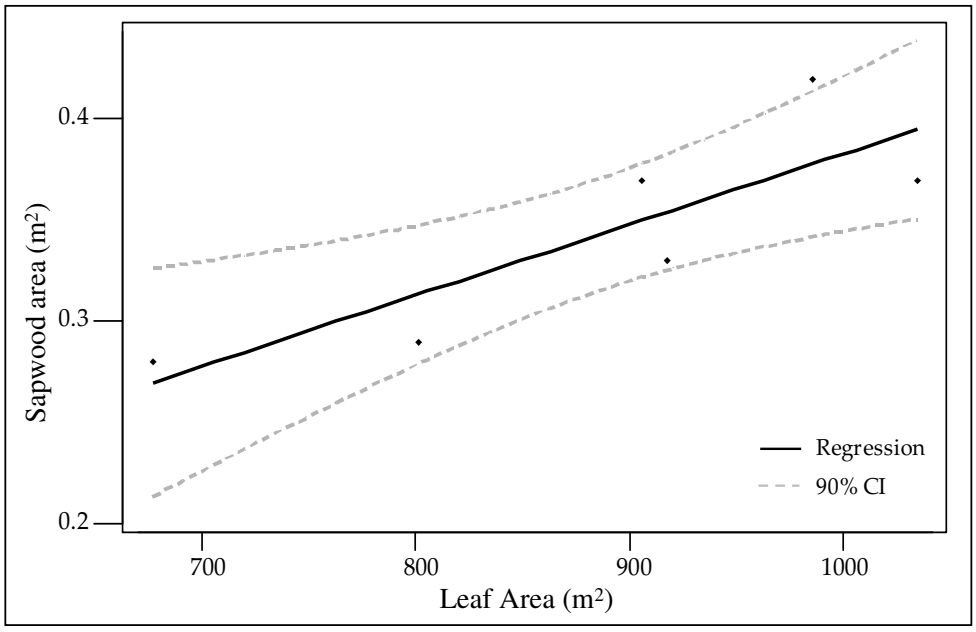

Figure 5.10: Conifers' SA_{plot} in relation to their LA_{plot}, and the regression model's fitted line. Plots of $10 \times 10m$.

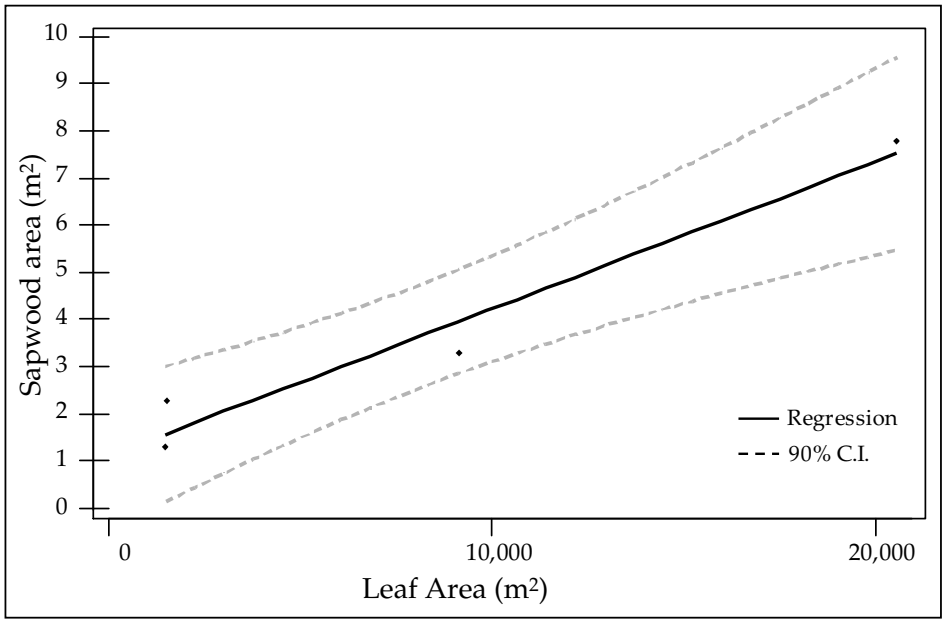

Figure 5.11: Conifers' SA_{plot} in relation to their LA_{plot}, and the regression model's fitted line. Plots of $60 \times 60m$.

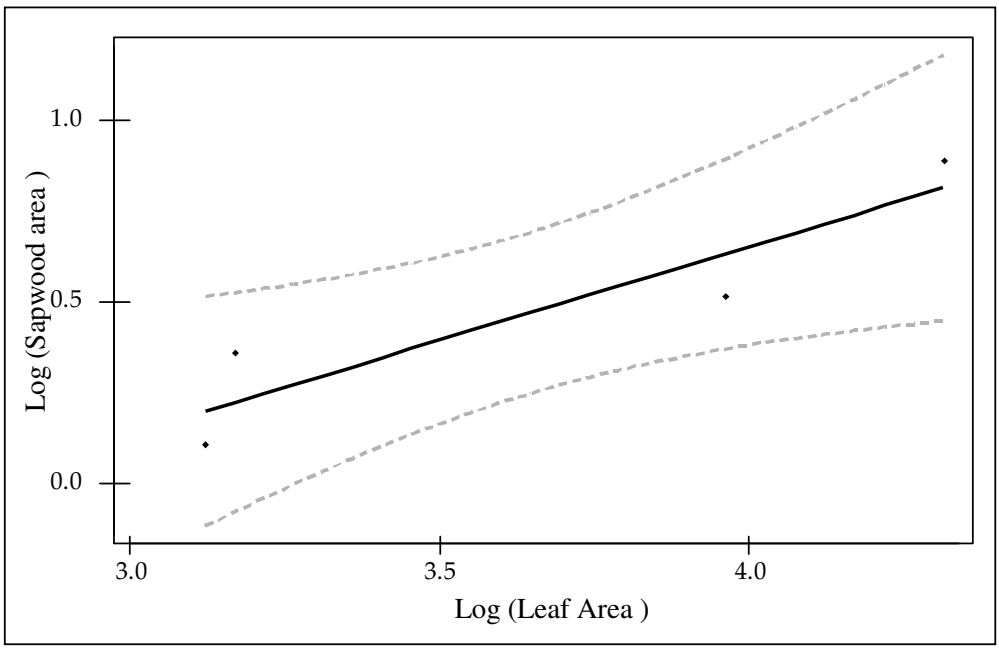

Figure 5.12: Plots of $60 \times 60m$. Conifers' Log(SA_{plot}) in relation to their Log(LA_{plot}) and the regression model's fitted line. Dotted lines are the 90% C.I. This figure is intended to decrease the large difference among LA_{plot} values, and make clearer visualization of the $60 \times 60m$ regression model.

Table 5.10: Coniferous and Deciduous plots' SA_{plot}, LA_{plot}, and LAI 95% C.I. for their COVs by applying Payton's equation.

Site type	Variable	COV	95% C.I.
Coniferous	SA_{plot}	0.79	0.4963–1.6222
	LA_{plot}	1.11	0.5943–1.9426
	LAI	0.32	0.2438–0.7976
Deciduous	SA_{plot}	1.46	0.6614–1.7885
	LA_{plot}	1.82	0.7026–1.8999
	LAI	0.17	0.1344–0.3633

5.2.4 Error propagation

Errors on sapwood area estimates.

The absolute error on SA_{plot} estimates (ΔSA_{plot}) is calculated based on the rules of error propagation that are derived from a Taylor series (Chapra and Canale, 1988).

Hence, having that Equation (5.5) is the summation of each tree's SA:

$$SA_{plot} = \sum_{i=1}^{tq} (DBH_{OB_i}\, \bar{sd_i}' - [\, \bar{sd_i}'\,]^{\,2})\, \pi$$

the error on SA_{plot} (ΔSA_{plot}) will be given by the summation of each tree's error on SA:

$$\Delta SA_{plot} = \sum_{i=1}^{tq} \left[\left| \frac{\partial SA_{plot}}{\partial DBH_{OB_i}} \right| \Delta\, DBH_{OB_i} + \left| \frac{\partial SA_{plot}}{\partial \bar{sd_i}'} \right| \Delta\, \bar{sd_i}' \right] \tag{5.13}$$

where ΔDBH_{OB_i} and $\Delta \bar{sd_i}'$ are the absolute errors on the ith tree's DBH_{OB} and $\bar{sd_i}'$ respectively. The CBH field mensurations were carefully verified by measuring the CBH on the same tree 50 times. Two trees were measured in this exercise. The tree with a DBH_{OB} of $0.98m$ was always measured as $0.98m$, thus the error was null. The second tree DBH_{OB} mensurations varied just between $1.24m$ and $1.25m$, thus the average error calculated was $\pm 0.0048m$. Since most of the trees are $\leq 1.00m$, it was decided to take as the ΔDBH_{OB_i} the average between the two calculated errors ($\pm 0.0024m$).

Naturally, for White spruce $\bar{sd}$ estimates (Equation [5.3]), $\Delta \bar{sd_i}'$ will be given by:

$$\begin{aligned} \Delta \bar{sd_i}' &= \left| \frac{\partial \bar{sd_i}'}{\partial DBH_{OB_i}} \right| \Delta DBH_{OB_i} \\ &= 0.0887\ \Delta DBH_{OB_i} \end{aligned} \tag{5.14}$$

In the Trembling aspen linear model (Equation [5.4]), ΔDBH_{OB_i} is given by:

$$\begin{aligned} \Delta \bar{sd_i}' &= \left| \frac{\partial \bar{sd_i}'}{\partial DBH_{OB_i}} \right| \Delta DBH_{OB_i} \\ &= 0.2441 \ \Delta DBH_{OB_i} \end{aligned} \tag{5.15}$$

Solving the partial derivatives on Equation (5.13) and substituting $\Delta \bar{sd_i}'$ for Equation (5.14), the White spruce's ΔSA_{plot} is:

$$\Delta SA_{plot} = \sum_{i=1}^{tq} \left[(\bar{sd_i}' \, \Delta DBH_{OB_i}) + (DBH_{OB_i} - 2\bar{sd_i}') \, 0.0887 \ \Delta DBH_{OB_i} \right] \tag{5.16}$$

And for Trembling aspen:

$$\Delta SA_{plot} = \sum_{i=1}^{tq} \left[(\bar{sd_i}' \, \Delta DBH_{OB_i}) + (DBH_{OB_i} - 2\bar{sd_i}') \, 0.2441 \ \Delta DBH_{OB_i} \right] \tag{5.17}$$

Finally, when SA_{plot} is given by the second approach (Equation [5.6]), ΔSA_{plot} is estimated by the following equation:

$$\Delta SA_{plot} = \left| \frac{\partial SA_{plot}}{\partial \overline{SA}_{sp}} \right| \Delta \overline{SA}_{sp} + \left| \frac{\partial SA_{plot}}{\partial tq} \right| \Delta \, tq \tag{5.18}$$

Due to the method used in this study to measure tq, it is considered an exact number (if some other approaches are used to estimate tree quantity, there may be an error associated with tq); therefore,

$$\Delta SA_{plot} = tq \ \Delta \overline{SA}_{sp} \tag{5.19}$$

where $\Delta\overline{SA}_{sp}$ is the absolute error on the SA average value that is given by:

$$\Delta\overline{SA}_{sp} = \sum_{i=1}^{n} \left[\left| \frac{\partial\overline{SA}_{sp}}{\partial DBH_{OB_i}} \right| \Delta DBH_{OB_i} + \left| \frac{\partial\overline{SA}_{sp}}{\partial \bar{sd}} \right| \Delta\bar{sd} + \left| \frac{\partial\overline{SA}_{sp}}{\partial n} \right| \Delta\, n \right] \quad (5.20)$$

where n is a constant; thus, the third term is null. And after derivation, the Equation to estimate the $\Delta\overline{SA}_{sp}$ becomes:

$$\Delta\overline{SA}_{sp} = \sum_{i=1}^{n} \left[\frac{(\bar{sd}_i\, \Delta DBH_{OB_i}) + (DBH_{OB_i} - 2\bar{sd})\, \Delta\bar{sd}_i}{n} \right] \quad (5.21)$$

According to previous reports (Sperry and Tyree, 1989), sapwood depth mensurations by means of the microscopical analysis gives an accuracy of 98%. Here, it is estimated that the error on $\bar{sd}$ is related to the accuracy of the ocular scale of the microscope (with divisions of $1\mu m$) and the ruler (with divisions of $1mm$) used to measure each core's sapwood depth. Thus, the Instrument Limit of Error (ILE) is estimated as 1/2 of the smallest measuring increment of the instrument (ruler). Hence, it is estimated that $\Delta\bar{sd}_i = ILE = 1/2(1mm)$ that gives a $\Delta\bar{sd}_i = \pm 0.0005m$. $\Delta\overline{SA}_{sp}$ for the Lodgepole and Jack pine sample set is $0.0002m^2$; and $\Delta\overline{SA}_{sp}$ for the Black spruce sample set is also $0.0002m^2$. Tables 5.2 and 5.1 report ΔSA_{plot} for the Coniferous and Deciduous sites.

Errors on leaf area estimates.

To estimate the error on LA_{plot} (ΔLA_{plot}), the Equation (5.12) is decomposed into:

$$\Delta LA_{plot} = \left| \frac{\partial LA_{plot}}{\partial LAI} \right| \Delta\, LAI + \left| \frac{\partial LA_{plot}}{\partial A_{plot}} \right| \Delta\, A_{plot} \quad (5.22)$$

Deriving the equation and substituting error values, we obtain:

$$\Delta LA_{plot} = A_{plot}\,\Delta\,LAI + LAI_{plot}\;\Delta\,A_{plot} \tag{5.23}$$

Remember that plots' ΔLAI is ± 0.10 for Deciduous and ± 0.13 for Coniferous, while $\Delta\,A_{plot}$ will be given by:

$$\Delta\,A_{plot} = \left|\frac{\partial A_{plot}}{\partial L}\right|\,\Delta\,L \tag{5.24}$$

Thus, on the whole we obtain:

$$\Delta\,A_{plot} = 2L\,\Delta\,L \tag{5.25}$$

where L is the plot's length, whose $\Delta\,L$ is $\pm 2.79m$ for Deciduous and $\pm 1.27m$ for Coniferous. The $10\times 10m$ plots $\Delta\,L$ is $\pm 0.05m$. Solving Equation (5.25), a Deciduous $60\times 60m$ plot's $\Delta\,A_{plot} = \pm 334.80m^2$ and $\pm 138.26m^2$ for the $415m^2$ plot. A Coniferous $60\times 60m$ plot has $\Delta\,A_{plot} = \pm 152.40m^2$. Notice that $\Delta\,A_{plot}$ of the plots named Conifer-11 and Conifer-12 (from Whitecourt) is $\pm 50.8m^2$ and $\pm 44.45m^2$, respectively (because they have a smaller surface area). For the $10\times 10m$ Deciduous plots, $\Delta\,A_{plot}$ equals $\pm 1.00m$. The errors on LA_{plot} estimates are given in Tables 5.4 and 5.5. Notice that the ΔLA_{plot} becomes larger as the plot size increases, being more notorious in the larger plots. Also, the contribution of ΔLAI to ΔLA_{plot} is small, but still the size of the plot influences the first term of the Equation (5.23), but if LAI increases in large plots, then ΔLA_{plot} becomes large (e.g. Conifer-4, Deciduous-6).

Errors associated to the linear regression models.

The prediction of SA_{plot} for Trembling aspen and Coniferous plots by means of the obtained linear models, establishes that $SA_{plot} = f(LA_{plot})$. Thus, the error propagation

on the linear models shown in Tables 5.9 and 5.7 is as follows:

$$\Delta\, SA'_{plot} = \left|\frac{\partial SA_{plot}}{\partial LA_{plot}}\right| \Delta\, LA_{plot} \tag{5.26}$$

For the Deciduous sites linear model, the $\Delta\, SA_{plot}$ produces the following Equation:

$$\Delta\, SA'_{plot} = 0.0007816 \Delta\, LA_{plot} \tag{5.27}$$

For the Coniferous linear model, the error on SA_{plot} is given by:

$$\Delta\, SA'_{plot} = 0.000312 \Delta\, LA_{plot} \tag{5.28}$$

in both cases, $\Delta\, LA_{plot}$ is estimated by means of Equation (5.23). Values of $\Delta\, LA_{plot}$ for the studied plots are shown in Tables 5.4 and 5.5.

5.3 Discussion and Conclusions

At the tree scale, there were two different responses with respect to $\bar{sd}$:DBH_{OB} allometric correlations. Firstly, White spruce and Trembling aspen individuals show a clear $\bar{sd}$:DBH_{OB} linear correlation. Secondly, the Jack pine/Lodgepole pine, and Black spruce individuals show a steady $\bar{sd}$ growth as the whole tree grows resulting in no $\bar{sd}$:DBH_{OB} correlation (opposite to what theory normally expects). Despite the latter outcome, notice that the results also show that for any of these three species, a tree's sapwood area still increases as the tree grows. And naturally, there is no doubt that it will be also the case for White spruce and Trembling aspen trees' sapwood area growth.

The White spruce and Trembling aspen linear models (for an single tree) show that there is a larger $\bar{sd}$ growth rate in Trembling aspen individuals, which can be explained by the site preferences and physiology of both species. Trembling aspen individuals are known for their preference for high soil moisture sites and their root ability to suck up large amounts of soil water; hence, more water conductive tissue (sapwood) is needed by these individuals. Besides, vessels in Trembling aspen are less efficient in conducting water than tracheids in White spruce. White spruce tracheids efficiency for conducting water and its preference for growing in xeric sites explains its lower growth $\bar{sd}$ rate. In these two linear models, the intercept was not significant (P-value > 0.05); however, it was decided to keep the models' intercept because in reality sapwood area does not become zero when the DBH_{OB} is at its minimum value.

With respect to Trembling aspen's linear regression, there is still a large amount of variation not explained by the model. It is considered that for future studies another variable should be integrated in the estimation of Trembling aspen. Due to the nature of Trembling aspen, soil moisture may be a parameter that drives sapwood depth. Thus, it would be interesting to integrate soil moisture classes as another estimator of Trembling aspen sapwood depth.

In summary, for White spruce and Trembling aspen species, it is feasible to estimate a tree's sapwood area by using a previously defined $\bar{sd}$:DBH_{OB} regression model. For Jack pine, Lodgepole pine and Black spruce species, DBH_{OB} and $\bar{sd}$ were not adequate

sapwood area predictors. As a result of these allometric correlation discrepancies, the five species have to be treated separately by using two approaches to aggregate sapwood area from a single tree to the plot scale. At the end, the combination of two approaches seem to give reliable SA_{plot} estimates that were significantly correlated to the SA_{plot} estimates. The final $SA_{plot} : LA_{plot}$ relationship (for both groups conifers and deciduous) allowed the development of linear models for predicting SA_{plot} as function of SA_{plot}.

The errors associated with the estimates were mainly influenced by the plot size. Indeed, the larger the plot the more the associated error. Particularly, reduction of error on leaf area estimates depends on accurate delimitation of plots. As the plot's size increases, it is more complicated to keep accurate plot delimitation. Still larger plots are needed in order to limit discrepancies associated with the footprint in LAI measurements. Even if small plots give the smallest errors on LA_{plot} estimates, there was a large discrepancy with SA_{plot} values due to the footprint influence. Consequently, the use of the $10 \times 10m$ linear model data set only helps to support the reliability of the $60 \times 60m$ linear model (since both follow the same linear pattern and the slope is practically the same). Lets keep in mind that it is the slope that practically defines the correlation between the two studied variables (Quinn and Keough, 2002).

Therefore, it has been learned here that plots delimitation should be as accurate as possible, and always keeping in mind the footprint influence for optical measurements. On the other hand, it is well known that in forested areas there are always area delimitation complications, even under the use of accurate devices such as a Total Station.

In conclusion, these results establish the uniqueness of each species allometry. Thus, it is necessary demonstrate caution before assuming a species' growth based on others species outcomes. Also, if there is any attempt to use the reported correlations for future estimations in different sites, it is suggested that one verifies that site conditions, topographic and climatic characteristics are similar.

It is possible to aggregate SA_{plot} to large areas by differentiating between deciduous and coniferous groups of trees, and by combining two different approaches, with an

error that is considered insignificant. Additionally, the plot size matters, and it is important to keep in mind that even if the $SA_{plot} : LA_{plot}$ relationship holds true, there are variations when the plot size changed in conifers.

Finally, the obtained results suggest that the $SA_{plot} : LA_{plot}$ relationship is maintained at larger scales in this particular area and for the five studied species. There is still some variation that is not explained with the models. This opens a study theme, since it would be worthwhile to introduce some other allometric characteristics of the trees, such as crown class or soil moisture, in order to observe what other factor(s) influence(s) SA_{plot}.

6 Scaling up transpiration

Chapter Outline

The Leaf Area at the plot scale (LA_{plot}) was determined to be an adequate predictor of the total sapwood area of a plot (SA_{plot}). The well correlated parameters and the good fit of the obtained regression models is attributed to the careful mensuration of single trees' sapwood area and the combination of two approaches to scale up SA_{sp} to SA_{plot}. It was then proved with these results that the correlation $SA_{plot}:LA_{plot}$ remains at large scales.

The next step is to aggregate the trees mass sap flow and to estimate the total canopy transpiration. This will be another form of proving the reliance of the SA_{plot} estimates, since it is expected that the scaled values will be a significant fraction of the forest evapotranspiration. The outcomes are dependent on the scaling factors and the method used to estimate tree transpiration. Since the reliance of the Granier method for measuring sap flow has been widely proven, once again SA_{plot} becomes the crucial parameter for scaling. Still, some constraints in sap flow mensuration due to the tree physiology are addressed here before scaling to the whole tree and beyond.

The means in which the scaled transpiration values are validated is through their comparison with the total forest evapotranspiration. And, as mentioned above, the canopy transpiration should represent a significant fraction of the forest evapotranspiration. Here, meteorology and soil moisture become a source of field data to estimate actual evapotranspiration and provide a point of comparison for our scaled transpiration values.

In summary, the expected aims of this dissertation chapter are:

1. To aggregate mass sap flow from single trees to the plot scale;
2. To estimate the transpiration rates of a single plot (i.e. canopy transpiration);
3. To obtain estimates of canopy transpiration and validate these results through their comparison with other well known and reliable methods (i.e. Penman-Monteith).

6.1 Material and methods

The Heat Dissipation technique was used to estimate sap flow in single trees (Granier, 1985). The technique was described in a previous chapter. At each site, a group of four trees were set up with TDP's for periods of 48 hours. The sensors were installed in the North side of the trees to avoid direct solar incidence and overheating of the sensors that might alter the logger readings. The sensors were covered with a special isolating material (Figures 6.1 and 6.2). At the same time, a set of soil moisture sensors (six sensors) was placed in the soil (below the litter) to observe the changes in soil moisture content and to later compare with the trees' water uptake. The soil moisture values are also used in the empirical calculation of the actual evapotranspiration. After 48 hours, another group of four trees was set up with the TDP's and the soil moisture sensors. The equipment set up has been also explained in detail in a previous Chapter.

The trees whose daily sap flow was measured were chosen in order to cover the range of trees' DBH_{OB} found inside the plot (i.e. the largest, the smallest, the mean and other intermediate DBH_{OB} values). This means that each tree's CBH_{OB} inside the plot was measured while the trees were counted. An exception was made in the Deciduous-6 site, where four trees were set up for a period of 96 hours. This was due to a failure in the power used to feed the logger and the thermosensors, and the data from the first two groups of trees set up in this site were completely lost. Thus, it was decided to set up a third group of trees and leave it for a longer period of time. A total of 16 Trembling aspen, 9 Lodgepole pine, and 9 White spruce trees were used to measured sap flow in

Figure 6.1: Thermal Dissipation Sensors (TDP's) installed in a coniferous tree.

Figure 6.2: Same coniferous tree with the isolation material (upper part of the picture) ready to cover the sensors.

KFC. In WC, 8 Jack pine trees were set up for sap flow mensurations. Not all the days and trees provided adequate data either because of power failures or problems with the trees (i.e. tree infestations that caused very different diurnal sap flow patterns in comparison to healthy trees). Based on the available sap flow data, it was decided to

use two plots to scale up mass sap flow and calculate the total rate of transpiration per plot. The sites are one Coniferous and one Deciduous (Conifer-4 and Deciduous-6 respectively).

The canopy transpiration estimates were computed after data was corrected for radial patterns of sap flow. The Trembling aspen individuals were excluded from the radial correction, since it has been proven that diffuse-porous tree radial sap flow does not vary significantly (Bovard et al., 2005; Phillips et al., 1996; Booker, 1984). Thereafter, the forest evapotranspiration using the Penman-Monteith equation was estimated. Finally, the agreement between forest evapotranspiration and rates of transpiration were compared for each plot. The mathematical theory behind all these computations is detailed in the following sections.

6.2 Spatial scaling: Canopy Transpiration

Radial patterns of sap flow.

The acropetal sap transport rate has a radial gradient that decreases from the outermost part of the sapwood towards the pith. Since there is enough evidence of the significance of the sap flow radial gradient while scaling up sap flux density from a single point to the entire tree (Mark and Crews, 1973; Granier et al., 1994; Phillips et al., 1996; Čermák and Nadezhdina, 1998; James et al., 2002; Čermák et al., 2004), a sap flow radial profile function developed by Ford et al. (2004) was used to calculate the sap flow velocity along the entire sapwood depth of each tree. The radial profile function accounts for the fractional changes in sap flow as a function of the maximum sap flow rate, the sapwood depth at which this rate occurs, the total sapwood depth and the rate at which the sap flow velocity decreases from the outer to the inner sapwood:

$$f(x) = \varpi \exp\left(-0.5\left[\frac{x - x_o}{\beta}\right]^2\right) \tag{6.1}$$

where $f(x)$ is the sap flow rate index (expressed as a fraction), ϖ is the maximum sap flow rate (equals one) occurring at the x_o sapwood depth, $1/\beta$ is the rate at which the sap flow radially decreases towards the pith's trunk. In order to calculate sap flow velocity changes instead of fractional changes, Equation (6.1) was modified slightly to the following form:

$$v_{0-3}/v_{max} = \frac{1}{\sqrt{2\pi}\,\beta}\int_0^3 \exp\left(-0.5\left[\frac{x-x_o}{\beta}\right]^2\right)dx \tag{6.2}$$

where v_{0-3} is the sap flow velocity in the first three centimetres of sapwood, and v_{max} is the maximum sap flow velocity. Most of the studies in variations of radial sap flow have found that in conifers the maximum velocity or the largest portion of sap flow occurs in the first centimetre (Granier et al., 1994), the first $2cm$ (Mark and Crews, 1973; Cohen et al., 1985), and $3cm$ (Mark and Crews, 1973) of sapwood depth (from cambium to pith). Čermák and Nadezhdina (1998) and Čermák et al. (2004) have reported graphs showing that maximum sap flow occurs at 20% of the depth (from cambium to pith as well). It seems that the depth at which the maximum sap flow occurs is a standard pattern independent of the tree size. Based on these previous results, here it is assumed that v_{max} occurs somewhere between the first two centimetres, thus $x_o = 2cm$. Other studies have reported that the rate of decrement in radial sap flow is about 20-24% in conifers (Delzon et al., 2004; Phillips et al., 1996), thus β has been assumed to equal 4 (i.e. a 25% of decrement). As v_{0-3} is known (i.e. it is calculated from the field measurements), v_{max} can be estimated:

$$v_{max} = v_{0-3} \div \left[\frac{1}{\sqrt{2\pi}\,\beta}\int_0^3 \exp\left(-0.5\left[\frac{x-x_o}{\beta}\right]^2\right)dx\right] \tag{6.3}$$

And then v_{max} is used to estimate the sap flow velocity along the entire sapwood

depth ($\bar{sd}$) at a specific time:

$$v_{0-\bar{sd}} = v_{max}\left[\frac{1}{\sqrt{2\pi}\,\beta}\int_0^{\bar{sd}} \exp\left(-0.5\left[\frac{x-x_o}{\beta}\right]^2\right)dx\right] \tag{6.4}$$

Note that $v_{0-\bar{sd}}$ is J_i, the original symbol used by Granier (1985) to define sap flow velocity (2.7). The sap flow velocity was computed with Equation (6.4) at each time step (5 minutes in this study) and then used to estimate the total volume of water transpired (F_s) by a tree on a daily basis. To calculate a single tree F_s at each time step, $v_{0-\bar{sd}}$ is multiplied by the total sapwood area of the tree, SA_{tree}:

$$\begin{aligned} F_s &= SA_{tree}\, J_i \\ &= SA_{tree}\, v_{0-\bar{sd}} \end{aligned} \tag{6.5}$$

Here, the main objective is to scale up these single tree values to the whole plot. This allows one to calculate the total average canopy water mass flow ($\bar{F}_{plot}$) and the average canopy transpiration rates (or transpiration rates per plot, [$\bar{T}_{plot}$]).

In order to do so, a diurnal average sap flow per species (and per plot) was estimated ($\bar{J}_{sp}$) and then multiplied by the total sapwood area of that species, SA_{sp}. Thus, the first calculations are:

$$\bar{J}_{sp} = \frac{1}{m}\sum_{i=1}^{m} \bar{v}_{0-\bar{sd}} \tag{6.6}$$

and

$$\bar{F}_{sp} = \bar{J}_{sp}\, SA_{sp} \tag{6.7}$$

where $\bar{J}_{sp}$ is the average sap flow of the species sp obtained by the summation of the diurnal average sap flow velocity of each ith individual and divided by the total m

individuals of the same species whose sap flow was measured. $\bar{F}_{sp}$ is the average of the total mass flow (units of sap volume per time^{-1}). Therefore, the calculation of $\bar{F}_{plot}$ is through the summation of each plot's species total mass flow:

$$\bar{F}_{plot} = \sum_{i=1}^{n} \bar{F}_{sp\,i} \tag{6.8}$$

similarly, the average sap flow of the plot ($\bar{J}_{plot}$) is:

$$\bar{J}_{plot} = \sum_{i=1}^{n} \bar{J}_{sp\,i} \tag{6.9}$$

The estimation of canopy transpiration ($\bar{T}_{plot}$) is normally based on a unit area factor that will divide the $\bar{F}_{plot}$ by a unit area of ground ($1\,ha$). This division allows one to observe the agreement between canopy transpiration and actual forest evapotranspiration ($E_{\rm a}$). Here, three different ground indices were used instead of the unit area of ground. The three indices were calculated as the ratio of SA_{plot}, LA, or LA_{eff} to the unit ground area ($1\,ha$). The indices were multiplied by $\bar{J}_{plot}$ to estimate $\bar{T}_{plot}$. Finally, $\bar{T}_{plot}$ values were compared with an average $E_{\rm a}$ for the same days when sap flow measurements were taken.

In the case of the Coniferous site, eight days of sap flow measurements were used to calculate the $\bar{F}_{plot}$ and $\bar{T}_{plot}$. The Deciduous site provided four days of sap flow measurements and meteorological data. For the same dates at each plot, the daily actual evapotranspiration was estimated with the Penman-Monteith equation and a daily average per plot was compared with the obtained $\bar{T}_{plot}$.

Two more methods were used to calculate forest evapotranspiration, the Penman combination equation for free water evaporation and the Penman equation for potential evapotranspiration (see § 6.3).

Water storage capacity.

Another factor that might influence the estimation of the total amount of water tran-

spired by a single tree is the tree's water storage capacity. Several authors have reported the contribution of a tree trunk's stored water to transpiration (Delzon et al., 2004; Loustau et al., 1996; Goldstein et al., 1998), under dry and wet conditions. On average, of the daily amount of water transpired by a tree, 14.8-20.0% corresponds to the trunk's stored water (ibidem). Hogg et al. (1997) found that in Trembling aspen, the water trunk provided 11.6 % of the mean daily transpiration. Most of the time, full replenishment for the tree trunk occurs at night time (Loustau et al., 1996), which creates a water balance between the tree water lost during the day and the water recharged at night. Thus, it is assumed that the water stored in the tree trunk equals the amount of water replenished at night. Loustau et al. (1996) determined that for scaling purposes, the error associated with water storage capacity is practically null if between individuals, the sap flux variability is low.

6.3 Computing forest evapotranspiration

6.3.1 Actual evapotranspiration

Since the direct estimation of transpiration is complex, it is more common to estimate evapotranspiration (ET) of forested areas as a close estimate of transpiration. For dense, homogenous vegetated areas, transpiration is usually considered the largest portion of total evapotranspiration in forested areas (Dugas, 1990; Kaufmann and Kelliher, 1991; Szilagy, 2000; Denmead, 1984). In Canada, it is estimated that forest transpiration has a large proportion of the total ET (varying between 45% and 67% of total ET), while the rest of the water lost is through soil evaporation or evaporation of water on surfaces (e.g. leaves, trunks) and sublimation (Liu et al., 2003). These statements are reinforced with detailed studies of ET in the boreal forest that demonstrate the large activity and amounts of energy and mass fluxes (Baldocchi and Vogel, 1996).

In this study, the Penman-Monteith equation (Monteith, 1965) is used to estimate the actual evapotranspiration of the vegetated areas under study. These evapotranspiration estimates will be used to validate the daily transpiration rate estimates at the

plot scale. The Penman-Monteith equation estimates the actual evapotranspiration of vegetated surfaces by accounting for all the micrometeorological factors that influence evapotranspiration as well as the influence of the canopy conductance and aerodynamic resistance in the rates of vegetation transpiration:

$$\lambda E_{\mathrm{a}} = \frac{\Delta(R_n - G) + \rho_a c_p (e^{\circ} - e_a)/r_a}{\Delta + \gamma \left[1 + \frac{r_c}{r_a}\right]} \tag{6.10}$$

where Δ is the slope of the saturation vapour pressure curve $[kPa\,^{\circ}\mathrm{C}^{-1}]$, λE_{a} is the latent heat of actual evapotranspiration, R_n is the net solar radiation, and G is the soil heat flux (all these terms in units of $[Jm^{-2}s^{-1}]$). The air density, ρ_a is in $[kgm^{-3}]$; c_p is the specific heat of air at constant pressure [i.e. $1010\,Jkg^{-1}\,^{\circ}\mathrm{C}^{-1}$]. The term $(e^o - e_a)$ is the vapour pressure deficit (VPD) calculated by the difference between the saturation vapour pressure (e°, $[kPa]$) and the actual vapour pressure (e_a, $[kPa]$). The psychrometric constant, γ, is in units of $[kPa\,^{\circ}\mathrm{C}^{-1}]$. The aerodynamic terms, r_a and r_c are the aerodynamic resistance to vapour and heat transfer, and the bulk canopy resistance (both expressed in sm^{-1}). The following paragraphs explain in detail the calculation of each Penman-Monteith equation's parameter. To convert the latent heat of evapotranspiration to actual evapotranspiration (E_{a}), use $E_{\mathrm{a}} = \lambda E_{\mathrm{a}}/\lambda$ in units of mms^{-1}.

Aerodynamic parameters.

To calculate the VPD term in the Penman-Monteith equation, the saturation vapour pressure was initially calculated using two different equations:

$$e^{\circ} = a_{\circ} + a_1 T_a + a_2 T_a^2 + a_3 T_a^3 + a_4 T_a^4 + a_5 T_a^5 + a_6 T_a^6 \tag{6.11}$$

and

$$e^{\circ} = \exp\left(\frac{16.78\,T_a - 116.9}{T_a + 237.3}\right) \tag{6.12}$$

In both equations, T_a is the air temperature ([°C], field weather station measurements). The first equation is the resultant of a Chebyshev fitting procedure used by Lowe (1977). The polynomial coefficients (i.e. $a_\circ$ to a_6) are reported in Lowe's paper and e° is calculated in $mbar$ units. The latter equation calculates e° in kPa, and it was derived by Murray (1967). Murray's equation estimates are considered of high reliability (Allen et al., 1996). The average difference between e° values calculated with both equations was of $0.00017kPa$. Thus, for further estimations, Equation (6.12) is applied. The actual vapour pressure is calculated using the estimated e° and the relative humidity (RH, [%]) that was measured in the field (Dingman, 2002):

$$e_a = \frac{RH\, e^\circ}{100} \tag{6.13}$$

The air density, ρ_a, can be derived from (Allen et al., 1996):

$$\rho_a = \frac{1000\, P}{T_v\, R} \tag{6.14}$$

where P is the daily mean atmospheric pressure calculated with the field measurements (barometer, units of $[kPa]$), R is the specific gas constant ($287Jkg^{-1}K^{-1}$). T_v is the virtual temperature in degrees Kelvin, calculated as (Allen et al., 1996):

$$T_v = \frac{\bar{T}_a}{1 - (0.378\, \bar{e}_a\, P^{-1})} \tag{6.15}$$

where $\bar{e}_a$ and $\bar{T}_a$ are taken as the daily average of e_a and T_a respectively. A sensitivity analysis was performed to observe how $\bar{T}_a$ values affect ρ_a or the evapotranspiration estimates. There were no significant changes in the values. Thus, $\bar{T}_a$ was used in the equation. This analysis was performed since Allen et al. did not specify if an average temperature or temperature at each hourly time-step values should be used.

The psychrometric constant can be expressed as (Smith, 1990):

$$\gamma = \frac{c_p\, P}{\varepsilon\, \lambda} \tag{6.16}$$

where γ is given in units of $kPa^{\circ}\mathrm{C}^{-1}$, c_p is entered as $1.010 kJ\,kg^{-1}\,^{\circ}C^{-1}$, P is in kPa. The water vapour ratio molecular weight (ε) is a constant value equal to 0.622, and λ is calculated using the following equation (Allen et al., 1996):

$$\lambda = 2.501 - 2.361 \times 10^{-3} T_a \tag{6.17}$$

where λ is given in units of $[MJ\,kg^{-1}]$ (i.e. multiply by 1000 to match units of c_p).

The slope of the saturation vapour pressure curve (Δ) is derived from the following equation:

$$\Delta = \frac{4098\, e^{\circ}}{(T_a + 237.3)^2} \tag{6.18}$$

The aerodynamic resistance to vapour and heat flux, r_a, is estimated with the following equation (Brutsaert, 1982; Allen et al., 1996):

$$r_a = \left(\left[\ln \frac{z_u - d}{z_{om}} \right] \left[\ln \frac{z_u - d}{z_{oh}} \right] \right) \div k^2 u_z \tag{6.19}$$

where k is von Karman's constant (0.40), z_u is the height $[m]$ at which the wind speed u_z $[ms^{-1}]$ has been recorded ($12.19\,m$ in this particular case), d is the zero-plane displacement $[m]$ that is assumed as 67% of the canopy height (i.e. $d = 0.67\,h_c$) for vegetation with $LAI > 2.0$. Here, the average canopy height is $15m$, which is the same height used in previous estimations (Chapter 5). The parameters z_{om} and z_{oh} are the roughness lengths for the momentum and heat transfer, respectively. Allen et al. (1996) suggested applying $z_{oh} = 0.1\,z_{om}$. In this study, the fact that z_{om} varies with cover has been taken into account; thus, z_{om} is calculated differently for the Deciduous and the Coniferous sites. For the Deciduous sites, whose vegetation is considered dense and homogeneous, the equation suggested by Brutsaert (1982) is applied:

$$z_{om} = \frac{1}{e}(\,h_c - d) = 0.37(\,h_c - d) \tag{6.20}$$

For the Coniferous sites, the equation suggested by Allen et al. (1996) is applied:

$$z_{om} = \varsigma(h_c - d) \tag{6.21}$$

where ς is an empirical factor that is independent of vegetation height (De Bruin and Moore, 1985). Based on their calculated values of z_{om} and d for conifers, De Bruin and Moore (1985) determined $\varsigma = 0.22$. Table 6.1 lists the constant terms of the aerodynamic resistance equation. The ratio $z_{om}/h_c = 0.7$ calculated for Coniferous sites concurs with the mean value reported by Allen et al. (1996) for this ratio. The Deciduous' sites z_{om} value is between the range of values listed for deciduous trees by Allen et al. (1996).

Table 6.1: Steady parameters in the calculation of the aerodynamic resistance to heat and vapour transfer, r_a. All parameters are reported in meters, with exception of ς, which is unitless.

Parameter	**Coniferous sites**	**Deciduous sites**
h_c	15	15
ς	0.22	0.37
d	10.05	10.05
z_{om}	1.089	1.82
z_{oh}	0.1089	0.1821

The canopy resistance is more complicated to estimate since it varies along the day and it is a function of several atmospheric parameters (Price and Black, 1989):

$$\mathrm{g_c} = \mathrm{g_{c_{max}}} \left[minimum(\mathrm{g}(LAI), \mathrm{g}(R_s), \mathrm{g}(VPD), \mathrm{g}(T_a), \mathrm{g}(\theta_{sm})) \right] \tag{6.22}$$

This equation implies that the canopy conductance ($\mathrm{g_c}$) is a function of the environmental parameters: LAI, R_s $[Wm^{-2}]$, VPD $[kPa]$, T_a [°C], and volumetric soil moisture

(θ_{sm}, in $[m^3m^{-3}]$). The parameter that reaches its minimum at a specific time (g_{env}), drives the canopy conductance. The lower the value of the environmental parameter reduction function, the lower the value of g_c, therefore the higher the r_c. Each parameter is represented by a reduction function that computes the value of the function between zero and one (i.e. $0 \leq g_c \leq 1$). Different authors have developed and calibrated reduction functions for calculating each one of the parameters in Equation (6.22). Allen et al. (1996) suggested that these equations can be replaced in the function above. Here, a set of equations was chosen and presented below. Most of the equations and empirical factors are taken from Stewart (1988), otherwise the author is cited. Stewart (1988) developed and calibrated these functions for Scots pine. This is the closest species to the species studied in this work with reported functions. In the case of the Deciduous site, the empirical factors were adjusted according to the response of r_c or g_c to the environmental parameters. This task was performed based on previous results and results obtained in this study.

The $g_{c_{max}}$ is the reciprocal of the minimum canopy or surface resistance ($r_{c_{min}}$). Typical values reported for coniferous forests $r_{c_{min}}$ range from $30sm^{-1}$ to $60sm^{-1}$ (Allen et al., 1996). Here, an average value of the reported ranges was taken for the Coniferous site (i.e. $51sm^{-1}$). Blanken et al. (1997) reported maximum values of canopy conductance for Trembling aspen ($31ms^{-1}$) and it is the one applied here for the Deciduous site.

To compute $g(LAI)$:

$$g(LAI) = \frac{LAI}{LAI_{max}} \tag{6.23}$$

where LAI_{max} is the maximum LAI along the year. Since data collection occurred during the peak of the summer (July and August), it is assumed that $g(LAI) \approx 1.0$ for both the Coniferous and the Deciduous sites.

The $g(R_s)$ is calculated with:

$$g(R_s) = \frac{R_s(1000 + K_R)}{1000(R_s + K_R)} \tag{6.24}$$

where R_s is in $[Wm^{-2}]$ and K_R is an empirical factor that was set up as $104.4 Wm^{-2}$.

The VPD function is established based on the two following equations:

$$\mathrm{g}(VPD) = 1 - K_{VPD} VPD \quad \text{for } 0 < VPD < VPD_c \tag{6.25}$$

and

$$\mathrm{g}(VPD) = 1 - K_{VPD_c} VPD \quad \text{for } VPD \geq VPD_c \tag{6.26}$$

with $K_{VPD} = 0.5\,kPa$. The VPD_c is called the "threshold vapour pressure deficit" and is set up as $1.5 kPa$ for the Coniferous site. For the Deciduous site, Bovard et al. (2005) reported the sap flow trend of four hardwood species in relation to VPD. One of the species studied is from the genus *Populus*. For that result, it was reported that the *Populus* sap flow did not significantly vary when VPD was greater than $1\,kPa$, unless the soil moisture content was limiting. The results presented by Bovard et al. perfectly concur with our study results. Thus, the threshold for the Deciduous site was assumed as $1\,kPa$. Since a K_{VPD} factor was not found in the Literature, its value was determined by using previously reported trends of $\mathrm{g_c}$ versus VPD. Thus, the value was assumed as $K_{VPD} = 0.79\,kPa$ initially. This decision was somehow conservative and based on the fact that deciduous r_c reported values have reached $160 sm^{-1}$ (Allen et al., 1996). Therefore, K_{VPD} was set up to make the reciprocal of $\mathrm{g_{max} g_{env}}$ to quasi match r_c to $160 sm^{-1}$ when VPD_c is greater than $1\,kPa$ and becomes the driving environmental parameter of r_c. Using Blanken et al. (1997) plots of half-hourly changes in $\mathrm{g_c}$ and VPD, it was observed that r_c can change from $81\,sm^{-1}$ to $200\,sm^{-1}$ as VPD reaches values greater than $1\,kPa$. In this case, a second run for E_a was performed assuming $K_{VPD} = 0.84\,kPa$, to make $r_c \approx 200\,sm^{-1}$ when $VPD > 1\,kPa$. Values of E_a obtained with both parameters are presented here.

For calculating $\mathrm{g}(T_a)$, a maximum and a minimum temperature (T_M and T_N, in [°C]) is required that constrain the stomas process, plus another empirical factor, K_T (called

the "optimum conductance temperature"):

$$g(T_a) = \frac{(T - T_N)(T_M - T)^{\varrho}}{(K_T - T_N)(T_M - K_T)^{\varrho}} \tag{6.27}$$

where

$$\varrho = \frac{T_M - K_T}{K_T - T_N} \tag{6.28}$$

and K_T is 18.35°C for the Coniferous site. In the case of the Deciduous site, reported half-hour Trembling aspen g_c and temperature values (Blanken et al., 1997) were used to estimate the optimum conductance temperature for Trembling aspen g_c. An average optimum temperature of 18.29°C was obtained.

Finally, to estimate the $g(\theta_{sm})$, a function reported by Allen et al. (1996), which is a slightly modified version of the one suggested by Stewart (1988), was used:

$$g(\theta_{sm}) = 1 - e^{-K_\theta \theta_e} \tag{6.29}$$

where K_θ is the empirical factor used to calculate $g(\theta_{sm})$ [$K_\theta = 6.7$]; and θ_e is the fraction available for transpiration, also called the "effective fraction of available soil moisture" (Allen et al., 1996):

$$\theta_e = \frac{\theta_{sm} - \theta_{\text{wp}}}{\theta_{\text{fc}} - \theta_{\text{wp}}} \tag{6.30}$$

where θ_{sm} is the volumetric soil moisture (field measurements, $[m^3 m^{-3}]$), θ_{wp} is the soil wilting point and θ_{fc} is the soil field capacity. The values of θ_{fc} and θ_{wp} are obtained based on the soil texture. Direct studies of the soil type and texture in the area of Kananaskis (Greenlee, 1973, 1976; Mcgregor, 1984; Archibald et al., 1996) were used to define the soil texture in the Coniferous and Deciduous sites. The soil texture, generally defined as fine sandy loam (for both areas), drew a soil field capacity ranging between 0.16 and 0.22, while the soil wilting point was estimated as 0.07 (all values in volumetric fraction).

Energy parameters.

The soil heat flux is calculated using a "universal relationship" developed by Choudhury (1989):

$$G = 0.4(e^{-0.5LAI})R_n \tag{6.31}$$

G has the units of R_n. The net solar radiation is derived from the following equation (Nokes, 1995; Allen et al., 1996):

$$R_n = (1 - \alpha)R_s + R_{nl} \tag{6.32}$$

where R_s is the shortwave solar radiation (measured in the field with a pyranometer), R_{nl} is the net outgoing longwave solar radiation, and α is the surface's albedo value. The term $(1-\alpha)$ helps to calculate the fraction of incident net shortwave solar radiation that is absorbed by a specific surface. For coniferous forests, mean α values are in the range of 0.09-0.15 (Jarvis et al., 1976; Brutsaert, 1982), and deciduous forests are in the range of $0.15 - 0.25$ (Brutsaert, 1982). Monthly albedo values for Mid-latitude forests are of 0.14 during the months of July and August (Dooge, 1988; Kondratyev et al., 1982; Henderson-Sellers and Wilson, 1983). The net longwave solar radiation is calculated based on the emissivities of four different surfaces and the air temperature, T_a (Liu et al., 2003):

$$\begin{aligned} R_{nl} = \Bigg\{ \epsilon_o \left[\epsilon_a \, \sigma_{sb} \, T_a^4 + \epsilon_u \, \sigma_{sb} \, T_a^4 \, (1 - e^{-0.5LAI_u \, \Omega_u / cos\, \bar{\theta_u}}) + \epsilon_g \, \sigma_{sb} \, T_a^4 \, (e^{-0.5LAI_u \, \Omega_u / cos\, \bar{\theta_u}}) \right] \\ - 2\epsilon_o \, \sigma_{sb} \, T_a^4 \Bigg\} (1 - e^{-0.5LAI_o \Omega_E / cos\, \bar{\theta_o}}) \end{aligned} \tag{6.33}$$

where σ_{sb} is the Stefan-Boltzmann constant ($5.675 \times 10^{-8} \, Jm^{-2}K^{-4}s^{-1}$), T_a is the air temperature (K). LAI_o and LAI_u are the Leaf Area indices of the overstory and understory respectively; Ω_E and Ω_u are the clumping indices of the overstory and understory; $cos\, \bar{\theta_u}$ and $cos\, \bar{\theta_o}$ are estimations of the transmission of diffuse radiant

energy through the understory and overstory. The emissivities of the overstory, ground, understory, and atmosphere are respectively represented by ϵ_o, ϵ_g, ϵ_u, and ϵ_a. Emissivity values for the first three surfaces are assigned from Liu et al. (2003) and Chen and Zhang (1989) as 0.98, 0.95 and 0.98, respectively . These emissivity values concur with values reported by Allen et al. (1996). Emissivity from the atmosphere is calculated with the following equation (Brutsaert, 1982):

$$\epsilon_a = 1.24 \left(\frac{e_a}{T_a} \right)^{1/7} \tag{6.34}$$

where e_a is in $[mba]$ and T_a is in degrees Kelvin. The transmission of diffuse radiant energy through the understory and overstory is given by the following two equations that were derived by Liu et al. (2003):

$$cos\,\bar{\theta_u} = 0.537 + 0.025 LAI_u \tag{6.35}$$

$$cos\,\bar{\theta_o} = 0.537 + 0.025 LAI_o \tag{6.36}$$

LAI_o was measured for every coniferous and deciduous site (i.e. $LAI_{plot} = LAI_o$); LAI_u is more complex to measure directly and it was derived from previous reports of understory NDVI and LAI values. Buermann et al. (2002) used the reflectance values to estimate the understory NDVI and calculate LAI indices based on understory NDVI-LAI scatterplots developed by Myneni et al. (1997). The LAI_u values reported by Buermann et al. range between 0.6-1.0 (being the largest values for Black spruce and the smallest for Jack Pine). Conifers understory NDVI ($NDVI_u$) values reported by Buermann et al. were compared with the studied Coniferous sites $NDVI_u$ calculated from the understory spectral reflectance that was recorded in the 2003 field campaign

at two Coniferous and two Deciduous sites (McAllister, 2005). For both Coniferous and Deciduous sites, the average $NDVI_u$ is 0.8, which is 0.3 larger than the values reported by Buermann et al. (their $NDVI_u$ range is 0.35-0.50). Using Myneni et al. information, Buermann et al. established that an $NDVI_u$ of 0.5 corresponded to an LAI_u of 1.0. On the other hand, Myneni et al. (1997) established a standard LAI_u value of 0.5 for broadleaf and needle-leaf forests.

Therefore, based on these previous results, LAI_u for the Coniferous sites in Kananaskis is assumed 1.0, and for Deciduous sites, 0.6. The latter value is also in the LAI_u range reported by Black et al. (1989) for deciduous stands in a boreal forest. Figure 6.3 is the typical understory spectral response at a Coniferous and a Deciduous site in KFS. It is convenient to stress the fact that these LAI_u values are approximate; however, the main objective is to acknowledge the importance of understory in the overall evapotranspiration estimates. Thus, as Liu et al. (2003) thought, it is convenient to somehow include the understory evapotranspiration based on assumptions about its LAI_u than ignore it.

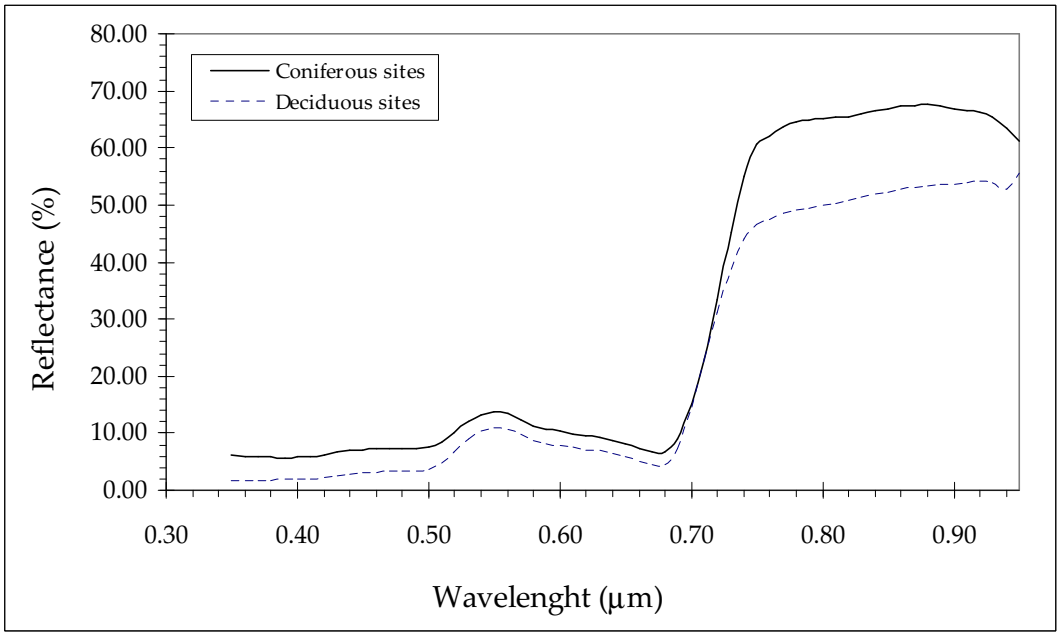

Figure 6.3: Typical understory spectral reflectance in KFS study sites during the summer of 2003.

The understory clumping index Ω_u, was derived by modifying the former Chen's equation (Equation [5.10]):

$$LAI = (1 - \alpha_l) LAI_{eff}\, \gamma_E / \Omega_E$$

where $\gamma_E/\Omega_E = 1/\Omega_E$ in vascular vegetation (Leblanc et al., 2002). Thus, for understory vegetation Ω_E does not have to be partitioned into fractions that account for the shoot effect. At the same time, the α_l value is zero since there is no fraction of wood to account for in the understory vegetation present at the study sites. Thus,

$$LAI_u = LAI_{eff}\, / \Omega_u \tag{6.37}$$

As LAI_u is known, LAI_{eff} can be approximated as 50% of LAI_u as suggested by Allen et al. (1989) for grasses (the closest that can be found to a forest understory). Hence,

$$\begin{aligned} \Omega_u &= LAI_{eff}/LAI_u \\ &= 0.5 LAI_u / LAI_u = 0.5 \end{aligned} \tag{6.38}$$

6.3.2 Potential evapotranspiration

The Penman combination equation estimates the potential evapotranspiration, or also, the free water evaporation. Potential rates of evapotranspiration assume that the water is never a limiting factor, the plant completely shades the ground (thus, there is no soil evaporation) and it has the optimal environmental conditions to transpire at its maximum rate (there is no canopy resistance). Two versions of the Penman-Monteith equation are used here to estimate the Potential Evapotranspiration (E_{p}), the combination equation for free water evaporation (Bavel, 1966; Bladon et al., 2006), and the Penman-Monteith equation that includes the aerodynamic parameter but sets $r_c = 0$

(Chang, 2002). The former equation is computed in the following form:

$$E_{\mathrm{p}} = \frac{\Delta(R_n - G) + \rho_a c_p (e^{\circ} - e_a) u_2}{\lambda(\Delta + \gamma)\rho_w} \tag{6.39}$$

where ρ_w is the water density in units of $[kg\, m^{-3}]$, and u_2 is the wind speed at $2\, m$ height. Wind speed measured at $3\, m$ height was scaled down to $2\, m$ using the aerodynamic function (McCuen, 1989):

$$\frac{u_2}{u_{\circ}} = \frac{z_2}{z_{\circ}} \tag{6.40}$$

where u_2 is the wind speed to be estimated at height $z_2 = 2\, m$ and $u_{\circ}$ is the wind speed at the reference height $z_{\circ}$ (in this case, $3\, m$). Wind differences of $\pm 6\, cm$ were registered between the two heights. The rest of the parameters were already defined. The G parameter is not included in the original equation; however it was decided to slightly modify the method and include G. Equation (6.39) gives E_{p} in units of ms^{-1}.

The second equation is Equation (6.10), making $r_c = 0$, and E_{p} is given in mms^{-1}:

$$E_{\mathrm{p}} = \frac{\Delta(R_n - G) + \rho_a c_p (e^{\circ} - e_a)/r_a}{\lambda\,[\Delta + \gamma]} \tag{6.41}$$

The obtained E_{a} and E_{p} daily values were averaged along the eight days (for the Coniferous site) and the four days (for the Deciduous site) and compared with the average $\bar{T}_{plot}$ value obtained for their respective period of time.

6.4 Computing canopy transpiration, modified Penman-Monteith equation

Liu et al. (2003) used a slightly modified version of the Penman-Monteith equation in order to estimate actual canopy transpiration at large scales. According to Liu et al.,

a model such as Penman-Monteith should be adjusted by separately estimating the transpiration of shaded and sunlit leaves as follows (stratified model):

$$T_{plant} = T_{sun} LAI_{sun} + T_{shade} LAI_{shade} \tag{6.42}$$

where T_{sun} and T_{shade} are the actual transpiration of sunlit and shaded leaves respectively; LAI_{sun} and LAI_{shade} are the Leaf Area Indexes for sunlit and shaded leaves as well.

The Penman-Monteith equation is then used by Liu et al. to estimate T_{sun} and T_{shade}:

$$\lambda T_{sun} = \frac{\Delta(R_{n,\,sun}) + \rho_a c_p (e^\circ - e_a)/r_a}{\Delta + \gamma\,[1 + r_s/r_a]} \tag{6.43}$$

and

$$\lambda T_{shade} = \frac{\Delta(R_{n,\,shade}) + \rho_a c_p (e^\circ - e_a)/r_a}{\Delta + \gamma\,[1 + r_s/r_a]} \tag{6.44}$$

where $R_{n,\,sun}$ and $R_{n,\,shade}$ are the net solar radiation available for sunlit and shaded leaves $[Jm^{-2}s^{-1}]$, and r_s is the stomatal resistance $[sm^{-1}]$. The rest of the parameters and units remain the same as in Equation (6.10); therefore, these parameters are estimated using the equations described in § 6.3.

The Boreal Ecosystem Productivity Simulator (BEPS) sets up a set of equations to calculate $R_{n,\,sun}$ and $R_{n,\,shade}$ (Liu et al., 1997, 2003). The equations compute the shortwave solar radiation for sunlit and shaded leaves as well. The net longwave solar radiation is assumed to behave equally for sunlit and shaded leaves; therefore, a single equation is used to calculate net longwave solar radiation. Thus, $R_{n,\,sun}$ and $R_{n,\,shade}$ are respectively given by:

$$R_{n,\,sun} = R_{s,\,sun} + R_{nl,\,sun} \tag{6.45}$$

and

$$R_{n,\,shade} = R_{s,\,shade} + R_{nl,\,shade} \tag{6.46}$$

where $R_{s,\,sun}$ and $R_{s,\,shade}$ are the shortwave solar radiation for sunlit and shaded leaves, $R_{nl,\,sun}$ and $R_{nl,\,shade}$ are the net longwave solar radiation for sunlit and shaded leaves. The shortwave solar radiation terms are calculated by the following equations:

$$R_{s,\,sun} = (1 - \alpha_L)(R_{s,\,dir}\, cos\, \alpha_{sa}/cos\, \theta) + R_{s,\,shade} \tag{6.47}$$

where α_L is the leaf scattering coefficient (constant that equals 0.25); α_{sa} is the mean leaf-sun angle, which is taken as 60° (Liu et al., 2003); θ is the solar zenith angle; $R_{s,\,dir}$ is the direct shortwave solar radiation. $R_{s,\,shade}$ is calculated with:

$$R_{s,\,shade} = (R_{s,\,dif} - R_{s,\,dif-under})/LAI_o + C \tag{6.48}$$

where $R_{s,\,dif}$ is the diffuse shortwave solar radiation; $R_{s,\,dif-under}$ is the diffuse shortwave solar radiation under the overstory; and C accounts for the multiple scattering of direct radiation, which is calculated by:

$$C = \alpha_L\, \Omega_E\, R_{s,\,dir}(1.1 - 0.1LAI_o)\, e^{-cos\, \theta} \tag{6.49}$$

$R_{s,\,dir}$ is a function of R_s and $R_{s,\,dif}$ as follows:

$$R_{s,\,dir} = R_s - R_{s,\,dif} \tag{6.50}$$

and $R_{s,\,dif}$ can be estimated using the following cases:

$$\frac{R_{s,\,dif}}{R_s} = \begin{cases} 0.13 & \text{if } \tilde{r} \geq 0.8 \\ 0.943 + 0.734\tilde{r} - 4.9\tilde{r}^2 + 1.796\tilde{r}^3 + 2.058\tilde{r}^4 & \text{if } \tilde{r} < 0.8 \end{cases} \tag{6.51}$$

where $\tilde{r}$ is calculated as a function of the solar constant ($SC = 1367 W m^{-2}$), R_s and θ:

$$\tilde{r} = \frac{R_s}{SC \cos\theta} \tag{6.52}$$

and finally, $R_{s,\,dif-under}$ can be calculated as a function of $R_{s,\,dif}$, Ω_E, LAI_o, and the angle for diffuse radiation ($\bar{\theta_o}$):

$$R_{s,\,dif-under} = R_{s,\,dif} \left(e^{-0.5\Omega_E LAI_o / \cos\bar{\theta_o}} \right) \tag{6.53}$$

where $\cos\bar{\theta_o}$ is calculated using Equation (6.36). The Ω_E is of course the clumping index of the overstory, which is taken as 0.83 and 0.64 for the Coniferous and Deciduous site respectively (values obtained in situ with the TRAC optical device).

As mentioned, the net longwave radiation terms are considered to behave the same for sunlit and shaded leaves. Thus, $R_{nl,\,sun} = R_{nl,\,shade}$, and their value is calculated by:

$$R_{nl,\,sun} = R_{nl,\,shade} = \frac{R_{nl}}{LAI_o} \tag{6.54}$$

and Equation (6.33) calculates R_{nl}.

As it is noticed, Equations (6.44) and (6.43) include the term r_s instead of r_c. The stomatal resistance is calculated based on the r_c values obtained with the set of reduction functions that resolve g_c [Equations (6.22) to (6.30)] and with the LAI_o:

$$r_s = LAI_o \, r_c \tag{6.55}$$

Allen et al. (1989) reported the previous equation using a LAI value which is standardized for crops and relatively tall grasses (i.e. $0.5\,LAI$). Here, the equation is modified to make it applicable to overstory. Besides, it is considered that shaded and sunlit leaves have similar stomatal resistances responses.

6.5 Results and analysis of results

6.5.1 Spatial scaling: Canopy transpiration

The Deciduous plot's ratio of SA_{plot} to the plot's basal area was of 0.57, while in the Conifer site, the ratio was 0.54 for the Lodgepole pine trees and 0.38 for the White Spruce trees. Thus, the Trembling aspen shows a larger sapwood area per unit basal area at the plot scale than the conifer species. That was expected since diffuse-porous trees have larger sapwood areas in order to meet their water demand (i.e they are less efficient at transporting water). As it is shown in the following sections, the Deciduous site drew larger mass flow per plot than the Conifer site.

The transpiration patterns of the sampled trees showed activity starting early in the morning (around 500 and 545 hours) and finishing between 1700 and 1900 hours. Changes in the time at which the tree stopped transpiring and started again was related to the meteorological changes. Thus, for each tree, its sap flow pattern was analyzed in order to determine the times of initial and final daily transpiration activity.

The use of the radial profile function to correct the sap flow velocity showed that the sap flow velocity values will have an underestimation of 12.5% in trees with a relatively small sapwood depth ($3.5cm \pm 1.5cm$). The average $\bar{sd}$ in conifers ranged between $3.10cm$ and $3.5cm$. Thus, in this particular case, if the radial profile correction could not be applied, the sap velocity will be underestimated when scaled to the entire tree. From Figure 6.4 to Figure 6.9 the diurnal sap flow pattern in Lodgepole pine, White spruce, and Trembling aspen, respectively is illustrated. In each plot, the dashed line is R_s and the solid line is J_i. Two individuals of different DBH_{OB} are presented in order to exemplify the differences in J_i due to the tree size. Notice that the Lodgepole pine J_i is somewhat tempered in comparison to R_s.

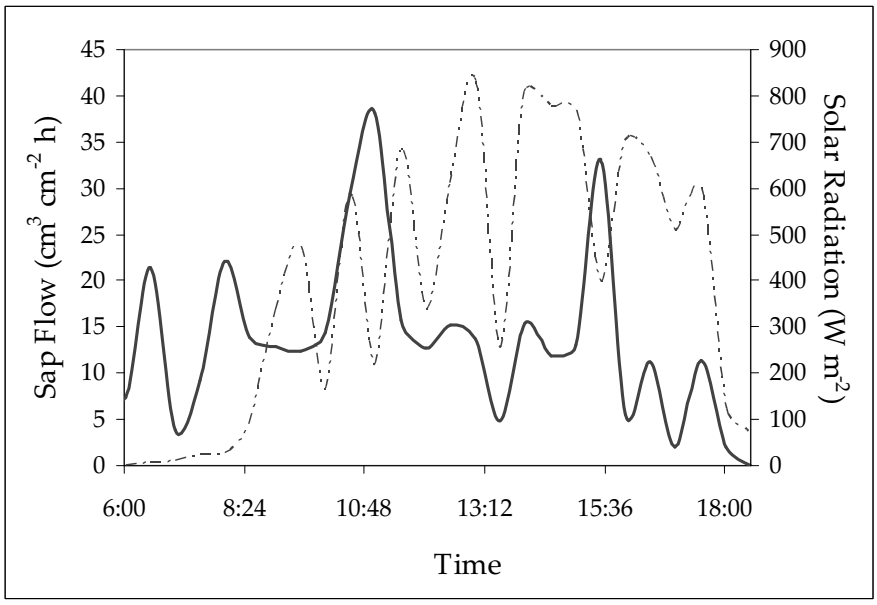

Figure 6.4: Diurnal sap flow of a Lodgepole pine tree. Tree's $DBH_{OB} = 24\,cm$. Day of the year: 212, in 2004.

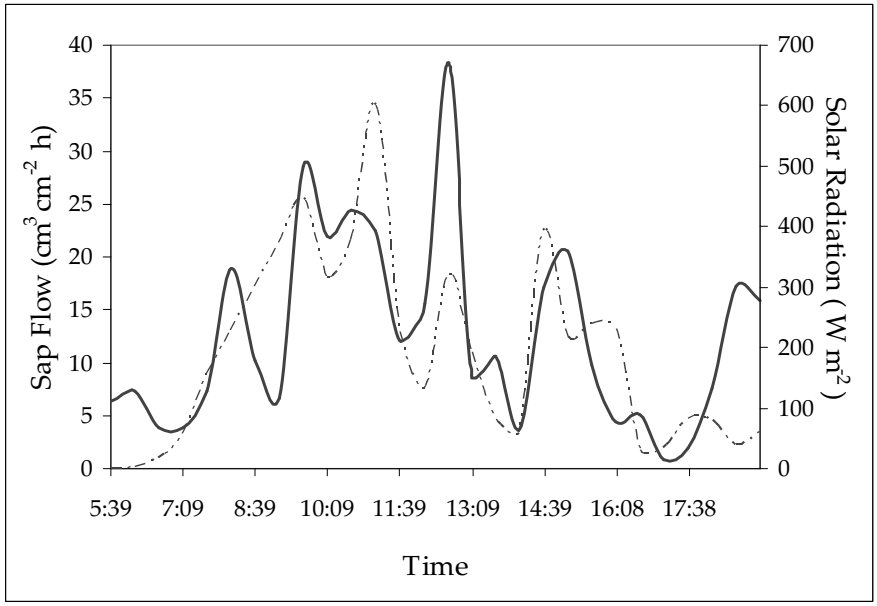

Figure 6.5: Diurnal sap flow of a Lodgepole pine tree. Tree's $DBH_{OB} = 17\,cm$. Day of the year: 216, in 2004.

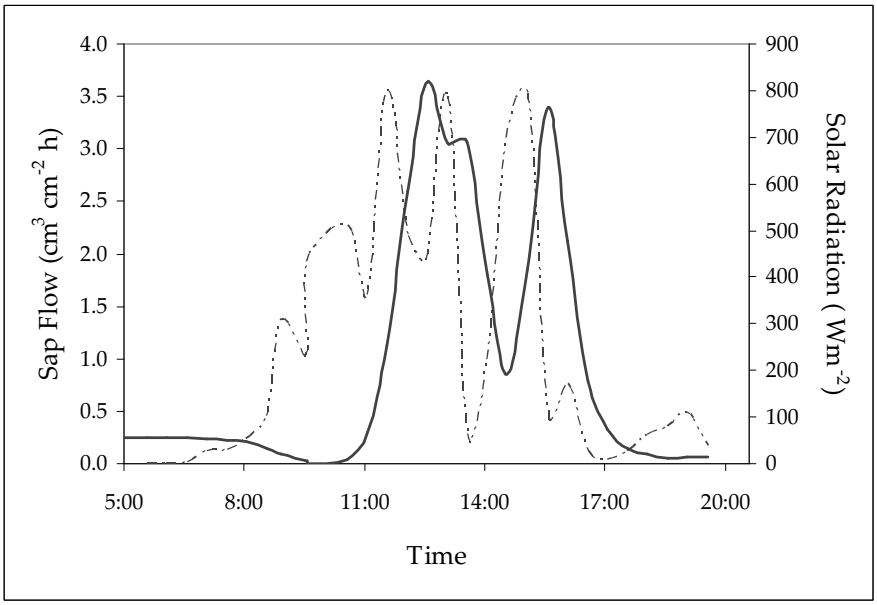

Figure 6.6: Diurnal sap flow of a White spruce tree. Tree's $DBH_{OB} = 18\,cm$. Day of the year: 232, in 2004.

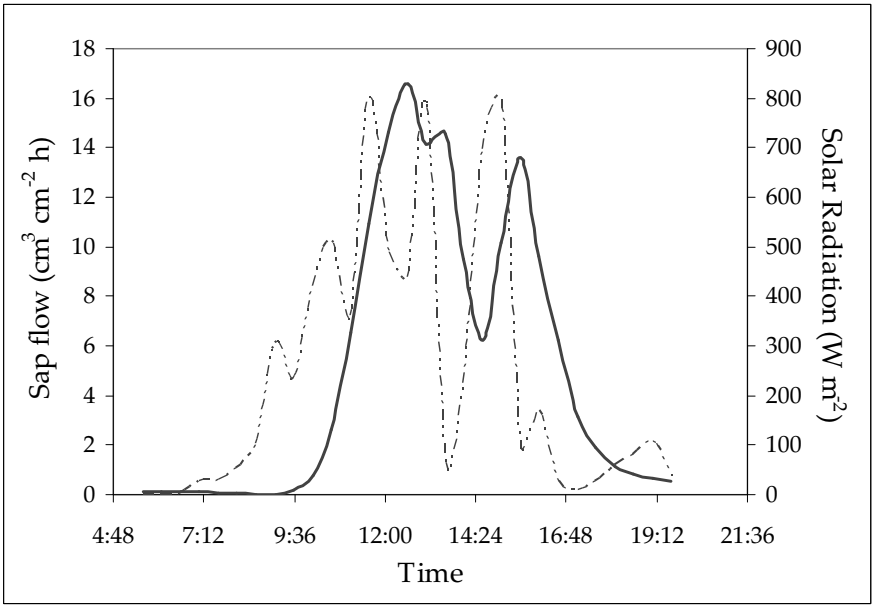

Figure 6.7: Diurnal sap flow of a White spruce tree. Tree's $DBH_{OB} = 32\,cm$. Day of the year: 232, in 2004.

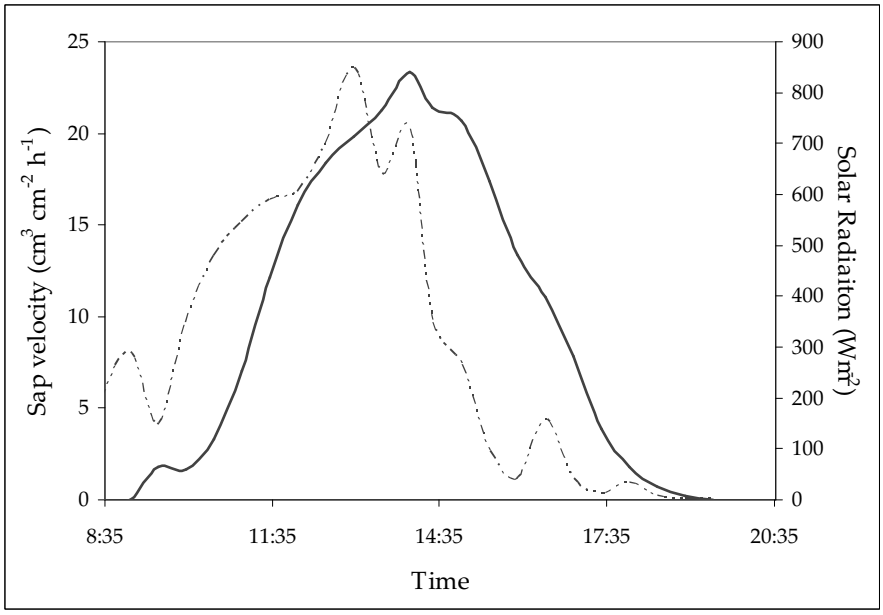

Figure 6.8: Diurnal sap flow of a Trembling aspen tree. Tree's $DBH_{OB} = 31\,cm$. Day of the year: 228, in 2004.

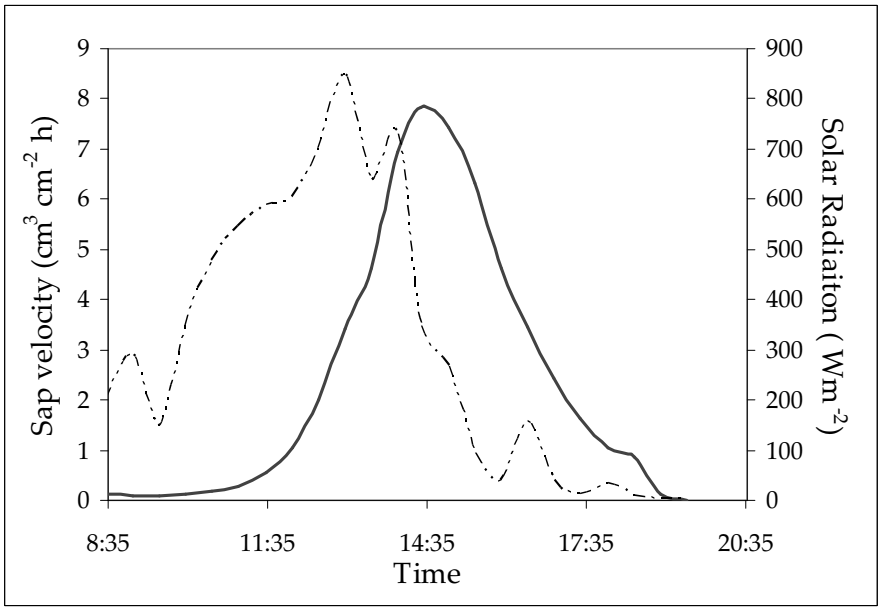

Figure 6.9: Diurnal sap flow of a Trembling aspen tree. Tree's $DBH_{OB} = 15\,cm$. Day of the year: 228, in 2004.

Each species $\bar{F}_{sp}$ and $\bar{F}_{plot}$ is reported in Table 6.2. The Coniferous site total mass flow is the summation of the two species populating the site. Not all the trees and not all the days registered adequate sap flow data. With the conifers, some individuals that were set up with TDP's had some pest problems (i.e. *Dendroctonus ponderosae* Hopkins [mountain pine beetle]) and their sap flows were inconsistent along the day with a healthy trees' response. The pest problem unfortunately was not that obvious at first sight (two trees). In some Coniferous and Deciduous groups set up with the TDP's there were some problems with the power feeding the logger and the sensors, which made the sap flow readings inconsistent and out of the expected ranges. Another problem that was faced were the rainy and cloudy days, that can inhibit tree transpiration and therefore during those days, there was no collection of data at all (i.e. Jack pine sites in WC). Hence, in the end, sap flow data was available for 5 Lodgepole pine and 4 White spruce in the Conifer-4 site. Eight days in total of sap flow data was collected at this site. The Deciduous site, the whole set was adequate, and four days in total were used to estimate the $\bar{F}_{plot}$.

Table 6.2: $\bar{F}_{sp}$ and $\bar{F}_{plot}$ at each site. The number of individuals used per plot (Ind. #) to estimate the mass flows and the number of days used to obtain the average values is shown in this table as well.

Site	**Tree type**	**Ind. #**	(m^3/d)		**Days averaged**
			$\bar{F}_{sp}$	$\bar{F}_{plot}$	
Conifer-4	Lodgepole pine	5	12.64		8
	White spruce	4	2.57	15.21	8
Deciduous-6	Trembling aspen	4	31.35	31.35	4

6.5.2 Forest evapotranspiration

Actual Evapotranspiration.

To calculate E_{a}, the most complex parameter to obtain is r_c. Here, the series of reduction functions used and the assumptions made provided half-hourly r_c values that are in reasonable agreement with the values listed by Allen et al. (1996), Perrier (1982), and Jarvis et al. (1976). The other parameter that was estimated in an uncommon way was the R_n. This was done by integrating parameters that take into account the influence of LAI, gap fraction and emissivity of understory and overstory. Since the determination of LAI_u and Ω_u was essentially based on previous reports, which at the same time are based on a few assumptions, it was necessary to observe the influence of LAI_u and Ω_u values on the calculation of E_{a}. Thus, a sensitivity analysis of E_{a} while varying LAI_u and Ω_u was performed. The range of values to test LAI_u and Ω_u were 0.6-1.5 and 0.5-0.9 respectively. The obtained estimates of E_{a} with respect to the initial E_{a} differ in the range of -2.0×10^{-4} to $9.0 \times 10^{-4}\, mm/d$. When LAI_u and Ω_u are set up as 0.6 and 0.9 respectively, E_{a} estimates are practically the same than when LAI_u and Ω_u are set up as 1.0 and 0.5 (the values used here). The sensitivity analysis was performed as well to see the impact on the average of E_{a} (i.e. $\bar{E}_{\mathrm{a}}$) per day. The analysis showed differences between values ($\bar{E}_{\mathrm{a}}$ here reported and the ones obtained with the sensitivity analysis) in the range of -2.0×10^{-4} to $6.0 \times 10^{-4}\, mm/d$. In conclusion, the variation is minimal and does not influence the final estimates. Final estimates of E_{a} are listed in Table 6.3. The E_{a} values are shown per date and sorted by the type of site that was set up for sap flow measurements in the same dates.

Liu et al. (2003) reported that Canadian boreal forest evapotranspiration values range between $100 - 300 mm/year$. Also, Liu et al. estimated that just a coniferous land cover could have a yearly transpiration of $123mm$ with an $s = 55m$; deciduous and mixed forests land covers were reported with yearly transpiration values of $327mm$ and $244mm$ respectively. On examination of the previous results, it would seem that there is an overestimation of E_{a}; however, 2004 had a particularly wet and hot summer, that exceeded reported rainfall normals (EC, 2006) by a magnitude of 0.75 in July and 2.27

Table 6.3: Penman-Monteith E_a and $\bar{E}_a$ estimates during the same days that sap flow was measured at each site. $\bar{E}_a$ is the average of the daily E_a . Field campaign 2004.

	Conifer-4		**Deciduous-6**
Day of the year	E_a (mm/d)	**Day of the year**	E_a (mm/d)
212	1.50	225	4.79
213	0.78	226	5.82
215	3.01	227	3.29
216	1.68	228	3.27
231	0.90		
232	0.87		
234	3.63		
235	0.07		
$\bar{E}_a$	1.56		4.29

in August. Also, daily maximum temperatures during the months of July and August were greater than the daily maximum values reported in the climate normals. That is, July and August maximum temperatures varied between 24 and 29°C, while the climate normals reported maximum temperatures of 21.5 and 21.1°C, respectively. Thus, the conditions for evapotranspiring large amounts could be considered reasonable for this wet and hot summer.

Variation of the soil field capacity.

The field capacity of a sandy loam soil varies between 0.16 and 0.22, and its wilting point is 0.073 (Dunne and Leopold, 1998). The reported E_a was calculated using an average value of the soil field capacity. Still, calculations of θ_e, g_s, and finally E_a were made using the lower and upper bounds of the soil's θ_{fc}.

Results showed that in days when $\theta_e \leq 0.00$, the function limiting E_a was $g(\theta_{sm})$, causing g_s to become practically null, and making r_c reach its maximum value. In these days, there was no difference in the final E_a since the computation of θ_e will always be

zero or negative, no matter the θ_{fc} value. Of course, in those days the factor limiting E_{a} was soil moisture to the point that observed E_{a} values were lower than $1mmd^{-1}$ (e.g. days 213 and 235, Coniferous site).

When $0.16 \geq \theta_{sm} \geq 0.22$, soil moisture is not limiting at all, and other environmental factors drive E_{a}. In these cases, there was no variation in the final E_{a} estimate. It was noticed as well that the immediate limiting factor was VPD, and then R_s (e.g. days 231, Coniferous site).

Finally, if $\theta_{sm} \approx \theta_{\text{wp}}$, there is variation in the estimates of E_{a}. This was noticeable for just two days in the whole data set used here (days 215 and 216, set up in Conifer-4). When θ_{sm} varied from 0.0750 to 0.0795, the changes in θ_{fc} generated E_{a} to vary between $2.54mmd^{-1}$ and $3.73mmd^{-1}$, when θ_{fc} was set up as 0.22 and 0.16, respectively (day 215). When θ_{sm} varied from 0.0735 to 0.0743, the changes in θ_{fc} caused an E_{a} value of $0.90mmd^{-1}$, either θ_{fc} was 0.22 or 0.16, respectively (day 216). The reported E_{a} values for these two days are $3.01mmd^{-1}$ and $1.68mmd^{-1}$. In those two days, it could be said that there is a variation in the E_{a} estimates between $0.47mmd^{-1}$ and $0.78mmd^{-1}$.

Potential Evapotranspiration.

E_{p} estimates are shown in Table 6.4. The obtained results with the Penman equation for free water evaporation are not displayed here since the results were just unreasonably high and not comparable with any of the evapotranspiration or transpiration values obtained here. The assumption that $r_c = 0$ creates very large evapotranspiration estimates was expected since it is supposed that there is no resistance from the canopy to transpire. These values are representative of an E_{p} in a forested area; however, they are not useful for comparisons with the obtained transpiration values due to the large differences in magnitude.

Table 6.4: E_{p} estimates during the same days that sap flow was measured at each site. Field campaign 2004.

	Conifer-4		**Deciduous-6**
Day of the year	E_{p} (mm/d)	**Day of the year**	E_{p} (mm/d)
212	41.65	225	194.47
213	26.89	226	234.09
215	37.32	227	110.31
216	25.10	228	98.60
231	19.19		
232	15.74		
234	27.68		
235	59.96		
$\bar{E}_{\mathrm{p}}$	31.69		159.36

6.5.3 Canopy transpiration, modified Penman-Monteith equation

The computation of T_{sun} and T_{shade} is very similar to the one applied for computing E_{a}. The main changes rely on substituting R_n by either R_{sun} or R_{shade} and the use of r_s instead of r_c. Tables 6.5 and 6.6 show the obtained transpiration estimates for shaded, sunlit leaves, and the total canopy transpiration, called T_{plant} by Liu et al. (2003), in the Conifer and Deciduous sites respectively. It is worth mentioning that for the Deciduous site, the T_{plant} estimates were based on the estimation of g(VPD) computed with $K_{VPD} = 0.84\,kPa$.

Variation of the soil field capacity.

Like in E_{a} estimates, there is variation in the estimates of T_{plant} if $\theta_{sm} \approx \theta_{\mathrm{wp}}$. At the Coniferous site, days 215 and 216 showed the variations at the Coniferous site. When θ_{sm} varied from 0.0750 to 0.0795, the changes in θ_{fc} generated T_{plant} to vary between $2.10 mm d^{-1}$ and $3.22 mm d^{-1}$, (keeping θ_{fc} equal to 0.22 and 0.16 respectively; day 215). When θ_{sm} varied from 0.0735 to 0.0743, the changes in θ_{fc} caused T_{plant} of $0.87 mm d^{-1}$,

either θ_{fc} was 0.22 or 0.16, respectively (day 216). The reported E_{a} values for these two days are $2.53 mmd^{-1}$ and $1.67 mmd^{-1}$. In those two days, it could be said that there is a variation in the E_{a} estimates between $0.43 mmd^{-1}$ and $0.80 mmd^{-1}$.

Table 6.5: Modified Penman-Monteith T_{plant} estimates during the same days that sap flow was measured at the Coniferous site. T_{plant} is the summation of T_{shade} and T_{sun}. $\bar{T}_{plant}$ is the average of the daily T_{plant}. Field campaign 2004.

Day of the year	T_{shade}	T_{sun}	T_{plant}
		(mm/d)	
212	0.38	1.08	1.46
213	0.19	0.56	0.75
215	1.80	0.73	2.53
216	1.26	0.41	1.67
231	0.56	0.66	1.22
232	0.52	0.64	1.16
234	2.59	0.95	3.54
235	0.11	0.04	0.15
$\bar{T}_{plant}$			1.56

Table 6.6: Modified Penman-Monteith T_{plant} estimates during the same days that sap flow was measured at the Deciduos site. Field campaign 2004. T_{plant} is the summation of T_{shade} and T_{sun}. $\bar{T}_{plant}$ is the average of the daily T_{plant}. Field campaign 2004.

Day of the year	T_{shade}	T_{sun}	T_{plant}
		(mm/d)	
225	3.00	1.75	4.75
226	3.67	2.13	5.80
227	2.44	1.42	3.86
228	2.05	1.20	3.25
$\bar{T}_{plant}$			4.42

6.5.4 Agreement between methods

Plot's sapwood area as unit ground area.

Before presenting results, recall that there are two main expectations:

1. That $\bar{T}_{plot} = \bar{T}_{plant}$, or at least $\bar{T}_{plot} \approx \bar{T}_{plant}$;
2. That $\bar{T}_{plot}$ estimates will be a significant proportion of $\bar{E}_{\mathrm{a}}$.

A third expectation is that $\bar{T}_{plant}$ will be a significant proportion of $\bar{E}_{\mathrm{a}}$. Even though the main focus is on validating $\bar{T}_{plot}$ estimates by comparing them with $\bar{E}_{\mathrm{a}}$ and $\bar{T}_{plant}$, the comparison between $\bar{T}_{plant}$ and $\bar{E}_{\mathrm{a}}$ will help to observe how significant is the contribution of forest transpiration to the total forest evapotranspiration. Specifically, the Coniferous site's daily average estimates of E_{a} and T_{plant} (Tables 6.3 and 6.5) are practically the same ($1.56 mm/d$). For the Deciduous site $\bar{T}_{plant} > \bar{E}_{\mathrm{a}}$ by $0.13 mm/d$. Hence, both Equations (6.10) and (6.42) give very similar estimates. The author wonders if such close similarity means that the wet, hot summer conditions of the studied area made the evaporation component negligible. Nevertheless this should be part of future studies that could observe the agreement between the original Penman-Monteith equation and the stratified model developed by Liu et al. (2003).

The comparison between $\bar{E}_{\mathrm{a}}$ and $\bar{T}_{plot}$ is shown in Table 6.7, while Table 6.8 shows the comparison between $\bar{T}_{plant}$ and $\bar{T}_{plot}$. For these comparisons, the transpiration values are expressed as the average of the sap flow $[mm^3_{\mathrm{sap}}\, mm^{-2}_{SA}\, d^{-1}]$ measured in trees inside of each plot multiplied by a ground index. This ground index was estimated as the ratio of SA_{plot} to $1ha$ (from now on named "SA_{plot} as unit ground area"). Additionally, E_{a} and T_{plant} were averaged (i.e. $\bar{E}_{\mathrm{a}}$ and $\bar{T}_{plant}$) on the same days for which $\bar{J}_{plot}$ was computed.

The agreement between the Coniferous $\bar{E}_{\mathrm{a}}$ and $\bar{T}_{plot}$ is acceptable and showed that $\bar{T}_{plot}$ is about 97% of the total forest evapotranspiration. The remaining 3% of $\bar{E}_{\mathrm{a}}$ may be attributed to the other sources of forest evapotranspiration such as surface evaporation and understory transpiration. The contribution of understory evapotranspiration

varies and it could be fairly large during the growing season; however, Black et al. (1989) listed different sources that measured understory ET in stands of different Pinaceas, and percentages range from 6% to 60% as understory contribution to forest ET. Thus, it is reasonable to attribute the difference between both methods to understory ET.

Equal results drew the comparison between $\bar{T}_{plant}$ and $\bar{T}_{plot}$; the $\bar{T}_{plot}$ is 97% of the $\bar{T}_{plant}$ estimates. Although both values are quite similar, the $\bar{T}_{plant}$is greater than $\bar{T}_{plot}$ by $0.04mm/d$. The agreement is acceptable as well; however, it was expected that both values will be equally the same (i.e. $\bar{T}_{plant} = \bar{T}_{plot}$).

The Deciduous showed a better agreement with the $\bar{E}_{\mathrm{a}}$ when K_{VPD} was set as $0.84\,kPa$ and the $VPD_c = 1.0\,kPa$. In this case, the $\bar{T}_{plot}$ is about 73% of the $\bar{E}_{\mathrm{a}}$, and about 71% of the $\bar{T}_{plant}$. The value is acceptable as well, since the days when the $\bar{J}_{sp}$ was measured, the soil moisture was not limiting, and VPD was the driving factor. As it has been shown in other works (Bovard et al., 2005), when this situation happens, the sap flow reaches a plateau and becomes quasi constant along the day. Just when water is limiting, the $\bar{J}_{sp}$ can decrease. Thus, the remnant 28% of the $\bar{E}_{\mathrm{a}}$ can be attributed to the understory transpiration and some other surfaces evaporating water.

Table 6.7: Daily average of E_{a} and T_{plot} at the Coniferous (8 days average) and Deciduous (4 days average) sites. SA_{plot} was used as the unit ground area to estimate $\bar{T}_{plot}$.

	(mm/d)			
Site	$\bar{E}_{\mathrm{a}}$	$\bar{T}_{plot}$	**Scale**	**Agreement**
Conifer-4	1.56	1.52	Canopy	$\bar{T}_{plot} = 0.97(\bar{E}_{\mathrm{a}})$
Deciduous-6	4.29	3.14	Canopy	$\bar{T}_{plot} = 0.73(\bar{E}_{\mathrm{a}})$
Deciduous-6[1]	5.31	3.14	Canopy	$\bar{T}_{plot} = 0.59(\bar{E}_{\mathrm{a}})$

[1]Results obtained when $K_{VPD} = 0.79\,kPa$

Table 6.8: Daily average of T_{plant} and T_{plot} at the Coniferous (8 days average) and Deciduous (4 days average) sites. SA_{plot} was used as the unit ground area to estimate $\bar{T}_{plot}$.

	(mm/d)			
Site	$\bar{T}_{plant}$	$\bar{T}_{plot}$	**Scale**	**Agreement**
Conifer-4	1.56	1.52	Canopy	$\bar{T}_{plot} = 0.97(\bar{T}_{plant})$
Deciduous-6[1]	4.42	3.14	Canopy	$\bar{T}_{plot} = 0.71(\bar{T}_{plant})$

[1]Results obtained when $K_{VPD} = 0.84\,kPa$

Leaf Area as unit ground area.

Looking for another unit area that could be helpful in transforming sap flux density values into a canopy transpiration rate, LA_{eff} and LA_{plot} were used as unit areas:

$$\bar{T}_{plot} = \bar{J}_{plot} \times SAI_{eff} \tag{6.56}$$

where

$$SAI_{eff} = SA_{sp}/(LAI_{eff} \times A_{plot}) \tag{6.57}$$

or:

$$\bar{T}_{plot} = \bar{J}_{plot} \times SAI_{actual} \tag{6.58}$$

where

$$SAI_{actual} = SA_{sp}/(LAI \times A_{plot}) \tag{6.59}$$

The same principle was applied with LA_{plot} as a unit area. It is important to remember that the same LA_{plot} values were used to create the regression model with SA_{plot}.

Results are shown in Tables 6.9 and 6.10. As it is appreciated, the LA_{plot} and LA_{eff} as unit ground areas describe the canopy transpiration of the Coniferous site as 48% and 67% of $\bar{E}_{\mathrm{a}}$ respectively; and the same agreements are shown with $\bar{T}_{plant}$. In the case of the Deciduous site, the $\bar{T}_{plot}$ is described as 64% and 83% of the $\bar{E}_{\mathrm{a}}$. On the other hand, $\bar{T}_{plot}$ is 62% and 80% of the $\bar{T}_{plant}$. The LA_{eff} as a unit area describes the Deciduous $\bar{T}_{plot}$ as a larger proportion of $\bar{E}_{\mathrm{a}}$ than the unit ground area (these values are based on $K_{VPD} = 0.84\,kPa$).

Table 6.9: LA_{plot}, LA_{eff} , and site average canopy transpiration along eight days, Coniferous site. L-p is Lodgepole pine, W-s is White spruce.

	Canopy transpiration (mm/d)			
Unit area	L-p	W-s	$\bar{T}_{plot}$	**Agreement**
$\mathbf{LA_{plot}}$	0.61	0.13	0.74	$\bar{T}_{plot} = 0.48(\bar{E}_{\mathrm{a}})$ $\bar{T}_{plot} = 0.48(\bar{T}_{plant})$
$\mathbf{LA_{eff}}$	0.86	0.18	1.04	$\bar{T}_{plot} = 0.67(\bar{E}_{\mathrm{a}})$ $\bar{T}_{plot} = 0.67(\bar{T}_{plant})$

Table 6.10: LA_{plot}, LA_{eff} , and site average canopy transpiration along four days, Deciduous site.

	(mm/d)	
Unit area	$\bar{T}_{plot}$	**Agreement**
$\mathbf{LA_{plot}}$	2.75	$\bar{T}_{plot} = 0.64(\bar{E}_{\mathrm{a}})$ $\bar{T}_{plot} = 0.62(\bar{T}_{plant})$
$\mathbf{LA_{eff}}$	3.55	$\bar{T}_{plot} = 0.83(\bar{E}_{\mathrm{a}})$ $\bar{T}_{plot} = 0.80(\bar{T}_{plant})$

6.6 Discussion and Conclusions

The main objectives of this study involve scaling issues in transpiration: firstly, to identify those parameters influencing transpiration at different scales in order to use them as scaling parameters if adequate models can be developed; and secondly (but no less important), the improvement of the final transpiration estimates at larger scales. This is a complex task since in Nature there exists large intra and interspecific variability that at the same time is controlled by biophysical characteristics. In this study, these problems were faced and addressed by using more accurate methods to estimate the scaling factors in order to avoid large uncertainty in the final estimates.

It is interesting that both Equations (6.10) and (6.42) drew practically the same daily average value. Still, the daily values of E_{a} and T_{plant} differ; and most days showed that indeed $E_{\mathrm{a}} > T_{plant}$ (i.e. Days 212, 215, 216, 234, 225, 226, and 228). However, other days oddly showed that $T_{plant} > E_{\mathrm{a}}$ (Days 231, 232, 235, and 227). Thus, it is considered the daily average estimates of both parameters is influenced by very large or very small numbers, making both $\bar{E}_{\mathrm{a}}$ and $\bar{T}_{plant}$ very similar. Furthermore, it was expected to observe that T_{plant} is a siginificant proportion E_{a}, and most of the days showed that T_{plant} was more than 90% of the E_{a}. Author feels that the closeness between these values is due to the particular conditions of the summer of 2004 (wet, hot summer). As mentioned in § 6.5.4, the agreement between T_{plant} and E_{a} should be part of future studies. Finally, the most important outcome is that either $\bar{T}_{plant}$ or $\bar{E}_{\mathrm{a}}$ are in good agreement with the $\bar{T}_{plot}$ estimates.

The $\bar{T}_{plot}$ values obtained showed an acceptable agreement with the computed actual forest evapotranspiration and the actual canopy transpiration (Equations [6.10] and [6.42]) of each site. In the Deciduous site case, the obtained $\bar{T}_{plot}$ motivates one to speculate if the agreement is good enough. In this particular case, there is an issue worth mentioning here (in case the reader considers the $\bar{T}_{plot}$ fraction small). The days in which the $\bar{T}_{plot}$ was calculated showed large E_{a} and T_{plant} values because θ_{sm} was not limiting, and VPD was driving E_{a} and T_{plant} transpiration as well. In this case, the empirical factor K_{VPD} was adjusted as much as possible by respecting previous reports

on the influence of VPD in g_s. The actual r_c of the Trembling aspen individuals could go beyond the empirical estimates, but there is no field data that could evince this and allow modification to K_{VPD}. Moreover, BEPS results evidenced that at larger scales, a deciduous forest's transpiration is about 67% of the anual actual forest evapotranspiration (Liu et al., 2003). Therefore, the Deciduous $\bar{T}_{plot}$ are reasonable estimates.

Specifically, in order to validate $\bar{T}_{plot}$ estimates obtained with the scaling approach created along this research, it was expected:

1. That $\bar{T}_{plot} = \bar{T}_{plant}$, or at least $\bar{T}_{plot} \approx \bar{T}_{plant}$;
2. That $\bar{T}_{plot}$ estimates will be a significant proportion of $\bar{E}_{\mathrm{a}}$.

And both points were observed for both the Coniferous and Deciduous sites. Even if the unit area factors used to express sap flux density of the plot as canopy transpiration rates drew dissimilar results, the estimated $\bar{T}_{plot}$ always met the expected agreements with $\bar{E}_{\mathrm{a}}$ and $\bar{T}_{plant}$. The Coniferous site $\bar{T}_{plot}$ estimated by means of SA_{plot} as a unit ground area (i.e. using $SA_{plot}/10\times10^6 m^2$) implies that there is a significant contribution of canopy transpiration to the total ET of the studied sites. Specifically, SA_{plot} as a unit area factor implies that the Coniferous site $\bar{T}_{plot}$ is 97% of the $\bar{E}_{\mathrm{a}}$, while the Deciduous site $\bar{T}_{plot}$ is 73% of the $\bar{E}_{\mathrm{a}}$.

Moreover, the estimated $\bar{T}_{plot} \approx \bar{T}_{plant}$, which proves the reliability of the developed scaling approach. The last results are in accordance with the now general knowledge of the importance of transpiration in forest water loss. Thus, using SA_{plot} as unit gound area, the canopy transpiration rates are in aggreement with previous works. However, using any Leaf Area as unit area factor, it seems that canopy transpiration is underestimated (in the Coniferous site), and overestimated (in the Deciduous site) in comparison with the obtained $\bar{T}_{plot}$ using SA_{plot} as unit area.

The LA_{eff} as a unit ground area (i.e. using SAI_{eff}) showed that $\bar{T}_{plot}$ of the Deciduous site is a larger fraction of the $\bar{E}_{\mathrm{a}}$ (than the estimated with the SA_{plot} as unit ground area); and $\bar{T}_{plot}$ becomes a closer value to the $\bar{T}_{plant}$ one. Conversely, LA_{eff} as a unit ground area defines the Coniferous site $\bar{T}_{plot}$ as a smaller fraction. Results suggest that SA_{plot} as unit ground area gives adequate $\bar{T}_{plot}$ estimates for the Coniferous site and

the SAI_{eff} gives adequate $\bar{T}_{plot}$ estimates for the Deciduous site. Thus, the chosen unit ground area considerably influences the $\bar{T}_{plot}$ estimates.

Furthermore, it is important to keep in mind that $\bar{F}_{plot}$ is influenced by the method used to estimate the sapwood area. In previous Chapters, the problem of over and underestimations of sapwood area was addressed using different methods for estimation. The most common methods showed under and overestimations between -61% and 35% of the sapwood area estimated with the microscopical analysis. Lets say that an average overestimation of 15% occurs for SA_{WS}, and an underestimation of 34% for SA_{LP}, then $\bar{F}_{plot}$ will be $15.16\,m^3/d$, which is $2.56\,m^3/d$ less than the reported value here. In an area of $60 \times 60m$ it could be a unimportant amount of water ($7.11 \times 10^{-4} m^3/d$), but it will significantly increase when scaling up to larger areas. For instance, the underestimation of total mass flow in the Lower Elbow River Basin (area of $431.7km^2$), would be $306,986.7m^3/d$. These numbers become of high importance when it comes to forest water yield estimations and management. Here, it was shown that this large over or underestimations can be avoided by using the microscopical wood tissue analysis to estimate sapwood depth, and thereupon to estimate sapwood area.

In the calculation of E_{a} (as well as T_{plant}), there could be significant variations in reported values if the volumetric soil moisture approximates its wilting point. Therefore, study of the variations of θ_e since it is a function of both, the θ_{fc} and θ_{wp}, on E_{a} is recommended. Here, it was fortunate that the soil was either extremelly dry (below its θ_{wp}) or very wet ($0.16 \geq \theta_{sm} \geq 0.22$), causing just two days of transition between dryness and wetness to affect E_{a} values.

In conclusion, the use of more accurate methods to measure and estimate the scaling factors improved the final canopy transpiration estimates. This conclusion is based on the good agreement observed with the computed $\bar{T}_{plant}$ and $\bar{E}_{\mathrm{a}}$ estimates, which validate this dissertation's final results. Hence, the creation of a robust scaling approach improved the final canopy transpiration estimates. It is considered that the key points for reaching such improvement are related to the use of robust mensuration techniques to collect the field data, which also allowed a decrease in the error associated with

the collected data. Moreover, this robust scaling approach is an appropriate way to quantify the variation of the scaling factors, and to prove their correlation at large scales. The last outcome helps to a better understanding of the canopy transpiration process, which indeed will improve future estimates at the canopy scale and predictions at larger scales than the canopy.

6.7 Future work

The next step is to observe the behaviour of this scaling approach at larger scales. This could be done by comparing the final canopy transpiration estimates with transpiration estimates obtained from remotely sensed data.

The canopy transpiration values calculated using the LA_{eff} as a unit ground area factor are meaningful due to the close relationship between the total amount of leaves that fully operate during transpiration. Hence, it is believed that a deeper understanding and testing of this canopy transpiration number will be a significant contribution to the study of the efficiency of trees in water use.

7 General discussion and conclusions

This dissertation dealt with the issues associated with aggregating single trees transpiration to the canopy scale. Its main focus was on finding and attempting to decrease the error associated with each one of the parameters involved in the final canopy transpiration estimates. Thus, it was foreseen that eliminating as much error as possible in the biometric (or scaling parameter) mensuration at small scales, will allow one to carry minor uncertainty while scaling up. To achieve this, existent mensuration methods were studied and evaluated to choose those that would help to generate minimum error. The biometrics measured were sapwood depth, outside bark circumference at breast height (to estimate DBH_{OB}), and leaf area index. Furthermore, one of the most difficult achievements of this research was the biometrics mensuration at a wide range of scales, embracing new information from the cellular scale ($10^{-4}\,m$) to the plot scale ($10^{2}\,m$). Nevertheless, it is thought that this achievement has contributed greatly to the interesting and reliable outcomes.

For instance, the sapwood depth values used to scale up and develop the regression models were obtained by using the microscopical analysis of wood tissues (i.e. cellular scale). Along with the microscopical method, three more non-thermal mensuration methods were applied and results compared among them in order to assess the reliability of the microscopical method. The other three non-thermal methods were the injection of dye in situ, the translucence, and the coloration methods. The final results showed that inter and intraspecific physiological and anatomical variations constrain the use of these three methods and the error associated with each one of them is not measurable. In conclusion, the microscopical method was chosen because it resulted in the most accurate method and the error associated with it is measurable.

Results reported in Chapter 4 show that intraspecific sapwood depth variability could not only be a matter of a tree's size, but also a mechanism of defence to avoid large water demand (i.e. greater transpiration rates). Also, some species showed larger sapwood depth variations around their tree trunks than others. Such variations may be attributed to habitat conditions, species water demands, and growth requirements. Finally, it was numerically and statistically proven that sapwood depth and sapwood area are not always proportional to the tree size and that sapwood depth may remain constant in some species.

The next step was to generate the mathematical models to obtain sapwood area estimates for each tree inside the plots. These models would be helpful to aggregate sapwood area and therefore estimate canopy transpiration. Here, it was found that not all the studied species have a linear correlation between sapwood depth and outer bark diameter at breast height (i.e. those species that sapwood depth does not change as the tree grows: Lodgepole pine, Jack pine and Black spruce). Therefore, it was necessary to combine two approaches for scaling up sapwood area. Scaled sapwood area was linearly correlated to plot leaf area. Here, the footprint influence of the LAI measurements in the coniferous sites was observed. Due to the footprint influence, the $10 \times 10m$ plots' $SA_{plot} : LA_{plot}$ relationship sat below the $60 \times 60m$ plot line. This result helped to observe the importance of choosing the adequate spatial scales to measure the scaling parameters (plot delimitation) and also to observe the equipment's footprint. It was also observed that in the Deciduous plots there was not a large footprint influence and the $10{\times}10m$ plots' $SA_{plot} : LA_{plot}$ relationship matched very well with the $60{\times}60m$ plots. This completely proves how the canopy structure (and therefore tree species) determines the relationship between scaling parameters as the spatial scale increases when optical instruments are used to estimate LAI. Another important outcome was that the error associated with LA_{plot} linearly increases with increases in the plot size. Thus, it is always valuable to carefully determine the adequate plot size (based on research aims) in order to avoid large error propagation. Additionally, the results presented in Chapters 4 and 5 showed the species-specific allometry; for that, it is highly recommended (and mentioned for a second time in this dissertation) to be cautious when assuming a species'

growth or allometric relationship based on results derived for other species.

At this point it was possible to achieve and cover the three specific objectives, and the most important is that the error associated with the scaled SA_{plot} is not significant. Still, the Coniferous and Deciduous sites were not combined into a single regression model since the canopy structure marked a difference in the $SA_{plot} : LA_{plot}$ relationships. But it was possible to take into account the inner plot vegetation heterogeneity to scale sapwood area by using the combined approach.

Finally, canopy transpiration estimates were computed using the sap flow measured in several individuals of each studied species. Here, it was observed that even if the HD method is reliable, there are still some mensuration issues. First, the HD method did not measure the sap flow radial variation; therefore it was necessary to adapt a brand new approach (Ford et al., 2004) to estimate each tree's sap flow radial profile. This approach has never been used to calculate sap flow (Chelcy Ford, personal communication, August 2006), but only to estimate sap flow fractions. Therefore, the modification to this approach is another contribution of this Dissertation. Second, the HD equipment requires large amounts of power, which at one point became difficult to fulfill and some of the measurements had to be dismissed because of problems in keeping an adequate level of power feeding the data logger and the thermosensors. Other trees were eliminated because they were infested with mountain pine beetle (not visually notorious) and their transpiration patterns were discrepant with healthy tree transpiration patterns.

Once these issues were solved, canopy mass flow and canopy transpiration estimates were computed. Canopy transpiration estimates need to be expressed in terms of a unit ground area; the SA_{plot} divided by a unit ground ($1ha$) seemed to be an adequate unit ground area to express mass flow as canopy transpiration. LA_{plot} and LA_{eff} as unit areas lead to a $\bar{T}_{plot}$ that is a smaller proportion of $\bar{E}_{\mathrm{a}}$. What is most interesting is that LA_{eff} as a unit area determines larger $\bar{T}_{plot}$ values than LA_{plot}. Since LA_{plot} is supposed to be a more accurate estimate of actual LAI, it would be expected to give more similar canopy transpiration values to the ones obtained with SA_{plot} as unit ground area. This

was expressed in Chapter 6 discussion as an underestimation; however, the results are very interesting and open a door for further investigation. The author's suggestion is to look for a theoretical explanation of the influence of LA_{eff} and LA_{plot} as unit ground areas to estimate canopy transpiration.

The estimation of actual forest evapotranspiration through the Penman-Monteith equations became a challenge since the estimation of the aerodynamic components requires large amounts of computation and data. Also, a recently suggested equation to estimate R_{nl} (Liu et al., 2003) was used which includes not only the influence of the canopy structure, but also the influence of the understory. The comparison between $\bar{T}_{plot}$ and $\bar{E}_{\mathrm{a}}$ were in good agreement, mostly using SA_{plot} as a unit ground area.

7.1 Conclusions and novel contribution

In conclusion, it is considered that the research objectives were met, and it included a decrease in the error associated with the scaling parameter mensuration and aggregation. The reader may find that the methods used (mainly the microscopical analysis) are not practical but arduous. However, in order to advance global climate change modelling (and watershed management) it is necessary to avoid large uncertainty while numerically describing and characterizing transpiration at smaller scales. A simple exercise of numerically estimating watershed transpiration demonstrated the importance of choosing the adequate mensuration methods in order to avoid large error propagation (Chapter 6).

Even though accurate or reliable canopy transpiration estimates are difficult to obtain, here it was demonstrated that the improvement of the mensuration methods significantly decreases the uncertainty in the final estimates. This research supports previous work stating that the complexity in obtaining reliable canopy transpiration values is due to the transpiration dependency on physiological and meteorological factors, besides the habitat vegetation heterogeneity.

Finally, this dissertation provided an improved approach to estimating the vegetation

structural attributes correlated to transpiration at larger scales using ground-based measurements. New findings for vascular boreal species are the following:

1. It was conclusively proven that there is a correlation between LA_{plot} and SA_{plot} at larger scales (i.e. plot scale).
2. The statement of linear correlation between $\bar{sd}$ and DBH_{OB} is not applicable to every tree species. In this case, it is not applicable to Lodgepole pine, Jack pine and Black spruce.
3. For some species, the sapwood remains constant as the tree grows. In this particular case, for Lodgepole pine, Jack pine and Black spruce.
4. Correlations at specific scales should be developed in order to reliably predict sapwood area.
5. This research also contributed the generation of applicable linear models at large scales to predict sapwood area and estimate transpiration.
6. It was possible to reduce the error propagation in the scaling process.

One strong suggestion is to characterize the intraspecific biometrics variations beforehand in order to develop an adequate scaling approach.

8 Glossary

Since this Dissertation is multidisciplinary, this glossary provides some concepts that may not be familiar to all readers.

Angiosperm : Vascular plants having the ovules and seeds enclosed in an ovary. Populus tremuloides is an angiosperm. Syn: flowering plant.

Diameter at breast height Outer bark diameter at breast height is the DBH value calculated directly from the outermost circumference of the tree trunk at the breast height.

Diameter classes : For purposes of forest surveys, trees are classified by their DBH_{OB}. Each class covers about 2 inches. For instance, the 2-inch class includes trees with DBH_{OB} from 1.0 to 2.9-inches.

Gymnosperm : Any of a class (Gymnospermae) of woody vascular seed plants (as conifers) that produce naked seeds not enclosed in an ovary and that in some instances have motile spermatozoids. *Pinus banksiana* and *Picea mariana* are gymnosperms.

Lumen : In wood anatomy, the cavity of a tubular tissue or cell.

Ontogenesis : The process of an individual organism growing organically; a purely biological unfolding of events involved in an organism changing gradually from a simple to a more complex level.

Phloem : In wood anatomy, the tissue concerned with the conduction of nutrients to the roots; consists primarily of sieve tubes. Syn: Inner bark, bast.

Pit : In wood anatomy, a recess in the secondary wall of a cell where a thin membrane may permit liquids to pass from one cell to another.

Pith : The small, soft core occurring in the structural center of a tree trunk, branch, twig, or log.

Sapwood : The active water conducting tissue of a vascular plant. Syn: secondary xylem, alburn.

Wood : The tissues of the stem, branches, and roots of a woody plant lying between the pith and cambium, serving for water conduction, mechanical strength, and food storage, and characterized by the presence of tracheids or vessels. Syn: Xylem, non-conducting tissue, primary xylem, bole, heartwood.

A The process of evapotranspiration

Evapotranspiration (ET) is the result of combined processes by which liquid or solid water is transformed to water vapour and transferred from the earth's land surface to the atmosphere, completing the hydrologic cycle. Thus, ET occurs through the combination of evaporation and vegetation transpiration (Dingman, 2002; Nokes, 1995). ET is a primary component of every ecosystem's water balance. Global estimates indicate that about 62% of Continental precipitation is evapotranspired (Dingman, 2002) and in parts of Africa this proportion can exceed 90% (Dunne and Leopold, 1998). Most of this quantity (about 97%) is evaporated from vegetation and soil, and the rest is open-water evaporation. Thus, in the long term, the difference between precipitation and ET is the water available for human use and eco-hydrological processes.

A.0.1 Evaporation

In the hydrologic cycle, evaporation is the process by which liquid and solid water transform to water vapour and are transferred to the atmosphere. Evaporation occurs mainly from liquid water in rivers and lakes, vegetation surfaces, ground surfaces and sublimation from ice and snow surfaces.

The process of evaporation occurs when some molecules of the liquid attain sufficient kinetic energy to overcome the forces of the surface tension and escape from the surface of the liquid in the form of water vapour. In other words, evaporation occurs when the supply of energy is enough to provide the latent heat of vaporization. Common sources of energy are solar radiation, sensible heat transfer from the atmosphere and advection of heat into a water body by inflowing warm water. Solar radiation is the

dominant energy source; therefore, evaporation is a function of latitude, time of the day, season and cloudiness. Net evaporation occurs when the quantity of the molecules in motion that are transferred to the atmosphere is greater than the quantity of molecules that are returned to the liquid by condensation. At the beginning of the evaporation process, the air space above the water surface contains a small concentration of water vapour molecules. Under this condition, liquid water evaporates at very high rates, but eventually, as the air space becomes more saturated by water vapour molecules, the concentration in the atmosphere-water interface tends to equilibrium. At this point, the net evaporation tends to decrease and the saturation vapour pressure is reached. If some mechanical energy, like the wind, moves the saturated air away from the evaporating surface, then the rate of evaporation will increase once again, generating a concentration gradient in the water vapour.

A.0.2 Transpiration

Transpiration is a physical mechanism of plants that consist of the extraction of water (i.e. water with a low concentration of nutrients, named "sap") from the soil through their roots. The extracted water is transported along the plant into the leaf, where water finally evaporates from the leaf's interior to the atmosphere. The rate at which water evaporates from the leaves determines both the rate at which water is taken from the roots and its ascent rate towards the leaves. The entire process of transpiration involves: absorption of soil water by plants, translocation in liquid form through the vascular system of roots, stem, and branches to the leaves; and translocation through the vascular system of the leaf to the walls of stomatal cavities, where evaporation takes place. The water vapour in these cavities then moves into the surrounding air through the stomata (Figure A.1).

The process of transpiration provides the necessary mineral nutrients to the plants, helps to cool the leaves, and the primary concomitant is to provide a place where CO_2 dissolution can occur and enter the plant tissues. Vegetation generates carbohydrates for its own consumption, and it happens when the CO_2 is dissolved in water (Ding-

man, 2002). However, transpiration is also the source of adverse effects due to water stress. About 95% of the absorbed water simply passes through the plant and is lost by transpiration; if the source of water is limited, the plant experiences water deficit that inhibits growth, causes injury and death by dehydration (Kozlowski and Pallardy, 1997).

Transpiration is driven by meteorological factors and plant characteristics. Some plant characteristics influencing transpiration are the leaf structure, leaf exposure, and the stomata response to meteorological factors. Transpiration occurs in two phases: evaporation of water from cell walls into intercellular spaces and diffusion of water vapour into the outside air. In theory, most of the water evaporates from the walls of mesophyll cells. Kramer and Boyer (1995) argued that there is no common agreement regarding the pattern of evaporation within the leaves.

In general, vegetation transpires water vapour through several pathways: some portion is released through the stomata; some passes out through the epidermis of leaves and its cuticular covering. In some woody species, water evaporates from the bark of stems, branches and twigs. Meteorological factors driving transpiration rates are: the available energy to vaporize water, the concentration gradient of water vapour and the resistances in the diffusion pathways.

A.0.2.1 Interception loss

In vegetated areas, the total amount of rainfall does not reach the soil surface directly. Some of this rainfall is caught by vegetation and stored in the wetted surface and evaporated during and after the storm. This retained portion is known as interception storage or interception loss. The rest of the rainfall is moved through the vegetation canopy by two processes: throughfall and stemflow. The quantity retained by interception storage depends on the type of vegetation and specific characteristics of the foliage, such as shape, density and surface texture of the leaves, twigs and branches. Senescence and stage of maturity are some other factors influencing interception storage.

There are differences in interception storage between deciduous and coniferous trees

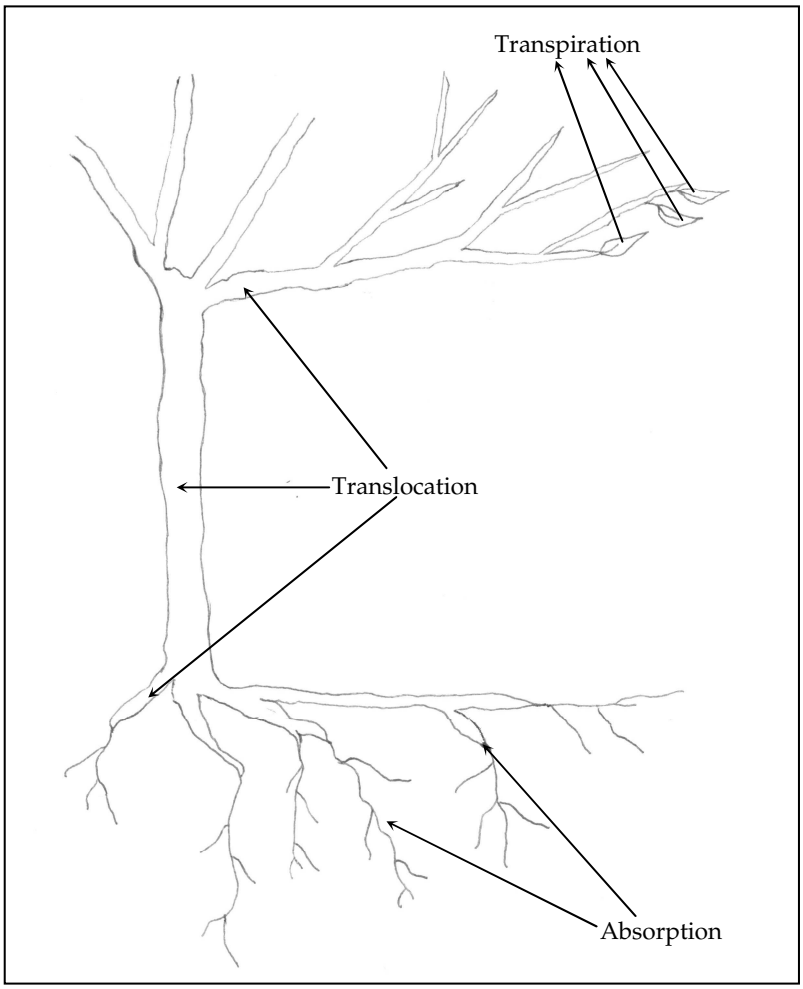

Figure A.1: The tree main physical phenomena involved in the transpiration process (modified from Dingman, 2002).

due to differences in their foliage density and canopy structure. Deciduous trees intercept different amounts of water during the growing and dormant seasons, while coniferous trees intercept almost the same amount due to their perennial foliage. Therefore the more the foliage density, the greater the amount of water intercepted. Leaf shape is an important factor driving the quantity of water stored by interception. On trees with broad leaves, the drops of rain are put together forming larger drops that overcome surface texture and fall to the soil surface. On a coniferous tree, drops are held apart on or between individual needles and do not fall so easily.

Throughfall is the rainfall that passes trough the canopy directly along spaces between leaves or by dripping from leaves, twigs and branches. Stemflow is rainfall that flows down through stems and trunks. Some water that reaches the forest floor by throughfall and stemflow passes through the litter layer to enter the mineral soil. Some of the water is intercepted by the litter layer and it is termed litter interception. Therefore, the net rainfall entering the soil is a function of gross rainfall and the process of interception.

According to Allen et al. (1996), evaporation of intercepted rainfall can be a significant portion of the water balance, especially in forests with large total leaf area and where single leaf stomatal resistances are large. Like Allen et al., Calder (1990) stated that interception may account for large losses of water which varied as function of rainfall intensity. Murakami et al. (2000) had concluded that changes in interception loss are of less impact than transpiration variations on the total evapotranspiration of forested areas.

A.1 Meteorological factors driving transpiration

Direct incident solar radiation is the primary source of energy for transpiration as well. Some of the solar radiation reaches either the surface vegetation or soil surface. Soil surfaces transmit a portion of this energy to deeper soil layers and the remaining energy is reflected and strikes the vegetation. This reflected solar radiation from the surrounding soil surface is an indirect source of energy. Advective flow of sensible heat from the adjacent areas also accounts as a source of energy available for transpiration. This available energy is dispersed by reflection to the atmosphere, convection of sensible heat and as a latent heat of transpiration. The actual radiation available to leaves is termed net radiation [R_n]

The most important role of meteorological parameters in transpiration rates is its influence on changes of R_n available at the evaporating surface (i.e. leaf) to be transformed into latent heat flux, λ. Daily changes in R_n are close correlated with daily changes in transpiration when soil water is not limiting. Daytime changes in R_n and

solar radiation (R_s) are also related to changes in transpiration rates (Allen et al., 1996). These daily and longer period variations are due to the potential amount of R_n that can reach the evaporating surface. Due to differences in the position of the sun, the potential radiation differs at various latitudes and in different seasons (Allen et al., 1998).

Available R_n is partitioned into other energy components of energy balance:

$$R_n = \lambda E + H + G \tag{A.1}$$

where G is soil sensible heat flux, and H is the sensible heat exchange with the environment by convection and advection.

For a single leaf (Tyree, 1999), the energy balance would be:

$$R_n = B + H + \lambda E \tag{A.2}$$

where B is the emittance of a single leaf. A leaf sensible heat transfer (H) occurs between the leaf surface and the surrounding air.

In both cases, partitioning of R_n is a function of the climatic factors such as air temperature (T_a), relative humidity (RH), wind velocity (u) and precipitation. These factors interact all together and generate different regional and seasonal climatic conditions creating seasonal trends of evapotranspiration.

The solar radiation absorbed by the atmosphere and the heat emitted by the earth increase the air temperature. The sensible heat of the surrounding air transfers energy to the vegetation and exerts a controlling influence on the rate of ET (Allen et al., 1996).

To illustrate, in hot, dry, and arid regions the loss of large amounts of water (if available) is due to high quantities of R_n and the desiccating power of the atmosphere.

In humid hot regions, the high humidity of the air reduces the transpiration rates independently of the high R_n available (Allen et al., 1998).

Additionally, clouds absorb and reflect upwards solar radiation and these may decrease the quantities of R_n. There is always an out of phase relationship between R_n and transpiration rates: the seasonal maximum rate of transpiration actually may follow seasonal maximum solar radiation and air temperature with several weeks (Hanson, 1991).

Authors have also stated that Vapour Pressure Deficit (VPD) together with Photosynthetic Active Radiation (PAR) determine transpiration variability (Bovard et al., 2005; Barbour and Whitehead, 2003; Oren et al., 1999; Hogg et al., 1997; Saugier et al., 1997; Meinzer et al., 1993). In fact, these two parameters are somehow related to some of the meteorological parameters mentioned above. For instance, atmosphere's concentration gradient of water vapour (VPD) is a function of wind, and at the same time, it influences transpiration rates. The concentration gradient consists on the removal of water vapour proximal to the evaporating surface, allowing to dry air to be placed over the evaporating surface and then maintain the transpiration rate.

B Angiosperms and Gymnosperms vascular structure

Wood tissues are composed of primary and secondary vascular systems. The latter vascular system (also secondary xylem, active xylem or sapwood) is located at the outermost part of the tree, after the vascular cambium. The sapwood is biologically active, having as a main function the transport of water and nutrients (sap) towards the leaves. The sapwood is formed (i.e. xylogenesis) when the vascular cambium produces new tissues by cell division and expands in a radial and tangential form. Sapwood becomes an active wood structure when its tracheary elements' cells lose their internal structures, forming empty capillaries that differ in structure and name according to their level of specialization. Gymnosperms have tracheids as conducting structures, while the conducting structures in angiosperms are vessels. In cross-section, vessels tend to be round and larger in diameter than tracheids (Aloni, 1991; Tyree and Zimmermann, 2002). Sapwood has other components such as ray parenchyma, fibres, and cells. Another unique characteristic of sapwood is the presence of starch grains stored in protoplasts (Jeffrey, 1922). Sequentially, the sapwood becomes nonfunctional, and it is incorporated in the heartwood while the cambium creates new tissues and thus new sapwood, giving place to the radial and tangential growth of the tree.

The primary vascular system (also known as primary xylem or heartwood) is located in the innermost or central part of the tree. The heartwood has mainly supporting functions, and its cells contain small concentrations of water or reserve compounds (e.g. extractives).

The major differences of these vascular systems result from tissues being composed of the same basic cells arranged into different proportions and giving a different function to every tissue (Tyree and Zimmermann, 2002; Aloni, 1991) as well as from the higher number of active vessels/tracheids always located in the sapwood area (Zimmermann and Jeje, 1981; Mauseth, 1988; Aloni, 1991; Sperry and Tyree, 1990).

C Regression analyses

Table C.1: Regression analysis, ANOVA, and unusual observations for the tree scale fitted linear regression model between $\bar{sd}$ and DBH_{OB} of White spruce.

Regression analysis

Predictor	Coefficient	SE Coefficient	T	P-value
Intercept	0.6828	0.3023	2.26	0.039
DBH_{OB}	0.08868	0.01005	8.83	<0.0001

$R^2 = 83.9\%$ $R^2_{adj} = 82.8\%$ $R^2_{pred} = 78.49\%$

$PRESS^1 = 3.8289$ $S = 0.4376$

Analysis of Variance

Source of variation	Degrees of Freedom	Sum of squares	Mean square	F_0	P-value
Regression	1	14.926	14.926	77.94	<0.0001
Residual Error	15	2.873	0.192		
Total	16	17.799			

Unusual observations

Observation	DBH_{OB}	$\bar{sd}$	Fit	SE Fit	Residual	StdRes
1	50.0	4.500	5.114	0.243	-0.614	-1.69
2	46.8	5.080	4.832	0.215	0.248	0.65
3	28.3	3.080	3.195	0.106	-0.115	-0.27
4	31.8	3.950	3.506	0.112	0.444	1.05
5	18.5	2.470	2.320	0.144	0.150	0.36
6	32.5	3.700	3.562	0.115	0.138	0.33
7	28.0	3.850	3.167	0.106	0.683	1.61
8	11.5	1.330	1.699	0.199	-0.369	-0.95
9	25.5	3.330	2.941	0.110	0.389	0.92
10	14.0	2.280	1.925	0.178	0.355	0.89

Unusual observations (cont.)

Observation	DBH_{OB}	$\bar{sd}$	Fit	SE Fit	Residual	StdRes
11	35.0	3.930	3.788	0.126	0.142	0.34
12	15.9	2.350	2.095	0.163	0.255	0.63
13	22.3	1.750	2.659	0.122	-0.909	-2.16^{R}
14	35.7	3.830	3.844	0.130	-0.014	-0.03
15	23.6	2.580	2.771	0.116	-0.191	-0.45
16	38.5	4.100	4.099	0.149	0.001	0.00
17	21.3	1.980	2.574	0.126	-0.594	-1.42

^{R} denotes an observation with a large standardized residual.

[1]

[1]Prediction Error Sum of Squares.

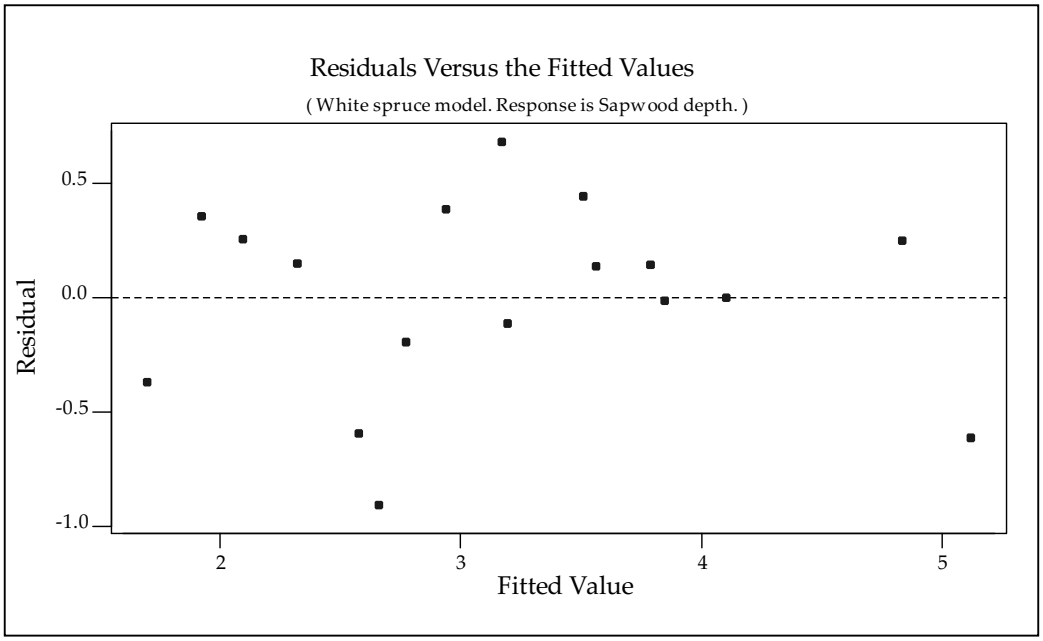
Residuals Versus the Fitted Values
(White spruce model. Response is Sapwood depth.)
Residual
0.5
0.0
-0.5
-1.0
2
3
4
5
Fitted Value

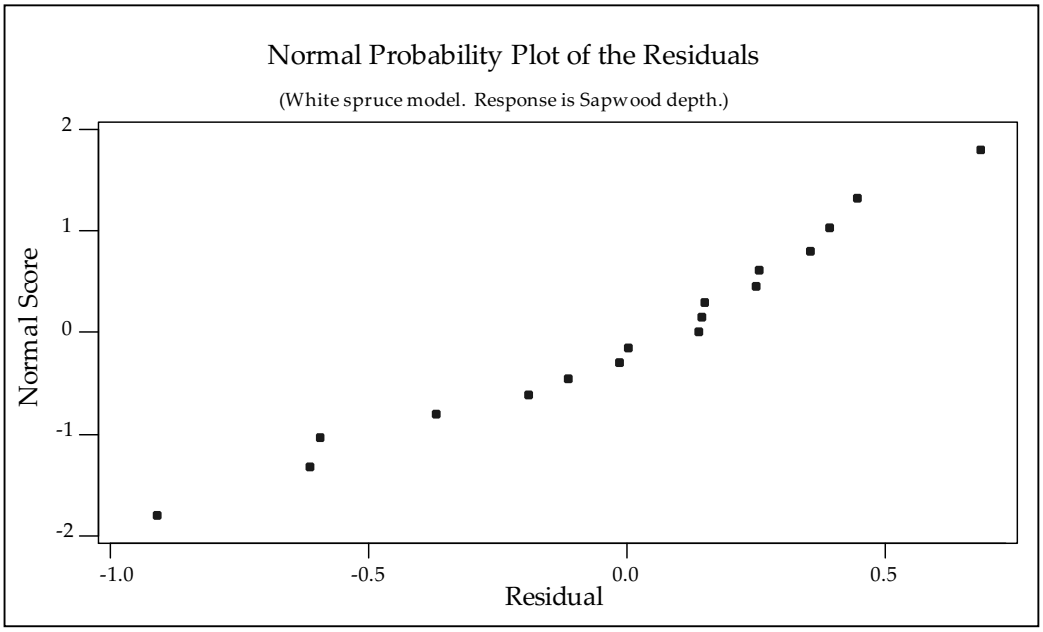
Normal Probability Plot of the Residuals
(White spruce model. Response is Sapwood depth.)
Normal Score
2
1
0
-1
-2
-1.0
-0.5
0.0
0.5
Residual

Table C.2: Regression analysis, ANOVA, and unusual observations for the tree scale fitted linear regression between SA_{plot} and LA_{plot} of Trembling aspen.

Regression analysis

Predictor	Coefficient	SE Coefficient	T	P-value
Intercept	-1.166	1.093	-1.07	0.297
DBH_{OB}	0.2441	0.04602	5.30	<0.0001

$R^2 = 54.0\%$ $R^2_{adj} = 52.0\%$ $R^2_{pred} = 45.32\%$

$PRESS = 65.46$ $S = 1.515$

Analysis of Variance

Source of variation	Degrees of Freedom	Sum of squares	Mean square	F_0	P-value
Regression	1	64.611	64.611	28.14	<0.0001
Residual Error	24	55.111	2.296		
Lack of Fit	19	51.610	2.716	3.88	0.069
Pure error	5	3.501	0.700		
Total	25	119.722			

Unusual observations

Observation	DBH_{OB}	$\bar{sd}$	Fit	SE Fit	Residual	StdRes
1	25.2	3.900	4.973	0.315	-1.073	-0.72
2	11.5	4.880	1.631	0.603	3.249	2.34^R
3	27.7	4.680	5.593	0.371	-0.913	-0.62
4	22.9	6.050	4.429	0.297	1.621	1.09
5	29.6	5.900	6.059	0.429	-0.159	-0.11
6	23.9	5.700	4.660	0.301	1.040	0.70
7	29.6	4.230	6.059	0.429	-1.829	-1.26
8	17.8	4.550	3.186	0.377	1.364	0.93
9	30.2	7.330	6.215	0.451	1.115	0.77
10	30.1	5.560	6.184	0.447	-0.624	-0.43

Unusual observations (cont.)

Observation	DBH_{OB}	$\bar{sd}$	Fit	SE Fit	Residual	StdRes
11	26.7	5.680	5.361	0.347	0.319	0.22
12	17.8	2.880	3.186	0.377	-0.306	-0.21
13	20.1	2.580	3.728	0.324	-1.148	-0.78
14	25.5	3.980	5.049	0.320	-1.069	-0.72
15	23.6	4.730	4.582	0.299	0.148	0.10
16	23.2	6.730	4.507	0.298	2.223	1.50
17	38.2	8.900	8.158	0.766	0.742	0.57^X
18	28.7	9.080	5.827	0.399	3.253	2.23^R
19	21.0	1.930	3.962	0.309	-2.032	-1.37
20	20.1	1.630	3.728	0.324	-2.098	-1.42
21	15.9	1.250	2.720	0.436	-1.470	-1.01
22	13.4	1.580	2.098	0.528	-0.518	-0.36
23	20.1	2.730	3.728	0.324	-0.998	-0.6
24	25.5	4.000	5.049	0.320	-1.049	-0.71
25	9.6	0.980	1.165	0.681	-0.185	-0.14
26	16.9	3.350	2.952	0.405	0.398	0.27

^{X} denotes an observation whose LA_{plot} value gives it large influence.
^{R} denotes an observation with a large standardized residual.

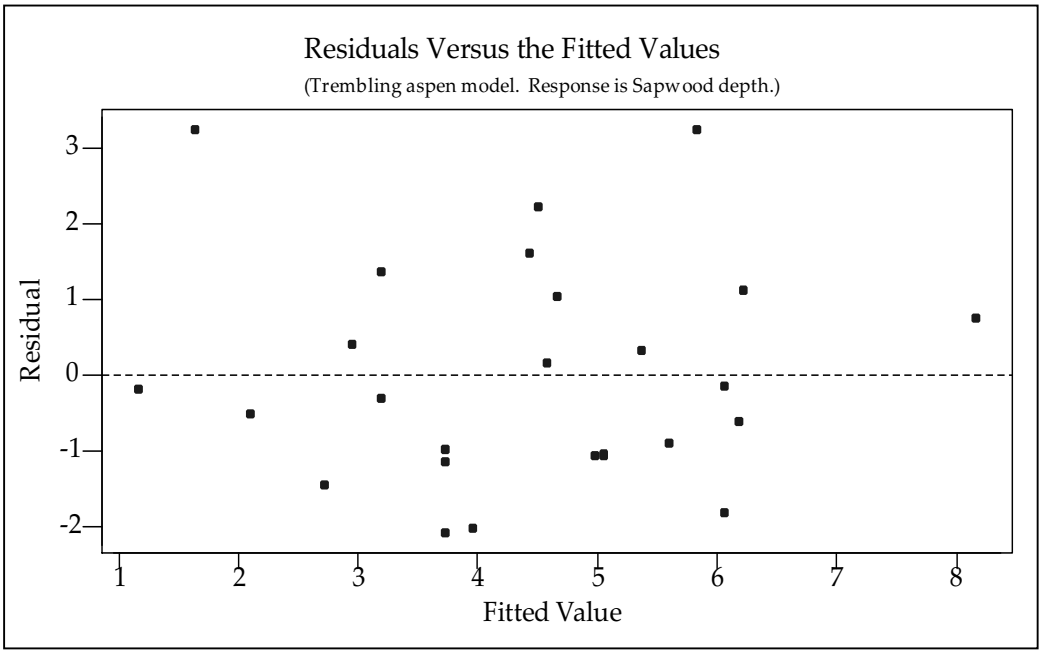
Residuals Versus the Fitted Values
(Trembling aspen model. Response is Sapwood depth.)
Residual
Fitted Value
3
2
1
0
-1
-2
1
2
3
4
5
6
7
8

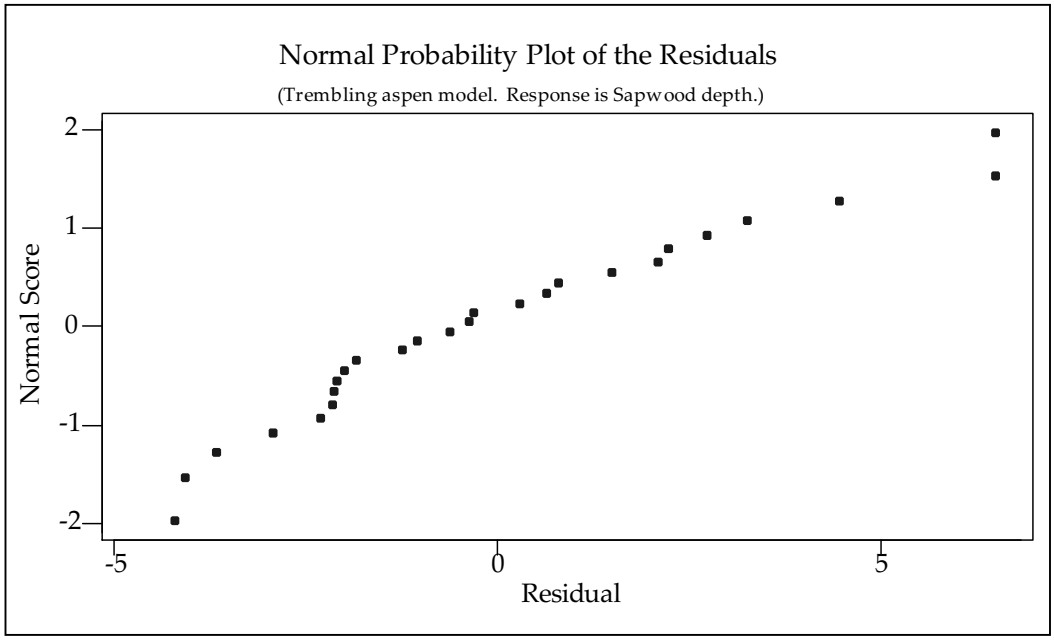
Normal Probability Plot of the Residuals
(Trembling aspen model. Response is Sapwood depth.)
Normal Score
Residual
2
1
0
-1
-2
-5
0
5

Table C.3: Regression analysis, ANOVA, and unusual observations for the first fitted linear regression between SA_{plot} and LA_{plot} of Trembling aspen.

Regression analysis

Predictor	Coefficient	SE Coefficient	T	P-value
Intercept	0.51779	0.04484	11.55	0.001
LA_{plot}	0.00078165	0.00000882	88.63	<0.0001

$R^2 = 100\%$ $R^2_{adj} = 99.9\%$ $R^2_{pred} = 98.61\%$

$PRESS = 0.7991$ $S = 0.08544$

Analysis of Variance

Source of variation	Degrees of Freedom	Sum of squares	Mean square	F_0	P-value
Regression	1	57.338	57.338	7855.07	<0.0001
Residual Error	3	0.022	0.007		
Total	4	57.360			

Unusual observations

Observation	LA_{plot}	SA_{plot}	Fit	SE Fit	Residual	StdRes
Deciduous-6	11,304.00	9.3500	9.3535	0.0853	-0.0035	-0.65^X
Deciduous-1	1,094.00	1.4200	1.3726	0.0406	0.0474	0.63
Deciduous-7	230.00	0.7000	0.6976	0.0438	0.0024	0.03
Deciduous-8	357.00	0.8700	0.7968	0.0433	0.0732	0.99
Deciduous-9	322.00	0.6500	0.7695	0.0434	-0.1195	-1.62

^{X} denotes an observation whose LA_{plot} value gives it large influence.

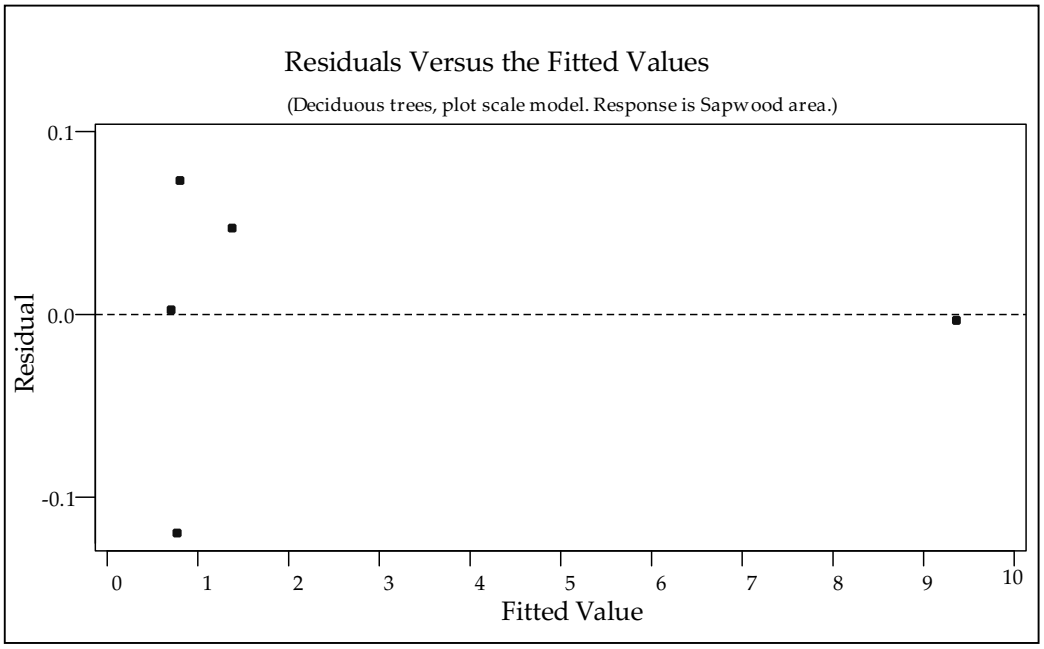
Residuals Versus the Fitted Values
(Deciduous trees, plot scale model. Response is Sapwood area.)
Residual
0.1
0.0
-0.1
0
1
2
3
4
5
6
7
8
9
10
Fitted Value

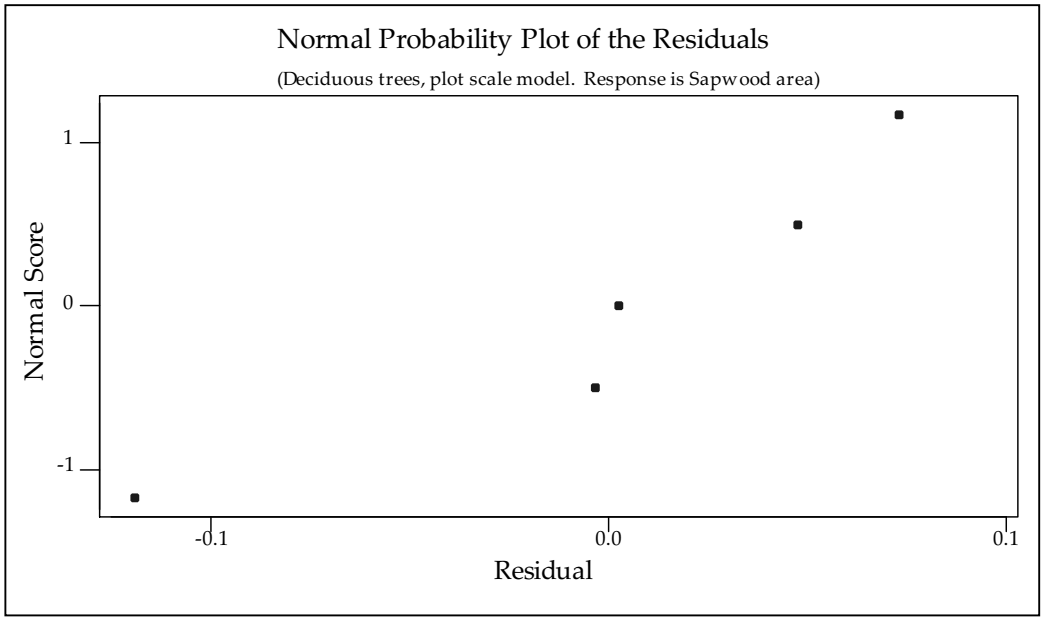
Normal Probability Plot of the Residuals
(Deciduous trees, plot scale model. Response is Sapwood area)
Normal Score
1
0
-1
-0.1
0.0
0.1
Residual

Table C.4: Regression analysis, ANOVA, and unusual observations for the second fitted linear regression between SA_{plot} and LA_{plot} of Trembling aspen. Observations from site "Deciduous-6" was removed to fit this model.

Regression analysis

Predictor	Coefficient	SE Coefficient	T	P-value
Intercept	0.47850	0.08537	5.60	0.030
LA_{plot}	0.0008619	0.0001404	6.14	0.026

$R^2 = 95.0\%$ $R^2_{adj} = 92.4\%$ $R^2_{pred} = 87.83\%$

$PRESS = 0.04544$ $S = 0.09697$

Analysis of Variance

Source of variation	Degrees of Freedom	Sum of squares	Mean square	F_0	P-value
Regression	1	0.35459	0.35459	37.71	0.026
Residual Error	2	0.01881	0.00940		
Total	3	0.37340			

Unusual observations

Observation	LA_{plot}	SA_{plot}	Fit	SE Fit	Residual	StdRes
Deciduous-1	1094	1.4200	1.4210	0.0963	-0.0010	-0.09
Deciduous-7	230	0.7000	0.6767	0.0616	0.0233	0.31
Deciduous-8	357	0.8700	0.7862	0.0525	0.0838	1.03
Deciduous-9	322	0.6500	0.7560	0.0546	-0.1060	-1.32

Table C.5: Regression analysis, ANOVA, and unusual observations for the fitted linear regression between SA_{plot} and LA_{plot} of the $10 \times 10m$ Coniferous sites.

Regression analysis

Predictor	Coefficient	SE Coefficient	T	P-value
Intercept	0.03406	0.09781	0.35	0.745
LA_{plot}	0.0003487	0.0001093	3.19	0.033

$R^2 = 71.8\%$ $R^2_{adj} = 64.7\%$ $R^2_{pred} = 38.37\%$
$PRESS = 0.00883$ $S = 0.03180$

Analysis of Variance

Source of variation	Degrees of Freedom	Sum of squares	Mean square	F_0	P-value
Regression	1	0.010289	0.010289	10.18	0.033
Residual Error	4	0.004044	0.001011		
Total	5	0.014333			

Unusual observations

Observation	LA_{plot}	SA_{plot}	Fit	SE Fit	Residual	StdRes
Conifer-1'	1035.00	0.3700	0.3949	0.0207	-0.0249	-1.03
Conifer-2'	906.00	0.3700	0.3500	0.0131	0.0200	0.69
Conifer-3'	986.00	0.4200	0.3777	0.0169	0.0423	1.57
Conifer-4'	801.00	0.2900	0.3133	0.0160	-0.0233	-0.85
Conifer-5'	677.00	0.2800	0.2699	0.0264	0.0101	0.57
Conifer10'	918.00	0.3300	0.3541	0.0134	-0.0241	-0.84

No evidence of lack of fit (P > 0.1).

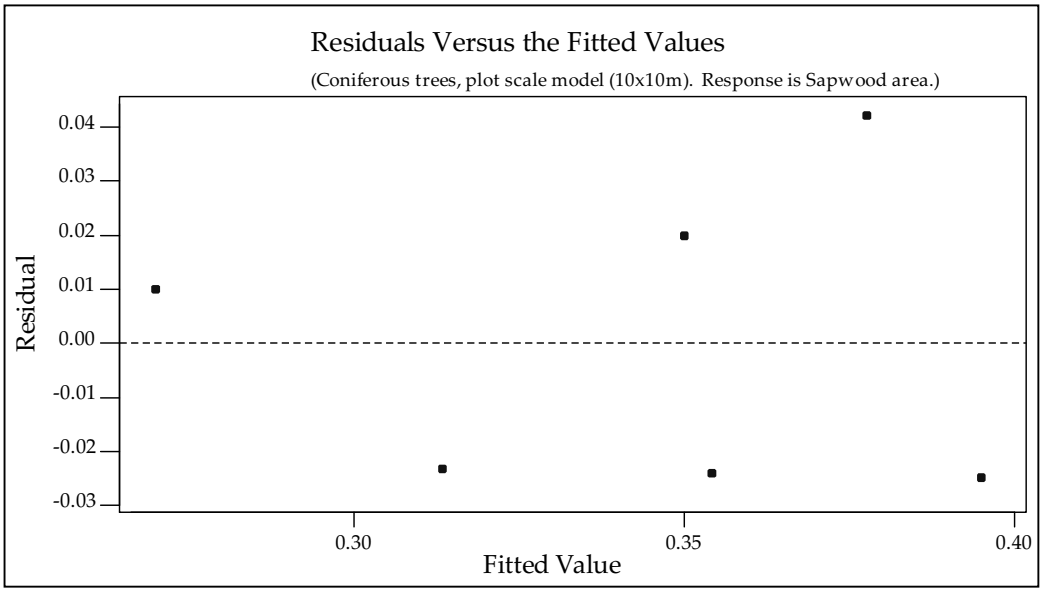
Residuals Versus the Fitted Values
(Coniferous trees, plot scale model (10x10m). Response is Sapwood area.)
Residual
0.04
0.03
0.02
0.01
0.00
-0.01
-0.02
-0.03
0.30
0.35
0.40
Fitted Value

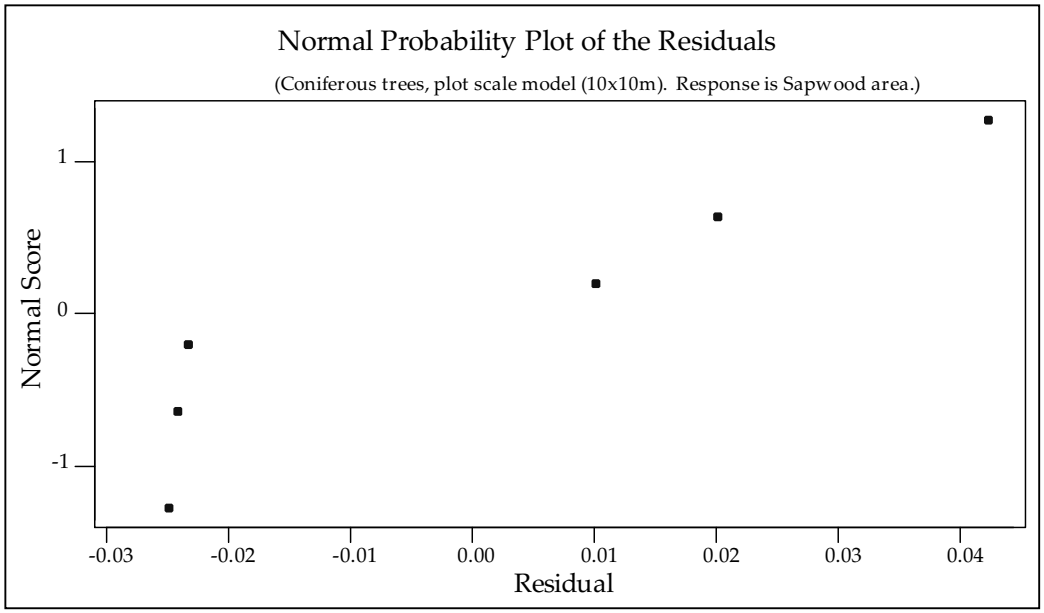
Normal Probability Plot of the Residuals
(Coniferous trees, plot scale model (10x10m). Response is Sapwood area.)
Normal Score
1
0
-1
-0.03
-0.02
-0.01
0.00
0.01
0.02
0.03
0.04
Residual

Table C.6: Regression analysis, ANOVA, and unusual observations for fitted linear regression between SA_{plot} and LA_{plot} of the Coniferous $60 \times 60m$ plots.

Regression analysis

Predictor	Coefficient	SE Coefficient	T	P-value
Intercept	1.1102	0.5408	2.05	0.176
LA_{plot}	0.00031169	0.00004786	6.51	0.023

$R^2 = 95.5\%$ $R^2_{adj} = 93.20\%$ $R^2_{pred} = 68.60\%$
$PRESS = 7.77693$ $S = 0.7468$

Analysis of Variance

Source of variation	Degrees of Freedom	Sum of squares	Mean square	F_0	P-value
Regression	1	23.655	23.655	42.41	0.023
Residual Error	2	1.115	0.558		
Total	3	24.770			

Unusual observations

Observation	LA_{plot}	SA_{plot}	Fit	SE Fit	Residual	StdRes
Conifer-4	20556	7.790	7.517	0.701	0.273	1.05
Conifer-5	9144	3.280	3.960	0.376	-0.680	-1.05
Conifer-11	1503	2.280	1.579	0.491	0.701	1.25
Conifer-12	1487	1.280	1.574	0.492	-0.294	-0.52

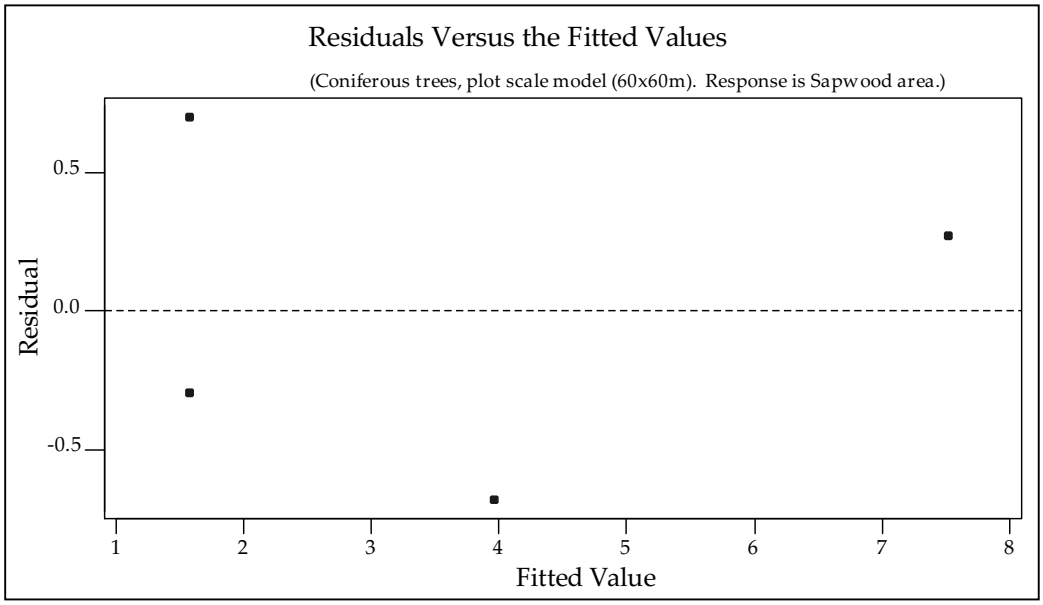
Residuals Versus the Fitted Values
(Coniferous trees, plot scale model (60x60m). Response is Sapwood area.)
Residual
0.5
0.0
-0.5
1
2
3
4
5
6
7
8
Fitted Value

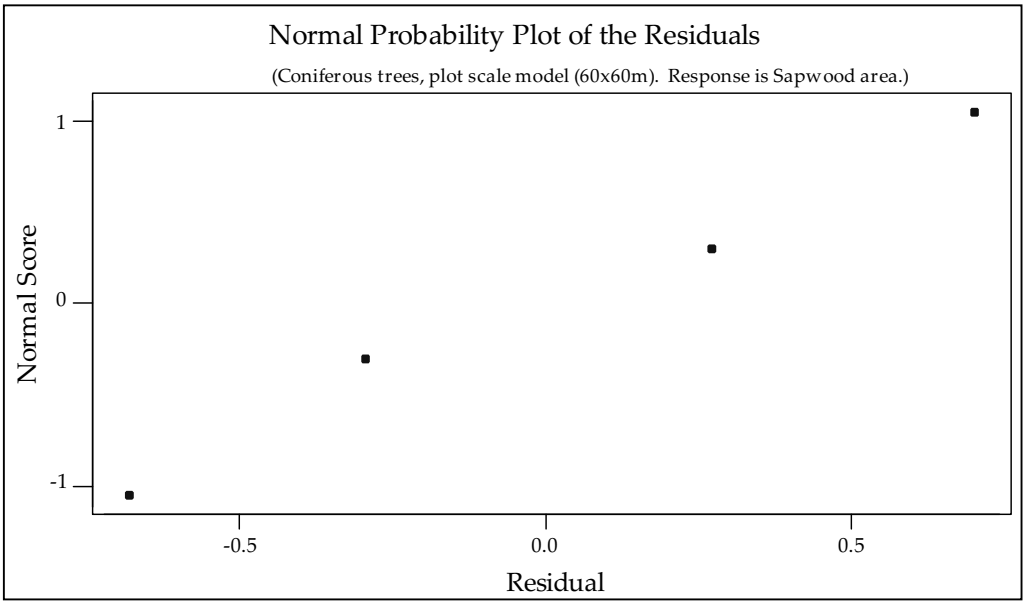
Normal Probability Plot of the Residuals
(Coniferous trees, plot scale model (60x60m). Response is Sapwood area.)
Normal Score
1
0
-1
-0.5
0.0
0.5
Residual

Bibliography

Allen, R. G., Jensen, M. E., Wright, J. L., and Burman, R. D. (1989). Operation estimates of reference evapotranspiration. *Agronomy Journal*, 81:650–662.

Allen, R. G., Pereira, L. S., Raes, D., and Smith, M. (1998). *Crop evapotranspiration. Guidelines for computing crop water requirements. FAO Irrigation and drainage paper 56.* FAO - Food and Agriculture Organization of the United Nations, Rome.

Allen, R. G., Pruitt, W. O., Businger, J. A., Fritschen, L. J., Jensen, M. E., and Quinn, F. H. (1996). Evaporation and transpiration. In Heggen, R. J., editor, *Hydrology Handbook. ASCE Manuals and Reports on Engineering Practice No. 28*, chapter 4. ASCE, New York, USA, second edition.

Aloni, R. (1991). *Wood formation in deciduous hardwood trees. In: Physiology of Trees*, chapter 8. John Wiley & Sons, Inc., USA.

Aloni, R., Alexander, J. D., and Tyree, M. T. (1997). Natural and experimentally altered hydraulic architecture of branch junctions in *Acer saccarum* Marsh, and *Quercus velutina* Lam. trees. *Trees*, 11:255–264.

AltaLIS, L. (2006). Digital base features. AltaLIS Ltd., Provincial Government GIS.

Archibald, J. H., Klappstein, G. D., and Corns, I. G. W. (1996). Field guide to ecosites of Southwestern Alberta. Special Report 8, Canadian Forest Service,Northwest Region, Northern Forestry Centre, Edmonton, Alberta. Canada-Alberta partnership agreement in Forestry funds.

Auslander, M., Nevo, E., and Inbar, M. (2003). The effects of slope orientation on plant growth, developmental instability and susceptibility to herbivores. *Journal of Arid Environments*, 2003(55):402–416.

Baldocchi, D. D. and Vogel, C. A. (1996). Energy and CO_2 flux densities above and below the temperature broad-leaved forest and a boreal pine forest. *Tree physiology*, 16:5–16.

Barbour, M. M., Hunt, J. E., Walcroft, A. S., Rogers, G. N. D., McSeveny, T. M., and Whitehead, D. (2005). Components of ecosystem evaporation in a temperate coniferous rainforest, with canopy transpiration scaled using sapwood density. *New Phytologist*, 165:549–558.

Barbour, M. M. and Whitehead, D. (2003). A demonstration of the theoretical prediction that sap velocity is related to wood density in the conifer *Dacrydium cupress-*

inum. *New Phytologist*, 158:477–488.

Bavel, C. H. M. V. (1966). Potential evaporation: the combination concept and its experimental verification. *Water Research Resources*, 2:455–467.

Baynes, J. and Dunn, G. M. (1997). Estimating foliage surface area index in 8-year-old stands of *Pinus elliottii* var. *elliottii* x *Pinus caribaea* var. *hondurensis* of variable quality. *Canadian Journal of Forest Research*, 27:1367–1375.

Biftu, G. F. and Gan, T. Y. (2001). Assessment of evapotranspiration models applied to a watershed of Canadian prairies with mixed land use. In Canadian Society for Civil Engineering, editor, *15th Canadian Hydrotechnical Conference of the Canadian Society for Civil Engineering*, Hydrotechnical, Victoria, British Columbia. Canadian Society for Civil Engineering, Canadian Society for Civil Engineering.

Binkley, D. and Reid, P. (1984). Long-term responses of stem growth and leaf area to thinning and fertilization in a Douglas-fir plantation. *Canadian Journal of Forest Research*, 15:1181–1184.

Black, T. A., Kelliher, F. M., Wallace, J. S., Stewart, J. B., Monteith, J. L., and Jarvis, P. G. (1989). Processes controlling understorey evapotranspiration. *Philosophical Transactions of the Royal Society of London. Series B. Biological Sciences*, 324(1223):207–231. Forest, Weather and Climate.

Bladon, K., Silins, U., Landhäuser, S. M., and Lieffers, V. J. (2006). Differential transpiration by three boreal species in response to increased evaporative demand after variable retention harvesting. *Agricultural and Forest Meteorology*. in print.

Blanche, C. A., Hodges, J. D., and Nebeker, T. E. (1985). A leaf area-sapwood area ratio developed to rate loblolly pine tree vigor. *Canadian Journal of Forest Research*, 15:1181–1184.

Blanken, P. D., Black, T. A., Yang, P. C., Newmann, H. H., Nesic, Z., Staebler, R., de Hartog, G., Novak, M. D., and Lee, X. (1997). Energy balance and canopy conductance of a boreal aspen forest: partitioning overstory and understory components. *Journal of Geophysical Research*, 102(D24):28915–28927.

Booker, R. E. (1984). Dye-flow apparatus to measure the variation in axial xylem permeability over a stem cross section. *Plant, Cell and Environment*, 7:623–628.

Borghetti, M., Vendramin, G. G., and Giannini, R. (1986). Specific leaf area and leaf area index distribution in a young Douglas-fir plantation. *Canadian Journal of Forest Research*, 16:1283–1288.

Bovard, B. D., Curtis, P. S., Vogel, C. S., Su, H. B., and Schmid, P. (2005). Environmental controls on sap flow in a northern hardwood forest. *Tree Physiology*, 25:31–38.

Brutsaert, W. H. (1982). *Evaporation into the atmosphere: theory, history, and applications*. Dordrecht, the Netherlands : Reidel, 1982., first edition.

Buermann, W., Wang, Y., Dong, J., Zhou, L., Zeng, X., Dickinson, R. E., Potter, C. S., and Myneni, R. B. (2002). Analysis of a multiyear global vegetation leaf area index data set. *Journal of Geophysical Research*, 107(D22):4646–4662.

Burns, R. M. and Honkala, B. H. (1990a). *Silvics of North America: Conifers. Agriculture handbook, 654*, volume 1. U.S. Department of Agriculture, Forest Service,, Washington, DC. 1383 pages.

Burns, R. M. and Honkala, B. H. (1990b). *Silvics of North America: Hardwoods. Agriculture handbook, 654*, volume 2. U.S. Department of Agriculture, Forest Service,, Washington, DC. 1711 pages.

Bussières, N. and Granger, R. (2000). Evapotranspiration and energy balance components from AVHRR. In Strong, G., editor, *The Mackenzie basin climate and water resources: understanding the past and predicting the future The Mackenzie GEWEX Study (MAGS), Phase 1. Final Reports and Proceedings of the 6th Scientific Workshop*, pages 251–257, Saskatoon, Saskatchewan.

Calder, I. R. (1990). *Evaporation in the uplands*. John Wiley & Sons, Ltd.

Calder, I. R. (1992). Deuterium tracing for the estimation of transpiration from trees. pat 2. estimation of transpiration parameters using a time-averaged deuterium tracing method. *Journal of Hydrology*, 130:27–35.

Calder, I. R., Narayanswamy, M., Srinivasalu, N., Darling, W., and Lardner, A. (1986). Investigation into the use of deuterium as a tracer for measuring transpiration from eucalyptus. *Journal of Hydrology*, 84:345–351.

Caselles, V., Artigao, M. M., Hurtado, E., Coll, C., and Brasa, A. (1998). Mapping actual evapotranspiration by combining Landsat TM and NOAA-AVHRR images: Application to the Barrax Area, Albacete, Spain. *Remote Sensing of Environment*, 63:1–10.

Čermák, J. (1989). Solar equivalent leaf area: an efficient biometrical parameter of individual leaves, trees and stands. *Tree physiology*, 5:269–289.

Čermák, J. (1998). Leaf distribution in large trees and stands of the floodplain forests in southern moravia. *Tree Physiology*, 18:727–737.

Čermák, J., Cienciala, E., Kučcera, J., Lindroth, A., and Bednářová, E. (1995). Individual variation of sap-flow rate in large pine and spruce trees and stand transpiration: a pilot study at the central NOPEX site. *Journal of Hydrology*, 168:17–27.

Čermák, J., Kučcera, J., and Nadezhdina, N. (2004). Sap flow measurements with some thermodynamic methods, flow integration within trees and scaling up from sample trees to entire forest stands. *Trees*, 18:529–546.

Čermák, J. and Nadezhdina, N. (1998). Sapwood as the scaling parameter defining according to xylem water content or radial pattern of sap flow? *Annales des Sciences Forestières*, 55:509–521.

Chang, M. (2002). Forests and vaporization. In Chang, M., editor, *Forest Hydrology. An introduction to water and forests*, chapter 9, pages 151–174. CRC Press LLC, Boca Ratón, USA, first edition.

Chapra, S. C. and Canale, R. P. (1988). *Numerical Methods for Engineers*. McGraw Hill, Inc., second edition.

Chen, J. M. and Black, T. A. (1992). Defining leaf area index for non-flat leaves. *Plant, Cell and Environment*, 15:421–429.

Chen, J. M. and Cihlar, J. (1996). Retrieving Leaf Area Index of boreal conifer forests using Landsat TM images. *Remote Sensing of Environment*, 55(2):153–162.

Chen, J. M., Rich, P. M., Gower, S. T., Norman, J. M., and Plummer, S. (1997). Leaf area index of boreal forests: Theory, techniques, and measurements. *Journal of Geophysical Research*, 102(D24):29,429–29,443.

Chen, J. M. and Zhang, R.-H. (1989). Studies on the measurements of crop emissivity and sky temperature. *Agricultural and Forest Meteorology*, 49:23–34.

Choudhury, B. J. (1989). Estimating evaporation and carbon assimilation using infrared temperature data: vistas in modeling. In Asrar, G., editor, *Theory and applications of optical remote sensing*, Remote Sensing Series, chapter 17, pages 628–. John Wiley & Sons, first edition.

Cienciala, E., Kučera, J., and Malmer, A. (2000). Tree sap flow and stand transpiration of two *Acacia mangium* plantations in Sabah, Borneo. *Journal of Hydrology*, 236:109–120.

Cienciala, E., Kučera, J., Lindroth, A., Cěrmák, J., Grelle, A., and Halldin, S. (1997). Canopy transpiration from a boreal forest in Sweden during a dry year. *Agricultural and Forest Meteorology*, 86:157–167.

Cienciala, E., Mellander, P. E., Kucera, J., Oplustilova, M., Ottosson-Lofvenius, M., and Bishop, K. (2002). The effect of a north-facing forest edge on tree water use in a boreal Scots pine stand. *Canadian Journal of Forest Research*, 32:693–702.

Cohen, Y., Kelliher, F. M., and Black, T. A. (1985). Determination of sap flow in Douglas-fir trees using the heat pulse technique. *Canadian Journal of Forest Research*, 15:422–428.

Coyea, M. R. and Margolis, H. A. (1992). Factors affecting the relationship between sapwood area and leaf area of balsam fir. *Canadian Journal of Forest Research*, 22:1684–1693.

De Bruin, H. A. R. and Moore, C. J. (1985). Zero-plane displacement an roughness length fir tall vegetation, derived from a simple mass conservation hypothesis. *Boundary-Layer Meteorology*, 31:39–49.

Dean, T. J. and Long, J. N. (1986). Variation in sapwood area-leaf area relations within two stands of Lodgepole pine. *Forest Science*, 32:749–758.

Dean, T. J., Long, J. N., and Smith, F. W. (1988). Bias in leaf area-sapwood area ratios and its impact on growth analysis in *Pinus contorta*. *Trees Journal*, 2:104–109.

Delzon, S., Sartore, M., Burlett, R., Dewar, R., and Loustau, D. (2004). Hydraulic responses to height growth in maritime pine trees. *Plant, Cell and Environment*, 2004(27):1077–1087.

Denmead, O. T. (1984). Plant physiological methods for studying evapotranspiration: problems of telling the forest from the trees. *Agricultural Water Management*, 8:167–189.

Dias, M. A. F. S., Rutledge, S., Kabat, P., Dias, P. L. S., Nobre, C., Fisch, G., Dolman, A. J., Zipser, E., Garstang, M., Manzi, A. O., Fuentes, J. D., Rocha, H. R., Marengo, J., Plana-Fattori, A., Sá, L. D. A., Alvalá, R. C. S., Andreae, M. O., Artaxo, P., Gielow, R., and Gatti, L. (2002). Cloud and rain processes in a bioshpere-atmosphere interaction context in the Amazon region. *Journal of Geophysical Research*, 107(D20):8072–8092.

Dingman, S. L. (2002). *Physical Hydrology*. Prentice-Hall, Inc., Upper Saddle River, New Jersey 07458, second edition.

Dooge, J. C. I. (1988). Modelling the behaviour of water. In Reynolds, E. R. C. and Thompson, F. B., editors, *Forests, Climate, and Hydrology. Regional impacts.*, chapter 7, page 227. The United Nations University, Kefford Press, Singapore, first edition.

Dugas, W. A. (1990). Sap flow in stems. In Goel, N. S. and Norman, J. M., editors, *Instrumentation for studying vegetation canopies for remote sensing in optical and thermal infrared regions*, number 1 in Remote Sensing Reviews, 225-236 14. Harwood Academic.

Dunne, T. and Leopold, L. B. (1998). *Water in environmental planning*. Freeman and Company Publishers, New York, USA, fifteenth edition.

EC (2006). Canadian climate normals 1971-2000. Report, Environment Canada, Canada.

Eckmüllner, O. and Sterba, H. (2000). Crown condition, needle mass, and sapwood area relationships of Norway spruce (*Picea abies*). *Canadian Journal of Forest Research*, 30:1646–1654.

Elliot-Frisk, D. L. (1988). The boreal forest. In Barbour, M. G. and Billings, W. D., editors, *North American Terrestrial Vegetation*, chapter 2, pages 33–62. Cambridge University Press, New York, first edition.

Farrar, J. L. (2003). *Trees in Canada*. Fitzhenry & Whiteside Limited, Markham, Ontario, eight edition.

Ford, C. R., Mcguire, M. A., Mitchell, R. J., and Teskey, R. O. (2004). Assessing variation in the radial profile of sap flux density in *Pinus* species and its effect on

daily water use. *Tree Physiology*, 24:241–249.

Gartner, B. (2002). Sapwood and inner bark quantities in relation to leaf area and wood density in Douglas-fir. *IAWA Journal*, 23(3):267–285.

Gedney, N. and Valdes, P. J. (2000). The effect of Amazonian deforestation on the Northern Hemisphere circulation and climate. *Geophysical Research Letters*, 27(19):30253–3056.

Gilmore, W. D., Seymour, S. R., and Maguire, A. (1996). Foliage-sapwood area relationships for *Abies balsamea* in Central Maine, USA. *Canadian Journal of Forest Research*, 26:2071–2079.

Goldstein, G., Andrade, J. L., Meinzer, F. C., Holbrook, N. M., Cavelier, J., Jackson, P., and Celis, A. (1998). Stem water storage and diurnal patterns of water use in tropical forest canopy trees. *Plant, Cell and Environment*, 21:397–406.

Granger, R. J. (1997). Comparison of surface and satellite-derived estimates of evapotranspiration using a feedback algorithm. In *Proceedings of the Third International workshop on the applications of Remotes Sensing Hydrology*, pages 71–81. NASA Goddard Space Center, NASA Goddard Space Center.

Granger, R. J. (2000). Satellite-derived estimates of evapotranspiration in the Gediz basin. *Journal of Hydrology*, 229(1-2):70–76.

Granier, A. (1985). Une nouvelle méthode pour la mesure du flux de sève brute dans le tronc des arbres. *Annales des Sciences Forestières*, 42:193–200.

Granier, A., Anfondillo, T., Sabatti, M., Cochard, H., Dreyer, E., Tomasi, M., Valentini, R., and Bréda, N. (1994). Axial and radial water flow in the trunks of oak trees: a quantitative and qualitative analysis. *Tree Physiology*, 14:1383–1396.

Granier, A., Aubinet, M., Epron, D., Falge, E., Gudmundsson, J., Jensen, N. O., Köstner, B., Matteucci, G., Pilegaard, K., Schmidt, M., and Tenhunen, J. (2003). Deciduous forests: carbon and water fluxes, balances and ecophysiological determinants. In Valentini, R., editor, *Fluxes of carbon, water and energy of European forests (Ecological Studies Vol. 163)*, pages 55–70. Springer, Berlin, Heidelberg, New York.

Granier, A., Biron, P., and Lemoine, D. (2000). Water balance, transpiration and canopy conductance in two beech stands. *Agricultural and Forest Meteorology*, 100:291–308.

Granier, A., Bobay, V., Gash, J. H. C., Gelpe, J., Saugier, B., and Shuttleworth, W. J. (1990). Vapour flux density and transpiration rate comparisons in a stand of Maritime pine (*Pinus pinaster* Ait) in Les Landes forest. *Agricultural and Forest Meteorology*, 51:309–319.

Granier, A., Huc, R., and Barigah, S. T. (1996). Transpiration of natural rain forest and its dependence on climatic factors. *Agricultural and Forest Meteorology*, 78:19–29.

Green, S. R., Mcnaughton, K. G., and Clothier, B. E. (1989). Observations of night-

time water use in kiwifruit vines and apple trees. *Agricultural and Forest Meteorology*, 48:251–261. 4.

Greenlee, G. M. (1973). Soils map of Bow Valley Provincial Park and adjacent Kananaskis area. Soils map, Alberta Research Council. Soils Division. Alberta Institute of Pedology, Edmonton, Alberta.

Greenlee, G. M. (1976). Soil survey of Kananaskis Lakes area and interpretation for recreational use. Final Report M-76-1, Alberta Research Council. Soils Division. Alberta Institute of Pedology, Edmonton, Alberta. Includes soils and landform maps of the studied areas.

Hacke, U. G., Sperry, J. S., and Pittermann, J. (2004). Analysis of circular bordered pit function II. Gymnosperm tracheids with torus-margo pit membranes. *American Journal of Botany*, 91(3):386–400.

Ham, J. M., Heilman, J. L., and Lascano, R. J. (1990). Determination of soil water evaporation and transpiration from energy balance and stem flow measurements. *Agricultural and Forest Meteorology*, 52:287–301.

Hanson, R. L. (1991). Evaporation and droughts. In Paulson, R. W., Chase, E. B., Roberts, R. S., and Moody, D. W., editors, *National Water Summary 1988-898-Hydrologic Events and Floods and Droughts: U.S. Geological Survey Water-Supply. Paper 2375*, pages 99–104. U.S. Geological Survey.

Hasager, C. B. and Jensen, N. O. (2001). Scaling-up evapotranspiration from field to regional scale based on optical remote sensing scenes. In IAHS, Publication, ., editor, *Remote Sensing and Hydrology 2000. Proceedings of a symposium held at Santa Fe, New Mexico, USA*, number 267, pages 292–295.

Hasager, C. B., Jensen, N. O., Pilegaard, K., and Boegh, E. (2003). MODIS and Landsat TM scaling study on the evapotranspiration at mid-latitude. In *International Geoscience and Remote Sensing Symposium. IGARSS '03. Proceedings. 2003 IEEE International*, number 5, pages 3335 – 3337. IEEE, IEEE.

Henderson-Sellers, A. and Wilson, M. F. (1983). Surface albedo data for climatic modeling. *Reviews of Geophysics and Space Physics*, 21(8):1743–1778.

Hillis, W. E. (1987). *Heartwood and Tree Exudates*. Series in Wood Science. Springer, Berlin. ISBN 3-540-17593-8.

Hipps, L. and Kustas, W. (2000). Patterns and organization in evaporation. In Grayson, R. and Blöshcl, G., editors, *Spatial Patterns in Catchment Hydrology*, pages 105–122. Cambridge University Press, United Kingdom, first edition.

Hogg, E. H., T, A. B., den Hartog, G., Newmann, H. H., Zimmermann, R., Blanken, P. A. H. P. D., Nesic, Z., Paul C, Y., Staebler, R. M., McDonald, K. C., and Oren, R. (1997). A comparison of sap flow and eddy fluxes of water vapor from a boreal deciduous forest. *Journal of Geophysical Research*, 102(D24):28929–28937.

Hungerford, R. D. (1987). Estimation of foliage area in dense Montane Lodgepole pine stands. *Canadian Journal of Forest Research*, 17:320–324.

Husch, B., Miller, C. I., and Beers, T. W. (1972). *Forest mensuration*. The Ronald Press Company, New York, USA, second edition.

IPCC (2001). Climate Change 2001:The Scientific basis. In Houghton, J. T., Ding, Y., Griggs, D. J., Noguer, M., van der Linden, P. J., Dai, X., Maskell, K., and Johnson, C. A., editors, *Contribution of working Group I to the third assessment report of the Intergovernmental Panel on Climate Change*, Scientific assessment, Cambridge, UK. Intergovernmental Panel on Climate Change, Cambridge University Press.

James, S. A., Clearwater, M. J., Meinzer, F. C., and Goldstein, G. (2002). Heat dissipation sensors of variable length for the measurement of sap flow in trees with deep sapwood. *Tree physiology*, 22:277–283.

Jarvis, P. G., James, G. B., and Landsberg, J. J. (1976). Coniferous forest. In Monteith, J. L., editor, *Vegetation and the Atmosphere*, chapter 7, pages 171–240. Academic Press Inc., New York, first edition.

Jeffrey, E. D. (1922). *The anatomy of woody plants*. . The University of Chicago Press, Chicago Illinois, USA, second edition.

Jeremic, D., Cooper, P., and Srinivasan, U. (2004). Comparative analysis of Balsam fir wetwood, heartwood and sapwood properties. *Canadian Journal of Forest Research*, 34:1241–1250.

Jiménez, M. S., Čermák, J., Kučcera, J., and Morales, D. (1996). Laurel forests in Tenerife, Canary Islands: the annual course of sap flow in *Laurus* trees and stand. *Journal of Hydrology*, 183:307–321.

Jonckheere, I., Fleck, S., Nackaerts, K., Muysa, B., Coppin, P., Weiss, M., and Baret, F. (2004). Review of methods for in situ leaf area index determination. Part I. Theories, sensors and hemispherical photography. *Agricultural and Forest Meteorology*, 121(1-2):19–35.

Jones (1997). Preliminary spatially distributed estimates of evapotranspiration using in-situ and satellite remote sensing data. In USGS, editor, *Proceedings of the Technical Symposium in Ft. Lauderdale, Florida*, number Open file report 97-385 in Proceedings. United States Geological Survey, USGS. Last date URL accessed: September 27, 2006.

Kakane, V. C. K. (1998). *Measurement of evapotranspiration by the Bowen ratio energy balance method and the investigation of evapotranspiration NDVI relations.* PhD thesis, University of Ghana.

Kant, Y. and Badarinath, K. V. S. (1998). Regional scale evapotranspiration estimation using satellite derived albedo and surface temperature. *Journal of the Indian Society of Remote Sensing*, 26(3):129–134.

Kaufmann, M. R. and Kelliher, F. M. (1991). Estimating tree transpiration rates in forest stands. In Lassoie, J. P. and Hinckley, T. M., editors, *Techniques and approaches in Forest tree Ecophysiology*, pages 117–140. CRC Press, Boca Raton, Florida, USA.

Kaufmann, M. R. and Troendle, C. A. (1981). The relationship of leaf area and foliage biomass to sapwood conducting area in four Subalpine forest tree species. *Forest Science*, 27(3):477–482.

Keane, M. G. and Weetman, G. F. (1987). Leaf area-sapwood cross-sectional area relationships in repressed stands of lodgepole pine. *Canadian Journal of Forest Research*, 17:205–209.

Kite, G., Granger, R., and Jayasinghe, G. (2001). Evapotranspiration at the basin scales estimated from satellite data and by a hydrological model. In IAHS, Publication, ., editor, *Remote Sensing and Hydrology 2000. Proceedings of a symposium held at Santa Fe, New Mexico, USA*, number 267, pages 265–270.

Kondoh, A. and Higuchi, A. (2001). Relationship between satellite-derived spectral brightness and evapotranspiration from a grassland. *Hydrological processes*, 15:1761–1770.

Kondratyev, K. Y., Korzov, V. I., Mukhenberg, V. V., and Dyachenko, L. N. (1982). The shortwave albedo and the surface emissivity. In Eagleson, P. S., editor, *Land surface processes in atmospheric general circulation models*, pages 463–514, Greenbelt, Maryland. WMO/ICSO Joint Scientific Committee, Cambridge University Press. Papers presented at the world climate research programme study Conference.

Köstner, B. (2001). Evaporation and transpiration from forests in Central Europe, relevance of patch-level studies for spatial scaling. *Meteorology and Atmospheric Physics*, 76:69–82.

Kozlowski, T. T. and Pallardy, S. G. (1997). *Physiology of woody plants*. Academic Press, Inc., USA, second edition.

Kramer, P. J. (1969). *Plant and soil water relationships: a modern synthesis*. Organismic Biology. McGraw-Hill Book Company, USA, first edition.

Kramer, P. J. and Boyer, J. S. (1995). *Water relations of plants and soils*. Academic Press Inc., San Diego, USA.

Kramer, P. J. and Kozlowski, T. T. (1979). *Physiology of woody plants*. Academic Press Inc., 111 Fifth Avenue, New York, New York, first edition.

Kumagai, T., Aoki, S., Nagasawa, H., Mabuchi, T., Kubota, K., Inoue, S., Utsumi, Y., and Otsuki, K. (2005). Effects of tree-to-tree and radial variations on sap flow estimates of transpiration in Japanese cedar. *Agricultural and Forest Meteorology*. In Press.

Kumagai, T., Saitoh, T. M., Sato, Y., Morooka, T., Manfroi, O. J., Kuraji, K., and

Suzuki, M. (2004). Transpiration, canopy conductance and the decoupling coefficient of a lowland mixed dipterocarp forest in Sarawak, Borneo: dry spell effect. *Journal of Hydrology*, 287:237–251.

Kustas, W. P., Albertsons, J. D., Scanlon, T. M., and Cahill, A. T. (2001). Issues in monitoring evapotranspiration with radiometric temperature observations. In IAHS, Publication, ., editor, *Remote Sensing and Hydrology 2000. Proceedings of a symposium held at Santa Fe, New Mexico, USA*, number 267, pages 239–245.

Lassen, L. E. and Okkonen, E. A. (1969). Sapwood thickness of douglas-fir and five other western softwoods. *Research Article PNW- Article FPL-124*, page 16p.

Leblanc, S. G., Chen, J. M., and Kwong, M. (2002). *Tracing Radiation and Architecture of Canopies. TRAC manual version 2.1.3*. Natural Resources Canada, Natural Resources Canada, Canada Centre for Remote Sensing; 588 Booth Street, Ottawa, Ontario Canada, K1A 0Y7., first edition.

Lefsky, M. A., Cohen, W. B., Acker, S. A., Parker, G. G., Spies, T. A., and Harding, D. (1999). Lidar remote sensing of the canopy structure and biophysical properties of Douglas-fir Western Hemlock forests. *Remote Sensing of Environment*, 70:339–361.

Liu, J., Chen, J. M., and Cihlar, J. (2003). Mapping evapotranspiration based on remote sensing: an application to Canada's landmass. *Water Resources Research*, 39(7):1189–1203.

Liu, J., Chen, J. M., Cihlar, J., and Park, W. M. (1997). A Process-Based Boreal Ecosystem Productivity Simulator Using Remote Sensing Inputs. *Remote Sensing of Environment*, 62(2):158–175.

López, B. C., Sabaté, S., Gracia, C. A., and Rodríguez, R. (2005). Wood anatomy, description of annual rings, and responses to ENSO events of *Prosopis pallida* H.B.K., a wide-spread woody plant of arid and semi-arid lands of Latin America. *Journal of Arid Environments*, 61:541–554.

Loustau, D., Berbigier, P., Roumagnac, P., Arruda-Pacheco, C., David, J. S., Ferreira, M. I., Pereira, J. S., and Tavares, R. (1996). Transpiration of 64-year-old maritime pine stand in Portugal. *Oecologia*, 107:33–42.

Lowe, P. R. (1977). An approximating polynomial for the computation of saturation vapour pressure. *Journal of Applied Meteorology*, 16:100–103.

MADGIC (2006). GEODE. Alberta Digital Elevation Models for the 11 NTS. GIS Resources, University of Calgary.

Marc, V. and Robinson, M. (2004). Application of the deuterium tracing method for the estimation of tree sap flow and stand transpiration of a beech forest (*Fagus silvatica* L.) in a mountainous Mediterranean region. *Journal of Hydrology*, 285:248–259.

Marchand, J. P. (1984). Sapwood area as an estimator of foliage biomass and projected leaf area for *Abies balsamea* and *Picea rubens*. *Canadian Journal of Forest Research*,

14:85–87.

Mark, W. R. and Crews, D. L. (1973). Heat-Pulse velocity and bordered pit condition in living Engelman spruce and Lodgepole pine trees. *Forest Science*, 19:291–296.

Matlack, G. R. (1993). Microenvironment variation within and among forest edge sites in the eastern United States. *Biological Conservation*, 66(3):185–194.

Mauseth, J. D. (1988). *Plant anatomy.* . The Benjamin Cummings, Inc., Menlo Park, California, USA.

McAllister, D. (2005). Remote estimation of Leaf Area Index in forested ecosystems. Master's thesis, University of Calgary, Calgary, Alberta.

McCuen, R. H. (1989). *Hydrological Analysis and Design*. Prentice Hall, Upper Saddle River, NJ, USA, third edition.

McDowell, N., Barnard, H., Bond, B. J., Hinckley, T., Hubbard, R. M., Ishii, H., Köstner, B., Magnani, F., Marshall, J. D., Meinzer, F. C., Phillips, N., Ryan, M. G., and Whitehead, D. (2002). The relationships between tree height and leaf area: sapwood area ratio. *Oecologia*, 132:12–20.

Mcgregor, C. A. (1984). Ecological land classification and evaluation. Kananaskis country. Natural Resource Summary, Alberta Energy and Natural Resources. Resource appraisal section. Resource evaluation branch, Edmonton, Alberta. Report No. T/11 - No. 10.

Meadows, S. J. and Hodges, D. J. (2002). Sapwood area as an estimator of leaf area and foliar weight in cherrybark oak and green ash. *Forest Science*, 48(1):69–76.

Means, J. E., Acker, S. A., Harding, D. J., Blair, J. B., Lefsky, M. A., Cohen, W. B., Harmon, M. E., and McKee, W. A. (1999). Use of large-footprint scanning airborne lidar to estimate forest stand characteristics in the western cascades of Oregon. *Remote Sensing of Environment*, 67:298–308.

Meinzer, F. C., Brooks, J. R., Domec, J. C., Gartner, B. L., Warren, J. M., Woodruff, D. R., Bible, K., and Shaw, D. C. (2006). Dynamics of water transport and storage in conifers studied with deuterium and heat tracing techniques. *Plant, Cell and Environment*, 29:105–114.

Meinzer, F. C., Goldstein, G., Holbrook, N. M., Jackson, P., and Cavelier, J. (1993). Stomatal and environmental control of transpiration in a lowland tropical forest. *Plant, Cell and Environment*, 16:429–436.

Mencuccini, M. and Grace, J. (1994). Climate influences the leaf area/sapwood area ratio in scots pine. *Tree physiology*, 15:1–10.

Monteith, J. L. (1965). Evaporation and environment. In Fogg, G. E., editor, *Symposia of the Society for experimental biology. The state and movement of water living organisms*, number XIX, pages 205–234, London, UK. Society for Experimental Biology, Cambridge University Press.

Montgomery, D. C. (2001). *Design and analysis of experiments*. John Wiley & Sons, Inc., USA.

Murakami, S., Tsuboyama, Y., Shimizu, T., Fijieda, M., and Noguchi, S. (2000). Variation of evapotranspiration with stand age and climate in a small Japanese forested catchment. *Journal of Hydrology*, 227:114–127.

Murray, F. W. (1967). On the computation of saturation vapour pressure. *Journal of Applied Meteorology*, 6:203–204.

Myneni, R. B., Nemani, R. R., and Running, S. W. (1997). Estimation of global Leaf Area Index and absorbed PAR using radiative transfer models. *IEEE Transactions on Geoscience and Remote Sensing*, 35(6):1380–1393.

Nadezhdina, N., Čermák, J., and Ceulemans, R. (2002). Radial patterns of sap flow in woody stems of dominant and understory species: scaling errors associated with positioning of sensors. *Tree Physiology*, 22:907–918.

Naglera, P. L., Cleverly, J., Glenna, E., Huetec, D. L. A., and Wand, Z. (2005). Predicting riparian evapotranspiration from MODIS vegetation indices and meteorological data. *Remote Sensing of Environment*, 94:17–30.

Nishida, K., Nemani, R. R., Running, S. W., and Glassy, J. M. (2003). Development of and evapotranspiration index from Aqua/MODIS for monitoring surface moisture status. *IEEE Transactions on Geoscience and Remote Sensing*, 41(2):493–501.

Nokes, S. E. (1995). Evapotranspiration. In Ward, A. D. and Elliot, W. J., editors, *Environmental Hydrology*, chapter 4, pages 91–132. CRC Press, USA, first edition.

Oren, R., Phillips, N., Ewerds, B. E., Pataki, D. E., and Megonigal, J. P. (1999). Sap-flux-scaled transpiration responses to light, vapour pressure deficit, and leaf area reduction in a flooded *Taxodium distichum* forest. *Tree Physiology*, 19:337–347.

Oren, R., Phillips, N., Katul., G., Ewers, B. E., and Pataki, D. E. (1998). Scaling xylem sap flux and soil water balance and calculating variance: a method for partitioning water flux in forests. *Annales des Sciences Forestières*, 55:191–216.

Payton, M. E. (1997). Confidence intervals for the coefficient of variation. In *Refereed Proceedings for the 1996 Kansas State University Conference for Applied Statistics in Agriculture*, pages 82–87, Kansas, USA. Kansas State University.

Payton, M. E., Miller, A. E., and Raun, W. R. (2000). Testing statistical hypothesis using standard error bars and confidence intervals. *Communications in Soil Science and Plant Analysis*, 31(5-6):547–551.

Peet, R. K. (1988). Forests of the Rocky Mountains. In Barbour, M. G. and Billings, W. D., editors, *North American Terrestrial Vegetation*, chapter 2, pages 33–62. Cambridge University Press, New York, first edition.

Perrier, A. (1982). Land surfaces processes: vegetation. In Eagleson, P. S., editor, *Land surface processes in atmospheric general circulation models*, pages 395–448,

Greenbelt, Maryland. WMO/ICSO Joint Scientific Committee, Cambridge University Press. Papers presented at the world climate research programme study Conference.

Philipson, W. R., Ward, J. M., and Butterfield, B. G. (1971a). Reaction of the cambium to gravity and to the displacement of branches. In Philipson, W. R., Ward, J. M., and Butterfield, B. G., editors, *In: The vascular cambium, its development and activity*, chapter 11, pages 159–169. Chapman and Hall LTD, The Chaucer Press, Ltd., Bungay, Suffolk, first edition.

Philipson, W. R., Ward, J. M., and Butterfield, B. G. (1971b). *Variations in the size of fusiform cambial initials. In: The vascular cambium, its development and activity*, chapter 4. Chapman and Hall LTD, The Chaucer Press, Ltd., Bungay, Suffolk.

Phillips, N., Oren, R., and Zimmerman, R. (1996). Radial patterns of xylem sap flow in non-diffuse and ring-porous tree species. *Plant, Cell and Environment*, 19:983–990.

Pimentel, D., Berger, B., Filiberto, D., Newton, M., Wolfe, B., Karabinakis, E., Clark, S., Poon, E., Abbett, E., and Nandagopa, S. (2004). Water Resources: Agricultural and Environmental issues. *BioScience*, 54(10):10.

Poyatos, R., Llorens, P., and Gallart, F. (2005). Transpiration of Montane *Pinus sylvestris* L. and *Quercus pubescens* Willd. forest stands measured with sap flow sensors in NE spain. *Hydrology and Earth System Sciences*, 9:493–505.

Price, D. T. and Black, T. A. (1989). Estimation of forest transpiration and CO_2 uptake using the Penman-Monteith equation and a physiological photosynthesis model. In Black, T. A., Spittlehouse, D. A., Novak, M. D., and T., P. D., editors, *Estimation of Aereal Evapotranspiration*, number 177 in IAHS, Red books, pages 213–227. IASH, first edition.

Price, J. C. (1990). Using spatial context in satellite data to infer regional scale evapotranspiration. *IEEE Transactions on Geoscience and Remote Sensing*, 28(5):940–948.

Prueger, J. H., Hips, L. E., Kustas, W. P., Neale, C. M. U., Hatfield, J. L., Bawazir, S., Eichinger, W. E., and Cooper, D. I. (2001). Feasibility of evapotranspiration monitoring of riparian vegetation with remote sensing. In IAHS, Publication, ., editor, *Remote Sensing and Hydrology 2000. Proceedings of a symposium held at Santa Fe, New Mexico, USA*, number 267, pages 246–251.

Quinn, G. P. and Keough, M. J. (2002). *Experimental design and Data Analysis for Biologists*. Cambridge University Press, Cambridge, UK, first edition.

Roberts, J. (1999). Plants and water in forests and woodlands. In Baird, A. J. and Wilby, R. L., editors, *Eco-Hydrology. Plants and water in terrestrial and aquatic environments*, Routledge physical environment series, chapter 4, pages 193–236. Routledge, Taylor and Francis Group, London and New York, first edition.

Roberts, J. (2000). The influence of physical and physiological characteristics of vegetation on their hydrological response. *Hydrological processes*, 14:2885–2901.

Robinson, D. E., Wagner, R. G., and Swanton, C. J. (2002). Effects of nitrogen on the growth of Jack pine competing with Canada blue-joint grass and large leaved aster. *Forest Ecology and Management*, 160(1-3):233–242.

Roderick, M. L. and Berry, S. L. (2001). Linking wood density with tree growth and environment: a theoretical analysis based on the motion of water. *New Phytologist*, 149:473–485.

Rowe, J. S. (1972). *Forest Regions of Canada*. Department of the Environment Canadian Forestry Service, Ottawa. Publication No. 1300.

Sakuratani, T. (1981). A heat balance method for measuring water flux in the stem of intact plants. *Journal of Agricultural Meteorology*, 40:273–277.

Samson, R. (2001). *An experimental and modelling approach to the actual evapotranspiration in a mixed deciduous forest ecosystem (Experimental forest Aelmoeseneie at Gontrode)*. PhD thesis, Ghent University, Ghent, Belguim.

Saugier, B., Granier, A., Pontailler, J. Y., E, D., and Baldochi, D. D. (1997). Transpiration of a boreal pine forest measured by branch bag, sap flow and micrometeorological methods. *Tree Physiology*, 17:511–519.

Schipka, F., Heimann, J., and Leuschner, C. (2005). Regional variation in canopy transpiration of central European beech forests. *Oecologia*, 143:260–270.

Schuler, T. M. and Smith, F. W. (1988). Effect of species mix on size/density and leaf-area relations in Southwest Pinyon/Juniper woodlands. *Forest Ecology and Management*, 25:211–220.

Schulze, E. D., Čermák, J., Matyssek, R., Penka, M., Zimmermann, R., Vasiceck, F., Gries, W., and Kucera, J. (1985). Canopy transpiration and water fluxes in the xylem of the trunk of *Larix* and *Picea* trees: a comparison of xylem flow, porometer and cuvette measurements. *Oecologia*, 66:475–483.

Shelburne, V. B., Hedden, R. L., and Allen, R. M. (1993). The effects of site, stand density and sapwood permeability on the relationship between leaf area and sapwood area in loblolly pine (*Pinus taeda* L.). *Forest Ecology and Management*, 58:193–209.

Sievänen, R., Nikinmaa, E., and Perttunen, J. (1997). Evaluation of importance of sapwood senescence on tree growth using the model lignum. *Silva Fennica*, 31(3):329–340.

Skene, D. S. and Balodis, V. (1968). A study of vessel length in *Eucalyptus obliqua* L'Herit. *Journal of Experimental Botany*, 19(4):825–830.

Smith, M. (1990). Report on the expert consultation on revision of FAO methodologies for crop water requirements. Report, Land and Water Development Division, Food and Agriculture Organization of the United Nations (FAO), Rome, Italy. With contributions from: R. Allen, J. L. Monteith, A. Perrier, L. Santos Pereira, and A. Segeren.

Smith, W. K. and Hinckley, T. M. (1995). *Ecophysiology of coniferous forests*. Physiological ecology. Academic Press Inc., 525B Street, Suite 1900, San Diego, California 92101-4495, first edition.

Sperry, J. S., Nichols, L. K., Sullivan, J. E. M., and Eastlack, S. E. (1994). Xylem embolism in ring-porous, diffuse-porous and coniferous trees of Northern Utah and interior Alaska. *Ecology*, 75(6):1736–1752.

Sperry, J. S., Perry, A. H., and Sullivan, J. E. M. (1991). Pit membrane degradation and air-embolism formation in ageing xylem vessels of *Populus tremuloides* Michx. *Journal of Experimental Botany*, 42(244):1399–1406.

Sperry, J. S. and Tyree, M. T. (1989). Water-stress-induced xylem embolism in three species of conifers. *Plant, Cell and Environment*, 13:427–436.

Sperry, J. S. and Tyree, M. T. (1990). Water stress-induced xylem embolism in three species of conifers. *Plant, Cell and Environment*, 1990(13):427–436.

Spicer, R. and Gartner, B. (2001). The effects of cambial age and position within the stem on specific conductivity in Douglas-fir (*Pseudotsuga menziesii*) sapwood. *Trees*, 15:222–229.

Steinberg, S. L. (1988). Dynamax trunk-flow gauge test. Technical application report 2. Insulation and time of attachment test. Dynamax Inc.

Steinberg, S. L., van Bavel, C. H. M., and McFarland, M. J. (1989). A gauge to measure mass flow rate of sap in stems and trunks of woody plants. *Journal of the American Society for Horticultural Science*, 114:466–472.

Stewart, J. B. (1988). Modelling surface conductance of pine forest. *Agricultural and Forest Meteorology*, 43(1988):19–35.

Strong, W. L. (1992). *Ecoregions and Ecodistricts of Alberta*, volume 1. Alberta Forestry, Lands and Wildlife, Edmonton, Alberta. Canada.

Strong, W. L. and Leggat, K. R. (1992). *Ecoregions of Alberta*. Alberta Forestry, Lands and Wildlife, Edmonton, Alberta. Canada.

Swanson, R. H. (1994). Significant historical developments in thermal methods for measuring sap flow. *Agricultural and Forest Meteorology*, 72:113–132.

Szilagy, J. (2000). Can a vegetation index derived from remote sensing be indicative of areal transpiration? *Ecological Modelling*, 127(5):65–79.

Szilagy, J. (2002). Vegetation indices to aid areal evapotranspiration estimations. *Journal of Hydrological Engineering*, 7(5):368–372.

Tyree, M. T. (1999). Water relations of plants. In Bard, S. J. and Wilby, R. L., editors, *Eco-hydrology, plants and water in terrestrial aquatic environments*, chapter 2. Routledge Publishers. Taylor & Francis Group, USA and Canada.

Tyree, M. T. and Zimmermann, M. H. (2002). *Xylem structure and the ascent of sap*. . Springer Series in Wood Science, Springer, Germany, second edition.

Vangel, M. G. (1996). Confidence intervals for a normal coefficient of variation. *The American Statistician*, 50(1):21–26.

Čermák, J., Deml, M., and Penka, M. (1973). A new method of sap flow rate determination in trees. *Biologia Plantarum (Praha)*, 15:171–178.

Čermák, J., Kučcera, J., and Penka, M. (1976). Improvement of the method of sap flow rate determination in full-grown trees based on heat balance with direct electric heating in xylem. *Biologia Plantarum PRAHA*, 18(2):105–110.

Veihmeyer, F. J. and Hendrickson, A. H. (1950). Soil moisture in relation to plant growth. In Arnon, D. I. and Machlis, L., editors, *Annual review of plant physiology. Vol. 1*, pages 285–304. Annual Review, Inc., Stanford California.

Verrill, S. (2003). Confidence bounds for normal and log normal distribution coefficients of variation. *The Forest Products Laboratory*, 2003:1–10. Research Paper FPL-RP-609, Madison WI; US.

Vertessy, R. A., Benyon, R. G., OSullivan, S. K., and Gribben, P. R. (1995). Relationships between stem diameter, sapwood area, leaf area and transpiration in a young mountain ash forest. *Tree physiology*, 15:559–567.

Vertessy, R. A., Hatton, T. J., Reece, P., O'Sullivan, S. K., and Benyon, R. G. (1997). Estimating stand water use of large mountain ash trees and validation of the sap flow. *Tree physiology*, 17:747–756.

Ward, J. C. and Pong, W. Y. (1980). Wetwood in trees: a timber resource problem. Technical Report PNW-112, Unites States Department of Agriculture, Forest Service, Pacific Northwest Forest and Range Experiment Station.

Waring, R. H. (1982). Estimating forest growth and efficiency in relation to canopy leaf area. *Advance Ecological Research*, 13:327–354.

Waring, R. H., Gholz, H. L., Grier, C. C., and Plummer, M. L. (1977). Evaluating stem conducting tissue as an estimator of leaf area in four woody angiosperms. *Canadian Journal of Botany*, 55:1474–1477.

Waring, R. H. and Roberts, J. M. (1979). Estimating water flux through stems of scots pine with tritiated water and phosphorous-32. *Journal of Experimental Botany*, 30:459–471.

White, D., Beadle, C., Worledge, D., Honeysett, J., and Cherry, M. (1998). The influence of drought on the relationship between leaf and conducting sapwood area in *Eucalyptus globulus* and *Eucalyptus nitens*. *Trees*, 1998(12):406–414. Springer-Verlag Pubs.

Whitehead, D. (1978). The estimation of foliage area from sapwood basal area in scots pine. *Forestry*, 51:137–149.

Wilson, K. B., Hanson, P. J., Mulholland, P. J., Baldocchi, D. D., and Wullschleger, S. D. (2001). A comparison of methods for determining forest evapotranspiration and

its components: sap-flow, soil water budget, eddy covariance and catchment water balance. *Agricultural and Forest Meteorology*, 106:153–168.

Woodward, F. I. (1995). Ecophysiological controls of conifer distributions. In Smith, W. K. and Hinckley, T. M., editors, *Ecophysiology of coniferous forests*, chapter 4, pages 79–94. Academic Press, USA, first edition.

Wullschleger, S. D. and Norby, T. J. (2001). Sap velocity and canopy transpiration in a sweetgum stand exposed to free-air CO_2 enrichment (FACE). *New Phytologist*, 150:489–498.

Yang, K. C. (1993). Survival rate and nuclear irregularity index of sapwood ray parenchyma cells in four tree species. *Canadian Journal of Forest Research*, 23:673–629.

Yazawa, K., Ishida, S., and Miyajima, H. (1965). On the wet heartwood of some broad leaved trees grown in Japan. *Journal of the Japan Research Society*, 11:71–75.

Yunhao, C., Xiaobing, L., and Guifei, J. (2003). An estimation model for daily regional evapotranspiration. *Internation Journal of Remote Sensing*, 24(1):199–205.

Zhang, H., Simmonds, L. P., Morison, J. I. L., and Payne, D. (1997). Estimation of transpiration by single trees: comparison of sap flow measurements with a combination equation. *Agricultural and Forest Meteorology*, 87:155–169.

Zimmermann, M. H. and Jeje, A. A. (1981). Vessel-length distribution of some American woody plants. *Canadian Journal of Botany*, 59:1882–1892.